Department of Chemical Engineering

Faculty of Science and Engineering

Aqueous Phase Adsorption of Organic/Inorganic Contaminants by Eucalyptus Bark (*Eucalyptus Sheathiana*) Biomass

Sharmeen Afroze

This thesis is presented for the Degree of

Doctor of Philosophy

of

Curtin University

April 2016

DECLARATION

To the best of my knowledge and belief this thesis contains no material previously published by any other person except where due acknowledgement has been made.

This thesis contains no material which has been accepted for the award of any other degree or diploma in any university.

Signature: ……S. Afroze……

Date: ……27.04.2016

DEDICATIONS

This work is dedicated to my mother and father for their loving support.

This work is also dedicated to my husband Md. Zahangir Alam Sarker and my two super kids, Arisha and Afrah for their love, support, understanding and encouragement during my whole period of study.

ACKNOWLEDGEMENT

In the beginning, all praises and glories to Almighty Allah (SWT) who has bestowed me courage and patience upholding this work.

I gratefully acknowledge and heartily express my sincere regards and gratitude to my supervisor, Associate Prof. Tushar Kanti Sen. His constant encouragement, invaluable advice, deep involvement and the patience has helped me to achieve this goal today. Sincere thanks to my co-supervisor Prof. Ming Ang for his enduring guidance and support towards the fulfilment of my research through detailed and constructive comments during my study.

My sincere thanks to all the laboratory technical staff members of Chemical Engineering Department, Curtin University, in particular Karen Haynes, Jason Wright, Araya Abera, Jimmy Xiao Hua, Andrew Chan and Roshanak Doroushi and my colleague Zana Rada for their assistance in the laboratory. Also, I must acknowledge the support provided by the entire staff of the department of Applied Physics at Curtin University for carrying out SEM and XRD analysis. Sincere thanks to my friends Sara Dawood and Anteneh Yeneneh Musfin for their support and advice whenever I needed.

I am indeed indebted to my mother whose understanding attitude, constant inspiration and patience to listen to my difficulties kept me in high spirits for completing this work. I cannot find words to express my gratitude to my lovely family members for their encouragement, support and endurance through my study. I owe my thanks and appreciation to my lovely sister Dilruba Afrose for her unconditional love, care and support throughout my life. Finally, I would like to thank all the other people not mentioned here, but in my sincerest mind and heart.

PUBLICATIONS

Refereed Journal Publications

- T. K. Sen, **S. Afroze**, and H. Ang, *Equilibrium, kinetics and mechanism of removal of methylene blue from aqueous solution by adsorption onto pine cone biomass of Pinus radiate,* Water, Air, & Soil Pollution, 2011. 218 (1-4): p. 499-515.

- T. K. Sen, M. T. Thi, **S. Afroze**, C. Phan, M. Ang, *Removal of anionic surfactant sodium dodecyl sulphate from aqueous solution by adsorption onto pine cone biomass of Pinus Radiate: equilibrium, thermodynamic, kinetics, mechanism and process design*, Desalination and Water Treatment, 2012. 45 (1-3): p. 263-275.

- M. T. Yagub, T. K. Sen, **S. Afroze**, H. M. Ang, *Fixed-bed dynamic column adsorption study of methylene blue (MB) onto pine cone*, Desalination and Water Treatment, 2014: p. 1-14.

- M. T. Yagub, T. K. Sen, **S. Afroze**, H. M. Ang, *Dye and its removal from aqueous solution by adsorption: A review*, Advances in Colloid and Interface Science, 2014. 209: p. 172-184.

- **S. Afroze**, T. K. Sen, *Agricultural Solid Wastes in Aqueous Phase Dye Adsorption: A Review. Agricultural Wastes Characteristics, Types and Management*, NOVA Publishers, New York, 2015. 1: p. 169-214.

- **S. Afroze**, T. K. Sen, M. Ang, H. Nishioka, *Adsorption of methylene blue dye from aqueous solution by novel biomass Eucalyptus sheathiana bark: equilibrium, kinetics, thermodynamics and mechanism*, Desalination and Water Treatment, 2016. 57(13): p. 5858-5878. DOI: 10.1080/19443994.2015.1004115

- **S. Afroze**, T. K. Sen, H. M. Ang, *Adsorption performance of continuous fixed bed column for the removal of methylene blue (MB) dye using Eucalyptus sheathiana bark biomass*, Research on Chemical Intermediates, 2016. 42(3): p. 2343-2364. DOI: 10.1007/s11164-015-2153-8

- **S. Afroze**, T. K. Sen, M. Ang, *Kinetic and Equilibrium Study for the Removal of Zinc (II) from Aqueous Phase by Raw and Base Modified Eucalyptus Sheathiana Bark*, Process Safety and Environmental Protection, 2016 (in press).

TABLE OF CONTENTS

Acknowledgement iii

Publications iv

Abstract xxii

Table of Contents vi

List of Figures xii

List of Tables xvi

List of Appendices xviii

Nomenclature xix

List of Abbreviations xxi

CHAPTER 1

INTRODUCTION

1.1 General Overview and Problem Statement 1

1.1.1 Classification of Organic and Inorganic Pollutants in Wastewater 2
1.1.2 Toxicity Effects of Organic and Inorganic Pollutants in Wastewater 3
1.1.3 Wastewater Treatment Technologies 4

1.2 Significance of Current Research 5

1.3 Aim and Objectives of This Research 7

1.3.1 Aim 7
1.3.2 Specific Objectives 7

1.4 Organisation of Thesis and Research Design 8

1.5 References 12

CHAPTER 2

LITERATURE REVIEW

2.1 Sources of Organic and Inorganic Contaminants in Wastewater and Their Removal 15

2.2 Classification of Organic and Inorganic Pollutants in Wastewater 17

2.3 Treatment Methods Available for Organic and Inorganic Removal from Wastewater 21

2.3.1 Physical Methods 25
2.3.2 Chemical Methods 25
2.3.3 Biological Methods 26
2.3.4 Combined Methods 28

2.4 Adsorption 28

2.4.1 Factors Affecting Adsorption of Organic and Inorganic Ions 29

2.4.1.1 Effect of Solution pH 30
2.4.1.2 Effect of Initial Adsorbate Concentration 33
2.4.1.3 Effect of Solution Temperature 36
2.4.1.4 Effect of Adsorbent Dosage 39
2.4.1.5 Effect of Ionic Strength 42

2.4.2 Role of Adsorbent Characteristics on Adsorption 45

2.4.2.1 Adsorption with Modified Adsorbents 46
2.4.2.2 Adsorption with Biomass Based Activated Carbon Adsorbents 48

2.5 Use of Various Adsorbents for the Removal of Organic and Inorganic Contaminants 49

2.5.1 Cost Effective Adsorbents for Organic and Inorganic Removal 50
2.5.1.1 Agricultural Solid Wastes 50
2.5.1.2 Modified Agricultural Solid Wastes 53
2.5.1.3 Biomass Based Activated Carbon 54
2.5.1.4 Inorganic Materials 56
2.5.1.5 Bioadsorbents & Microbial Biomass 59

2.6 Batch Adsorption Kinetic-Study 61

2.6.1 Application of Lagergren Pseudo-first-order and Pseudo-second order model Kinetics on Organic/Inorganic Adsorption 61
2.6.2 Application of Intra-particle Diffusion Model on Organic/Inorganic Adsorption 62

2.7 Batch Adsorption Isotherms 65

2.7.1 Langmuir Adsorption Isotherm Model 65
2.7.2 Freundlich Adsorption Isotherm Model 66

2.8 Thermodynamics Study 69

2.9 Column Adsorption Studies for Organic Dye Removal 70

2.9.1 Theory of Breakthrough Curve (BTC) 71

2.9.2 Modelling of Column Dynamic Adsorption 72

2.9.2.1 Thomas Model 73
2.9.2.2 Yoon-Nelson model 73
2.9.2.3 Bed Depth Service Time (BDST) Model 74

2.10 Summary 75

2.11 References 77

CHAPTER 3

MATERIALS, METHODS AND CHARACTERISATION

3.1 Introduction 100

3.2 Research Methodology 100

3.2.1 Materials 100

3.2.1.1 Collection and Preparation of Adsorbents 100
3.2.1.2 Adsorbent Characterisation 104

3.2.2 Experimental Methods 105

3.2.2.1 Batch Adsorption Kinetic Studies 105
3.2.2.2 Isotherm Studies 108
3.2.2.3 Desorption Studies 108
3.2.2.4 Column Studies 109

3.3 Characterisation of Raw and Modified Eucalyptus *Sheathiana* Bark Biomass 109

3.3.1 Surface Morphology 109
3.3.2 EDS Observation 111
3.3.3 X-Ray Diffraction Spectrum Study 112
3.3.4 FTIR Spectrum Study 113
3.3.5 Particle Size Distribution 117
3.3.6 BET Analysis 118
3.3.7 Bulk Density Measurement 120
3.3.8 C-H-N Analysis 121
3.3.9 Point of Zero Charge (pH_{pzc}) Study 122

3.4 Summary 125

3.5 References 127

CHAPTER 4

BATCH ADSORPTION STUDIES ON THE REMOVAL OF ORGANIC METHELYNE BLUE (MB) DYE BY RAW EUCALYPTUS BARK

4.1 Introduction 129

4.2 Materials and Methods 130

4.2.1 Adsorbent 130
4.2.2 Adsorbate and Other Chemicals 130
4.2.3 Adsorption Experiments 130

4.3 Results and Discussion 131

4.3.1 Effect of Initial Solution pH on MB Dye Adsorption Kinetics 131
4.3.2 Effect of Initial Dye Concentration and Contact Time on MB Dye Adsorption Kinetics 133
4.3.3 Effect of Adsorbent Dosage on MB Dye Adsorption Kinetics 135
4.3.4 Effect of Temperature and Thermodynamic Parameters Calculation for MB Dye Adsorption Kinetics 137
4.3.5 Effect of Surfactant on MB Dye Adsorption Kinetics 140
4.3.6 Effect of Presence of Mixed Dye 141
4.3.7 Effect of Inorganic Mono, Di and Trivalent Ions on MB Dye Adsorption Kinetics 142

4.4 Desorption Studies 144

4.5 Application of Adsorption Kinetic Models 146

4.5.1 Pseudo First Order Kinetic Model 147
4.5.2 Pseudo Second Order Kinetic Model 150
4.5.3 Intraparticle Diffusion Model and Mechanism of Adsorption 153
4.5.4 Validity of Kinetic Models 157

4.6 Adsorption Equilibrium Isotherm Models 157

4.7 Design of Single Stage Batch Adsorber from Isotherm Data 161

4.8 Summary 163

4.9 References 164

CHAPTER 5

ADSORPTION OF METHYLENE BLUE (MB) DYE THROUGH FIXED BED COLUMN STUDY BY RAW EUCALYPTUS BARK

5.1 Introduction 169

5.2 Materials and Methods 170

5.2.1 Adsorbent and its characterisation 170
5.2.2 Adsorbate and Other Chemicals 170

5.3 Fixed Bed Adsorption Column Design and Experimental Procedure 171

5.4 Modelling and Column Adsorption Process Analysis 173

5.5 Results and Discussion 176

5.5.1 Effect of Initial MB Dye Flow Rate 176
5.5.2 Effect of Initial MB Dye Concentration 178
5.5.3 Effect of Adsorbent Bed Height 180

5.6 Kinetic Modelling of Fixed Bed Column Studies 182

5.6.1 Application of Thomas Model 182
5.6.2 Application of Yoon-Nelson Model 185
5.6.3 Application of Bed Depth Service Time (BDST) Model 187

5.7 Summary 189

5.8 References 190

CHAPTER 6

BATCH ADSORPTION STUDIES ON THE REMOVAL OF ZINC (II) METAL IONS BY RAW AND MODIFIED EUCALYPTUS BARK

6.1 Introduction 194

6.2 Materials and Methods 194

6.2.1 Adsorbent 194
6.2.2 Adsorbate and Other Chemicals 195
6.2.3 Adsorption Experiments 195

6.3 Results and Discussion 196

6.3.1 Effect of Initial Solution pH on Zn^{2+} Adsorption Kinetics 196
6.3.2 Effect of Initial Metal Concentration and Contact Time on Zn^{2+} Adsorption Kinetics 199
6.3.3 Effect of Adsorbent Dosage on Zn^{2+} Adsorption Kinetics 202
6.3.4 Effect of Temperature on Zn^{2+} Adsorption Kinetics and Thermodynamic Studies 204
6.3.5 Effect of Presence of Salts on Zn^{2+} Adsorption Kinetics 207

6.4 Desorption Studies 210

6.5 Application of Adsorption Kinetic Models 211

6.5.1 Pseudo First Order Kinetic Model 211
6.5.2 Pseudo Second Order Kinetic Model 216
6.5.3 Intraparticle Diffusion Model and Mechanism of Adsorption 220

6.6 Adsorption Equilibrium Isotherm Models and Error Analysis 225

6.7 Design of Single Stage Batch Adsorber from Isotherm Data 231

6.8 Summary 232

6.9 References 233

CHAPTER 7

CONCLUSIONS AND RECOMMENDATIONS

7.1 Introduction 236

7.2 Conclusion 237

7.2.1 Chapter 3: Characterisation of Prepared Adsorbents 237
7.2.2 Chapter 4: Batch Adsorption Study of Raw Eucalyptus Bark for MB Dye Removal 238
7.2.3 Chapter 5: Column Adsorption Study of Raw Eucalyptus Bark for MB Dye Removal 239
7.2.4 Chapter 6: Batch Adsorption Study of Raw and Modified Eucalyptus Bark for Zn^{2+} Removal 240

7.3 Recommendations for Future Research 241

LIST OF FIGURES

Figure 2.1	Effect of solution pH on Light Green dye adsorption on modified peanut husk	31
Figure 2.2	Effect of initial Cu(II) concentration onto acid treated Tomato waste	35
Figure 2.3	Effect of temperature on the adsorption of Pb(II) by peanut shell	37
Figure 2.4	Effect of adsorbent dose on the adsorption of Basic Green 4 on Olive Pomace at equilibrium time	40
Figure 2.5	The effect of ionic strength (NaCl) to the adsorption rate of MB-5G on expanded perlite	44
Figure 2.6	Adsorption in a flow-through packed-bed column	72
Figure 3.1	(a) Eucalyptus *sheathiana* tree and (b) bark from eucalyptus *sheathiana* tree	101
Figure 3.2	Preparation of base modified eucalyptus bark powder	101
Figure 3.3	Chemical structure of (a) Methylene Blue (MB) dye and (b) Zine Nitrate Hexahydrate	102
Figure 3.4	SP-8001 UV/VIS Spectrophotometer	103
Figure 3.5	Calibration curve of initial Methylene Blue (MB) dye concentrations	104
Figure 3.6	Measuring pH of solution using pH Meter: WP 81	104
Figure 3.7	Thermo Line Scientific Orbital Shaker Incubator	106
Figure 3.8	Centrifugal analyser	106
Figure 3.9	Shimadzu AA-7000 atomic absorption spectrophotometer (AAS)	107
Figure 3.10	(a) Raw eucalyptus bark and (b) NaOH modified eucalyptus bark before adsorption	110
Figure 3.11	(a) Raw eucalyptus bark after MB dye adsorption, (b) raw eucalyptus bark after Zn^{2+} adsorption and (c) NaOH modified eucalyptus bark after Zn^{2+} adsorption	111
Figure 3.12	EDS surface chemical properties of raw eucalyptus bark (106 µ)	112
Figure 3.13	X-ray diffraction spectra's of (a) raw and (b) NaOH modified eucalyptus bark (EB) powder	113
Figure 3.14	Spectrum 100 FT-IR Spectrometer	114
Figure 3.15	FTIR spectrum of (a) raw and (b) NaOH modified eucalyptus bark powder	116
Figure 3.16	Malvern MasterSizer 2000S	117
Figure 3.17	Particle size distribution of raw eucalyptus bark	118
Figure 3.18	Micromeritics Tristar II 3020 and degassing chambers	119
Figure 3.19	CHNS/O analyser 2400 Series II by Perkin Elmer	122

Figure 3.20	Point of zero charge (pHpzc) of (a) raw eucalyptus bark and (b) NaOH modified eucalyptus bark	124
Figure 4.1	Effect of initial solution pH by raw eucalyptus bark on (a) the amount of MB dye adsorption (b) percentage (%) removal of MB dye	133
Figure 4.2	Effect of initial solution concentration by raw eucalyptus bark on (a) the amount of MB dye adsorption (b) percentage (%) removal of MB dye	135
Figure 4.3	Effect of adsorbent dosages by raw eucalyptus bark (a) on the amount of MB dye adsorption (b) percentage (%) removal of MB dye	136
Figure 4.4	Effect of temperature on the adsorption of MB dye onto EB powder	138
Figure 4.5	Van't Hoff plot for adsorption of MB dye on raw eucalyptus bark	140
Figure 4.6	Effect of surfactant on the amount of adsorption of MB dye onto EB powder	141
Figure 4.7	Effect of mixture of adsorbents on the adsorption onto EB powder	142
Figure 4.8	Effect of electrolytes on the adsorption of MB dye onto EB powder	144
Figure 4.9	Batch desorption of MB dye from raw eucalyptus bark using different solvents	145
Figure 4.10	Pseudo-first-order kinetic model for the adsorption of MB dye onto raw eucalyptus bark at different (a) initial pH (b) initial concentrations (c) adsorbent dosages and (d) solution temperatures	148
Figure 4.11	Pseudo-second-order kinetic model for the adsorption of MB dye onto raw eucalyptus bark at different (a) initial pH (b) initial concentrations (c) adsorbent dosages and (d) solution temperatures	151
Figure 4.12	Intraparticle diffusion model for the adsorption of MB dye onto raw eucalyptus bark at different (a) initial pH (b) initial concentrations (c) adsorbent dosages and (d) solution temperatures	154
Figure 4.13	(a) Langmuir-I plot and (b) Langmuir-II plot	158
Figure 4.14	Freundlich plot	159
Figure 4.15	Adsorbent mass (g) against volume (litres) of solution treated	162
Figure 5.1	Schematic Diagram of Fixed bed Column	172
Figure 5.2	Ideal Breakthrough Curve	174
Figure 5.3	Comparison of experimental breakthrough curves (BTC) of MB dye adsorption on raw eucalyptus bark at different flow rates	177
Figure 5.4	Comparison of experimental breakthrough curves (BTC) of MB Dye adsorption on raw eucalyptus bark at different initial MB dye concentrations	180
Figure 5.5	Comparison of experimental breakthrough curves (BTC) for MB dye adsorption on raw eucalyptus bark at different bed heights	181

Figure 5.6	Thomas kinetic plot for the adsorption of MB on eucalyptus bark: Effect of flow rate	183
Figure 5.7	Thomas kinetic plot for the adsorption of MB on eucalyptus bark: Effect of inlet MB dye concentration	184
Figure 5.8	Thomas kinetic plot for the adsorption of MB on eucalyptus bark: Effect of adsorbent bed height	184
Figure 5.9	Yoon–Nelson kinetic plot for the adsorption of MB on eucalyptus bark: Effect of flow rate	186
Figure 5.10	Yoon–Nelson kinetic plot for the adsorption of MB on eucalyptus bark: Effect of inlet MB dye concentration	186
Figure 5.11	Yoon–Nelson kinetic plot for the adsorption of MB on eucalyptus bark: Effect of adsorbent bed height	187
Figure 5.12	Bed Depth Service Time (BDST) kinetic plot for the adsorption of MB on eucalyptus bark	188
Figure 6.1	Effect of initial solution pH by raw and NaOH modified EB powder	198
Figure 6.2	Effect of initial metal concentration by raw EB powder on (a) the amount of Zn^{2+} adsorption (b) percentage (%) removal of Zn^{2+}	200
Figure 6.3	Effect of initial metal concentration by NaOH modified EB on (a) the amount of Zn^{2+} adsorption (b) percentage (%) removal of Zn^{2+}	201
Figure 6.4	Effect of adsorbent dosages by raw and NaOH modified EB on (a) the amount of Zn^{2+} adsorption (b) percentage (%) removal of Zn^{2+}	203
Figure 6.5	Effect of temperature on Zn^{2+} adsorption onto raw and NaOH modified EB powder	205
Figure 6.6	Van't Hoff plot for adsorption of Zn^{2+} onto raw and NaOH modified EB	206
Figure 6.7	Effect of presence of salts on the amount of Zn^{2+} adsorption onto raw EB powder	208
Figure 6.8	Effect of presence of salts on the amount of Zn^{2+} adsorption onto NaOH modified EB powder	208
Figure 6.9	Pseudo-first-order kinetic model for the adsorption of Zn^{2+} onto raw eucalyptus bark at different (a) initial pH (b) initial concentrations (c) adsorbent dosages and (d) solution temperatures	213
Figure 6.10	Pseudo-first-order kinetic model for the adsorption of Zn^{2+} onto NaOH modified eucalyptus bark at different (a) initial pH (b) initial concentrations (c) adsorbent dosages and (d) solution temperatures	214
Figure 6.11	Pseudo-second-order kinetic model for the adsorption of Zn^{2+} onto raw eucalyptus bark at different (a) initial pH (b) initial concentrations (c) adsorbent dosages and (d) solution temperatures	217

Figure 6.12 Pseudo-second-order kinetic model for the adsorption of Zn^{2+} onto NaOH modified eucalyptus bark at different (a) initial pH (b) initial concentrations (c) adsorbent dosages and (d) solution temperatures 218

Figure 6.13 Intraparticle diffusion model for the adsorption of Zn^{2+} onto raw eucalyptus bark at different (a) initial pH (b) initial concentrations (c) adsorbent dosages and (d) solution temperatures 222

Figure 6.14 Intraparticle diffusion model for the adsorption of Zn^{2+} onto NaOH modified eucalyptus bark at different (a) initial pH (b) initial concentrations (c) adsorbent dosages and (d) solution temperatures 223

Figure 6.15 Equilibrium Adsorption Isotherm fitted to (a) Langmuir-I and (b) Langmuir-II model 226

Figure 6.16 Freundlich plot for raw and NaOH treated EB 227

Figure 6.17 Adsorbent mass (g) against volume (litres) of solution treated for (a) raw eucalyptus bark system (b) NaOH modified eucalyptus bark 231

LIST OF TABLES

Table 2.1:	Classification of dyes according to the chemical structure	17
Table 2.2:	Classification of dyes based on their usage	18
Table 2.3:	Class A and Class B metals adopted from	20
Table 2.4:	Classification of inorganic heavy metals based on their toxicity sequences on a range of organisms	20
Table 2.5:	Principal advantages and limitations of dyes removal methods	22
Table 2.6:	Current treatment technologies for inorganic heavy metals removal involving physical and/or chemical processes	24
Table 2.7:	The effect of solution pH on the adsorption of dyes and heavy metal ions by different adsorbents	32
Table 2.8:	The results of various reported studies on the initial dye concentration effect on dyes and heavy metals adsorption by various adsorbents	35
Table 2.9:	Influence of solution temperature on the adsorption of dyes and heavy metals using various adsorbents	38
Table 2.10:	The effect of adsorbent dosage on the percentage of organic dyes and inorganic heavy metals removal using several adsorbents	41
Table 2.11:	The results of various reported studies on the effect of ionic strength on dyes and heavy metals adsorption by various adsorbents	44
Table 2.12:	Technical advantages and disadvantages of existing modification techniques	46
Table 2.13:	Various adsorbents and their modifying agents for dyes and heavy metal ions removal	47
Table 2.14:	The classification of pre-treatment methods for the production of activated adsorbents	49
Table 2.15:	Adsorption capacities q_m (mg/g) of waste materials from raw agricultural solid wastes	51
Table 2.16:	Adsorption capacities q_m (mg/g) for modified agricultural waste materials	53
Table 2.17:	Adsorption capacities q_m (mg/g) for activated carbon materials made from agricultural solid wastes	55
Table 2.18:	Adsorption capacities q_m(mg/g) of natural inorganic materials	58
Table 2.19:	Adsorption capacities q_m (mg/g) for various natural organic materials as biosorbents	60
Table 2.20:	Pseudo-second-order kinetic studies for organic dyes and inorganic heavy metals adsorption by several adsorbents	64
Table 2.21:	Various isotherm studies of dyes and heavy metals adsorption by various adsorbents	68
Table 3.1:	BET surface area for raw and NaOH modified eucalyptus bark (EB)	119

Table 3.2:	Bulk density of raw and NaOH modified eucalyptus bark (EB)	121
Table 3.3:	Elemental analysis of raw eucalyptus bark (EB)	122
Table 4.1:	Thermodynamic parameters for adsorption of MB dye onto raw eucalyptus bark at different temperature	140
Table 4.2:	Pseudo-first-order kinetic model parameters for adsorption of MB dye on raw eucalyptus bark	149
Table 4.3:	Pseudo-second-order kinetic model parameters for adsorption of MB dye on raw eucalyptus bark	152
Table 4.4:	Intraparticle diffusion model parameters for adsorption of MB dye on raw eucalyptus bark	156
Table 4.5:	Calculated values of model parameters obtained from Freundlich and Langmuir isotherms	160
Table 4.6:	Comparison of the adsorption capacity (q_m in mg/g) of different sorbents for the removal of methylene blue (MB) dye	161
Table 5.1:	Breakthrough curves (BTCS) parameters of fixed bed column at different MB dye flow rates for its removal by eucalyptus bark biomass	178
Table 5.2:	Breakthrough curves (BTCS) parameters of fixed bed column at different inlet MB dye concentration for its removal using eucalyptus bark biomass	180
Table 5.3:	Breakthrough curves (BTCS) parameters of fixed bed column at different bed height of eucalyptus bark biomass for the removal of MB dye	182
Table 5.4:	Thomas kinetic model parameters at different experimental conditions by non-linear regression analysis	185
Table 5.5:	Yoon–Nelson kinetic model parameters at different experimental conditions by non-linear regression analysis	187
Table 6.1:	Thermodynamic parameters for adsorption of Zn^{2+} at different temperatures onto raw and NaOH modified eucalyptus bark	207
Table 6.2:	Percentage desorption of Zn^{2+} from raw and NaOH modified eucalyptus bark	210
Table 6.3:	Pseudo-first-order kinetic model parameters for adsorption of Zn^{2+} on raw and NaOH modified eucalyptus bark	215
Table 6.4:	Pseudo second order model parameters for adsorption of Zn^{2+} on raw and NaOH modified eucalyptus bark (EB)	219
Table 6.5:	Intraparticle diffusion model parameters for adsorption of Zn^{2+} on raw and NaOH modified eucalyptus bark (EB)	224
Table 6.6:	A summary of Langmuir and Freundlich calculated values	228
Table 6.7:	Comparison of the adsorption capacity (q_m in mg/g) of different sorbents for the removal of Zn^{2+}	230

LIST OF APPENDICES

Appendix A	Raw data for the adsorption of methylene blue (MB) dye onto raw eucalyptus bark	243
Appendix B	Raw data for the adsorption of methylene blue (MB) dye onto raw eucalyptus bark through fixed bed column study	266
Appendix C	Raw data for the adsorption of Zinc (II) metal ions onto raw and modified eucalyptus bark	275

NOMENCLATURE

Symbol	Description	Unit
C_e	Equilibrium adsorbate concentration	ppm or (mg/L)
C_0	Initial adsorbate concentration	ppm or (mg/L)
C_t	Adsorbate concentration at time *t*	ppm or (mg/L)
D_p	Diffusion coefficient	(cm^2/s)
ΔG^0	Gibbs free energy change	(kJ/mol)
ΔH^0	Enthalpy change	(kJ/mol)
h	Initial adsorption rate	(mg/g min)
H_B	used bed length up to the break point	(cm)
H_T	Total bed height	(cm)
H_{UNB}	Unused bed length	(cm)
Ka	Langmuir isotherm constant	(L/mg)
K_1	Pseudo-first-order rate constant	(min^{-1})
K_2	Pseudo-second-order rate constant	(mg/g min)
K_a	BDST rate constant	(L mg^{-1} min^{-1})
K_f	Freundlich isotherm constant	[$(L/g)^{1/n}$]
K_{id}	Intra-particle rate constant	(mg/g. $min^{0.5}$)
K_{Th}	Thomas rate constant	(mL/min mg)
K_{YN}	Yoon–Nelson constant	(min^{-1})
M	Mass of adsorbent per unit volume	(g L^{-1})
m	Amount of adsorbent added	(g)
m_{total}	Total amount of adsorbate sent to the column	(mg)
N_o	Adsorption capacity of the column bed per unit bed volume	(mg L^{-1})

n	Freundlich constant	-
p	Number of parameters for MPSD calculation	-
Q	Adsorbate volumetric flow rate	(mL/min)
q_e	Amount of adsorbate per gram of adsorbent at equilibrium	(mg/g)
q_m	Maximum adsorption capacity	(mg/g)
q_o	Maximum solid phase concentration	(mg/g)
q_t	Amount of adsorbate per gram of adsorbent at any time t	(mg/g)
q_{total}	Total adsorbed quantity of adsorbate	(mg)
R^2	Linear regression coefficient	-
R_L	Dimensionless constant separation factor	-
r_0	Radius of adsorbent particle	cm
ΔS^0	Entropy change	(J/k mol)
t	Time	(min)
t_b	Breakthrough time	(min)
t_t	Time equivalent to total or Stoichiometric Capacity	(min)
t_{total}	Total flow time	(min)
t_u	Time equivalent to usable capacity	(min)
T	Absolute temperature	(K)
V	Volume of adsorbate solution	(L)
V_{eff}	Total effluent volume	(mL)
x	Number of data point for MPSD calculation	-
χ^2	Chi-square	-
τ	Time required for 50% sorbate breakthrough	(min)

ABBREVIATIONS

AAS	Atomic Absorption Spectrophotometer
BBS	British Standard Sieves
BDST	Bed Depth Service Time BDST
BET	Brunauer–Emmett–Teller
BTC	Breakthrough Curve
CR	Congo red
$CaCl_2$	Calcium Chloride
CH_3COOH	Acetic Acid
EDS	Electron Diffraction Spectrum
EB	Eucalyptus bark
$FeCl_3$	Ferric Chloride
FTIR	Fourier Transform Infrared
HCl	Hydrochloric Acid
H_2O	Water
hr	Hour
MB	Methylene blue
mins	Minutes
MPSD	Marquardt's percent standard deviation
NaOH	Sodium Hydroxide
NaCl	Sodium Chloride
pzc	Point of Zero Charge
SEM	Scanning electron microscopy
SSE	Sum of Squared Errors
Temp	Temperature
XRD	X-ray Diffraction
Zn^{2+}	Zinc (II) ion

ABSTRACT

Wastewater generated from various industrial activities has contributed to environmental contamination by producing organic and inorganic pollutants. These pollutants are a major threat to surrounding ecosystem and human health if left untreated before discharging to environment. Hence, among several treatment strategies, adsorption is regarded to be an effective and preferred method for the removal of these organic and inorganic pollutants from wastewater and in recent years, agricultural solid waste resources have attracted great research interest in their use as adsorbents in this regard. Eucalyptus bark (*Eucalyptus Sheathiana*) biomass, an evergreen, fast growing and abundantly available worldwide, has been extensively studied as a novel adsorbent for the removal of natural organic matters and heavy metal ions from wastewater effluents. This thesis describes the adsorption capacity and efficiency of raw eucalyptus bark adsorbent towards selected pollutants, methylene blue (MB) dye as organic and Zinc (II) heavy metal ions as inorganic pollutants on the sorbent. Further, the adsorbent was modified with (0.1 M) sodium hydroxide (NaOH) in order to improve its capacity for extraction of Zinc (II) metal ions from aqueous solutions. The main focus of the proposed study was to formulate cheap and sustainable ways of purifying contaminated water by exploiting the pollutants affinity towards adsorbents.

The raw and NaOH treated eucalyptus bark samples were characterized by Scanning electron microscopy (SEM) to examine the surface micro-morphology of materials, Electron diffraction spectrum (EDS) for elemental analysis, Fourier transform infrared spectroscopy (FTIR) for the determination of the functional groups and X-ray diffractometer (XRD) to observe the minerals that are present in the biomass adsorbents. Some other analyses such as bulk density, particle size, surface area and point of zero charge of the raw and modified adsorbents were also determined.

The undertaken study showed the adsorption potential of raw eucalyptus bark to remove methylene blue (MB) dye from its aqueous solutions. Effects of various process parameters such as initial dye concentration, adsorbent loading, solution pH, temperature, mixture of dyes, presence of salts and surfactant onto MB dye

adsorption by raw bark material were studied. The amount of MB dye adsorption on eucalyptus bark was found to increase with an increase in initial solution pH, initial MB dye concentration, contact time, ionic strength and system temperature; but decreased with increase in the amount of adsorbent and non-ionic surfactant. Around 90% MB dye removal percentage was achieved by raw eucalyptus bark biomass at a MB dye solution pH of 10.0 with 20 ppm initial concentration. The studied kinetic models including Pseudo-first order and Pseudo second-order models showed that the Pseudo second-order model best described the kinetics of MB dye adsorption onto raw eucalyptus bark adsorbent. The mechanism of MB dye adsorption was analysed by intraparticle diffusion model and desorption study, implying a multilayer chemisorption process. The adsorption equilibrium data prescribed to Langmuir model with monolayer adsorption. The maximum Langmuir monolayer adsorption capacity of raw eucalyptus bark for MB dye was found to be 204.08 mg/g at 30°C. A single-stage batch adsorber design for MB dye adsorption onto eucalyptus bark biomass has been presented based on the Langmuir isotherm model equation. The results of determined thermodynamic parameters with positive enthalpy change (ΔH^o) accompanied by positive entropy change (ΔS^o) and negative decrease in Gibbs free energy change (ΔG^o), revealed that the adsorption process is endothermic, irreversible and spontaneous in nature.

The dynamic adsorption of methylene blue (MB) dye by raw eucalyptus bark was also performed in packed bed up-flow column. The column studies were conducted with a fixed column of internal diameter 2.5 cm and a height of 30 cm. On evaluating the breakthrough curves, a series of column experiments were studied with varying inlet MB dye flow rate, initial MB dye concentration and adsorbent bed height. High bed height, low flow rate and high initial dye concentration were found to be the better conditions for maximum dye adsorption. For a given initial dye concentration, the lower the flow rate and the higher the bed depth is, the higher are the breakthrough and exhaustion times. A maximum uptake of 45.24, 48.29 and 49.55 mg g^{-1} for MB dye adsorption by raw eucalyptus bark was observed at 10 mL min^{-1} flow rate, 100 mg L^{-1} initial dye concentration and 10 cm bed height respectively. For continuous process design, the obtained experimental dynamic results were fitted to determine column kinetic parameters using Thomas, Yoon-Nelson and bed depth service time (BDST) models. All models were found suitable with high correlation

coefficients for describing the dynamic behaviour of the column, with respect to the examined process parameters.

In the same manner to organic pollutant (MB dye), the applicability of eucalyptus bark (in its raw and base modified form) was studied for the removal of inorganic heavy metal ions Zn^{2+} from its aqueous solutions. In general, the results of the adsorption studies showed that base treated eucalyptus bark is more efficient than raw ones. BET analysis confirmed that modification improved the surface area and pore size of adsorbent which exhibits higher adsorption capacity of modified eucalyptus bark compared to the raw eucalyptus bark to adsorb Zn^{2+} ions on the adsorbent surface. The adsorption process was found to be dependent on adsorbent weight, pH, initial metal ion concentration, contact time, presence of salts and temperature. The kinetic experiments revealed that the adsorption of metal ions were rapid at initial stage followed by a slower phase where equilibrium was attained. Based on kinetic study of adsorption of Zn^{2+} ions on raw and modified adsorbent, the Pseudo second order model fitted best for both the systems. The evaluated equilibrium adsorption studies showed that both Freundlich and Langmuir models are applicable to fit the data well for both raw and base modified eucalyptus systems. MPSD error function was used to treat the equilibrium data using non-linear optimization technique for evaluating the fit of the isotherm equations. Upon modification, it was observed that the sorption capacity for Zn^{2+} improved from 128.21 mg g^{-1} to 250 mg g^{-1}. With the following experimental process parameters as: initial metal Zn^{2+} ion concentration, 20 ppm; solution temperature, 30^0C; shaking speed,120 rpm; contact time, 100 minutes; adsorbent dosage, 20 mg; and pH, 5.01; the maximum percent recovery of Zn^{2+} adsorbed was found to be 40.12% and 69.38% for raw and modified adsorbent respectively which were higher than many other reported systems. The increased free energy of activation (ΔG^o) with NaOH treatment indicated more spontaneous behaviour of adsorbent biomass with NaOH treatment. This implies, therefore, that the base modified eucalyptus bark has potential application as a tool to remove heavy metal Zn^{2+} ions from wastewater effluents.

In conclusion, eucalyptus bark biomass with good mechanical strength, high adsorption capacity, excellent adsorption selectivity and wide pH application range

has been successfully developed as a novel adsorbent for organic (MB dye) and inorganic (Zn^{2+} metal ions) pollutants removal. Therefore, raw and modified eucalyptus bark adsorbents showed good adsorption potential in environmental applications to remove organic and inorganic ions from water or wastewater and their adsorption capacity is very much comparative with other adsorbents including commercial activated carbon to treat MB dye and Zn^{2+} from their aqueous solutions.

CHAPTER 1

INTRODUCTION

1.1 General Overview and Problem Statement

The availability of clean water continues to be a challenge worldwide. In recent decades, environmental contamination through excessive release of organic and inorganic pollutants into water has contributed to high volumes of wastewater effluents. Contaminated liquid wastes that are produced and promoted on the water resources by human activities via increased population, industrialization, unplanned urbanization, agricultural activities including expanded use of chemicals, has become an increasingly serious problem worldwide. As most of the industrial processes are to be found close to the water bodies, they are increasingly polluted by a number of organic and inorganic materials. Synthetic dyes and heavy metals are widely used in many fields of advanced technology and hence treatment of their effluents in water is vital because of their carcinogenesis, mutagenesis, chromosomal fractures and respiratory toxicity effects to organisms including humans (Afroze and Sen 2015). Among the various potential pollutants of waterbodies, dyes are a large and important group of industrial chemicals. In up-to-date data, more than 100,000 commercial dyes are known with an annual production of over 7 $x10^5$ tonnes/year (Yagub, Sen et al. 2014). The total consumption of dyes in textile industries worldwide is more than 10,000 tonnes/year and approximately 100 tonnes/year of dyes are discharged into water streams (Yagub, Sen et al. 2012, Yagub, Sen et al. 2014). The presence of dyes in water even at low concentration is highly visible and undesirable. Among inorganic pollutants, heavy metals such as lead, copper, cadmium, zinc and nickel are the most common hazardous pollutants found in industrial effluents. According to the World Health Organization, the most toxic metals are aluminium, chromium, magnesium, iron, cobalt, nickel, copper, zinc, cadmium, mercury and lead (Karatas 2012). Basically exact data on the amount of organic dyes and inorganic heavy metals discharged from various industrial processes in the environment are unknown. However, the release and presence of these pollutants of synthetic dyes and heavy metals to the environment and development of effective technologies to remove these pollutants from their aqueous phase has posed has posed challenges to the scientists and engineers.

Motivation for The Work (Problem Statement)

Fresh water is scarce in many parts of the world and even our oceans, rivers, and other inland waters quality is reduced by various human activities which means water pollution. Basically fresh water resources are very limited and quality of fresh water is deteriorating day by day due to increased industrialization, urbanization, population growth and climate change and hence produces polluted water. Therefore development of sustainable water treatment process to alleviate water pollution has been a challenging and demanding task for engineers and researchers. This study was also carried out in Western Australia where the discharged industrial wastes include petroleum hydrocarbons, heavy metals, surfactants, mining activities may pollute receiving waters rendering them unsuitable as a water supply and pose a threat to aquatic life (Australia 2009). Some industrial wastes are volatile or release toxic gases which may become responsible for several health problems with plants, animals and human beings. Recent reports show that in South Australia, wastewater effluents are discharged into the marine environment which is a very complex issue. Pollutants through these wastewater effluents including sewage, industrial effluent, anti-foulants and ballast water that contain nutrients, organic sediments, heavy metals, and agricultural chemicals may impact significant risk to sensitive water resources including marine habitats and species (Department of Environment 2004). When pollutants in the waste interact with drinking water, they get incorporated, leading to accumulation of toxic dyes and heavy metals, making it unsuitable for human and animal consumption. Hence, it becomes necessary to remove these contaminants from these wastewaters by an appropriate treatment method before releasing them into the environment. Therefore, this project attempts to address and analyse above problems together with the development of removal methods of pollutants from contaminated waters.

1.1.1 Classification of Organic and Inorganic Pollutants in Wastewater

The constituents of the wastewater effluents comprise of organic and inorganic pollutants. Among the organic pollutants, commercial dyes are the leading ones while the main inorganic pollutants of concern are heavy metals in nature. Dyes can be classified according to their origin (natural/synthetic), chemical and/or physical

properties or characteristics related to the application process (Agustina 2013). Another categorization is based on the application classes. Dyes are also usually classified based on their particle charge upon dissolution in aqueous application medium (Hadi, Samarghandi et al. 2011) such as cationic (all basic dyes), anionic (direct, acid, and reactive dyes), and non-ionic (dispersed dyes).

Heavy metals can be classified according to their periodic table, or through the trends in the magnitude of equilibrium constants that describe the formation of metal ion/ligand complexes. According to the classification illustrated by Nieboer and Richardson (Nieboer and Richardson 1980), metals can be classified into three groups: class A (hard metals), class B (soft metals) and borderline (intermediate metals).

1.1.2 Toxicity Effects of Organic and Inorganic Pollutants in Wastewater

The evaluation of the toxicity of organic and inorganic pollutants (mainly dyes and heavy metals) is very important, mainly due to the different effects that they cause in the environment and the organisms exposed to them. Dyes are considered as an objectionable type of pollutants because they are toxic to food chain organisms (Gupta 2009). Generally, dyes can cause oral ingestion and inhalation, skin and eye irritation, and also carcinogenicity (Rai, Bhattacharyya et al. 2005, Christie 2007). They impart colour to water which is visible to human eye and therefore, highly objectionable on aesthetic grounds. Furthermore, dyes may cause micro-toxicity to fish and other organisms, also interfere with the transmission of light and upset the biological metabolism processes which cause the destruction of aquatic communities present in ecosystem (Afroze, Sen et al. 2015). Additionally dyes can have harmful effects on human beings such as dysfunction of kidneys, reproductive system, liver, brain and central nervous systems (Kadirvelu, Kavipriya et al. 2003). In several dyes classification, basic dyes have been classified as toxic colorants (El Qada, Allen et al. 2008). Basic dyes have high intensity of colours and the tinctorial value of basic dyes is very high, less than 1 ppm of dye is greatly visible in solution (McKay 1982). Anthroquinone based dyes made from known carcinogens such as benzidine and other aromatic compounds are resistant to degradation due to their fused aromatic ring structure, and disperse dyes have good ability to bioaccumulation (Carmen and

Daniela 2012). Azo dyes are one of the more detrimental toxic classes because it is highly persistent in the aquatic environment, due to its chemical compositions, involving aromatic rings, azoic linkages and amino groups (Ventura-Camargo and Marin-Morales 2013). Many studies have shown that reactive dyes can cause allergic dermatoses and respiratory diseases (Manzini, Motolese et al. 1996, Klemola, Pearson et al. 2007, Afroze and Sen 2015).

Among inorganic pollutants, heavy metals are hazardous pollutants of wastewaters that have become a serious public health concern (Demirbas, Sari et al. 2006). Although many heavy metals are micronutrients but higher concentration may give toxic effect. The most significant toxic metal ions that pose risks to humans and the environment include Cr, Cu, Pb, Hg, Mn, Cd, Ni, Zn, and Fe (Chatterjee, Bhattacharjee et al. 2010, Vakili, Rafatullah et al. 2014). Duruibe et al. (Duruibe, Ogwuegbu et al. 2007) reported that heavy metals cause adverse health effects, such as gastrointestinal disorders, diarrhoea, stomatitis, tremors, hemoglobinuria, ataxia, paralysis, vomiting, and convulsions, although each of these heavy metals exhibits its specific toxicity profile.

In addition to being toxic, it is also mentioned earlier that dyes and heavy metals containing effluents also contain chemicals that has been informed to cause carcinogenesis, mutagenesis or teratogenesis and respiratory toxicity to various organisms (Novotný, Dias et al. 2006, Mathur and Bhatnagar 2007). As such it is important to treat wastewater effluents for the removal of dyes and heavy metal ions. Therefore, this study will focus on specific methods and technologies for the removal of dyes and heavy metals bearing wastewater.

1.1.3 Wastewater Treatment Technologies

Various physical, chemical and biological methods are adopted in water and wastewater treatment process to produce acceptable water quality and satisfying governmental and environmental protocol agencies law and regulations (Sen 2015). A number of treatment methods such as reverse osmosis (RO), filtration, adsorption, chemical precipitation, coagulation, foam flotation, solvent extraction, electroplating, evaporation, oxidation/reduction, ion exchange, activated sludge, aerobic and anaerobic treatment, electrolysis, magnetic separation, membrane filtration,

adsorption on activated carbon have been used to remove the pollutants (Crini 2006, Barakat and Schmidt 2010, Bhatnagar and Sillanpää 2010, Miretzky and Cirelli 2010, Abdolali, Guo et al. 2014).

Among the possible techniques for wastewater treatments, the adsorption process by solid adsorbents meet great attention from the researchers by showing its efficient and potentially high pollutant–binding capacities for the removal of both organic and inorganic contaminants from wastewater. Fundamentally, adsorption is a process wherein a material is concentrated at a solid surface from its liquid or gaseous surroundings. It is a solid/liquid or solid/gas interfacial phenomena. When a solution containing adsorbable solute comes into contact with a solid with a highly porous surface structure, liquid–solid intermolecular forces of attraction cause some of the solute molecules from the solution to be concentrated or deposited at the solid surface and hence the solute retained on the solid surface in adsorption processes is called adsorbate, whereas, the solid on which it is retained is called as an adsorbent (Dabrowski 2001). This surface accumulation of adsorbate on adsorbent is called adsorption. Adsorption has advantages over the other methods mainly because of simple design, easy operation and regeneration, and involvement of low investment in term of both initial cost and land required. Further it is more advantageous when the selected adsorbents become naturally biomass based materials.

1.2 Significance of Current Research

The amount and variety of chemicals discharged into wastewaters has been increasing significantly which in turn accelerates the concentration of toxic contaminants in water and wastewater. This increase is as a result of rapid development of agricultural, chemical, petroleum processing, mining and allied industries around the world. Due to the presence of organic/inorganic chemical and biological pollutants in wastewater streams, when these discharged wastewaters come into contact with ground and surface water, make it unfit for human and animal consumption.

The increase of various hazardous chemicals in water bodies has made conventional methods of wastewater treatment ineffective and inefficient. As a result, a new

method of treatment has become necessary. Among various water purification and recycling technologies, adsorption has been found to be superior to other conventional methods for the removal of wastewater pollutants especially which are not easily biodegradable such as dyes and heavy metal ions. Adsorption can function in solid or liquid media and its pollutant removal mechanism is a result of adsorption and ion exchange. Adsorption is influenced by many physico-chemical factors such as sorbate/sorbent interaction, sorbent surface area, particle size, temperature, solution pH, concentration and contact time (Sulak, Demirbas et al. 2007). The sorbent molecular structure and presence of variety of functional groups in the sorbents make them selective and highly capable of sorption of contaminants from wastewater.

Among various techniques developed using adsorption method, commercially available activated carbon is commonly used highly effective adsorbent for the removal of organic/inorganic from aqueous solution but they are quite expensive and difficult to regenerate. Due to the high cost of commercial activated carbons, there is a need for an alternative, locally abundant, less expensive, efficient and effective means of adsorbent for removing pollutants from wastewaters. This search has put major consideration on locally available materials such as natural materials, agricultural wastes and industrial wastes which are called as low-cost adsorbents. The application of agricultural solid wastes as effective adsorbents offer several advantages; their easy availability in large quantities, requirement of less processing time, renewable in nature, low cost, eco-friendly and good adsorption potential due to their unique chemical composition makes the adsorption process more attractive for heavy metal and dye remediation (Choi, Chung et al. 2012, Singha and Das 2013). Considering all these facts, barks of eucalyptus trees (*Eucalyptus sheathiana*) which are one type of lignocellulose carbonaceous material, fast growing in nature and abundantly available in Australia can be proved effective and efficient for adsorption capacity. In this project, these issues have been considered carefully during the selection of adsorbent together with its economic viability for commercial application. Therefore, this work was undertaken:

- To investigate adsorption capacity and kinetic modelling of dyes and heavy metals uptake from their aqueous solutions by using agricultural waste

biomass eucalyptus bark (*Eucalyptus sheathiana*) as potential raw material for the development of sustainable cost effective adsorbent and efficient solid waste management.

- The significance of this study was to utilize raw and treated agricultural wastes eucalyptus bark biomass for the removal of cationic dye methylene blue (MB) and zinc metal ions (Zn^{2+}) in a better economical way.
- To investigate the mechanism and kinetics of adsorption of MB dye by raw eucalyptus bark and Zn^{2+} ions by raw and treated eucalyptus bark biomass.
- Commercial production of eucalyptus bark adsorbent can start using the methodology for the preparation of modified adsorbent established in this work and may also be useful in the removal of other organic and inorganic ions from industrial wastewater effluents.

1.3 Aim and Objectives of This Research

1.3.1 Aim

The overall objective of this research work is to develop a cost effective, environmentally friendly and readily available alternative biomass based sustainable adsorbent such as eucalyptus bark and its applications in the removal of organic MB dye and inorganic heavy metal ions Zn^{2+} pollutants from its aqueous solution, system identification and optimization of various physico-chemical process parameters by adsorption.

1.3.2 Specific Objectives

The specific objectives of this research project are arranged according to the thematic areas by which the Thesis (mainly the results chapters) is structured.

- Collection and synthesis of raw and base modified eucalyptus bark (*Eucalyptus Sheathiana*) biomass adsorbents.
- Characterisation of raw and base modified eucalyptus bark adsorbents to investigate the adsorption properties using different analytical instruments such as Scanning Electron Microscopy (SEM), Electron Diffraction Spectrum (EDS), X-ray Diffractometer (XRD), Fourier Transform Infrared

Spectroscopy (FTIR), CHN elemental analyser, Brunauer–Emmett–Teller (BET) method, and Malvern particle size analyser.

- Selections of methylene blue (MB) dye as an organic and heavy metal Zn^{2+} ions as an inorganic adsorbate model pollutants.
- To conduct batch kinetic adsorption studies under various physico-chemical process conditions such as initial solution pH, initial adsorbent dosage, initial adsorbate concentration, contact time, solution temperature and presence of different salts concentrations to identify and evaluate optimum process conditions for the adsorption of organic as well as inorganic ions distinctly.
- To investigate the adsorption kinetics, thermodynamics and mechanism of adsorption.
- To find out the applicability of different kinetic and isotherm models under a selected range of process conditions to find out maximum adsorption capacity.
- To examine desorption study for identification of mechanism of adsorption and regeneration.
- To perform continuous fixed bed column operation containing raw eucalyptus bark adsorbent for methylene blue (MB) dye adsorption by varying inlet dye flow rate, inlet dye concentration and adsorbent bed height to justify the process feasibility in industrial situation.
- To establish several breakthrough plots and assess the applications of various kinetic mass transfer models under different column experimental conditions.
- To compare the adsorption results between batch and column study.

1.4 Organisation of Thesis and Research Design

This thesis has been organised into seven chapters that covers all the details of this research work. In each chapter, there will be an introduction which will consist of a brief statement of the problem, objectives, the literature review, the experimental work explaining the analysis conducted throughout the research, and a conclusion based on the discussion of results obtained from the study. A list of references used appears at the end of each chapter. An overview of the summarized structure for this

thesis is presented in Figure 1.1 which is a schematic diagram showing the activities carried out in this research.

Chapter 1 outlines a brief introduction about the research project which is related to the background of water pollution, classification of pollutants, the need for remediation of pollutants to mitigate their effects and progress in this area, the significance of the study along with justification and scope of work. This chapter also gives an overview of the research design and a flow chart of the research activities.

Chapter 2 presents a detailed review of the literature including sources of organic-inorganic pollutants in wastewater, treatment technologies for their removal and current state of the developments for the use of inexpensive abundant materials to remove organic and inorganic pollutant ions from contaminated water. Later sections give a brief explanation on the theory of adsorption process together with isotherm models and kinetics of the batch and column adsorption processes.

Chapter 3 covers the research methodology and the characterisation of the raw and modified eucalyptus bark materials.

Chapter 4 includes the treatment of dye wastewater, using the raw eucalyptus bark biomass by discussing the findings in batch experiments followed by desorption study. Next sections provide the results on the equilibrium and kinetics studies and mechanism.

Chapter 5 reports the experimental results of fixed bed laboratory column operation. In this chapter, emphasis has been given to plot and examine several breakthrough curves on different examined process conditions such as amount of bark adsorbent, inlet dye adsorbate flow rate and its concentration for the removal of methylene blue.

Chapter 6 describes the experimental results for the removal of inorganic heavy metal (Zn^{2+}) ions together with the discussion using raw and treated eucalyptus bark material respectively to compare the performance between raw and treated adsorbent for the adsorption process. The discussion includes the findings in adsorption and

desorption experiments. The appropriate models are also employed to fit the experimental data.

Chapter 7 gives an overview of the major conclusions drawn from the chapters of the thesis, based on research findings from the data obtained along with some suggestions and recommendations for future scientific work to be carried out.

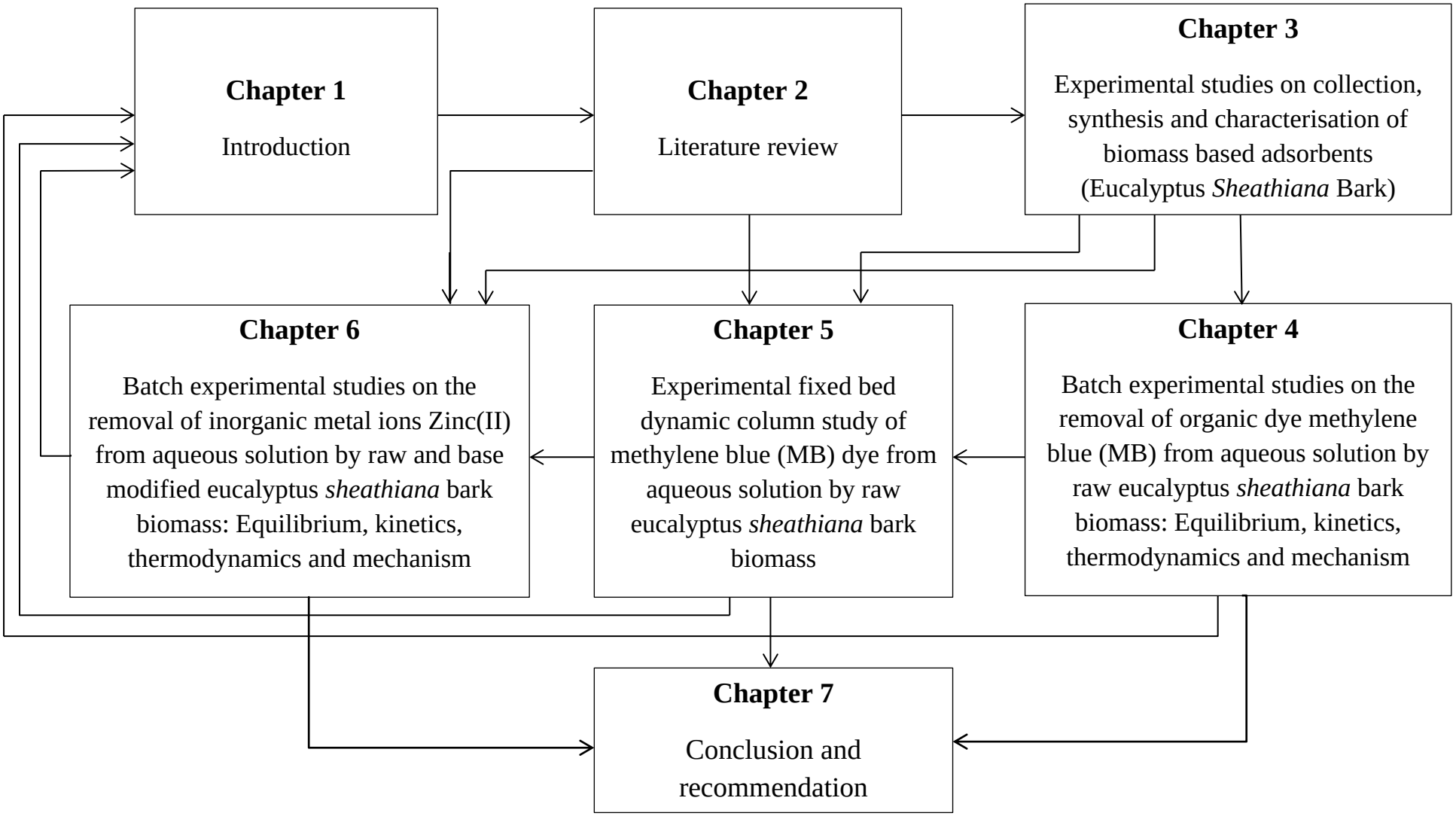

Figure 1.1 Schematic diagram of research activities

1.5 References

Abdolali, A., Guo, W., Ngo, H., Chen, S., Nguyen, N. and Tung, K. (2014). "Typical lignocellulosic wastes and by-products for biosorption process in water and wastewater treatment: a critical review." Bioresource Technology **160**: 57-66.

Afroze, S. and Sen, T. K. (2015). Agricultural Solid Wastes in Aqueous Phase Dye Adsorption: A Review. Agricultural Wastes Characteristics, Types and Management. C. N. Foster. New York, NOVA Publishers. **1:** 169-214.

Afroze, S., Sen, T. K., Ang, M. and Nishioka, H. (2015). "Adsorption of methylene blue dye from aqueous solution by novel biomass Eucalyptus sheathiana bark: equilibrium, kinetics, thermodynamics and mechanism." Desalination and Water Treatment **57**(13): 5858-5878.

Agustina, T. E. (2013). AOPs Application on Dyes Removal. Wastewater Reuse and Management, Springer**:** 353-372.

Australia, G. o. W. (2009). Industrial wastewater management and disposal. D. o. Water. Western Australia**:** 1-28.

Barakat, M. and Schmidt, E. (2010). "Polymer-enhanced ultrafiltration process for heavy metals removal from industrial wastewater." Desalination **256**(1): 90-93.

Bhatnagar, A. and Sillanpää, M. (2010). "Utilization of agro-industrial and municipal waste materials as potential adsorbents for water treatment—a review." Chemical Engineering Journal **157**(2): 277-296.

Carmen, Z. and Daniela, S. (2012). "Textile organic dyes–characteristics, polluting effects and separation/elimination procedures from industrial effluents–a critical overview." ISBN: 978-953.

Chatterjee, S., Bhattacharjee, I. and Chandra, G. (2010). "Biosorption of heavy metals from industrial waste water by Geobacillus thermodenitrificans." Journal of Hazardous Materials **175**(1): 117-125.

Christie, R. (2007). Environmental aspects of textile dyeing, Elsevier.

Crini, G. (2006). "Non-conventional low-cost adsorbents for dye removal: a review." Bioresource Technology **97**(9): 1061-1085.

Dabrowski, A. (2001). "Adsorption--from theory to practice." Advances in Colloid and Interface Science **93**(1-3): 135.

Demirbas, A., Sari, A. and Isildak, O. (2006). "Adsorption thermodynamics of stearic acid onto bentonite." Journal of Hazardous Materials **135**(1): 226-231.

Department of Environment, W. a. N. R. (2004). "DEH Living Coast Strategy for South Australia".

Duruibe, J., Ogwuegbu, M. and Egwurugwu, J. (2007). "Heavy metal pollution and human biotoxic effects." International Journal of Physical Science **2**(5): 112-118.

El Qada, E. N., Allen, S. J. and Walker, G. M. (2008). "Adsorption of basic dyes from aqueous solution onto activated carbons." Chemical Engineering Journal **135**(3): 174-184.

Gupta, V. (2009). "Application of low-cost adsorbents for dye removal–A review." Journal of Environmental Management **90**(8): 2313-2342.

Hadi, M., Samarghandi, M. R. and McKay, G. (2011). "Simplified fixed bed design models for the adsorption of acid dyes on novel pine cone derived activated carbon." Water, Air, & Soil Pollution **218**(1-4): 197-212.

Kadirvelu, K., Kavipriya, M., Karthika, C., Radhika, M., Vennilamani, N. and Pattabhi, S. (2003). "Utilization of various agricultural wastes for activated carbon preparation and application for the removal of dyes and metal ions from aqueous solutions." Bioresource Technology **87**(1): 129-132.

Karatas, M. (2012). "Removal of Pb (II) from water by natural zeolitic tuff: kinetics and thermodynamics." Journal of Hazardous Materials **199**: 383-389.

Klemola, K., Pearson, J. and Lindstrom-Seppä, P. (2007). "Evaluating the toxicity of reactive dyes and dyed fabrics with the HacaT cytotoxicity test." Autex Research Journal **7**: 217-223.

Manzini, B. M., Motolese, A., Conti, A., Ferdani, G. and Seidenari, S. (1996). "Sensitization to reactive textile dyes in patients with contact dermatitis." Contact Dermatitis **34**(3): 172-175.

Mathur, N. and Bhatnagar, P. (2007). "Mutagenicity assessment of textile dyes from Sanganer (Rajasthan)." Journal of Environmental Biology **28**(1): 123-126.

McKay, G. (1982). "Adsorption of dyestuffs from aqueous solutions with activated carbon I: Equilibrium and batch contact-time studies." Journal of Chemical Technology and Biotechnology **32**(7-12): 759-772.

Miretzky, P. and Cirelli, A. F. (2010). "Cr (VI) and Cr (III) removal from aqueous solution by raw and modified lignocellulosic materials: a review." Journal of Hazardous Materials **180**(1): 1-19.

Nieboer, E. and Richardson, D. H. (1980). "The replacement of the nondescript term 'heavy metals' by a biologically and chemically significant classification of metal ions." Environmental Pollution Series B, Chemical and Physical **1**(1): 3-26.

Novotný, Č., Dias, N., Kapanen, A., Malachová, K., Vándrovcová, M., Itävaara, M. and Lima, N. (2006). "Comparative use of bacterial, algal and protozoan tests to study toxicity of azo-and anthraquinone dyes." Chemosphere **63**(9): 1436-1442.

Rai, H. S., Bhattacharyya, M. S., Singh, J., Bansal, T., Vats, P. and Banerjee, U. (2005). "Removal of dyes from the effluent of textile and dyestuff manufacturing

industry: a review of emerging techniques with reference to biological treatment." Critical Reviews in Environmental Science and Technology **35**(3): 219-238.

Sen, T. (2015). Physical Chemical and Biological Treatment Processes for Water and Wastewater. USA, Nova Publishers.

Sulak, M., Demirbas, E. and Kobya, M. (2007). "Removal of Astrazon Yellow 7GL from aqueous solutions by adsorption onto wheat bran." Bioresource Technology **98**(13): 2590-2598.

Vakili, M., Rafatullah, M., Ibrahim, M. H., Abdullah, A. Z., Salamatinia, B. and Gholami, Z. (2014). Oil palm biomass as an adsorbent for heavy metals. Reviews of Environmental Contamination and Toxicology Springer. **232:** 61-88.

Ventura-Camargo, B. d. C. and Marin-Morales, M. A. (2013). "Azo Dyes: Characterization and Toxicity– A Review." Textiles and Light Industrial Science and Technology (TLIST) **2**(2).

Yagub, M. T., Sen, T. K., Afroze, S. and Ang, H. (2014). "Dye and its Removal from aqueous solution by Adsorption: A review." Advances in Colloid and Interface Science **209**: 172-184.

Yagub, M. T., Sen, T. K. and Ang, H. (2012). "Equilibrium, kinetics, and thermodynamics of methylene blue adsorption by pine tree leaves." Water, Air, & Soil Pollution **223**(8): 5267-5282.

Every reasonable effort has been made to acknowledge the owners of copyright material. I would be pleased to hear from any copyright owner who has been omitted or incorrectly acknowledged.

CHAPTER 2

LITERATURE REVIEW

2.1 Sources of Organic and Inorganic Contaminants in Wastewater and Their Removal

The continuous release of toxic organic and inorganic wastes bearing effluents from industries into water bodies has become a major concern for environmentalists, academics and engineers. A dye is a coloured, ionising and aromatic organic compound that can attach itself to surfaces or fabrics to impart colour. They have a synthetic origin and complex molecular structures and make them inert and difficult to biodegrade when discharged into waste streams (Afroze and Sen 2015). The residual dyes from different sources of industries such as textile (Sokolowska-Gajda, Freeman et al. 1996, Carmen and Daniela 2012) , paper and pulp manufacturing (Ivanov, Gruber et al. 1996, Carmen and Daniela 2012), agricultural sector (Kross, Nicholson et al. 1996, Cook and Linden 1997), food technology (Bhat and Mathur 1998), light-harvesting arrays (Bensalah, Alfaro et al. 2009), photo electrochemical cells (Wróbel, Boguta et al. 2001), hair colourings (Scarpi, Ninci et al. 1998), dye and dye intermediates (Carmen and Daniela 2012) , pharmaceutical (Carmen and Daniela 2012) , tannery (Kabdaşli, Tünay et al. 1999, Tünay, Kabdaşli et al. 1999), and kraft bleaching industries (Carmen and Daniela 2012), etc. are considered a wide variety of organic pollutants introduced into the natural water resources or wastewater treatment systems (Ravikumar, Deebika et al. 2005). Among all industrial sectors, textile industries are rated as high dye polluters, taking into consideration the volume of discharge and effluent composition (El Qada, Allen et al. 2008). The total dye consumption in textile industry worldwide is more than 10,000 tonnes/year and approximately 100 tonnes of dyes per year are discharged into water streams (Yagub, Sen et al. 2012). Recent studies indicate that approximately 12% of synthetic dyes are lost during manufacturing and processing operations and approximately 20% of these lost dyes enter the industrial wastewaters (Demirbas 2009).

Heavy metals are inorganic elements having atomic weights between 63.5 and 200.6, and a specific gravity greater than 5.0 (Srivastava and Majumder 2008, Fu and Wang 2011).

The part of this chapter has been published in Agricultural Wastes Characteristics, Types and Management by C. N. Foster, New York, NOVA Publishers; as book chapter.

Unlike organic contaminants, heavy metals are not biodegradable and tend to accumulate in living organisms and many heavy metal ions are known to be toxic or carcinogenic. Toxic heavy metals of particular concern in treatment of industrial wastewaters include zinc, copper, nickel, mercury, cadmium, lead and chromium (Vakili, Rafatullah et al. 2014). The industrial sources of commonly encountered heavy metals are refineries, coal fired power plants, municipal wastewater for mercury (Urgun-Demirtas, Benda et al. 2012), mining operations, tanneries, electronics for copper (Kazemipour, Ansari et al. 2008), cadmium–nickel batteries, phosphate fertilizers, pigments and stabilizers for cadmium (Mortaheb, Kosuge et al. 2009), metal smelters, paints and ceramics for manganese (Li, Imaizumi et al. 2010), effluents from plastics, textiles, microelectronics and wood preservatives producing industries for lead (Bhatti, Mumtaz et al. 2007) production. The main sources of zinc are the manufacturing of brass and bronze alloys, car radiator manufacturing, agricultural sources, steel production, electroplating (Abdelwahab, Amin et al. 2013) where highly concentrated zinc is coming from pharmaceuticals, galvanizing, paints, pigments, insecticides, cosmetics, etc. (Bhattacharya, Mandal et al. 2006).

Hence, these organic dyes and heavy metals can cause irreparable damage to natural environment and human health and further these toxic effluents pose a major threat to the surrounding ecosystem if left untreated. Various methods such as adsorption, coagulation, advanced oxidation, membrane separation, etc. are used for the removal of pollutants from wastewater. Among all these methods, adsorption is considered as one of the most effective processes of advanced wastewater treatment which industries employ to reduce hazardous inorganic/organic presence in the effluent. Many industries use commercial activated carbon for the treatment of wastes containing dyes and heavy metals. Activated carbons are expensive due to their regeneration and reactivation procedures. The current research is focused on the need for a more cost effective adsorbent to commercial activated carbon. Many researchers have reported the feasibility of using various low cost adsorbents derived from natural materials, industrial solid wastes, agricultural by-products and biosorbents as viable alternatives to activated carbon for the treatment of contaminated wastewater containing different classes of dyes (Robinson, McMullan et al. 2001, Rafatullah, Sulaiman et al. 2010, Salleh, Mahmoud et al. 2011, Kharat 2015) and heavy metal ions (Fu and Wang 2011, Vakili, Rafatullah et al. 2014).

2.2 Classification of Organic and Inorganic Pollutants in Wastewater

Commercial dyes are usually a mixture of large complex and often unreported molecular structure and diverse properties and also vary widely in chemical composition (El Qada, Allen et al. 2008). There are several ways for classification of commercial dyes. Each class of dye has a very unique chemistry, structure, and particular way of bonding. As mentioned in Chapter 1 (Section 1.1.1), dyes are usually classified based on their particle charge upon dissolution in aqueous application medium (Hadi, Samarghandi et al. 2011) such as cationic (all basic dyes), anionic (direct, acid, and reactive dyes), and non-ionic (dispersed dyes). A systematic classification of dyes according to chemical structure is the colour index (Agustina 2013). However, due to the complexities of the colour nomenclature from the chemical structural system, the classification based on application is often preferable (Gupta 2009). The classification based on chemical structure for the common class of dyes is presented in Table 2.1, whereas Table 2.2 represents the classification based on dye usage.

Table 2.1: Classification of dyes according to the chemical structure (Ali 2010, Yagub, Sen et al. 2014)

Class	*Chromospheres*	*Example*
Azo dyes	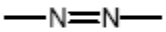	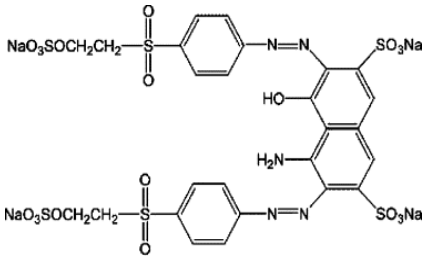 Reactive Black 5
Anthraquinone dyes	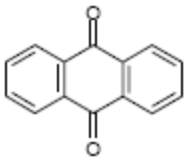	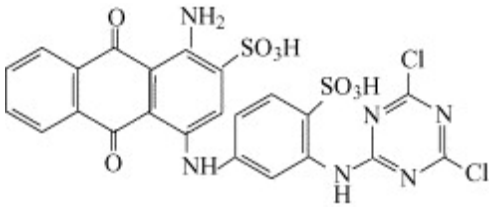 Reactive Blue 4

Indigoid dyes	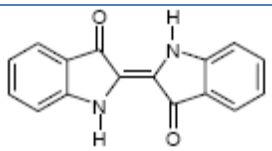	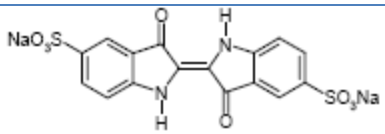 Acid Blue 71
Nitroso dyes	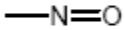	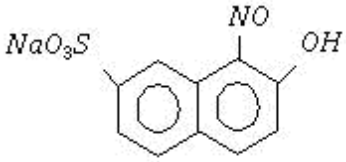 Acid green 1
Nitro dyes	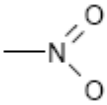	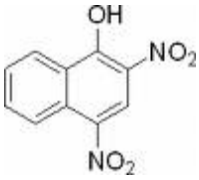 Acid Yellow 24
Triarylmethane dyes	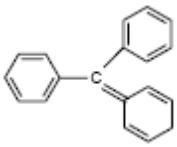	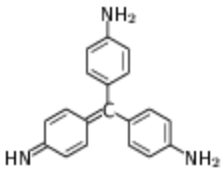 Basic red 9

Table 2.2: Classification of dyes based on their usage (Kochher and Kumar 2012)

Class	***Principle Substrates***	***Application Method***	***Chemical Types***
Acid	Nylon, wool, silk, paper, inks and leather	Usually from neutral to acidic dye baths	Azo (including premetallized), anthraquinone, triphenylmethane, azine, xanthenes, nitro, nitroso
Azoic components and compositions	Cotton, rayon, cellulose acetate and polyester	Fiber impregnated with coupling component and treated with a solution of stabilized diazonium salt	Azo
Basic	Paper, polyacrylonitrile, modified nylon, inks, polyester	Applied from acidic dye baths	Cyanine, Diaz cyanine, hemidiazacyanine, diphenymethane, azo, xanthenes

Direct	Cotton, rayon, paper, leather and nylon	Applied from neutral or slightly alkaline baths containing additional electrolytes	Azo, Phthalocyanine, stilbene and oxazine
Disperse	Polyester, polyamide, acetate, acrylic and plastics	Fine aqueous dispersion often applied by high temperature/pressure or low temperature carrier methods	Azo, anthraquinone, styryl, nitro and benzodifuranone
Fluorescent brighteners	Soaps, detergents, all fibres,paints,oil and plastic	From solution, dispersion or suspension in mass	Naphtha imides, stilbene, pyrazoles, coumarin
Food, cosmetics and drugs	Food, drug and cosmetics		Azo, anthraquinone, carotenoid and triarylmethane
Mordent	Wool, leather and anodized aluminum	Applied in conjunction with Cr salts	Azo, anthraquinone
Oxidation bases	Hair, fur and cotton	Aromatic amines and phenols oxidized on substrate	Aniline black and indeterminate structures
Reactive	Cotton, wool, silk and nylon	Reactive site on dye reacts with functional group on fiber to bind dye covalently under influence of heat and pH(alkaline)	Azo, anthraquinone, phthalocyanine, oxazine and basic
Solvent	Plastic, gasoline, varnishes, ink, fats and waxes	Dissolution in substrate	Azo, triphenylmethane, phthalocyanine, oxazine
Sulphur	Cotton and rayon	Aromatic substrate vatted with sodium sulphide and reoxidized to insoluble sulphur-containing products on fiber	Indeterminate structures
Vat	Cotton, rayon, wool	Water insoluble dyes solubilized by reducing with sodium hydrogen sulphite, then exhausted on fiber and reoxidized	Anthraquinone (including polycyclic quinones) and indigoids

Chemical classification of heavy metals using the periodic table may divide metallic elements into four broad categories: s-block, p-block, d-block transition, and f-block (lanthanides and actinides) (Duffus 2002). Table 2.3 lists the classification of metal ions according to the Lewis acid classification (Da Silva and Williams 2001) which indicates the formation of bonding in metal complexes. Another way of presenting the classification of heavy metal ions is based on their toxicity efficacy towards humans and aquatic biota which is shown in Table 2.4.

Table 2.3: Class A and Class B metals adopted from (Da Silva and Williams 2001)

Class A (hard) metals
Lewis acids (electron acceptors) of small size and low polarizability (deformability of the electron sheath or hardness) Li, Be, Na, Mg, Al, K, Ca, Sc, Ti, Fe(III), Rb, Sr ,Y, Zr, Cs, Ba, La, Hf, Fr, Ra, Ac, Th.
Class B (soft) metals
Lewis acids (electron acceptors) of large size and high polarizability (softness) Cu(I), Pd, Ag, Cd, Ir, Pt, Au, Hg, Ti, Pb(II).
Borderline (intermediate) metals
V, Cr, Mn, Fe(II), Co, Ni, Cu(II), Zn, Rh, Pb(IV), Sn.

Table 2.4: Classification of inorganic heavy metals based on their toxicity sequences on a range of organisms (Nieboer and Richardson 1980)

Organisms	***Sequence[a]***	***Reference***
Algae[c] Chlorella vulgaris	Hg>Cu>Cd>Fe>Cr>Zn>Ni>Co>Mn	(Sakaguchi, Horikoshi et al. 1977)
Fungi[d]	Ag>Hg>Cu>Cd>Cr>Ni>Pb>Co> Zn>Fe>Ca	(Khangarot and Ray 1989)
Flowering plant[c] berley	Hg>Pb>Cu>Cd>Cr>Ni>Zn	(Oberlander and Roth 1978)
Protozoa[c] Paramecium	Hg, Pb>Ag>Cu, Cd> Ni, Co> Mn>Zn	(Shaw 1954)
Annelida[c] Neanthes, a polychaete	Hg>Cu>Zn> Pb>Cd	(Reish, Martin et al. 1976)
Mammalia[b'c] rat, mouse, rabbit	Ag, Hg, TI, Cd>Cu, Pb, Co, Sn, Be > In, Ba > Mn, Zn, N i, Fe, Cr>Y, La>Sr, Sc>Cs, Li, AI	(Venugopal and Luckey 1975)

[a] In this table the atomic symbols represent tripositive ions for In, AI, Cr, La, Y, Sc and Au; dipositive ions for Ni, Hg, Cu, Pb, Cd, Zn, Fe, Sn, Co, Mn, Mg, Ba, Be, Sr and Ca and monopositive ions for Ag, TI, Cs, Li, H, Na and K.

[b] Based upon a sequence synthesised from data on lethal doses (LD or LD_{50}) to small mammals administered iv, ip, sc or orally. The data were abstracted from (Venugopal and Luckey 1975).

[c] In these sequences the metal concentrations resulting in toxicity were expressed on a molar basis and this accounts for any discrepancies with the originally reported sequences. Metals administered as oxo anions were omitted.

[d] Concentration units were unavailable.

2.3 Treatment Methods Available for Organic and Inorganic Removal from Wastewater

Environmental contamination resulting from the emission of effluents from industries is a global problem, therefore different methods of effluents treatment have been used in an attempt to minimize the problems resulted from this contamination. Coagulation, foam flotation, precipitation, ozonation, ion exchange, filtration, solvent extraction, electrolysis, chemical oxidation, membrane separation technology, liquid-liquid extraction and adsorption on activated carbon have been used for the removal of dye contaminants from wastewater (Bhatnagar and Minocha 2006, Gupta 2009, Vakili, Rafatullah et al. 2014). The technologies can be divided into three categories: physical, chemical and biological. The advantages and disadvantages for the removal of dyes and heavy metals (organic and inorganic) contaminated effluents from industrial wastewater applied into different industrial units which are summarized in Table 2.5 and Table 2.6 respectively.

Table 2.5: Principal advantages and limitations of dyes removal methods adapted from (Carmen and Daniela 2012, Afroze and Sen 2015)

Treatment methodology	***Advantages***	***Limitations***
	Physico-chemical treatments	
Precipitation, Coagulation-flocculation	Short detention time and low capital costs. Relatively good removal efficiencies.	Agglomerates separation and treatment. Selected operating condition
Electrokinetic coagulation	Economically feasible.	High sludge production
Ozonation	Effective for azo dye removal. Applied in gaseous state: no alteration of volume.	Not suitable for dispersed dyes. Releases aromatic dyes. Short half-life of ozone (20 min)
Oxidation with NaOCl	Low temperature requirement. Initiates and accelerates azobond cleavage	Cost intensive process. Release of aromatic amines
Adsorption with solid adsorbents such as:		
Activated carbon	Economically attractive. Good removal efficiency of wide variety of dyes.	Very expensive; cost intensive regeneration process
Peat	Effective adsorbent due to cellular structure. No activation required.	Surface area is lower than activated carbon
Industrial solid wastes such as coal ashes, red mud, etc.	Economically attractive. Good removal efficiency.	Slow kinetics. Specific surface area for adsorption is lower than activated carbon
Wood chips/ Wood sawdust	Effective adsorbent due to cellular structure. Economically attractive. Good adsorption capacity for acid dyes.	Long retention time and huge quantities are required
Silica gels	Effective for basic dyes	Side reactions prevent commercial application
Ion exchange	Regeneration with low loss of adsorbents.	Specific and effective for dyes removal and softening of water
	Biological treatments	
Aerobic process	Partial or complete decolourization for all classes of dyes.	Expensive treatment
Anaerobic process	Resistant to wide variety of complex coloured compounds. Bio gas produced is used for	Longer acclimatization phase

	stream generation.	
Microbial processes	Good removal efficiency for low volumes and concentrations. Very effective for specific colour removal.	Culture maintenance is cost intensive. Cannot cope up with large volumes of wastewater.
	Advanced separation treatments	
Electrochemical oxidation	No additional chemicals required and the end products are non-dangerous/hazardous.	High cost
Membrane filtration	Removes all dye types; recovery and reuse of chemicals and water.	High running cost. Concentrated sludge production. Dissolved solids are not separated in this process.
Photo catalysis	Process carried out at ambient conditions. Inputs are no toxic and inexpensive. Complete mineralization with shorter detention times.	Effective for small amount of coloured compounds. Expensive process.
Sonication	Simplicity in use. Very effective in integrated systems.	Relatively new method and awaiting full scale application.
Irradiation	Effective oxidation at lab scale	Requires a lot of dissolved oxygen (O_2)
Photochemical process	No sludge production	Formation of by-products
Redox mediators	Easily available and enhances the process by increasing. electron transfer efficiency	Concentration of redox mediator may give antagonistic effect. Also depends on biological activity of the system.
Engineered wetland systems	Cost effective technology and can be operated with huge volumes of wastewater	High initial installation cost. Requires expertise and managing during monsoon becomes difficult.

Table 2.6: Current treatment technologies for inorganic heavy metals removal involving physical and/or chemical processes (Kurniawan, Chan et al. 2006, Barakat 2011, Sharma 2014)

Treatment methodology	***Advantages***	***Limitations***
	Physico-chemical treatments	
Oxidation	Rapid process for toxic pollutants removal	High energy costs and formation of by-products
Ion exchange	No sludge generation, less time consuming, high regeneration	Adsorbent requires regeneration or disposal, not all ion-exchange resins are suitable for metal removal, high capital cost
Membrane filtration (Reverse osmosis, ultrafiltration, nanofiltration)	Low solid waste generation, low chemical consumption, small space required, high separation selectivity	Limited flow rate, high initial cost, high maintenance and operation, membrane fouling
Adsorption	Low cost, easy operating conditions, having wide pH range, high capacity, fast kinetics, insensitivity to toxic pollutants	Low selectivity, production of waste products, physical or chemical activation to improve its sorption capacity
Coagulation/flocculation	Good sludge settling, economically feasible	High sludge production and formation of large particles
Electrochemical treatment	Rapid process and effective for certain metal ions	High energy costs and formation of by-products
Ozonation	Applied in gaseous state: alteration of volume	Short half-life
Photochemical irradiation	No sludge production, effective at lab scale	Formation of by-products, requires a lot of dissolved O_2
Electrokinetic coagulation	Economically feasible	High sludge production
Fentons reagents	Effective and capable of treating variety of wastes and no energy input necessary to activate hydrogen peroxide	Sludge generation
Chemical precipitation	Low capital cost, simple operation	Sludge generation, extra operational cost for sludge disposal
Photo catalysis	Removal of metals and organic pollutant simultaneously, less harmful by-products	Long duration time, limited applications
Dissolved air flotation	Low cost, shorter hydraulic retention time	Subsequent treatments are required to improve the removal efficiency of heavy metals

2.3.1 Physical Methods

Different physical methods are widely used in wastewater treatment applications such as sedimentation, ion exchange, membrane filtration techniques and adsorption. ***Sedimentation*** is the basic form of industrial-wastewater treatment facilities with a number of process options including chemical flocculants, sedimentation basins and clarifiers (Cheremisinoff 2001). ***Filtration technologies*** of drinking water and wastewater treatment applications include microfiltration, ultrafiltration, nanofiltration, and reverse osmosis. This process with different types of membranes shows great promise for their high efficiency, easy operation and space saving for dyes and heavy metals removal (Fu and Wang 2011). However, application of these processes to only smaller wastewater flow rate, high cost of membrane system, high working pressure to push the wastewater flow through membrane, inability to reduce dissolved solid content and relatively shorter life time of membrane due to frequent clogging on the membrane pores limit its potential as a sustainable separation system for effluent treatment (Pang and Abdullah 2013). ***Ion exchange*** have been widely used to remove heavy metals from wastewater due to their many advantages, such as high treatment capacity, high removal efficiency and fast kinetics (Kang, Lee et al. 2004). Ion-exchange resin, either synthetic or natural solid resin, has the specific ability to exchange its cations with the metals in the wastewater and synthetic resins are commonly preferred as they are effective to nearly remove the heavy metals from the solution (Fu and Wang 2011). The main drawback for the success of ion exchange method in treating dye bearing effluents is mainly due to its ineffectiveness in removing several types of dyes. Ion exchange is a good method to separate soluble cationic, anionic and toxic dyes although the high capital cost associated with the process limit its use (Dawood and Sen 2013). Meanwhile, the advantages of ion exchange treatment method include the recovery of adsorbent upon successful regeneration and reclamation of solvent after use (Pang and Abdullah 2013).

2.3.2 Chemical Methods

Chemical methods include coagulation or flocculation combined with flotation and filtration, precipitation-flocculation with $Fe^{2+}/Ca(OH)_2$, electro-flotation, electro-kinetic coagulation, conventional oxidation methods by oxidizing agents, irradiation or electrochemical processes. ***Chemical Oxidation*** is one of the traditional methods

where oxidizing agents are used for the removal of organic/inorganics from wastewater without the need of microorganism for the reactions to proceed. ***Advanced Oxidation Processes*** (AOPs) are the processes involving simultaneous use of more than one oxidation processes, since sometimes a single oxidation system is not sufficient for the total decomposition of dyes (Gupta 2009). AOPs include techniques as Fenton's reagent oxidation, ozonation, ultra violet (UV) photolysis and sonolysis. ***Ozonation*** by ozone, a powerful oxidant with a relatively short life time, is capable of degrading chlorinated hydrocarbons, phenols, pesticides and aromatic hydrocarbons (Robinson, McMullan et al. 2001). One major advantage is that ozone can be applied in its gaseous state and therefore does not increase the volume of wastewater and sludge. Ozone reacts with most organic and several inorganic molecules.The drawbacks of this method include pre-treatment of raw textile wastewater before the ozonation process to prevent excessive consumption of ozone by other pollutants (such as inorganic salts, surfactants) that are present in the water (Pang and Abdullah 2013). ***Electrokinetic coagulation*** (EC) is one of the most important physio-chemical processes used in wastewater treatment. EC technique uses a direct current source between metal electrodes such as aluminium and iron immersed in water effluent to cause the dissolution of metal plates into wastewater (Aoudj, Khelifa et al. 2010, Fu and Wang 2011). EC process provides a simple, reliable and low cost method for the removal of dyes such as Direct Red 81 from wastewater (Aoudj, Khelifa et al. 2010), Reactive Blue 140 (Phalakornkule, Polgumhang et al. 2010) and Disperse Red (Merzouk, Gourich et al. 2011). Heidmann and Calmano (Heidmann and Calmano 2008) studied the performance of an EC system with aluminium electrodes for removing Zn^{2+}, Cu^{2+}, Ni^{2+}, Ag^{+} and $Cr_2O_7^{2-}$. The main advantages of electro coagulation in comparison to other conventional technique such as chemical coagulation are the compactness of equipment used and no generation of secondary pollution (Phalakornkule, Polgumhang et al. 2010). The disadvantages associated with this process are high amount of sludge production and the need for further treatment by flocculation and filtration (Dawood and Sen 2013).

2.3.3 Biological Methods

Biological treatment may involve the use of microorganisms in either aerobic or anaerobic conditions to degrade organic dyes and dilute heavy metal contaminations.

The most common biological treatment approaches are trickling filter and activated sludge due to their simplicity and lower treatment cost as compared to some physical and chemical methods (You and Teng 2009). The process can be aerobic (in presence of oxygen), anaerobic (without oxygen) or combined aerobic-anaerobic. The possible microorganisms used for biodegradation of dyes and to treat dilute heavy metal wastewater are microbial biomass, e.g. fungi, bacteria, yeasts; algal biomass, and non-living biomass such as shrimp, krill, squid, crab shell, etc. (Fu and Wang 2011, Pang and Abdullah 2013).

Aerobic treatment Bacteria and fungi are the most common microorganisms used in the decolourization of dyes under aerobic conditions. In many reported works, microbial removal of metal ions from wastewater has been indicated as being highly effective (Fu and Wang 2011). Removal of heavy metals in aqueous solutions by bacteria includes *Bacillus cereus* (Sinha, Pant et al. 2012), *Micrococcus luteus* (Puyen, Villagrasa et al. 2012), *Lysinibacillus sp.* (Prithviraj, Deboleena et al. 2014), etc. Fungi and yeasts are easy to grow, produce high yields of biomass and at the same time can be manipulated genetically and morphologically. The use of fungi in the removal of dyes and metal ions is more effective compared to bacteria and algae such as removal of cationic dye Methylene blue by Dead macro fungi (Maurya, Mittal et al. 2006), Acid blue 29 by living fungus (Fu and Viraraghavan 2001), Direct red 28 and Disperse red 1 by *Aspergillus niger* (Fu and Viraraghavan 2002), removal of Zn^{2+}, Cd^{2+}, Hg^{2+} metal ions by *Lentinus edodes* fungi (Bayramoğlu and Arıca 2008), etc. But the problem associated with aerobic biological degradation are such as sludge bulking, rising sludge, and floc formation (Pang and Abdullah 2013) which are undesirable and could reduce the efficiency of organic/inorganic biodegradation in many processes.

Anaerobic treatment The potential of anaerobic treatment applications for the degradation of a wide variety of synthetic dyes has been well demonstrated and established by researchers such as removal of Methyl orange (MO) and Naphthol green B (NGB) by Shewanella oneidensis MR-1 (Cao, Xiao et al. 2013) and Reactive red by Halomonas variabilis and Halomonas glaciei (Balamurugan, Thirumarimurugan et al. 2011). The disadvantages of this process include requirement of long acclimatization time because of slow growth rate of microorganism, production of toxic by-products and the need for further treatment

under aerobic conditions. Thus a combination of anaerobic and aerobic process is recommended for the biodegradation of textile dye. However, the advantage of this treatment method is that methane gas is generated from the anaerobic digestion process and can be utilized as renewable energy (Pang and Abdullah 2013).

2.3.4 Combined Methods

Combined methods are considered rather than using physical, chemical or biological technologies separately; two or three treatment methods may be used together for treating water pollutants. Several researchers have been working on combined methods for last several years as reported in literature. Chen et al. (Chen, Ding et al. 2013) reported that a combination of adsorption, condensation, and electrochemical degradation techniques can achieve a satisfactory outcome for the degradation of low-concentration azo dye-Congo red effluents with large volume. By combining membrane filtration, acid precipitation and cooling crystallization, separation of organic and inorganic compounds from black liquor was investigated by Niemi et al (Niemi, Lahti et al. 2011). Lin and Chang (Lin and Chang 2000) found the combined chemical oxidation and biological treatment to be highly efficient to offer an extractive alternative in dealing with the high variability of pollutant content in the landfill leachate. Rashed (Rashed 2015) investigated the combined effect of photocatalytic degradation and adsorption of the heavy metals Cu^{2+}, Cd^{2+}, Pb^{2+} and Zn^{2+} using glass waste as adsorbent.

2.4 Adsorption

Adsorption is a separation process by which certain components of a fluid phase are attracted to the surface of a solid adsorbent and form attachments via physical or chemical bonds, thus removing the component from the fluid phase (McCabe, Smith et al. 1993, McKay, Guendi et al. 1997). Adsorption processes usually occur in interfacial layers which are regarded as two regions: the surface layer of the adsorbent (often simply called the adsorbent surface) and the adsorption space, in which the enrichment of the adsorbate can occur (Sing 1985). The exact nature of the bonding depends on the details of the species involved, but in general the adsorption process may be classified into two groups: physical and chemical sorption. Depending on the nature of the interactions of ionic species and molecular species

carrying different functional groups may be held to the surface through electrostatic attraction to sites of opposite charge at the surface or physiosorbed due to action of Van der Waals forces or chemisorbed involving strong adsorbate–adsorbent bonding which may lead to attachment of adsorbate molecules at specific functional group on adsorbent surface (Sharma, Kaur et al. 2011). The main physical forces controlling adsorption are Van der Waals forces, hydrogen bonds, polarity, dipole-dipole π-π interaction, etc. (Ali 2010).

Adsorption is a surface phenomenon, which besides being widely used for the removal of organic and inorganic pollutants also has wide applicability in wastewater treatment (Bansal and Goyal 2010). As compared to conventional methods for wastewater treatment, the adsorption process offers the advantages of low operating cost, minimization of the volume of chemical and/or biological sludge to be disposed of, high efficiency in detoxifying very dilute effluents, and no requirement of nutrients (Kratochvil and Volesky 1998, Rafatullah, Sulaiman et al. 2010) . These advantages have served as the primary incentives for developing full-scale adsorption processes to clean up toxic pollutants from industrial effluents using different kinds of natural and synthetic adsorbents, especially if the sorbent is inexpensive and does not require an additional pre-treatment step before its application. At present, the interests in utilization of cheap alternatives have been significantly increased and many attempts have been made by researchers on feasibility of adsorption potential of lignocellulosic materials (either natural substances or agro-industrial wastes and by-products) as economic and eco-friendly options (Abdolali, Guo et al. 2014).

2.4.1 Factors Affecting Adsorption of Organic and Inorganic Ions

Many physico-chemical factors influence the adsorption process and these include; adsorbate/adsorbent interaction, adsorbent surface area and pore structure, chemistry of the surface, nature of the adsorbate, effect of other ions, particle size, pH, temperature, contact time, etc. (Smith, Koonce et al. 1993, Allen and Koumanova 2005, Crini 2006). Thus, the effects of these parameters are to be taken into account. Optimization of such conditions will greatly help in the development of industrial-scale organic/inorganic removal treatment. In this section, some of the leading factors affecting adsorption of dyes and heavy metal ions are therefore discussed:

2.4.1.1 Effect of Solution pH

In wastewater treatment, it is repeatedly reported that pH of the adsorbate (solution) is the first and perhaps the most crucial parameter that plays a vital role on the adsorption capacity by influencing the chemistry of adsorbate and adsorbent in aqueous solution (Kyzas, Siafaka et al. 2015). Initial pH of aqueous solution influences not only site dissociation, but also the solution chemistry of the adsorbate molecules: hydrolysis, complexation by organic and/or inorganic ligands, redox reactions and precipitation are strongly influenced by pH (Ahalya, Chandraprabha et al. 2014). The effect of solution pH on the adsorption can be determined by preparing adsorbent–adsorbate solution with fixed dye/metal concentration and adsorbent dose but with different pH by adding NaOH (1 M) or HCl (1 M) solutions (Salleh, Mahmoud et al. 2011, Yagub, Sen et al. 2014). On the adsorption capacity, the impact of the pH of aqueous solution is significant due to its impact on both the surface binding sites of the adsorbent, concentration of the counter ions on the functional groups of the adsorbent and the degree of ionization of the adsorbate during reaction (Saifuddin and Kumaran 2005, Franca, Oliveira et al. 2009).

Khalid et al. (Khalid, Ngah et al. 2015) studied the effect of solution pH for the removal of Acid Blue 25 dye from aqueous solutions by using Rubber leaf powder (phosphporic acid treated) and noticed that at a pH range from 2 – 10, the maximum dye adsorption was found at pH of 2.0. Pavan et al. (Pavan, Camacho et al. 2014) studied the effect of solution pH on the adsorption of Crystal Violet (CV) by Formosa papaya seed powder and they noticed that at a pH range from 2 to 8, the dye removal percentage was maximum at pH 8. Wu et al. (Wu, Kuo et al. 2015) studied the effect of solution pH for the removal of Lead and Zinc ions from aqueous solutions by using Coffee residues and observed that the maximum adsorption was found at pH of 5.0. Zhao et al. (Zhao, Xiao et al. 2014) reported that adsorption of anionic dye Light Green (LG) onto surfactant modified peanut husk biomass was decreased with increase in solution pH (Fig. 2.1). The compilation of different studies on the effect of solution pH on dyes and heavy metals adsorption is presented in Table 2.7.

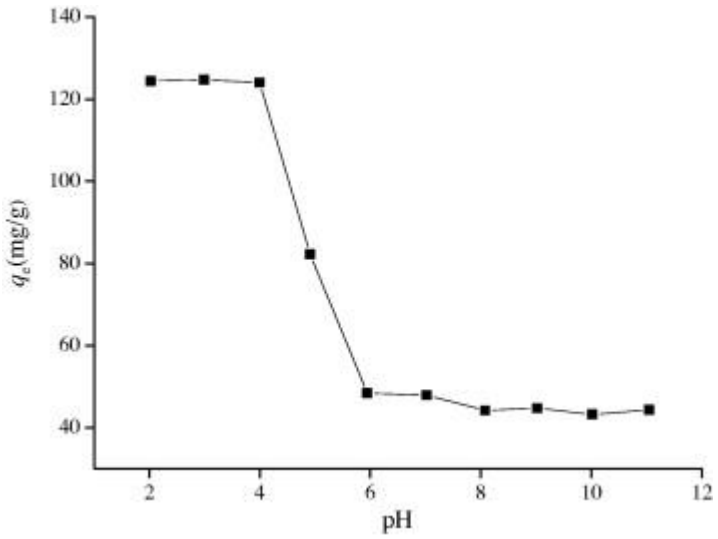

Figure 2.1 Effect of solution pH on Light Green dye adsorption (T = 303 K, C_0 = 100 mg/L) on modified peanut husk (Zhao, Xiao et al. 2014).

Any oxide surface creates a charge (positive or negative) on its surface is proportional to the pH of the solution which surrounds the oxide particles (Allen and Koumanova 2005). The pH at which the surface charge is zero is called the point of zero charge (pHpzc). The point of zero charge (pzc) relates to the adsorption phenomenon and it describes the condition when the electrical charge density on a surface is zero. Therefore the adsorption ability of the surface and the type of surface active centres are indicated by the point of zero charge (pH_{pzc}) (Liu, Yao et al. 2012) for systems where H^+/OH^- are the potential-determining ions. Due to presence of functional groups such as OH^- group, cationic dye adsorption is favoured at $pH>pH_{pzc}$, whereas, anionic dye adsorption is favoured at $pH< pH_{pzc}$ (Tan, Zhang et al. 2012). In order to understand the adsorption mechanism, the point of zero charge (pH_{pzc}) of various adsorbents prepared from agricultural solid wastes was investigated by many researchers (Jain and Jayaram 2010, Saeed, Sharif et al. 2010, Pavan, Camacho et al. 2014). Han et al. (Han, Niu et al. 2012) studied the adsorption of Methylene blue (MB) onto poplar leaf and they found that the zero point of charge (pH_{pzc}) for the poplar leaf was around 5.6, while the maximum adsorption capacity of MB was at pH 9, in other words $pH>pH_{pzc}$. The adsorption of Cu^{2+} onto pine cone powder has been studied by Ofamaja et al. (Ofomaja, Naidoo et al. 2009) and they found that the maximum adsorption capacity of Cu^{2+} was at pH 5.0, while the point of zero charge (pH_{pzc}) for the pine cone powder was 7.49.

Table 2.7: The effect of solution pH on the adsorption of dyes and heavy metal ions by different adsorbents

Adsorbents	*Adsorbates (Dyes and heavy metals)*	*pH range*	*Percentage (%) removal range*	*References*
Rubber leaf (Phosphoric acid treated)	Acid blue 25	2-10	99.34-7.68	(Khalid, Ngah et al. 2015)
Coffee waste	Toluidine blue	2.0-10.5	50-95	(Lafi, ben Fradj et al. 2014)
Formosa papaya seeds	Crystal violet	2.0-8.0	41.3-97.3	(Pavan, Camacho et al. 2014)
Parsley stalks	Methylene blue	2-10	20.72-82.84	(Akkaya and Güzel 2014)
Cucumber peels	Methylene blue	2-10	13.44-77.70	(Akkaya and Güzel 2014)
Potato peel waste	Acid blue 1	2-11	Decrease	(Hoseinzadeh, Samarghandi et al. 2014)
Tobacco stem ash	Methylene blue	2.08-7.93	60-81	(Ghosh and Reddy 2013)
Activated- Carbon	Methylene blue	2-11	Increase	(Kannan and Sundaram 2001)
Fe_2O_3	Acid red 27	1.5-10.5	98-27	(Nassar 2010)
Activated- Rice husk	Acid yellow 36	2-9	80-45	(Imam Maarof, Hameed et al. 2003)
Spent coffee grounds	Methylene blue	3-11	81-95	(Franca, Oliveira et al. 2009)

Tomato leaf powder	Ni^{2+}	2-5.5	Increase	(Gutha, Munagapati et al. 2015)
Rice husk	Zn^{2+}	4-8	Increase	(Galletti, Russo et al. 2015)
Modified orange peel	Pb^{2+}	2.5-6	93.2-99.4	(Feng and Guo 2012)
Pine cone (base modified)	Cu^{2+}	2-5	Increase	(Ofomaja and Naidoo 2011)
Papaya wood	Cu^{2+}	2-5	17.3-97.3	(Saeed, Akhter et al. 2005)

2.4.1.2 Effect of Initial Adsorbate Concentration

The adsorptive dye/metal removal mechanism is of great significance for developing sorbent-based water technology and is particularly dependent on the initial dyes and heavy metal ions concentration. The effect of initial adsorbate (dye and heavy metal ions) concentration depends on the immediate relation between the concentration of the adsorbate and the available sites on an adsorbent surface. The effect of initial adsorbate concentration can be studied by preparing adsorbent–adsorbate solution with fixed adsorbent dose and different initial dyes or heavy metal ions concentration for different time intervals and shaken until equilibrium (Salleh, Mahmoud et al. 2011, Yagub, Sen et al. 2014).

In adsorbent-adsorbate solution, the initial organic/inorganic adsorbate concentration provides the driving force to overcome the resistance to the mass transfer of adsorbate between the aqueous and the solid phase. At low concentrations, adsorption sites take up the available adsorbates more quickly. However, at higher concentrations, adsorbate needs to diffuse to the sorbent surface by intra-particle diffusion. Also, the steric repulsion between the solute molecules may slow down the adsorption process (Hameed 2008). However, after the initial adsorption stages, a competition occurs between adsorbate molecules for the adsorption sites on the surface of adsorbent, resulting in a decrease of adsorption rate (Pavan, Camacho et al. 2014). Therefore, in general, it is evident that the higher percentage of organic/inorganic (dye and heavy metals) removal decreases with an increase in the

initial solute concentration. However, the amount of dye or heavy metals adsorbed per unit adsorbent mass increase with increase in initial adsorbate concentration due to the decrease in resistance to the uptake of solute from aqueous solution (Yagub, Sen et al. 2014, Wang, Chen et al. 2015).

Imaga et al. (Imaga, Abia et al. 2015) studied the effect of initial Zn^{2+} metal concentration on raw Sorghum hulls and found that the percentage of metal ions removal decreased from 50.98% to 12.81% with an initial concentration range of 10 – 50 mg/L at 106 µm hull particle size. Senthil Kumar et al. (Senthil Kumar, Palaniyappan et al. 2014) studied the effect of initial dye concentration on the adsorption of Methylene Blue (MB) dye by Raw mango seeds and they reported that at an initial dye concentration range from 50 mg/L to 250 mg/L, the percentage of dye removal was decreased from 99.136% to 92.523%. Low et al. (Low, Teng et al. 2013) studied the effect of initial dye concentration on the adsorption of methylene blue (MB) dye by modified bagasse and they reported that at an initial dye concentration range from 100 mg/L to 300 mg/L, the percentage of dye removal was decreased from 99.94% to 86.59%. Zhang et al. (Zhang, Zhou et al. 2012) studied the adsorption of Methyl Orange by Chitosan/Alumina interface and it was found that when the Methyl Orange concentration increase from 20 mg/L to 400 mg/L, while the percentage of dye removal decreased from 99.53% to 83.55% with the same MB concentration range. Fig. 2.2 showed that adsorption of Cu^{2+} by chemically treated Tomato waste decreased with increase in initial metal ion concentration (Yargıç, Şahin et al. 2015). Table 2.8 presented the results of various reported studies on the of initial dye concentration effect on dye adsorption.

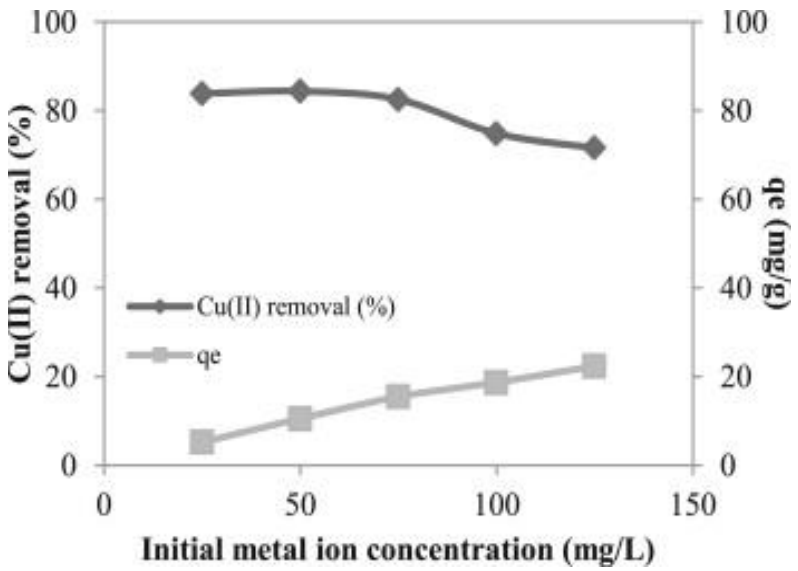

Figure 2.2 Effect of initial Cu(II) concentration onto acid treated Tomato waste (pH: 8, biosorbent dosage: 0.2 g/50 mL, temperature: 293 K, contact time: 1 h) (Yargıç, Şahin et al. 2015).

Table 2.8: The results of various reported studies on the initial dye concentration effect on dyes and heavy metals adsorption by various adsorbents

Adsorbents	*Adsorbates (Dyes and heavy metals)*	*Initial concentration range (mg/L)*	*Percentage (%) removal range*	*References*
Activated carbon (modified from egg shell waste)	Acid blue 25, Zn^{2+}, Ni^{2+}, Cd^{2+}	20-500	Increase	(Tovar-Gómez, del Rosario Moreno-Virgen
Olive pomace	Basic green 4	20-100	96.9-98	(Koçer and Acemioğlu 2015)
Tomato seeds	Acid Red 14	50-150	89-85	(Najafi, Pajootan et al. 2015)
Mango seeds	Methylene blue	50-250	99.14-92.52	(Senthil Kumar, Palaniyappan et al. 2014)
Kaolin	Methylene	10-40	90-62	(Tehrani-Bagha,

	blue			Nikkar et al. 2011)
Oil palm tree sawdust (tartaric acid modified)	Malachite green	100-300	99.97-83.46	(Low, Teng et al. 2013)
Pine leaves	Methylene blue	10-90	96-41	(Yagub, Sen et al. 2012)
Sugarcane bagasse	Basic Blue 9	250-500	94-55.5	(Zhang, O'Hara et al. 2013)
Modified Sawdust	Methylene blue	25-500	91.2-66.3	(Zou, Bai et al. 2013)
Nanostructure TiO_2	Reactive blue 21	32-56	10.93-8.28	(Srivastava, Goyal et al. 2013)
Modified wheat residue	Cr(VI)	150-500	Increase	(Chen, Yue et al. 2010)
ZnO	Malachite green	10-40	83-73	(Kumar, Muralidhara et al. 2013)
Magnetite nanorods	Fe^{2+}, Pb^{2+}, Zn^{2+}	10-200	Decrease	(Karami 2013)
Raw pomegranate peel	Pb^{2+}, Cu^{2+}	10-80	Decrease	(El-Ashtoukhy, Amin et al. 2008)

2.4.1.3 Effect of Solution Temperature

Temperature is an important parameter for adsorption processes. Changing temperature changes the equilibrium capacity of the adsorbent for a particular adsorbate. To study the effect of temperature on the adsorption process, it can be carried out by preparing adsorbent–adsorbate solution with fixed adsorbate concentration and adsorbent dose but with different temperature (Yagub, Sen et al. 2014).

Increasing the temperature is known to increase the rate of diffusion of the adsorbate molecules across the external boundary layer and in the internal pores of the adsorbent particle, owing to the decrease in the viscosity of the solution (Hameed

and Ahmad 2009). If the amount of adsorption increases with increasing temperature then the adsorption is an endothermic process. This may be a result of increase in the mobility of adsorbate (dye or heavy metals) molecule with an increase in their kinetic energy, as well as an enhanced rate of intraparticle diffusion of sorbate with the rise in temperature (Bouguettoucha, Chebli et al. 2015). An increasing number of molecules may also acquire sufficient energy to undergo an interaction with active sites at the surface (Hameed and Ahmad 2009, Bouguettoucha, Chebli et al. 2015). Decrease of adsorption capacity with increasing temperature indicates that the adsorption is an exothermic process. This may be due to increasing temperature causing the decrease of adsorptive forces between the organic or inorganic adsorbate species and the active sites on the adsorbent surface as a result of decreasing the amount of adsorption (Salleh, Mahmoud et al. 2011). Öztürk and Malkoc (Öztürk and Malkoc 2015) reported that the adsorption capacity of waste manure ash for the removal of Basic yellow 2 increased from 60.6 % to 89.09% with the increase in solution temperature from 25^0C to 45^0C. Taşar et al. (Taşar, Kaya et al. 2014) observed that the adsorption capacity of Peanut shell for the removal of heavy metal Pb^{2+} ions decreased with increase in temperature (Fig. 2.3). Table 2.9 showed previous studies on the effect of temperature on the dyes and heavy metals adsorption by various adsorbents.

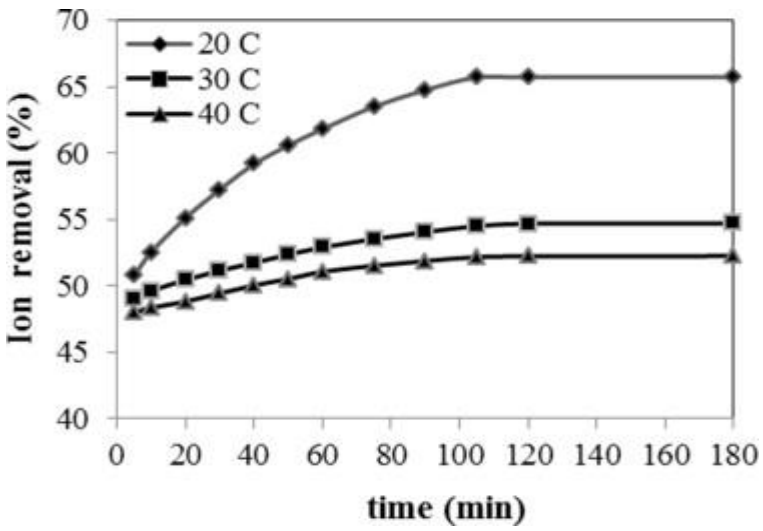

Figure 2.3 Effect of temperature on the adsorption of Pb(II) by peanut shell (peanut shell concentration: 2 g/L; initial Pb(II) concentration: 100 ppm; pH: 5.5 ± 0.02; temperature: 20, 30, 40°C; contact time 180 min) (Taşar, Kaya et al. 2014)

Table 2.9: Influence of solution temperature on the adsorption of dyes and heavy metals using various adsorbents

Adsorbents	*Adsorbates (Dyes and heavy metals)*	*Temperature range (°K)*	*Type of process*	*References*
Chitosan/bentonite	Methylene blue	298-313	Endothermic	(Bulut and Karaer 2015)
Waste manure ash	Basic yellow 2	298-318	Endothermic	(Öztürk and Malkoc 2015)
Peanut hull	Novacorn golden yellow	303-333	Exothermic	(Nawaz, Bhatti et al. 2014)
Modified magnetic corn straw	Methylene blue	303-323	Exothermic	(Zhao, Xia et al. 2014)
Pomelo (*Citrus grandis*) peel	Reactive blue 114	303-323	Endothermic	(Argun, Güclü et al. 2014)
Rice husk (nitric acid treated)	Malachite green	303-333	Endothermic	(Ramaraju, Manoj Kumar Reddy et al. 2013)
Saw dust	Acid Yellow 23	298-318	Endothermic	(Banerjee and Chattopadhyaya 2013)
Sugarcane bagasse	Rhodamine B	303-323	Endothermic	(Zhang, O'Hara et al. 2013)
Activated clay	Methyl orange	293-303	Endothermic	(Ma, Shen et al. 2013)
Residue sludge	Congo Red	288-323	Endothermic	(Attallah, Ahmed et al. 2013)

Activated Bamboo waste	Reactive Black 5	303-323	Endothermic	(Ahmad, Idris et al. 2013)
Activated carbon	Methylene blue	308-333	Endothermic	(Kavitha and Namasivayam 2007)
Bentonite	Cd^{2+}, Cr^{2+}	293.15-343.15	Exothermic	(Barkat, Chegrouche et al. 2014)
Biochar (derived from tomato waste)	Co^{2+}	293-313	Endothermic	(Önal, Özbay et al. 2014)
Fe_2O_3 nanoparticle	Pb^{2+}	298-318	Endothermic	(Ahmadi, Heidarzadeh et al. 2014)
Chlorella vulgaris algae	Cd^{2+}	293-323	Exothermic	(Aksu 2001)

2.4.1.4 Effect of Adsorbent Dosage

Adsorbent dosage is also an important parameter for the optimisation of adsorption system. The effect of the amount of adsorbent on the adsorption process can be determined by preparing adsorbent–adsorbate solution with different amount of adsorbents added to fixed initial organic/inorganic adsorbate concentration and fixed initial solution pH then shaken together until equilibrium time (Yagub, Sen et al. 2014). Generally the percentage removal of adsorbate organic dyes and inorganic heavy metals increases with increasing adsorbent dosage. This higher percentage removal at higher adsorbent dosage is due to the increase in surface area resulting from the increase in adsorbent mass, thus increasing the number of active adsorption sites for adsorption.

Hussain et al. (Hussin, Talib et al. 2015) studied the adsorption of Methylene blue onto NaOH modified Durian leaf powder at different amount of adsorbent dose and

they concluded that the percentage of adsorption increased by increasing the amount of adsorbent using the treated leaf. Pandharipanda et al. (Pandharipande and Kalnake 2013) studied the effect of adsorbent dose (0.0025-0.01 gm/10 mL) on the removal of Cr(VI) by tamarind fruit shell and they found 50% to 85% removal percentage of Cr(VI) with increasing adsorbent dose. Feng et al. (Feng, Zhou et al. 2012) studied the effect of adsorbent dose on the removal of Methylene blue dye by Swede rape straw and they observed dye removal percentage increased with decreased adsorbent dose. Fig. 2.4 presented the effects of doses on the removal of Basic Green 4 (BG4) dye using Olive Pomace (Koçer and Acemioğlu 2015). The compilation results evaluated from many research studies on the effect of adsorbent dosage on organic dyes and inorganic heavy metals adsorption by various adsorbents are presented in Table 2.10.

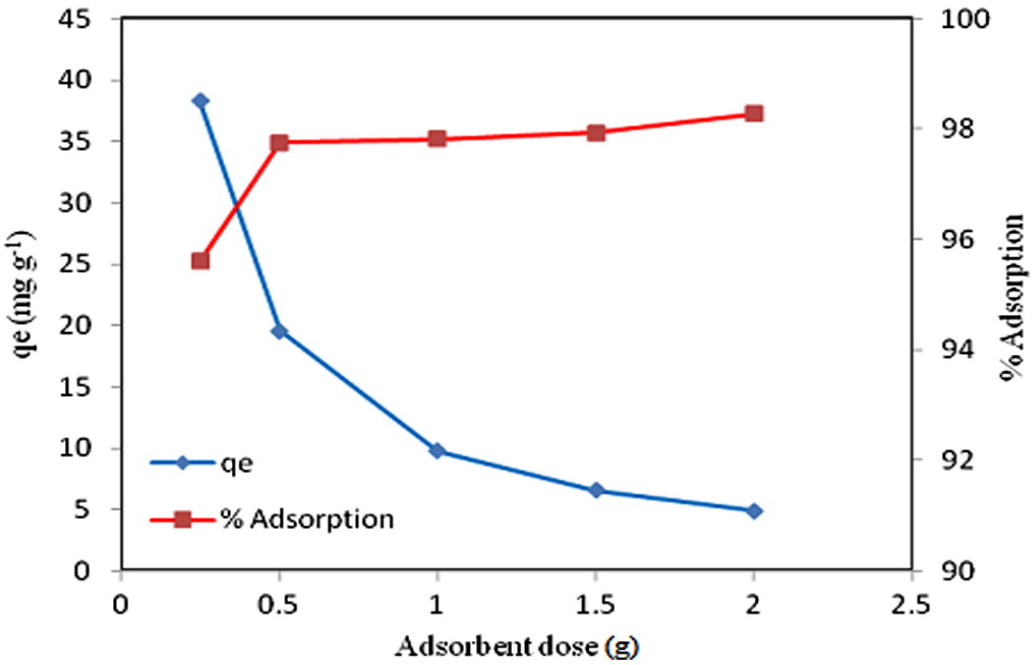

Figure 2.4 Effect of adsorbent dose on the adsorption of Basic Green 4 on Olive Pomace at equilibrium time (Koçer and Acemioğlu 2015)

Table 2.10: The effect of adsorbent dosage on the percentage of organic dyes and inorganic heavy metals removal using several adsorbents

Adsorbents	*Adsorbates (Dyes and heavy metals)*	*Adsorbent dosage*	*Percentage (%) removal range*	*References*
Activated carbon	Rhodamine B	2.5-50 mg	Increase	(Maneerung, Liew et al. 2016)
Watermelon seed hull	Methylene Blue	0.1-1.0 g/50 mL	27.71-97.65	(Akkaya and Güzel 2014)
Modified sawdust	Methylene blue	1.5-5 g	34.4-96.6	(Zou, Bai et al. 2013)
Modified Mango Seed	Methylene blue	0.1-1.2 g	99.8-79	(Senthil Kumar, Palaniyappan et al. 2013)
Tea waste	Acid orange 7	2-20 $g.L^{-1}$	90-99	(Khosla, Kaur et al. 2013)
Chitosan/Alumina composite	Methyl orange	1-12 $g.\ L^{-1}$	92.84-99.23	(Zhang, Zhou et al. 2012)
Loquat seed	Reactive black 5	5-30 $g.L^{-1}$	83.52-90.36	(Handan 2011)
Papaya Seeds	Methylene blue	0.05-1.0 g	43.6-80	(Hameed 2009)
Treated saw dust	Brilliant Green	1-30 $g.L^{-1}$	61-99.9	(Mane and Babu 2011)
Modified Alumina	Crystal violet	5-20 $g.L^{-1}$	58-99	(Adak, Bandyopadhyay et al. 2005)
Rice hull	Reactive Orange 16	0.02-0.08 g	21.7-56.2	(Ong, Lee et al. 2007)
Activated carbon (sulphurised)	Zn^{2+}	0.5-8 $g.L^{-1}$	Increase	(Krishnan, Sreejalekshmi et al. 2016)
Iron Oxide	Ni^{2+}	0.1-0.5 g	Increase	(Adolphe, Merlain et al. 2015)
Sugarcane bagasse (sulphuric acid treated)	Cu^{2+}	0.5-2 gm/100 mL	Increase	(Rana, Shah et al. 2014)

Tamarind fruit shell	Ni^{2+}	0.01-0.08 gm/10 mL	20-90	(Pandharipande and Kalnake 2013)
Modified wheat residue	Cr(VI)	0.2-1 $g.L^{-1}$	49-97	(Chen, Yue et al. 2010)

2.4.1.5 Effect of Ionic Strength

Industrial wastes and natural water often contain dissolved salts in a wide range of concentrations depending on the source and the quality of water. Presence of electrolytes in solution strongly influences interfacial potential, compete with adsorbate ions for binding sites on the sorbent which affect the sorption of adsorbate (dye/heavy metal ions) and thus influences adsorption process. The wastewater containing organic and inorganic materials has commonly higher salt concentration; therefore ionic strength effect is of some importance in dye/heavy metal ions adsorption onto adsorbents. The effect of ionic strength on adsorption can be carried out by adding different doses of salts (normally NaCl) to the adsorbent–adsorbate solution and shaking up to equilibrium time (Bharathi and Ramesh 2013). Generally, the removal efficiency of adsorbent decreases with increase in salt (NaCl) concentrations. This behaviour is attributed to the competitive effect between adsorbent ions and Na^{+} for the limited active sites available during the adsorption process (Guechi and Hamdaoui 2011). This implied that the mechanism is mainly ion exchange and the activity of adsorption sites reduce as the salt concentration increases (Ren, Xiao et al. 2015). Additionally, the electrostatic interaction between sorbent and sorbate may be screened by Na^{+}, and the higher ionic strength affects the activity coefficient of adsorbents (Wang, Yuan et al. 2014). The increase in salt concentration changes the equilibrium constant between the interface and the bulk of the liquid ultimately affects adsorption. Further, percentage removal efficiency by dye adsorption with various salt concentrations is due to the change in diffuse double layer thickness of Gouy-Chapman adsorption model and hence change in electrostatic force of attraction. Theoretically, when the electrostatic forces between the adsorbent surface and adsorbate ions are attractive, an increase in ionic strength will decrease the adsorption capacity. Conversely, when the electrostatic attraction is repulsive, an increase in ionic strength will increase adsorption (Bharathi and

Ramesh 2013). This behaviour may be due to dye dimerization in solution or formation of dye aggregation induced by the effect of salt ions which is known as “salting-out-effect” (Kuo, Wu et al. 2008, Fedoseeva, Fita et al. 2010). This phenomenon comprises of two facts: (i) reduction of dye solubility due to bulk phase addition of salts and (ii) stimulate the MB adsorption at the interface by changing the equilibrium constant between adsorbed dye molecules at interface and those being dissolved in bulk phase (Fedoseeva, Fita et al. 2010). Basically, various types of short range forces such as Van der Waals force, dipole-dipole and ion-dipole force increased with salt concentration during dye dimerization (Fedoseeva, Fita et al. 2010). On the other hand, the trend of decreasing adsorption for the removal of metal ions in the presence of monovalent salt and further significant reduction of the metal removal efficiency with increasing salt concentration is due to the presence of ionic strength which could be attributed to the competitive effect between metal ions and cations from the salt (Na^+) for the same binding sites available on the adsorbent surface for the sorption process. Another reason behind this may be the increase in salt concentration (Na^+) changes the equilibrium constant between the interface and the bulk of the liquid ultimately influencing adsorption. Additionally, an increase in ionic strength will decrease the adsorption capacity in the system if the electrostatic forces between the adsorbent surface and adsorbate ions were attractive, and vice versa (Yang, Lin et al. 2014). The reported studies on the effect of ionic strength on the percentage of dyes and heavy metals removal using various materials as adsorbents are shown in Table 2.11. Demirbaş and Alkan (Demirbaş and Alkan 2015) studied the effect of ionic strength on the removal of Maxilon Blue 5G (MB-5G) using perlite (Fig. 2.5).

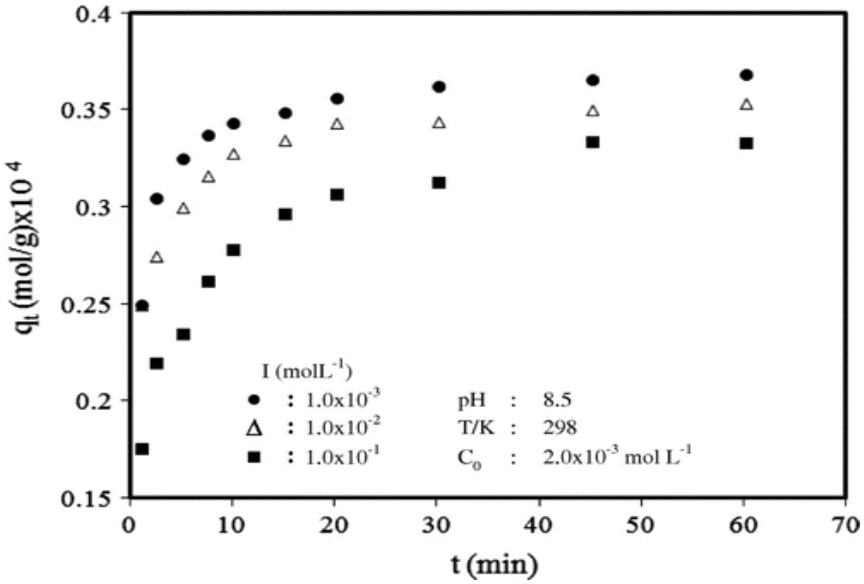

Figure 2.5 The effect of ionic strength (NaCl) to the adsorption rate of MB-5G on expanded perlite (Demirbaş and Alkan 2015)

Table 2.11: The results of various reported studies on the effect of ionic strength on dyes and heavy metals adsorption by various adsorbents

Adsorbents	***Adsorbates (Dyes and heavy metals)***	***Initial salt (NaCl) concentration range (mg/L)***	***Percentage (%) removal range***	***References***
Eucalyptus *sheathiana* bark	Methylene blue	100-300	58.78-69.92	(Afroze, Sen et al. 2016)
Cinnamomum camphora sawdust	Malachite green	0-0.05	89.21-64.75	(Wang, Yuan et al. 2014)
Modified peanut husk	Light green	0-0.1	decrease	(Zhao, Xiao et al. 2014)
Pirina (treated with nitric acid)	Remazon brilliant blue	0.05-0.3	96.45-86.15	(Dağdelen, Acemioğlu et al. 2014)
Pleurotus ostreatus	Malachite green	0.05-0.2 M	87.22-49.01	(Chen, Deng et al. 2014)
Modified breadnut peel	Malachite green	0.0-1.0 M (KNO_3)	decrease	(Chieng, Lim et al. 2015)

Modified phoenix tree leaves	Crystal violet	0.0-0.1 M	decrease	(Ren, Xiao et al. 2015)
Lotus leaf	Malachite Green	0-0.2 M	81.7-62.5	(Han, Yuan et al. 2014)
Pine cone	Methylene blue	0-200	decrease	(Sen, Afroze et al. 2011)
Potato peel	Malachite green	0-2.0 g	decrease	(Guechi and Hamdaoui 2011)
Activated Carbon	CN^-	0.01-0.1 M (KNO_3)	decrease	(Stavropoulos, Skodras et al. 2015)
Eucalyptus bark	Cd^{2+}	0-10 $g.L^{-1}$(Na_2SO_4)	decrease	(Ghodbane, Nouri et al. 2008)
Ulmas tree leaves	Pb^{2+}, Cu^{2+}, Cd^{2+}	0-0.1 M	decrease	(Sangi, Shahmoradi et al. 2008)
Eucalyptus bark	Hg^{2+}	0-20 g/500 mL	decrease	(Ghodbane and Hamdaoui 2008)

2.4.2 Role of Adsorbent Characteristics on Adsorption

Adsorption method is quite popular due to its simplicity as well as the availability of a wide range of adsorbents and it is proved to be an effective and attractive process for removal of refractory pollutants (including dyes, heavy metal ions, etc.) from wastewater (Crini 2006, Gupta 2009). The major contributing characteristic parameters of adsorbents for good adsorption capacity are specific surface area, pore-size distribution, pore volume, particle size, point of zero charge and presence of surface functional groups. Usually, adsorption capacity increases with increase in specific surface area due to the availability of a number of adsorption sites, while pore size and micropore distribution are closely related to the composition of the adsorbents and the type of raw biomass material supplied for their synthesis (Gautam, Mudhoo et al. 2014). The presence of variety of functional groups such as hydroxyl, nitro and azo groups in the sorbents makes them selective and highly capable of sorption of pollutants from wastewater. Further, the direct application of untreated agricultural by products or wastes as adsorbents sometimes can bring problems linked with lower adsorption capacity for anionic pollutants (as

characteristic of the adsorbent with positive charge on surface) and the release of soluble organic compounds contained in the raw materials (resulted in secondary pollution) (Zhao, Shang et al. 2014). Hence, physical and chemical modification or activation of these materials are necessary to get the desired physical and chemical attributes to enhance their affinities toward dyes and metal ions uptake from aqueous solutions which in turn influences the adsorption capacity of adsorbents for better application.

2.4.2.1 Adsorption with Modified Adsorbents

The techniques of modification can be categorized into three broad groups: modification of physical, chemical and biological characteristics. Among these three methods, modification with chemical compounds has been more frequently employed to increase the adsorption and removal capacity of adsorbents. The physical treatments include vacuum and freeze-drying, boiling or heating, autoclaving and mechanical disruption. The various chemical treatments used for modification include washing the raw adsorbent material with detergents, treatment with various organic and inorganic compounds, such as acid and caustic, methanol, formaldehyde, etc. Table 2.12 lists and compares the advantages and disadvantages of existing modification techniques with regard to technical aspects and Table 2.13 lists some of the adsorbents and their modifying agents for the removal of dyes and heavy metal ions.

Table 2.12: Technical advantages and disadvantages of existing modification techniques (Gautam, Mudhoo et al. 2014)

Modification	***Treatment***	***Advantages***	***Disadvantages***
Chemical characteristics	Acidic	Increases acidic functional groups on activated carbon surface enhances chelation ability with metal species	May decrease BET surface area and pore volume
	Basic	Enhances uptake of organics	In some cases, decrease the uptake of metal ions
	Impregnation of foreign materials	Enhances in-built catalytic oxidation capability	May decrease BET surface area and pore volume

Physical characteristics	Heat	Increases BET surface area and pore volume	Decreases oxygen surface functional groups
Biological characteristics	Bioadsorption	Prolongs activated carbon bed life by rapid oxidation of organics by bacteria before the material can occupy adsorption sites	Thick biofilm encapsulating activated carbon may impede diffusion of adsorbate species

Table 2.13: Various adsorbents and their modifying agents for dyes and heavy metal ions removal

Adsorbents	***Modifying agent***	***Adsorbates (Dyes and heavy metals)***	***References***
Bentonite clay	Cationic Surfactant	Methylene blue (MB), Crystal violet (CV) and Rhodamine B (RB)	(Anirudhan and Ramachandran 2015)
Wheat straw	cationic surfactant	Congo red	(Zhao, Shang et al. 2014)
Pirina	Nitric acid (HNO_3)	Remazon brilliant blue	(Dağdelen, Acemioğlu et al. 2014)
Magnetic corn straw	Glutamic acid	Methylene blue	(Zhao, Xia et al. 2014)
Rice husk	Nitric acid (HNO_3)	Malachite green	(Ramaraju, Manoj Kumar Reddy et al. 2013)
Clay	Physical activation (Drying)	Methyl orange	(Ma, Shen et al. 2013)
Coconut coir	Sulphuric acid (H_2SO_4)	Methylene blue, Acid orange 7	(Ong, Ho et al. 2013)
Olive stone	Phosphoric acid (H_3PO_4)	Cu^{2+}, Ni^{2+}, Pb^{2+}	(Bohli, Ouederni et al. 2015)
Leaf biomass	Nitric acid (HNO_3)	Pb^{2+}	(Madala, Mudumala et al. 2015)

Guava leaves	Sodium hydroxide (NaOH)	Cd^{2+}	(Abdelwahab, Fouad et al. 2015)
Melia azedarach L. leaves	Hydrochloric acid (HCl)	Fe^{2+}, Pb^{2+}	(Khokhar and Siddique 2015)
Sugarcane bagasse	Sulphuric acid (H_2SO_4)	Cu^{2+}	(Rana, Shah et al. 2014)
Orange peel	Sodium hydroxide (NaOH) and calcium chloride ($CaCl_2$) solutions	Cu^{2+}, Pb^{2+}, Zn^{2+}	(Feng and Guo 2012)
Wheat residue	Epichlorohydrin and triethylamine	Cr(VI)	(Chen, Yue et al. 2010)

2.4.2.2 Adsorption with Biomass Based Activated Carbon Adsorbents

Activated carbon adsorbent is prepared by modification and activation of a large number of raw biomass and constitutes one of the most important types of industrial carbon. Because of its high adsorption capacity it is used extensively in environmental applications for the removal of impurities from gases and liquids. The high adsorptive capacities of activated carbons are mainly associated with their internal pore properties such as pore surface area, pore volume, and pore size distribution (Gautam, Mudhoo et al. 2014). Activated carbons are mostly produced by a two-stage process: carbonization (to enrich the carbon content and to create an initial porosity) and next, activation process (to enhance the pore structure of the selected adsorbent). The activation processes for the preparation of activated carbon are physical and chemical activation. Two important advantages of chemical activation over physical activation are lower temperature to accomplish the process and the other is global yield of the chemical activation tends to be greater since burn off char is not required (Bansal and Goyal 2010). Table 2.14 shows the classification of pre-treatment methods for the production of activated biosorbents.

Table 2.14: The classification of pre-treatment methods for the production of activated adsorbents adopted from (Gautam, Mudhoo et al. 2014)

Physical methods	***Chemical and Physicochemical methods***	***Biological methods***
Milling: - Ball milling - Two-roll milling - Hammer milling *Irradiation*: - Ultrasound irradiation - Gamma-ray irradiation - Electron-beam irradiation - Microwave irradiation *Others*: - Hydrothermal - High pressure steaming - Extrusion - Pyrolysis	*Explosion*: - Steam, Ammonia, CO_2, SO_2, Acids *Alkali*: - CaO, $ZnCl_2$, NaOH, NH_3, $(NH_4)_2SO_3$ *Acid*: - H_2SO_4, HCl, HNO_3 and H_3PO_4acids *Gas*: - ClO_2, NO_2, SO_2 *Oxidizing agents*: - H_2O_2 - O_3 -*Wet oxidation* *Solvent extraction of lignin*: - Ethanol–water extraction - Benzene–water extraction - Butanol–water extraction	*Fungi and actinomycetes*: - Lignin peroxidase, manganese peroxidase, laccase - White-rot and brown-rot fungi

2.5 Use of Various Adsorbents for the Removal of Organic and Inorganic Contaminants

Among all the proposed sorbent materials, commercial activated carbon is the most popular and ideal choice for its effectiveness of adsorption for removal of a large variety of toxic pollutants from wastewater. However, the high cost associated with use and regeneration of commercial activated carbon (CAC) in adsorption leads the researchers to search for more economic and alternative adsorbents. At present, the interests in utilization of low-cost and easily available alternatives have been significantly increased and many attempts have been made by researchers on feasibility of adsorption potential of agricultural solid waste materials (either in its raw or modified form) as economic and eco-friendly options which are discussed below:

2.5.1 Cost Effective Adsorbents for Organic and Inorganic Removal

Cost is an important parameter for comparing the sorbent materials. The precursor for the development of low cost adsorbents should be freely available, in-expensive and non-hazardous in nature. In general, a sorbent can be assumed to be "low cost" if it requires little processing and is abundant in nature, or a waste material or a by-product from another industry. Commonly, biosorption processes can significantly reduce capital costs, operational costs and total treatment costs compared with the conventional systems. Waste treatment by adsorption using low cost adsorbent is a demanding area as it has double benefits i.e. water treatment and waste management. To date, hundreds of studies on the use of various low-cost adsorbents derived from agricultural wastes, certain waste products from industrial operations, natural materials and biosorbents have been investigated intensively and have resulted in potentially economical alternative sorbents for organic dyes and inorganic heavy metals removal from contaminated wastewater.

2.5.1.1 Agricultural Solid Wastes

The raw agricultural solid wastes such as leaves, fibres, fruit peels, seeds, etc. and waste materials from forest industries such as sawdust, bark, etc. have been used as adsorbents. The sorption onto agricultural solid wastes is becoming a potential alternative for inorganic/organic removal from aqueous solution. These materials are available in large quantities, low-cost, environmental friendly, efficient and are able to replace the most widely used commercial activated carbon. These materials may have potential as sorbents due to their physio-chemical characteristics. Recently many researchers reported that the effective removal capabilities of various agricultural solid wastes as adsorbents to remove inorganic/organic pollutants. Geetha and Belagali (Geetha and Belagali 2013) reported a review article on the use of agricultural solid wastes to remove heavy metals and dyes and readers are encouraged to go through this review article. Table 2.15 presents the compilation results of various agricultural by-products in the removal of dyes and heavy metals and their adsorption capacity.

Table 2.15: Adsorption capacities q_m (mg/g) of waste materials from raw agricultural solid wastes

Adsorbents	*Dyes and heavy metals*	*Maximum adsorption capacity q_m (mg/g)*	*References*
Tomato seeds	Acid Red 14, Acid Blue 92	125, 36.23	(Najafi, Pajootan et al. 2015)
Olive pomace	Basic green 4	41.66	(Koçer and Acemioğlu 2015)
Mango seeds	Methylene blue	25.36	(Senthil Kumar, Palaniyappan et al. 2014)
Formosa papaya seed	Crystal violet	85.99	(Pavan, Camacho et al. 2014)
Coffee waste	Toluidine blue	142.5	(Lafi, ben Fradj et al. 2014)
Pineapple leaf powder	Crystal violet	78.22	(Chakraborty, Chowdhury et al. 2012)
Peach gum	Methylene blue, methyl violet	298, 277	(Zhou, Huang et al. 2014)
Coffee residues	Basic Blue 3G	179	(Kyzas, Lazaridis et al. 2012)
Poplar leaf	Methylene blue	135.35	(Han, Niu et al. 2012)
Peanut hull	Reactive Black 5	55.55	(Tanyildizi 2011)
Rice husk	Crystal violet	44.87	(Chakraborty, Chowdhury et al. 2011)
Pine cone	Methylene blue	109.89	(Sen, Afroze et al. 2011)
Pine Tree Leaves	Basic red 46	71.94	(Deniz and Karaman 2011)
Grapefruit peel	Crystal violet	254.16	(Saeed, Sharif et al. 2010)
Pineapple stem	Methylene blue	119.05	(Hameed, Krishni et al. 2009)
Garlic peel	Methylene blue	82.64	(Hameed and Ahmad 2009)
Coconut bunch waste	Methylene blue	70.92	(Hameed, Mahmoud et al. 2008)
Yellow passion	Methylene	44.7	(Pavan, Lima et al. 2008)

fruit waste	blue		
Coffee husk	Methylene blue	90.1	(Oliveira, Franca et al. 2008)
Cherry sawdust	Methylene blue	39.84	(Ferrero 2007)
Ground hazelnut shells	Methylene blue	76.9	(Ferrero 2007)
Walnut sawdust	Methylene blue	59.17	(Ferrero 2007)
Rice husk	Methylene blue	40.59	(Vadivelan and Kumar 2005)
Pine sawdust	Acid yellow 132, Acid blue 256	398.8, 280.3	(Ozacar and Sengil 2005)
Chitosan	Acid green 25	645.1	(Wong 2004)
Peat	Acid Blue 25	14.4	(Ho and McKay 2003)
Coconut tree sawdust	Zn^{2+}	23.81	(Putra, Kamari et al. 2014)
Eggshell	Pb^{2+}	90.90	(Putra, Kamari et al. 2014)
Sorghum hulls	Cu^{2+}	148.93	(Imaga, Abia et al. 2015)
Coffee residues	Pb^{2+}, Zn^{2+}	9.7 (Pb^{2+}), 4.4 (Zn^{2+})	(Wu, Kuo et al. 2015)
Papaya wood	Cu^{2+}, Cd^{2+}, Zn^{2+}	19.88 (Cu^{2+}), 17.22 (Cd^{2+}), 13.45 (Zn^{2+})	(Saeed, Akhter et al. 2005)
Peanut shell	Pb^{2+}	39	(Taşar, Kaya et al. 2014)
Eucalyptus bark	Cd^{2+}	14.53	(Ghodbane, Nouri et al. 2008)
***Ulmas carpinifolia* tree leaves**	Cd^{2+}	80.0	(Sangi, Shahmoradi et al. 2008)
***Fraxinus excelsior* tree leaves**	Cu^{2+}	33.1	(Sangi, Shahmoradi et al. 2008)

2.5.1.2 Modified Agricultural Solid Wastes

Literature demonstrates that modification of agricultural adsorbents is a good method to improve surface properties of agricultural wastes which is better for dye removal and metal ions sequestration from wastewater (Gautam, Mudhoo et al. 2014). Chemical treatment removes natural fats, waxes and low-molecular weight lignin compounds from agricultural adsorbent surfaces, thus revealing chemically reactive functional groups and the removal of surface impurities also develops the surface roughness of the particles, thus opening more reactive functional groups on the surface (Auta and Hameed 2012, Dawood and Sen 2012). Due to these facts, modification with a chemical treatment is considered for the raw adsorbent to be used for remediation of dyes and heavy metals contaminated wastewater. Few reported research works on applicability of chemically modified adsorbents for remediation of wastewater contaminated with dyes and heavy metals are presented in Table 2.16.

Table 2.16: Adsorption capacities q_m (mg/g) for modified agricultural waste materials

Modified Adsorbents	***Dyes and heavy metals***	***Maximum adsorption capacity, q_m (mg/g)***	***References***
Rubber leaf	Acid blue 25	28.09	(Khalid, Ngah et al. 2015)
Durian leaf powder	Methylene blue	125	(Hussin, Talib et al. 2015)
Neem (*Azadiracta indica*) bark	Malachite green	500	(Sharma, Tiwari et al. 2014)
Mango seeds	Methylene blue	58.08	(Senthil Kumar, Palaniyappan et al. 2014)
Peanut husk biomass	Light Green (LG)	146.2±2.4	(Zhao, Xiao et al. 2014)
Magnetic corn straw	Methylene blue	196.46	(Zhao, Xia et al. 2014)
Breadnut peel	Malachite green	353	(Chieng, Lim et al. 2015)

Phoenix tree leaves	Crystal violet	510.3	(Ren, Xiao et al. 2015)
Rice husk	Malachite green	26.6	(Ramaraju, Manoj Kumar Reddy et al. 2013)
Bagasse	Methylene blue	69.93 (at 60°C)	(Low, Teng et al. 2013)
Oil palm tree sawdust	Malachite green	65.36 (at 60°C)	(Low, Teng et al. 2013)
Coconut coir	Methylene Blue	121	(Ong, Ho et al. 2013)
Pine cone	Methylene Blue	142.24	(Yagub, Sen et al. 2013)
Saw dust	Methylene Blue	111.46	(Zou, Bai et al. 2013)
Rice straw	Malachite green	256.41	(Gong, Jin et al. 2007)
Okra biomass	Cu^{2+}, Zn^{2+}, Cd^{2+}, Pb^{2+}	72.72 (Cu^{2+}), 57.11 (Zn^{2+}), 121.51 (Cd^{2+}), 273.97 (Pb^{2+})	(Singha and Guleria 2015)
Leaf biomass	Pb^{2+}	100.0	(Madala, Mudumala et al. 2015)
Melia azedarach L. leaves	Fe^{2+}, Pb^{2+}	35.06, 38.46	(Khokhar and Siddique 2015)
Sugarcane bagasse	Cu^{2+}	30.9	(Rana, Shah et al. 2014)
Orange peel	Cu^{2+}, Pb^{2+}, Zn^{2+}	70.73 (Cu^{2+}), 209.8 (Pb^{2+}) and 56.18 (Zn^{2+})	(Feng and Guo 2012)

2.5.1.3 Biomass Based Activated Carbon

Activated carbon (AC) obtained from agricultural by-product has the advantage of offering an effective low cost replacement for non-renewable coal based granular

activated carbon (CACS) provided that they have similar or better adsorption efficiency (Yagub, Sen et al. 2014). The abundant availability of agricultural by-product makes them good sources of raw materials for activated carbon (AC) production. Table 2.17 presents the compilation of various biomass based activated carbon and their maximum adsorption capacity towards dyes and heavy metals removal. Biomass based activated carbon for the removal of organic dyes and inorganic metals are reviewed by Ali et al. (Ali 2010) and Gautam et al. (Gautam, Mudhoo et al. 2014) and readers are encouraged to go through these review articles.

Table 2.17: Adsorption capacities q_m (mg/g) for activated carbon materials made from agricultural solid wastes

AC from waste materials	***Dyes and heavy metals***	***Maximum adsorption capacity q_m (mg/g)***	***References***
Egg shell wastes	Acid blue 25	109.80	(Tovar-Gómez, del Rosario Moreno-Virgen et al. 2015)
Coconut Shell	Malachite Green	214.63	(Bello and Ahmad 2012)
Hazelnut husks	Methylene Blue	204.0	(Ozer, Imamoglu et al. 2012)
Walnut shell-carbon	Methylene Blue	315.0	(Yang and Qiu 2010)
Pine fruit shell-carbon	Methylene Blue	529.0	(Royer, Cardoso et al. 2009)
Oil palm shell-carbon	Methylene Blue	243.9	(Tan, Ahmad et al. 2008)
Coal-based mesoporous	Congo red	189	(Lorenc-Grabowska and Gryglewicz 2007)
Pinewood	Basic blue 9	556	(Tseng, Wu et al. 2003)
Rice husk	Basic green 4	511	(Guo, Yang et al. 2003)
Bagasse fly ash	Malachite green	42.18	(Mall, Srivastava et al. 2005)
Bagasse	Acid blue 80	391	(Valix, Cheung et al. 2004)
Bamboo dust	Methylene blue	143.2	(Kannan and Sundaram
Groundnut shell	Methylene blue	164.9	(Kannan and Sundaram
Egg shell wastes	Zn^{2+}, Ni^{2+}, Cd^{2+}	1.6 (Zn^{2+}), 2.31 (Ni^{2+}), 2.70 (Cd^{2+})	(Tovar-Gómez, del Rosario Moreno-Virgen et al. 2015)

Tomato wastes	Co^{2+}	166.67	(Önal, Özbay et al. 2014)
Sugarcane bagasse	Zn^{2+}	23.7 (at 100 mg L^{-1})	(Krishnan, Sreejalekshmi et al. 2016)
Tamarind wood	Cr(VI)	28.019	(Acharya, Sahu et al. 2009)
Olive bagasse	Cr(VI)	109.89 (at 45^0C)	(Demiral, Demiral et al. 2008)
***M.baccifera Roxburgh* (bamboo)**	Pb^{2+}	53.76	(Lalhruaitluanga, Jayaram et al. 2010)

2.5.1.4 Inorganic Materials

A) *Clay minerals*: Among natural inorganic materials, clay minerals are well known and familiar to use as adsorbents because of low cost, available in abundance, have good sorption properties and potential for ion exchange. Clays always contain exchangeable ions mainly Ca^{2+}, Mg^{2+}, H^+, K^+, NH_4^+, Na^+, and SO_4^{2-}, Cl^-, PO_4^{3-}, NO_3^- on their surface and these ions can be exchanged with other cations and/or anions without affecting the structure of clay mineral (Rafatullah, Sulaiman et al. 2010). Hence, clay minerals show a strong affinity for both cations and anions. Clay mineral possesses a layered structure and is considered as host materials for the adsorbates and counter ions by playing important role in the environment by acting as a natural scavenger of contaminants. According to the layered structures, clays are classified as smectites (montmorillonite, saponite), mica (illite), kaolinite, serpentine, pylophyllite (talc), vermiculite and sepiolite (Yagub, Sen et al. 2014). There are various types of clay such as ball clay, bentonite, common clay, sepiolite, fire clay, fuller's earth and kaolin. In recent years, there has been an increasing interest in utilizing clay raw materials for their capacity to absorb inorganic ions and organic molecules. Clays can be modified to improve their sorption capacity by giving some treatment like replacing cations present in clay by heat treatment and acid treatment (Gupta 2009). The good removal capabilities of clays to uptake dyes and heavy metal ions have been demonstrated by many researchers (Table 2.18).

B) *Siliceous materials*: The natural siliceous sorbents such as silica beads, alunite, dolomite and perlite are progressively used for wastewater treatment because of their

low cost, abundance and high sorption properties and availability (Yagub, Sen et al. 2014). The porous texture, mechanical stability, chemical reactivity of hydrophilic surface and high surface area of silica beads make them attractive as sorbents for pollution removal applications (Crini 2006). They are resistant towards alkaline solution and the surface of siliceous materials contains acidic silanol (among other surface groups) which causes a strong and often irreversible non-specific adsorption. Therefore it is necessary to eliminate the negative features of these sorbents (Crini 2006). In order to promote their interaction with dyes, the silica surface can be modified using silane coupling agents with the amino functional group (Krysztafkiewicz, Binkowski et al. 2002). Other siliceous materials such as alunite, dolomite, perlite and glass have also been proposed for organic and inorganic toxic pollutants removal from wastewater. Alunite is very cheap and approximately contains 50% SiO_2. Dolomite is both a mineral and a rock. Burnt dolomite has a higher equilibrium capacity for reactive dye removal than activated carbon. Perlite is a glassy volcanic rock that has high silica content, inexpensive and simply available in several countries. Perlite is a good adsorbent for decontamination uses. Therefore, siliceous materials are good adsorbents for the removal of wastewater pollutants which it has been reported by several researchers and is presented in Table 2.18.

C) *Zeolites*: Zeolites are highly porous aluminosilicate with different cavity structures. Their structures consist of a three dimensional framework having a negatively charged lattice (Rafatullah, Sulaiman et al. 2010). The negative charge is balanced by cations which are exchangeable with certain cations in solutions. Among over 40 natural types of variety, the most abundant and commonly studied zeolite is clinoptilolite, a mineral of the heulandite group (Yagub, Sen et al. 2014). Zeolites are considered as attractive adsorbents because of their relatively high specific surface areas, high ion-exchange capacity and more importantly low-cost (Rafatullah, Sulaiman et al. 2010).

Zeolite have been extensively studied recently because of their applicability in removing trace quantities of contaminants such as heavy metal ions, phenols, dyes, etc. Several studies have been conducted on the sorbent characteristics and applications of zeolites and readers are encouraged to go through the review article by Ghobarker et al. (Ghobarkar, Schäf et al. 1999). The sorption mechanism on

zeolite particles is complex because of their porous structure and variable surface change. However, it is recognized that, like clay, the adsorption properties of zeolites result mainly from their ion-exchange capabilities. Although the removal efficiency of zeolites may not be as good as that of clay materials, their easy availability and low cost may compensate to some extent for the associated drawbacks (Crini 2006) .

Table 2.18: Adsorption capacities q_m(mg/g) of natural inorganic materials

Adsorbents	***Dyes and heavy metals***	***Maximum adsorption capacity q_m (mg/g)***	***References***
Kaolinite	Basic fuchsin (BF), crystal violet (CV)	10.36, 20.64	(Khan and Khan 2015)
Natural clay	Reactive Red 120, Reactive Orange 84 and Reactive Blue 160	30.3	(Abidi, Errais et al. 2015)
Magnetic perlite	Direct red 81	416.66	(Shirkhodaie, Hossein Beyki et al. 2016)
Raw Ball clay	Methylene blue	34.65	(Auta and Hameed 2012)
Modified Ball clay	Methylene blue	100	(Auta and Hameed 2012)
Gypsum	Basic Red 46	39.17	(Deniz and Saygideger 2010)
Na-Bentonite	Congo red	35.84	(Vimonses, Lei et al. 2009)
Spent activated clay	Methylene blue	127.5	(Weng and Pan 2007)
Pyrophyllite	Methylene blue	70.42	(Gücek, Şener et al. 2005)
Charred dolomite	Reactive dye E-4BA	950	(Walker, Hansen et al. 2003)
Sepiolite	Hg^{2+}	54.7	(Vaġzoğullar, Uğurlu et al. 2015)
Modified Sepiolite	Hg^{2+}	104.1	(Vaġzoğullar, Uğurlu et al. 2015)

Dolomite–palygorskite	Cu^{2+}	225.7	(Qiu, Xie et al. 2015)
clay	Hg^{2+}	68.1	(Caner, Sarı et al. 2015)
Diatomite	Cr(VI)	309.60	(Deng, Shi et al. 2014)
Modified kaolin clay	Cu^{2+}, Pb^{2+}, Zn^{2+}, Cd^{2+}	78.86 (Cu^{2+}), 154.08 (Pb^{2+}), 67.25 (Zn^{2+}), 66.67 (Cd^{2+})	(Jiang, Sun et al. 2006)
Tourmaline			

2.5.1.5 Bioadsorbents & Microbial Biomass

Biosorption is a physiochemical process that naturally allows certain biological materials to passively concentrate and bind contaminants from aqueous solutions onto its cellular structure. Biosorption is particularly suitable to treat dilute dye molecules and heavy metal ions from wastewater using inactive and dead biomass (Fu and Wang 2011, Asgher and Bhatti 2012). Biological materials, such as chitin, chitosan, peat, yeasts, fungi or bacterial biomass, are used as sorbents in order to remove dyes and heavy metal ions from aqueous solutions. The biosorbents are often much more selective than traditional ion-exchange resins and commercial activated carbons, and can reduce dye to low levels concentration (Ali 2010, Rafatullah, Sulaiman et al. 2010). Biosorption is a new approach, competitive, low-priced and has been established as an effective technology. A significant number of biosorption studies on the removal of dyes from aqueous solutions have been conducted worldwide which has been compiled by Asgher (Asgher and Bhatti 2012). Bioadsorption of heavy metals from aqueous solutions is a relatively new process and its recent advances have been reported by Ghosh et al. (Ghosh, Ghosh Dastidar et al. 2015) . Diverse functional groups such as carboxyl, hydroxyl, sulphate, and amino groups which all originally present on the biosorbent are responsible for possible binding mechanism (Yagub, Sen et al. 2014). Biosorption is an alternative technology for the removal of inorganic and organic pollutants from dilute solution by employing biomass as adsorbents e.g. agricultural and fermentation wastes and various types of microorganism. Table 2.19 presented compilation results of various natural biosorbents and microbial biomasses for the removal of dyes and heavy metal ions.

Table 2.19: Adsorption capacities q_m (mg/g) for various natural organic materials as biosorbents

Biosorbents	***Dyes and heavy metals***	***Maximum adsorption capacity q_m (mg/g***	***References***
Bacillus catenulatus JB-022 (bacteria)	Basic blue 3	139.74	(Kim, Jin et al. 2015)
Red Marine Alga *Kappaphycus alvarezii*	Methylene blue	74.4	(Vijayaraghavan, Bhagavathi Pushpa et al. 2015)
Saccharomyces cerevisiae	Eosin B, Eosin Y	200, 1000	(Bahramifar, Tavasolli et al. 2015)
Algae Gelidium	Methylene blue	171	(Vilar, Botelho et al. 2007)
Algal waste	Methylene blue	104	(Vilar, Botelho et al. 2007)
Composite material	Methylene blue	74	(Vilar, Botelho et al. 2007)
Dead macro fungi (F)	Methylene blue	232.73	(Maurya, Mittal et al. 2006)
Green alga	Reactive red 5	555.6	(Aksu and Tezer 2005)
Duckweed	Methylene blue	144.93	(Waranusantigul, Pokethitiyook et al. 2003)
Rhizopusarrhizus	Reactive orange 16	190	(O'Mahony, Guibal et al. 2002)
Aspergillus niger	Direct red 28, Disperse red 1	14.72, 5.59	(Fu and Viraraghavan 2002)
Living fungus	Acid blue 29	6.63	(Fu and Viraraghavan 2001)
Bacillus catenulatus JB-022	Cd^{2+}	64.28	(Kim, Jin et al. 2015)
***Lysinibacillus* sp. BA2 (bacteria)**	Ni^{2+}	238.04	(Prithviraj, Deboleena et al. 2014)
***Spirulina* algae**	Cr(VI)	90.91	(Rezaei 2013)

***Micrococcus luteus* DE2008 (bacteria)**	Cu^{2+}, Pb^{2+}	408, 1965	(Puyen, Villagrasa et al. 2012)
***Bacillus cereus* bacteria**	Hg^{2+}	104.1	(Sinha, Pant et al. 2012)
***Lentinus edodes* fungi**	Zn^{2+}, Cd^{2+}, Hg^{2+}	33.7 (Zn^{2+}), 78.6 (Cd^{2+}), 336.3 (Hg^{2+}) 88.9	(Bayramoğlu and Arıca 2008)
***Oedogonium sp.* algae**	Cd^{2+}		(Gupta and Rastogi 2008)

2.6 Batch Adsorption Kinetic-Study

For process design and to control the adsorption phenomenon, it is significant to understand the adsorption kinetics and mechanism of a system. The kinetics of dyes and heavy metal ions adsorption onto adsorbent materials is a prerequisite for choosing the best operating conditions for the full-scale batch process (Yagub, Sen et al. 2014). The study of adsorption dynamics describes the solute uptake rate and evidently this rate controls the residence time of the adsorbate uptake at the solid-solution interface. To design the adsorption system, this solute uptake rate plays the most significant role by determining the residence time required for completing the adsorption reaction and can be enumerated from kinetic analysis. Therefore the adsorption rate is an important factor for a better choice of material to be used as an adsorbent; where the adsorbent should have a large adsorption capacity and a fast adsorption rate (Bharathi and Ramesh 2013). In order to study the mechanism of sorption and potential rate determining steps, most of the adsorption studies used pseudo-first-order and pseudo-second-order models which are presented below:

2.6.1 Application of Lagergren Pseudo-first-order and Pseudo-second order Model Kinetics on Organic/Inorganic Adsorption

Pseudo-first-order Model The pseudo-first-order considers the rate of occupation of adsorption sites to be proportional to the number of unoccupied sites. The linearized

integral form of the pseudo-first-order model is generally expressed as (Lagergren 1898) :

$$\log (q_e - q_t) = \log q_e - \frac{k_1}{2.303} t \quad (2.1)$$

where q_t and q_e are the adsorption capacity at time t and at equilibrium, respectively (mg g^{-1}), k_1 is the rate constant of pseudo-first-order adsorption (min^{-1}) and t is the contact time (min). The slope and intercept of a linear plot of log ($q_e - q_t$) versus t will give the value of k_1 and q_e respectively. A straight line of log ($q_e - q_t$) versus t indicates the application of the first-order kinetics model. In a true first-order process log q_e should be equal to the intercept of the plot of log ($q_e - q_t$) against t.

Pseudo-second-order Model Lagergren pseudo-second-order adsorption kinetic was described by (Ho and McKay 1999) and the linearized form of the equation is :

$$\frac{t}{q_t} = \frac{1}{k_2 q_e^2} + \frac{1}{q_e} t \quad (2.2)$$

where k_2 (g mg^{-1} min^{-1}) is pseudo-second-order rate constant of adsorption. A plot between t/q_t vs. t gives the value of rate constant k_2 (g/mg min), initial sorption rate h (mg/g-min) and also q_e (mg/g) can be calculated. A plot of t/q_t against t should give a linear relationship for the applicability of the second-order kinetic.

The constant k_2 is used to calculate the initial sorption rate h, at t→0, as follows:

$$h = k_2 q_e^2 \quad (2.3)$$

Thus, the rate constant k_2, initial adsorption rate h and predicted q_e can be calculated from the plot of t/q_t versus time t using Eq. (2.2).

2.6.2 Application of Intra-particle Diffusion Model on Organic/Inorganic Adsorption

The mechanism of adsorption techniques involve four steps: migration of dye molecules from bulk solution to the surface of the sorbent, diffusion through the boundary layer to the surface of the sorbent, adsorption at a site, and intra-particle diffusion into the interior of the sorbent (Oladoja, Aboluwoye et al. 2008). According to Weber and Morris (Weber and Morris 1963), the amount of adsorption varies

almost proportional with $t^{1/2}$ rather than with the contact time for most adsorption processes and can be expressed as:

$$q_t = K_{id} t^{0.5} + C \quad (2.4)$$

where q_t is the adsorption capacity at time t, $t^{0.5}$ is the half-life time in second, K_{id} (mg/g $min^{0.5}$) is the rate constant of intraparticle diffusion. C (mg/g) is a constant that gives an idea about the thickness of the boundary layer. To find out the rate constants, plot q_t versus $t^{0.5}$ give a linear relationship, K_{id} can be determined from the slope of the plot.

Generally the best-fit model can be chosen based on the higher values of the linear regression correlation coefficient R^2. The R^2 values for pseudo-first-order are determined by fitting experimental data at various physico-chemical conditions using plots of log ($q_e - q_t$) vs. t for Eq.(2.1) and likewise commencing the slope and intercept of plot t/q_t vs. t using Eq.(2.2) for pseudo-second-order model. Usually the kinetic adsorption data is better represented by pseudo-second-order model for most dyes and heavy metal ions adsorption system. Wang et al. (Wang, Ma et al. 2016) studied the adsorption of Methylene Blue by citric acid modified peanut shell and they found very high (>0.99) regression correlation coefficient R^2 values for the Pseudo-second-order model. Surgin et al. (Sargın, Arslan et al. 2016) studied the use of chitosan-algal biomass composite for adsorption of Zn^{2+} ions. They found that the values of the regression correlation coefficient R^2 for Pseudo-second-order model was 0.992 which was higher than the value of R^2 (0.659) for the pseudo first order model. Dursun et al. (Dursun, Tepe et al. 2013) evaluated the adsorption of Remazol Black B dye using sugar beet pulp and they found that the applicability of Pseudo-second order over Pseudo-first order model. Table 2.20 presents compilation results of the applicability of Pseudo-second-order Kinetic models for dye adsorption using several agricultural solid wastes.

Table 2.20: Pseudo-second-order kinetic studies for organic dyes and inorganic heavy metals adsorption by several adsorbents

Adsorbents	*Adsorbate (Dyes and heavy metals)*	*References*
Sepiolite	Maxilon Red GRL	(Demirbaş, Turhan et al. 2015)
Reed	Basic yellow 28	(Boudrahem, Aissani-Benissad et al. 2015)
Peach gum	Methyl violet	(Zhou, Huang et al. 2014)
Modified oil palm tree sawdust	Malachite green	(Low, Teng et al. 2013)
Modified phoenix tree leaves	Crystal violet	(Ren, Xiao et al. 2015)
Raw and modified Mango Seed	Methylene blue	(Senthil Kumar, Palaniyappan et al. 2013)
Fe_3O_4 nanospheres	Neutral red	(Iram, Guo et al. 2010)
Almond shell	Methyl Violet	(Duran, Ozdes et al. 2011)
Wood apple shell	Crystal Violet	(Jain and Jayaram 2010)
Activated charcoal	Brilliant red HE-3B	(Suteu and Bilba 2005)
Chitosan-algal biomass composite	Cu^{2+}	(Sargın, Arslan et al. 2016)
Coal bottom ash	Fe^{2+}, Mn^{2+}, Cu^{2+}, Zn^{2+}	(Asokbunyarat, van Hullebusch et al. 2015)
Raw and activated guava leaves	Cd^{2+}	(Abdelwahab, Fouad et al. 2015)
Carbon nanospheres (from willow fallen leaves)	Cu^{2+}, Zn^{2+}	(Qu, Zhang et al. 2015)
Melia azedarach L. leaves (HCl treated)	Fe^{2+}, Pb^{2+}	(Khokhar and Siddique 2015)

2.7 Batch Adsorption Isotherms

Adsorption isotherms are crucial in understanding the mechanism of adsorption, and the analysis of the isotherm data by fitting them to different isotherm models is an important step to understand the suitable model that can be used for design purposes. Adsorption equilibrium is established when the concentration of sorbate in the bulk solution is in dynamic balance with that at the interface (Oladoja, Aboluwoye et al. 2008). The adsorption isotherm indicates how the adsorbate molecules distribute between the liquid phase and the solid phase at equilibrium during the process of adsorption. Thus they play an important role to understand the mechanism of adsorption. The surface phase may be considered as a monolayer or multilayer. Among several isotherm models presented in the literature (Allen, Mckay et al. 2004), Langmuir and Freundlich models are the earliest and simplest models (El-Halwany 2010) and hence most widely used to describe adsorption isotherms.

2.7.1 Langmuir Adsorption Isotherm Model

The Langmuir model of adsorption is based on the ideal assumption that the intermolecular forces decrease rapidly with distance, and consequently, predicts the existence of monolayer coverage of adsorbate at the outer surface of the adsorbent, which is assumed to be structurally homogeneous (Langmuir 1918). The activities of the surface sites are proportional to their concentration and the number of sorption sites is fixed; no further adsorption can take place after the saturation point. For solid/liquid systems, the linear form of the Langmuir equation is:

$$q_e = \frac{q_m K_a C_e}{1 + K_a C_e} \tag{2.5}$$

where q_e is the amount of adsorbate adsorbed at equilibrium time (mg g^{-1}), C_e is equilibrium concentration of adsorbate in solution (mg L^{-1}), q_m is maximum adsorption capacity (mg g^{-1}) and K_a is isotherm constants for Langmuir (L mg^{-1}).

The linearized form of Langmuir isotherm can be written in two different forms:

a) Langmuir-I isotherm model

$$\frac{C_e}{q_e} = \frac{C_e}{q_m} + \frac{1}{K_a q_m} \quad (2.6)$$

The slop and intercept of plot between C_e/q_e vs. C_e will give q_m and K_a respectively.

b) Langmuir-II isotherm model

$$\frac{1}{q_e} = \frac{1}{K_a q_m}\frac{1}{C_e} + \frac{1}{q_m} \quad (2.7)$$

In this form q_m and K_a are determined from plotted between $1/q_e$ vs. $1/C_e$. The essential characteristics of Langmuir isotherm can be expressed by a separation or equilibrium parameter, which is a dimensionless constant defined as:

$$R_L = \frac{1}{1+K_a C_0} \quad (2.8)$$

where K_a is the Langmuir constant and C_0 is the initial solute concentration (ppm). R_L indicates the nature of adsorption (Baskaralingam, Pulikesi et al. 2006) as indicated below:

- unfavorable $R_L > 1$;
- linear $R_L = 1$;
- favorable $0 < R_L < 1$;
- irreversible $R_L = 0$.

2.7.2 Freundlich Adsorption Isotherm Model

The Freundlich adsorption isotherm model considers a heterogeneous adsorption surface that has unequal available sites with different energies of adsorption. The Freundlich adsorption isotherm model is represented as follow (Freundlich 1906):

$$q_e = K_f\, C_e^{\frac{1}{n}} \quad (2.9)$$

The linearized form of Freundlich can be expressed as:

$$\ln q_e = \ln K_f + \frac{1}{n}(\ln C_e) \quad (2.10)$$

where q_e is the amount of adsorbate adsorbed at equilibrium time (mg g^{-1}), C_e is equilibrium concentration of adsorbate in solution (mg L^{-1}). K_f and n are Freundlich empirical constants related to adsorption phenomenon. The plot of $\ln q_e$ versus $\ln C_e$ is employed to determine the K_f and n from intercept and slope respectively. Generally the value of the linear regression correlation coefficient R^2 gives the indication which model to be chosen to give best-fit. Najafi et al. (Najafi, Pajootan et al. 2015) used tomato seeds for the removal of Acid Blue 92 (AB92) dye from its aqueous solution and they have found that the maximum monolayer adsorption capacity was 36.23 mg g^{-1} and the Langmuir adsorption isotherm model is the best-fit. Cantuaria et al. (Cantuaria, de Almeida Neto et al. 2016) investigated the adsorption of Silver by modified Bentonite clay and they reported that the data were fitted well with Langmuir isotherm model with a maximum adsorption capacity of 61.48 mg g^{-1}. Ong et al. (Ong, Ho et al. 2013) reported that the adsorption of Methylene Blue (MB) onto acid treated coconut coir could be well described by the Langmuir and Freundlich isotherm models as the correlation coefficients for all adsorption data was greater than 0.9. Table 2.21 shows various isotherm studies of dyes and metals adsorption by various adsorbents.

Table 2.21: Various isotherm studies of dyes and heavy metals adsorption by various adsorbents

Adsorbents	*Adsorbates (Dyes and heavy metals)*	*Isotherm Model*	*References*
Carbon nanospheres (from willow fallen leaves)	Rhodamine B	Langmuir	(Qu, Zhang et al. 2015)
Peanut husk	Drimarine Red HF-3D	Freundlich	(Nausheen, Bhatti et al. 2014)
Cucumber peel	Methylene blue	Langmuir	(Akkaya and Güzel 2014)
Pistachio shell	Remazol red	Freundlich	(Armagan and Toprak 2015)
Pumpkin husk	Reactive red 120	Freundlich	(Çelekli, Çelekli et al. 2014)
Activated clay	Methyl orange	Langmuir	(Ma, Shen et al. 2013)
Coconut coir (acid treated)	Acid orange 7	Langmuir and Freundlich	(Ong, Ho et al. 2013)
Poplar leaf	Methylene blue	Langmuir	(Han, Niu et al. 2012)
Pine cone (acid treated)	Congo red	Fruendlich	(Dawood and Sen 2012)
Green pea peels	Methylene blue	Langmuir	(Dod, Banerjee et al. 2012)
Pine leaves	Basic red 46	Langmuir	(Deniz and Karaman 2011)
Activated carbon (derived from olive stone)	Cu^{2+}, Ni^{2+}, Pb^{2+}	Langmuir	(Bohli, Ouederni et al. 2015)
Coal bottom ash	Cu^{2+}, Zn^{2+}	Freundlich	(Asokbunyarat, van Hullebusch et al. 2015)
Modified leaf biomass	Pb^{2+}	Langmuir	(Madala, Mudumala et al. 2015)
Carbon nanospheres (from willow fallen leaves)	Cr^{6+}	Langmuir	(Qu, Zhang et al. 2015)
Melia azedarach L. leaves (NaOH treat)	Fe^{2+}, Pb^{2+}	Langmuir	(Khokhar and Siddique 2015)

2.8 Thermodynamics Study

Thermodynamic studies are used to investigate the temperature effect on adsorption capacity. The determination of the basic thermodynamic parameters: enthalpy of adsorption (ΔH^o), Gibb's free energy of adsorption (ΔG^o) and entropy of adsorption (ΔS^o), is important as can be used to evaluate the feasibility of the process from thermodynamic point of view, to assess the spontaneity of the system and to ascertain the exothermic or endothermic nature of the process (Yaneva and Georgieva 2012). Change in Gibb's free energy of activation (ΔG^o), change in enthalpy of activation (ΔH^o) and change in entropy of activation (ΔS^o) are calculated by using the following equations (Sen and Gomez 2011):

$$\Delta G^o = \Delta H^o - T\Delta S^o \tag{2.11}$$

$$\log\left(\frac{q_e}{C_e}\right) = \frac{\Delta S^o}{2.303R} + \frac{-\Delta H^o}{2.303RT} \tag{2.12}$$

where q_e is the solid-phase concentration at equilibrium (mg L^{-1}), C_e is equilibrium concentration in solution (mg L^{-1}), T is temperature in K and R is the gas constant (8.314 J/mol K). The entropy change (ΔS^o) and enthalpy change (ΔH^o) can be calculated from the intercept and slope of the linear Van't Hoff plot log (q_e/C_e) versus $1/T$. From those values, change in Gibb's free energy of activation (ΔG^o) can be calculated using the Eq. (2.11). The absolute magnitude of the change in Gibbs energy (ΔG^o) can be also used to verify if the process is controlled by physical adsorption (ranges from 0 to −20 kJ mol^{-1}) or chemisorption (ranges from −400 to −80 kJ mol^{-1}) (Cantuaria, de Almeida Neto et al. 2016). Also, the negative value of ΔH^o specifies adsorption process as exothermic where positive value of ΔH^o indicates the process as endothermic in nature and the negative ΔS^o indicates a decrease in randomness at the solid/solution interface (Yaneva and Georgieva 2012). The study of Najafi et al. (Najafi, Pajootan et al. 2015) demonstrated the thermodynamic behaviour during Acid Red 14 (AR14) adsorption on Tomato seeds. Negative values of ΔG^o (-6.45, -5.09, -5.71, -6.18 kJ mol^{-1} at 30, 40, 50 and 60^0C, respectively) are indicative of a spontaneous adsorption process. Moreover, negative value of ΔH^o (-7.23 kJ mol^{-1}) and positive ΔS^o value (0.004 kJ/mol K) show that the

removal of AR14 by tomato seeds is an exothermic reaction with increasing randomness at the interface of solid/liquid. Also, the obtained ΔG values are within the ranges of physisorption mechanisms ($-20<\Delta G^o<0$ kJ mol^{-1}). Cantuaria et al. (Cantuaria, de Almeida Neto et al. 2016) investigated the adsorption of Silver by modified Bentonite clay and from the obtained negative values of ΔG^o (-2.45, -2.005, -1.573, -0.539 kJ mol^{-1} at 10, 20, 30, and 50^0C, respectively), they revealed that the adsorption is physical and the process was spontaneous. Madala et al. (Madala, Mudumala et al. 2015) studied the removal of Pb^{2+} ions on *Tephrosia Purpuria Leaf* (TPL) biomass and explained that the negative values of ΔG^o demonstrate the process to be spontaneous and positive values of ΔH^o indicating the process to be endothermic in nature. The ΔH^o value obtained (37.9 kJ mol^{-1}) showed that chemisorption plays a dominant role in the adsorption process. The positive value of ΔS^o suggested the increase of randomness at the solid/solution interface during the adsorption of Pb^{2+} metal ions on Tephrosia Purpuria Leaf (TPL) biomass.

2.9 Column Adsorption Studies for Organic Dye Removal

Adsorption performance of adsorbents in continuous system is important in accessing the feasibility of adsorbent in real industrial applications and to find key parameters required for the design of fixed-bed adsorber. The study of adsorption dynamics through fixed bed column operation permits more efficient utilization of the adsorption capacity than batch studies. The most important condition for the design of a fixed bed adsorption system is the accurate generation of breakthrough curves through the whole service period of column operation which verify the process lifetime of the bed. Therefore, to determine the operation and dynamic response of an adsorption column, it is significantly important to know the breakthrough curve shape and the breakthrough time appearance characteristics via various column operating parameters such as adsorbate velocity, concentration of solute in the feed and the bed height of adsorbent that affect the shape of the curve (Sarin and Pant 2006).

Öztürk and Malkoc (Öztürk and Malkoc 2015) evaluated the efficiency of a waste substance, manure ash for the removal of Basic Yellow 2 (BY2) in batch and fixed-bed studies. Fixed-bed adsorption systems were found to perform better for BY2

uptake by manure ash at a lower initial dye concentration (100mg L^{-1}) and higher bed depth (6 cm). For BY2 adsorption, the column adsorption data were fitted well to the Thomas and Yoon–Nelson models. The studied work showed manure ash as an effective low-cost adsorbent for the removal of BY2 from wastewater.

Adsorption of Congo Red (CR) from solution using cationic surfactant modified wheat straw in column model was studied by Zhao et al. (Zhao, Shang et al. 2014) and effects of initial CR concentration, flow rate, bed depth and common salt existed in solution on breakthrough curves were presented. Lower flow rate, lower CR concentration and higher bed depth were found to be advantageous of CR removal from solution. The adsorption data were fitted to the Thomas model at different process conditions.

Ahmad and Hameed (Ahmad and Hameed 2010) investigated the adsorption potential of bamboo waste based granular activated carbon to remove Reactive Black 5 (RB5) from aqueous solution using fixed bed adsorption column. The effects of inlet RB5 concentration, feed flow rate and adsorbent bed height on the breakthrough characteristics of the adsorption system were studied. The maximum bed capacity of 39.02 mg g^{-1} was obtained using 100 mg L^{-1} inlet dye concentration, 80 mm bed height of activated carbon with 10 mL min^{-1} flow rate, and Thomas model was found suitable to describe the breakthrough curve at various experimental conditions.

2.9.1 Theory of Breakthrough Curve (BTC)

In a fixed bed adsorption system, the adsorbent located closest to raw water saturates first where maximum adsorption takes place initially. As time passes, this mass transfer zone moves further to approach the exit of the bed, the adsorption zone moves through the column and the concentration of the adsorbate at the exit becomes equal to the feed concentration. The breakthrough curve is defined as a column effluent concentration over time and the overall performance of fixed bed columns is strongly related to the length and shape of breakthrough curve or ion-exchange zone that develops during adsorption and regeneration. This zone develops between the column section saturated with adsorbate species and the section with fresh adsorbent. When the sorbent saturation zone approaches the end of the column, the adsorbate concentration in the outlet stream increases sharply and the useful life of the column

is ended by approaching the breakthrough point, and the time before breakthrough occurs is the service time of the column (Kratochvil and Volesky 1998). In adsorption studies, the breakthrough curve often observed is the 'S' shape in nature (Fig. 2.6).The shorter the dynamic breakthrough curve zone in the column, the longer the column service time and the larger the fully utilized sorbent portion inside the column.

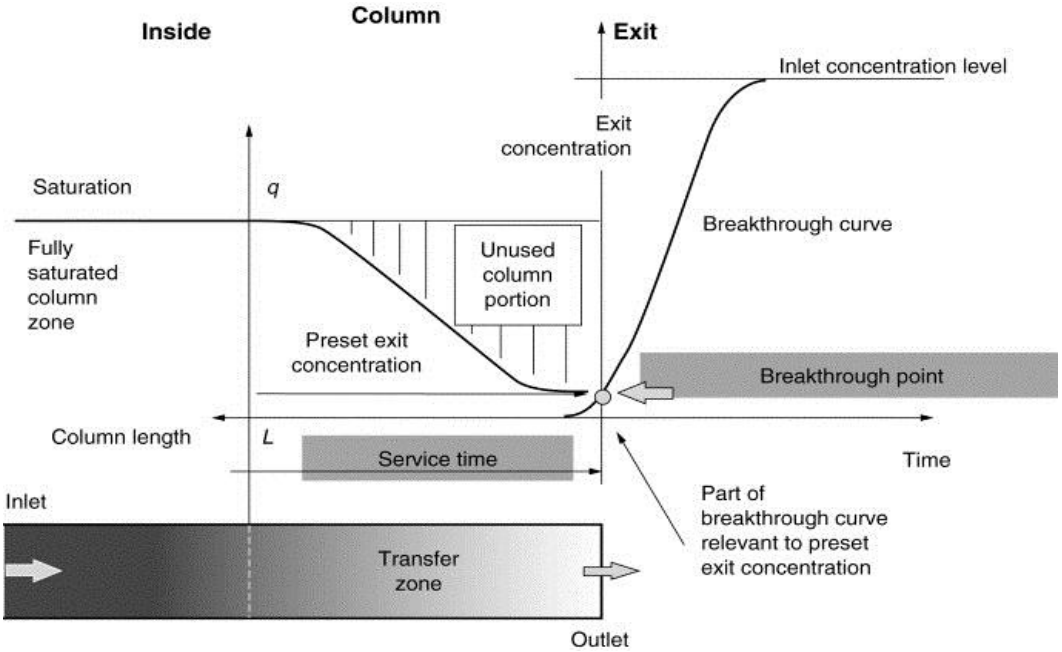

Figure 2.6 Adsorption in a flow-through packed-bed column (Kratochvil and Volesky 1998)

2.9.2 Modelling of Column Dynamic Adsorption

In order to describe the fixed-bed column behaviour and to scale it up for industrial applications, an accurate model needs to be used (Goel, Kadirvelu et al. 2005, Han, Zhang et al. 2006, Han, Zou et al. 2006). Several simple mathematical models have been developed to describe and possibly predict the dynamic behaviour of the bed in column performance (Mobasherpour, Salahi et al. 2014). Hence, to investigate the breakthrough performance, to describe the adsorption kinetics for the calculation of column kinetic parameters and to determine the adsorption capacity of the fixed bed column; Thomas, Yoon–Nelson and BDST models are widely used column dynamics.

2.9.2.1 Thomas Model

The Thomas model (Thomas 1944) is one of the most widely used models in describing the column performance and prediction of breakthrough curves. It assumes plug flow behaviour in the bed (Ahmad and Hameed 2010) and follows the Langmuir kinetics of adsorption. The suitability of Thomas model may be explained that this model assumes negligible axial dispersion in the column adsorption since the rate driving force obeys the second-order reversible reaction kinetics (Futalan, Kan et al. 2011) and considers that sorption is not limited by the chemical reaction but controlled by the mass transfer at the interface (Hasan, Ranjan et al. 2010).

The linearized form of the model is given as (Chowdhury, Zain et al. 2012):

$$\ln\left(\frac{C_O}{C_t} - 1\right) = \left(\frac{K_T\, q_0 m}{Q}\right) - \left(\frac{K_T\, C_0\, V_{eff}}{Q}\right) \qquad (2.13)$$

where K_T is the Thomas rate constant (mL min^{-1} mg^{-1}), q_o is the equilibrium adsorbate uptake (mg g^{-1}), m is the amount of adsorbent in the column (g), C_o is the inlet adsorbate concentration (mg L^{-1}), C_t is the effluent adsorbate concentration (mg L^{-1}), Q is the flow rate (ml min^{-1}) and V_{eff} is the effluent volume (ml).

A linear plot of ln [(C_o/C_t) - 1] against time (t) is to be employed to determine the values of K_T and q_o from the intercept and slope of the plot.

2.9.2.2 Yoon-Nelson model

The Yoon and Nelson model (Yoon and NELSON 1984) is judged as the less complicated column model because it requires no detailed data concerning the characteristics of adsorbate, the type of adsorbent and the physical properties of adsorption bed (Yagub, Sen et al. 2014). The assumption of this model is based on the rate of decrease in the probability of adsorption for each adsorbate molecule is proportional to the probability of adsorbate adsorption and the probability of adsorbate breakthrough on the adsorbent (Yoon and NELSON 1984).

The linearized form of Yoon-Nelson model for a single component system is expressed as:

$$\ln\left(\frac{C_t}{C_0 - C_t}\right) = K_{YN}\, t - K_{YN}\, \tau \qquad (2.14)$$

where K_{YN} is the Yoon and Nelson rate constant (min^{-1}), C_o is the inlet or initial concentration (mg L^{-1}), C_t is the effluent adsorbate concentration (mg L^{-1}), t is the breakthrough (sampling) time (min), and τ is the time required for 50% adsorbate breakthrough (min). The plot of ln [C_t/ (C_o−C_t)] versus sampling time (t) according to Eq. (2.14) will result in a straight line with slope of K_{YN} and intercept K_{YN} τ.

2.9.2.3 Bed Depth Service Time (BDST) Model

BDST is a simple model which states that column bed depth and service time bears a linear relationship in terms of process concentration and adsorption parameters. The Bed Depth Service Time (BDST) model was derived from the equation described by Adams–Bohart, but was modified by Hutchins (Hutchins 1973). This model assumes that forces like intra-particular diffusion and external mass transfer resistance are negligible and that the adsorption kinetics is controlled by surface chemical reaction between the solute in the solution and the unused adsorbent (Baral, Das et al. 2009). It is another most widely used models for comparing adsorption capacity of the adsorption columns under different process variables.

The equation of BDST model can be expressed as (Hutchins 1973) follows :

$$t = \left(\frac{NoH_T}{CoU}\right) - \left(\frac{1}{KoCo}\right) \ln\left(\frac{C_O}{C_t} - 1\right) \quad (2.15)$$

where C_t is the effluent concentration of solute in the liquid phase (mg L^{-1}), C_o is the inlet solute concentration (mg L^{-1}), U is the influent linear velocity (cm min^{-1}), N_o is the adsorption capacity (mg L^{-1}), K_o is the rate constant in BDST model (L mg^{-1} min^{-1}), t is time (min), H_T is the bed height of column (cm).

A plot of t vs. bed height H_T should yield a straight line where N_o and K_o can be determined. A simplified form of the BDST model is as follows:

$$t = az + b \quad (2.16)$$

where slope, a = N_o/C_oU and intercept, b = − $(1/K_oC_o)$ ln $[(C_o/C_t) - 1)]$

2.10 Summary

This chapter presented several treatment techniques for water and wastewater treatment and highlighted a wide range of adsorbent materials especially agricultural solid waste materials as adsorbents for the treatment of industrial effluents that contain a large number of organic dyes and inorganic heavy metals. This chapter provides extensive literature information about dyes and heavy metals, their classification and toxicity, various treatment methods for dyes and heavy metals adsorption and characteristics of various adsorbents. It is clear from the present literature survey that non-conventional adsorbents may become potential and effective adsorbents for dealing with dyes and heavy metal species. Literature also reveals that in some cases the modification of the adsorbent increased the removal efficiency. Therefore, these inexpensive, abundant, locally available and effective raw and treated natural waste materials from agriculture, plant waste, fruit waste and agricultural by-products are an interesting alternative to the traditionally available aqueous waste processing methods such as coagulation, flocculation, chemical oxidation, biological treatment, etc. especially replacing the use of expensive commercial activated carbon for the removal of toxic contaminants (dyes and heavy metals) from wastewater effluents. They also possess some other advantages that make them excellent materials for environmental purposes, such as high capacity and rate of adsorption, high selectivity for different concentrations and also rapid kinetics. From the large number of published literature reviewed here, it is observed that the mechanism and kinetics of dyes and heavy metals adsorption on various adsorbents depend on the chemical nature of the materials and various physico-chemical experimental conditions such as solution pH, initial dye concentration, adsorbent dosage, temperature, ionic load of the system, etc. Therefore the mechanism and dye adsorption behaviour of various adsorbents under these physico-chemical process parameters have been critically analysed here. This review analysis also includes column adsorption study and the application of various column models to carry out the feasibility of various low cost alternative adsorbents at an industrial scale. Hence, the widespread use of low-cost agricultural solid waste adsorbents today will undoubtedly offer a lot of promising benefits for industrial wastewater treatment in commercial purposes due to their local availability, technical feasibility, engineering applicability, and cost effectiveness. This chapter can also help to

propose optimum operating conditions for future studies on water and wastewater detoxification, as well as to improve environmental issues of solid and aquatic industrial waste disposal. As far as the author is concerned, to date only a few modified agricultural by-product waste materials were used to remove organic and inorganic ions from wastewater. This study was undertaken to utilize raw and treated agricultural wastes eucalyptus *sheathiana* bark in the removal of cationic dye methylene blue and inorganic heavy metal Zn^{2+} ions in a more economical way.

2.11 References

Abdelwahab, O., Amin, N. and El-Ashtoukhy, E. Z. (2013). "Removal of zinc ions from aqueous solution using a cation exchange resin." Chemical Engineering Research and Design **91**(1): 165-173.

Abdelwahab, O., Fouad, Y. O., Amin, N. K. and Mandor, H. (2015). "Kinetic and thermodynamic aspects of cadmium adsorption onto raw and activated guava (Psidium guajava) leaves." Environmental Progress & Sustainable Energy **34**(2): 351-358.

Abdolali, A., Guo, W., Ngo, H., Chen, S., Nguyen, N. and Tung, K. (2014). "Typical lignocellulosic wastes and by-products for biosorption process in water and wastewater treatment: a critical review." Bioresource Technology **160**: 57-66.

Abidi, N., Errais, E., Duplay, J., Berez, A., Jrad, A., Schäfer, G., Ghazi, M., Semhi, K. and Trabelsi-Ayadi, M. (2015). "Treatment of dye-containing effluent by natural clay." Journal of Cleaner Production **86**: 432-440.

Acharya, J., Sahu, J., Sahoo, B., Mohanty, C. and Meikap, B. (2009). "Removal of chromium (VI) from wastewater by activated carbon developed from Tamarind wood activated with zinc chloride." Chemical Engineering Journal **150**(1): 25-39.

Adak, A., Bandyopadhyay, M. and Pal, A. (2005). "Removal of crystal violet dye from wastewater by surfactant-modified alumina." Separation and Purification Technology **44**(2): 139-144.

Adolphe, K. S. P.-M., Merlain, T. G., Blaise, L. N. R., Desire, B. B. P., Julius, N., Daouda, K., Julius, G. N., Solomon, A. G. and Joseph, K. M. (2015). "Kinetics and equilibrium studies of the adsorption of nickel (II) ions from aqueous solution onto modified natural and synthetic iron oxide." International Journal of Basic and Applied Sciences **4**(3): 277-287.

Afroze, S. and Sen, T. K. (2015). Agricultural Solid Wastes in Aqueous Phase Dye Adsorption: A Review. Agricultural Wastes Characteristics, Types and Management. C. N. Foster. New York, NOVA Publishers. **1:** 169-214.

Afroze, S., Sen, T. K., Ang, M. and Nishioka, H. (2016). "Adsorption of methylene blue dye from aqueous solution by novel biomass eucalyptus *sheathiana* bark: equilibrium, kinetics, thermodynamics and mechanism." Desalination and Water Treatment **57**(13): 5858-5878.

Agustina, T. E. (2013). AOPs Application on Dyes Removal. Wastewater Reuse and Management, Springer**:** 353-372.

Ahalya, N., Chandraprabha, M., Kanamadi, R. and Ramachandra, T. (2014). "Adsorption of Fast Green on to Coffee Husk." Journal of Chemical Engineering and Research **2**(1): 201-207.

Ahmad, A. and Hameed, B. (2010). "Fixed-bed adsorption of reactive azo dye onto granular activated carbon prepared from waste." Journal of Hazardous Materials **175**(1): 298-303.

Ahmad, A., Idris, A. and Hameed, B. (2013). "Organic dye adsorption on activated carbon derived from solid waste." Desalination and Water Treatment **51**(13-15): 2554-2563.

Ahmadi, A., Heidarzadeh, S., Mokhtari, A. R., Darezereshki, E. and Harouni, H. A. (2014). "Optimization of heavy metal removal from aqueous solutions by maghemite (γ-Fe 2 O 3) nanoparticles using response surface methodology." Journal of Geochemical Exploration **147**: 151-158.

Akkaya, G. and Güzel, F. (2014). "Application of some domestic wastes as new low-cost biosorbents for removal of methylene blue: kinetic and equilibrium studies." Chemical Engineering Communications **201**(4): 557-578.

Aksu, Z. (2001). "Equilibrium and kinetic modelling of cadmium (II) biosorption by C. vulgaris in a batch system: effect of temperature." Separation and Purification Technology **21**(3): 285-294.

Aksu, Z. and Tezer, S. (2005). "Biosorption of reactive dyes on the green alga Chlorella vulgaris." Process Biochemistry **40**(3): 1347-1361.

Ali, H. (2010). "Biodegradation of synthetic dyes—a review." Water, Air, & Soil Pollution **213**(1): 251-273.

Ali, H. (2010). "Biodegradation of synthetic dyes—a review." Water, Air, & Soil Pollution **213**(1): 251-273.

Allen, S. and Koumanova, B. (2005). "Decolourisation of water/wastewater using adsorption." Journal of the University of Chemical Technology and Metallurgy **40**(3): 175-192.

Allen, S., Mckay, G. and Porter, J. (2004). "Adsorption isotherm models for basic dye adsorption by peat in single and binary component systems." Journal of Colloid and Interface Science **280**(2): 322-333.

Anirudhan, T. and Ramachandran, M. (2015). "Adsorptive removal of basic dyes from aqueous solutions by surfactant modified bentonite clay (organoclay): Kinetic and competitive adsorption isotherm." Process Safety and Environmental Protection **95**: 215-225.

Aoudj, S., Khelifa, A., Drouiche, N., Hecini, M. and Hamitouche, H. (2010). "Electrocoagulation process applied to wastewater containing dyes from textile industry." Chemical Engineering and Processing: Process Intensification **49**(11): 1176-1182.

Argun, M. E., Güclü, D. and Karatas, M. (2014). "Adsorption of Reactive Blue 114 dye by using a new adsorbent: Pomelo peel." Journal of Industrial and Engineering Chemistry **20**(3): 1079-1084.

Armagan, B. and Toprak, F. (2015). "Using pistachio shell for Remazol Red removal from aqueous solutions: equilibrium, kinetics and thermodynamics." Desalination and Water Treatment **56**(1): 136–145.

Asgher, M. and Bhatti, H. N. (2012). "Evaluation of thermodynamics and effect of chemical treatments on sorption potential of (Citrus) waste biomass for removal of anionic dyes from aqueous solutions." Ecological Engineering **38**(1): 79-85.

Asokbunyarat, V., van Hullebusch, E. D., Lens, P. N. and Annachhatre, A. P. (2015). Adsorption of Heavy metals from Acid Mine Drainage by Coal Bottom Ash. 4th International Conference on Research Frontiers in Chalcogen Cycle Science & Technology.

Attallah, M., Ahmed, I. and Hamed, M. M. (2013). "Treatment of industrial wastewater containing Congo Red and Naphthol Green B using low-cost adsorbent." Environmental Science and Pollution Research **20**(2): 1106-1116.

Auta, M. and Hameed, B. (2012). "Modified mesoporous clay adsorbent for adsorption isotherm and kinetics of methylene blue." Chemical Engineering Journal **198-199**: 219-227.

Bahramifar, N., Tavasolli, M. and Younesi, H. (2015). "Removal of eosin Y and eosin B dyes from polluted water through biosorption using Saccharomyces cerevisiae: Isotherm, kinetic and thermodynamic studies." Journal of Applied Research in Water and Wastewater **2**(1): 108-114.

Balamurugan, B., Thirumarimurugan, M. and Kannadasan, T. (2011). "Anaerobic degradation of textile dye bath effluent using Halomonas sp." Bioresource Technology **102**(10): 6365-6369.

Banerjee, S. and Chattopadhyaya, M. (2013). "Adsorption characteristics for the removal of a toxic dye, tartrazine from aqueous solution by a low cost agricultural by-product." Arabian Journal of Chemistry.

Bansal, R. C. and Goyal, M. (2010). Activated Carbon Adsorption, CRC press.

Barakat, M. (2011). "New trends in removing heavy metals from industrial wastewater." Arabian Journal of Chemistry **4**(4): 361-377.

Baral, S., Das, N., Ramulu, T., Sahoo, S., Das, S. and Chaudhury, G. R. (2009). "Removal of Cr (VI) by thermally activated weed Salvinia cucullata in a fixed-bed column." Journal of Hazardous Materials **161**(2): 1427-1435.

Barkat, M., Chegrouche, S., Mellah, A., Bensmain, B., Nibou, D. and Boufatit, M. (2014). "Application of Algerian Bentonite in the Removal of Cadmium (II) and Chromium (VI) from Aqueous Solutions." Journal of Surface Engineered Materials and Advanced Technology **2014**.

Baskaralingam, P., Pulikesi, M., Elango, D., Ramamurthi, V. and Sivanesan, S. (2006). "Adsorption of acid dye onto organobentonite." Journal of Hazardous Materials **128**(2): 138-144.

Bayramoğlu, G. and Arıca, M. Y. (2008). "Removal of heavy mercury (II), cadmium (II) and zinc (II) metal ions by live and heat inactivated Lentinus edodes pellets." Chemical Engineering Journal **143**(1): 133-140.

Bello, O. S. and Ahmad, M. A. (2012). "Coconut (Cocos nucifera) shell based activated carbon for the removal of malachite green dye from aqueous solutions." Separation Science and Technology **47**(6): 903-912.

Bensalah, N., Alfaro, M. and Martínez-Huitle, C. (2009). "Electrochemical treatment of synthetic wastewaters containing Alphazurine A dye." Chemical Engineering Journal **149**(1): 348-352.

Bharathi, K. and Ramesh, S. (2013). "Removal of dyes using agricultural waste as low-cost adsorbents: a review." Applied Water Science **3**(4): 773-790.

Bhat, R. and Mathur, P. (1998). "Changing scenario of food colours in India." Current Science **74**(3): 198-202.

Bhatnagar, A. and Minocha, A. (2006). "Conventional and non-conventional adsorbents for removal of pollutants from water-A review." Indian Journal of Chemical Technology **13**(3): 203-217.

Bhattacharya, A., Mandal, S. and Das, S. (2006). "Adsorption of Zn (II) from aqueous solution by using different adsorbents." Chemical Engineering Journal **123**(1): 43-51.

Bhatti, H. N., Mumtaz, B., Hanif, M. A. and Nadeem, R. (2007). "Removal of Zn (II) ions from aqueous solution using Moringa oleifera Lam.(horseradish tree) biomass." Process Biochemistry **42**(4): 547-553.

Bohli, T., Ouederni, A., Fiol, N. and Villaescusa, I. (2015). "Single and binary adsorption of some heavy metal ions from aqueous solutions by activated carbon derived from olive stones." Desalination and Water Treatment **53**(4): 1082-1088.

Boudrahem, F., Aissani-Benissad, F. and Soualah, A. (2015). "Removal of basic yellow dye from aqueous solutions by sorption onto reed as an adsorbent." Desalination and Water Treatment **54**(6): 1727-1734.

Bouguettoucha, A., Chebli, D., Mekhalef, T., Noui, A. and Amrane, A. (2015). "The use of a forest waste biomass, cone of Pinus brutia for the removal of an anionic azo dye Congo red from aqueous medium." Desalination and Water Treatment **55**(7): 1956-1965.

Bulut, Y. and Karaer, H. (2015). "Adsorption of methylene blue from aqueous solution by crosslinked chitosan/bentonite composite." Journal of Dispersion Science and Technology **36**(1): 61-67.

Caner, N., Sarı, A. and Tüzen, M. (2015). "Adsorption Characteristics of Mercury (II) Ions from Aqueous Solution onto Chitosan-Coated Diatomite." Industrial & Engineering Chemistry Research **54**(30): 7524-7533.

Cantuaria, M. L., de Almeida Neto, A. F., Nascimento, E. S. and Vieira, M. G. (2016). "Adsorption of silver from aqueous solution onto pre-treated bentonite clay: complete batch system evaluation." Journal of Cleaner Production **112**: 1112–1121.

Cao, D.-M., Xiao, X., Wu, Y.-M., Ma, X.-B., Wang, M.-N., Wu, Y.-Y. and Du, D.-L. (2013). "Role of electricity production in the anaerobic decolorization of dye mixture by exoelectrogenic bacterium Shewanella oneidensis MR-1." Bioresource Technology **136**: 176-181.

Carmen, Z. and Daniela, S. (2012). "Textile organic dyes–characteristics, polluting effects and separation/elimination procedures from industrial effluents–a critical overview." ISBN: 978-953.

Çelekli, A., Çelekli, F., Çiçek, E. and Bozkurt, H. (2014). "Predictive modeling of sorption and desorption of a reactive azo dye by pumpkin husk." Environmental Science and Pollution Research **21**(7): 5086-5097.

Chakraborty, S., Chowdhury, S. and Das Saha, P. (2011). "Adsorption of Crystal Violet from aqueous solution onto NaOH-modified rice husk." Carbohydrate Polymers **86**(4): 1533-1541.

Chakraborty, S., Chowdhury, S. and Saha, P. D. (2012). "Insight into biosorption equilibrium, kinetics and thermodynamics of crystal violet onto Ananas comosus (pineapple) leaf powder." Applied Water Science: 1-7.

Chen, M., Ding, W., Wang, J. and Diao, G. (2013). "Removal of azo dyes from water by combined techniques of adsorption, desorption, and electrolysis based on a supramolecular sorbent." Industrial & Engineering Chemistry Research **52**(6): 2403-2411.

Chen, S., Yue, Q., Gao, B. and Xu, X. (2010). "Equilibrium and kinetic adsorption study of the adsorptive removal of Cr (VI) using modified wheat residue." Journal of Colloid and Interface Science **349**(1): 256-264.

Chen, Z., Deng, H., Chen, C., Yang, Y. and Xu, H. (2014). "Biosorption of malachite green from aqueous solutions by Pleurotus ostreatus using Taguchi method." Journal of Environmental Health Science and Engineering **12**(1): 63.

Cheremisinoff, N. P. (2001). Handbook of water and wastewater treatment technologies. Boston, Butterworth-Heinemann.

Chieng, H. I., Lim, L. B. and Priyantha, N. (2015). "Enhancing adsorption capacity of toxic malachite green dye through chemically modified breadnut peel: equilibrium, thermodynamics, kinetics and regeneration studies." Environmental Technology **36**(1): 86-97.

Chowdhury, Z., Zain, S., Rashid, A., Rafique, R. and Khalid, K. (2012). "Breakthrough curve analysis for column dynamics sorption of Mn (II) ions from wastewater by using Mangostana garcinia peel-based granular-activated carbon." Journal of Chemistry **2013**.

Cook, S. M. F. and Linden, D. R. (1997). "Use of rhodamine WT to facilitate dilution and analysis of atrazine samples in short-term transport studies." Journal of Environmental Quality **26**(5): 1438-1440.

Crini, G. (2006). "Non-conventional low-cost adsorbents for dye removal: a review." Bioresource Technology **97**(9): 1061-1085.

Da Silva, J. F. and Williams, R. J. P. (2001). The biological chemistry of the elements: the inorganic chemistry of life, Oxford University Press.

Dağdelen, S., Acemioğlu, B., Baran, E. and Koçer, O. (2014). "Removal of Remazol Brilliant Blue R From Aqueous Solution by Pirina Pretreated with Nitric Acid and Commercial Activated Carbon." Water, Air, & Soil Pollution **225**(3): 1-15.

Dawood, S. and Sen, T. K. (2012). "Removal of anionic dye Congo red from aqueous solution by raw pine and acid-treated pine cone powder as adsorbent: Equilibrium, thermodynamic, kinetics, mechanism and process design." Water Research **46**(6): 1933-1946.

Dawood, S. and Sen, T. K. (2013). "Review on dye removal from its aqueous solution into alternative cost effective and non-conventional adsorbents." Journal of Chemical and Process Engineering **1**(1): 1.

Demiral, H., Demiral, I., Tümsek, F. and Karabacakoğlu, B. (2008). "Adsorption of chromium (VI) from aqueous solution by activated carbon derived from olive bagasse and applicability of different adsorption models." Chemical Engineering Journal **144**(2): 188-196.

Demirbas, A. (2009). "Agricultural based activated carbons for the removal of dyes from aqueous solutions: a review." Journal of Hazardous Materials **167**(1): 1-9.

Demirbaş, Ö. and Alkan, M. (2015). "Adsorption kinetics of a cationic dye from wastewater." Desalination and Water Treatment **53**(13): 3623-3631.

Demirbaş, Ö., Turhan, Y. and Alkan, M. (2015). "Thermodynamics and kinetics of adsorption of a cationic dye onto sepiolite." Desalination and Water Treatment **54**(3): 707-714.

Deng, L., Shi, Z., Li, B., Yang, L., Luo, L. and Yang, X. (2014). "Adsorption of Cr (VI) and phosphate on Mg–Al hydrotalcite supported kaolin clay prepared by ultrasound-assisted coprecipitation method using batch and fixed-bed systems." Industrial & Engineering Chemistry Research **53**(18): 7746-7757.

Deniz, F. and Karaman, S. (2011). "Removal of Basic Red 46 dye from aqueous solution by pine tree leaves." Chemical Engineering Journal **170**(1): 67-74.

Deniz, F. and Saygideger, S. D. (2010). "Investigation of adsorption characteristics of Basic Red 46 onto gypsum: Equilibrium, kinetic and thermodynamic studies." Desalination **262**(1): 161-165.

Dod, R., Banerjee, G. and Saini, S. (2012). "Adsorption of methylene blue using green pea peels (Pisum sativum): A cost-effective option for dye-based wastewater treatment." Biotechnology and Bioprocess Engineering **17**(4): 862-874.

Duffus, J. H. (2002). ""Heavy metals" a meaningless term? (IUPAC Technical Report)." Pure and Applied Chemistry **74**(5): 793-807.

Duran, C., Ozdes, D., Gundogdu, A. and Senturk, H. B. (2011). "Kinetics and isotherm analysis of basic dyes adsorption onto almond shell (Prunus dulcis) as a low cost adsorbent." Journal of Chemical & Engineering Data **56**(5): 2136-2147.

Dursun, A. Y., Tepe, O., Uslu, G., Dursun, G. and Saatci, Y. (2013). "Kinetics of Remazol Black B adsorption onto carbon prepared from sugar beet pulp." Environmental Science and Pollution Research **20**: 2472-2483.

El-Ashtoukhy, E.-S., Amin, N. and Abdelwahab, O. (2008). "Removal of lead (II) and copper (II) from aqueous solution using pomegranate peel as a new adsorbent." Desalination **223**(1): 162-173.

El-Halwany, M. (2010). "Study of adsorption isotherms and kinetic models for Methylene Blue adsorption on activated carbon developed from Egyptian rice hull (Part II)." Desalination **250**(1): 208-213.

El Qada, E. N., Allen, S. J. and Walker, G. M. (2008). "Adsorption of basic dyes from aqueous solution onto activated carbons." Chemical Engineering Journal **135**(3): 174-184.

Fedoseeva, M., Fita, P., Punzi, A. and Vauthey, E. (2010). "Salt effect on the formation of dye aggregates at liquid/liquid interfaces studied by time-resolved surface second harmonic generation." The Journal of Physical Chemistry C **114**(32): 13774-13781.

Feng, N.-c. and Guo, X.-y. (2012). "Characterization of adsorptive capacity and mechanisms on adsorption of copper, lead and zinc by modified orange peel." Transactions of Nonferrous Metals Society of China **22**(5): 1224-1231.

Feng, Y., Zhou, H., Liu, G., Qiao, J., Wang, J., Lu, H., Yang, L. and Wu, Y. (2012). "Methylene blue adsorption onto swede rape straw (Brassica napus) modified by tartaric acid: equilibrium, kinetic and adsorption mechanisms." Bioresource Technology **125**: 138-144.

Ferrero, F. (2007). "Dye removal by low cost adsorbents: Hazelnut shells in comparison with wood sawdust." Journal of Hazardous Materials **142**(1): 144-152.

Franca, A. S., Oliveira, L. S. and Ferreira, M. E. (2009). "Kinetics and equilibrium studies of methylene blue adsorption by spent coffee grounds." Desalination **249**(1): 267-272.

Freundlich, H. (1906). "Over the adsorption in solution." J. Phys. Chem **57**: 385-470.

Fu, F. and Wang, Q. (2011). "Removal of heavy metal ions from wastewaters: a review." Journal of Environmental Management **92**(3): 407-418.

Fu, Y. and Viraraghavan, T. (2001). "Fungal decolorization of dye wastewaters: a review." Bioresource technology **79**(3): 251-262.

Fu, Y. and Viraraghavan, T. (2002). "Dye biosorption sites in Aspergillus niger." Bioresource Technology **82**(2): 139-145.

Futalan, C. M., Kan, C.-C., Dalida, M. L., Pascua, C. and Wan, M.-W. (2011). "Fixed-bed column studies on the removal of copper using chitosan immobilized on bentonite." Carbohydrate Polymers **83**(2): 697-704.

Galletti, C., Russo, N. and Fino, D. (2015). "Zn2+ removal from wastewater using rice husk as an adsorbent." Journal of Chemical Engineering Research Studies **2**(1): 2.

Gautam, R. K., Mudhoo, A., Lofrano, G. and Chattopadhyaya, M. C. (2014). "Biomass-derived biosorbents for metal ions sequestration: Adsorbent modification and activation methods and adsorbent regeneration." Journal of Environmental Chemical Engineering **2**(1): 239-259.

Geetha, K. and Belagali, S. (2013). "Removal of heavy metals and dyes using low cost adsorbents from aqueous medium—a review." IOSR Journal of Environmental Science and Toxicology Food Technology **4**(3): 56-68.

Ghobarkar, H., Schäf, O. and Guth, U. (1999). "Zeolites—from kitchen to space." Progress in Solid State Chemistry **27**(2): 29-73.

Ghodbane, I. and Hamdaoui, O. (2008). "Removal of mercury (II) from aqueous media using eucalyptus bark: kinetic and equilibrium studies." Journal of Hazardous Materials **160**(2): 301-309.

Ghodbane, I., Nouri, L., Hamdaoui, O. and Chiha, M. (2008). "Kinetic and equilibrium study for the sorption of cadmium (II) ions from aqueous phase by eucalyptus bark." Journal of Hazardous Materials **152**(1): 148-158.

Ghosh, A., Ghosh Dastidar, M. and Sreekrishnan, T. (2015). "Recent Advances in Bioremediation of Heavy Metals and Metal Complex Dyes: Review." Journal of Environmental Engineering: C4015003.

Ghosh, R. K. and Reddy, D. D. (2013). "Tobacco Stem Ash as an Adsorbent for Removal of Methylene Blue from Aqueous Solution: Equilibrium, Kinetics, and Mechanism of Adsorption." Water, Air, & Soil Pollution **224**(6): 1-12.

Goel, J., Kadirvelu, K., Rajagopal, C. and Garg, V. K. (2005). "Removal of lead (II) by adsorption using treated granular activated carbon: batch and column studies." Journal of Hazardous Materials **125**(1): 211-220.

Gong, R., Jin, Y., Chen, J., Hu, Y. and Sun, J. (2007). "Removal of basic dyes from aqueous solution by sorption on phosphoric acid modified rice straw." Dyes and Pigments **73**(3): 332-337.

Gücek, A., Şener, S., Bilgen, S. and Mazmancı, M. A. (2005). "Adsorption and kinetic studies of cationic and anionic dyes on pyrophyllite from aqueous solutions." Journal of Colloid and Interface Science **286**(1): 53-60.

Guechi, E.-K. and Hamdaoui, O. (2011). "Sorption of malachite green from aqueous solution by potato peel: kinetics and equilibrium modeling using non-linear analysis method." Arabian Journal of Chemistry.

Guo, Y., Yang, S., Fu, W., Qi, J., Li, R., Wang, Z. and Xu, H. (2003). "Adsorption of malachite green on micro-and mesoporous rice husk-based active carbon." Dyes and Pigments **56**(3): 219-229.

Gupta, V. (2009). "Application of low-cost adsorbents for dye removal–A review." Journal of Environmental Management **90**(8): 2313-2342.

Gupta, V. and Rastogi, A. (2008). "Equilibrium and kinetic modelling of cadmium (II) biosorption by nonliving algal biomass Oedogonium sp. from aqueous phase." Journal of Hazardous Materials **153**(1): 759-766.

Gutha, Y., Munagapati, V. S., Naushad, M. and Abburi, K. (2015). "Removal of Ni (II) from aqueous solution by Lycopersicum esculentum (Tomato) leaf powder as a low-cost biosorbent." Desalination and Water Treatment **54**(1): 200-208.

Hadi, M., Samarghandi, M. R. and McKay, G. (2011). "Simplified fixed bed design models for the adsorption of acid dyes on novel pine cone derived activated carbon." Water, Air, & Soil Pollution **218**(1-4): 197-212.

Hameed, B. (2008). "Equilibrium and kinetic studies of methyl violet sorption by agricultural waste." Journal of Hazardous Materials **154**(1): 204-212.

Hameed, B. (2009). "Evaluation of papaya seeds as a novel non-conventional low-cost adsorbent for removal of methylene blue." Journal of Hazardous Materials **162**(2): 939-944.

Hameed, B. and Ahmad, A. (2009). "Batch adsorption of methylene blue from aqueous solution by garlic peel, an agricultural waste biomass." Journal of Hazardous Materials **164**(2): 870-875.

Hameed, B., Krishni, R. and Sata, S. (2009). "A novel agricultural waste adsorbent for the removal of cationic dye from aqueous solutions." Journal of Hazardous Materials **162**(1): 305-311.

Hameed, B., Mahmoud, D. and Ahmad, A. (2008). "Equilibrium modeling and kinetic studies on the adsorption of basic dye by a low-cost adsorbent: Coconut (Cocos nucifera) bunch waste." Journal of Hazardous Materials **158**(1): 65-72.

Han, R., Zhang, J., Zou, W., Xiao, H., Shi, J. and Liu, H. (2006). "Biosorption of copper (II) and lead (II) from aqueous solution by chaff in a fixed-bed column." Journal of Hazardous Materials **133**(1): 262-268.

Han, R., Zou, W., Li, H., Li, Y. and Shi, J. (2006). "Copper (II) and lead (II) removal from aqueous solution in fixed-bed columns by manganese oxide coated zeolite." Journal of Hazardous Materials **137**(2): 934-942.

Han, X., Niu, X. and Ma, X. (2012). "Adsorption characteristics of methylene blue on poplar leaf in batch mode: Equilibrium, kinetics and thermodynamics." Korean Journal of Chemical Engineering: 1-9.

Han, X., Yuan, J. and Ma, X. (2014). "Adsorption of malachite green from aqueous solutions onto lotus leaf: equilibrium, kinetic, and thermodynamic studies." Desalination and Water Treatment **52**(28-30): 5563-5574.

Handan, U. (2011). "Equilibrium, thermodynamic and kinetics of reactive black 5 biosorption on loquat (Eriobotrya japonica) seed." Science Research Essays **6**(19): 4113-4124.

Hasan, S., Ranjan, D. and Talat, M. (2010). "Agro-industrial waste 'wheat bran'for the biosorptive remediation of selenium through continuous up-flow fixed-bed column." Journal of Hazardous Materials **181**(1): 1134-1142.

Heidmann, I. and Calmano, W. (2008). "Removal of Zn (II), Cu (II), Ni (II), Ag (I) and Cr (VI) present in aqueous solutions by aluminium electrocoagulation." Journal of Hazardous Materials **152**(3): 934-941.

Ho, Y.-S. and McKay, G. (1999). "Pseudo-second order model for sorption processes." Process Biochemistry **34**(5): 451-465.

Ho, Y. S. and McKay, G. (2003). "Sorption of dyes and copper ions onto biosorbents." Process Biochemistry **38**(7): 1047-1061.

Hoseinzadeh, E., Samarghandi, M.-R., McKay, G., Rahimi, N. and Jafari, J. (2014). "Removal of acid dyes from aqueous solution using potato peel waste biomass: a kinetic and equilibrium study." Desalination and Water Treatment **52**(25-27): 4999-5006.

Hussin, Z. M., Talib, N., Hussin, N. M., Hanafiah, M. A. and Khalir, W. K. (2015). "Methylene Blue Adsorption onto NaOH Modified Durian Leaf Powder: Isotherm and Kinetic Studies." American Journal of Environmental Engineering **5**(3A): 38-43.

Hutchins, R. (1973). "New method simplifies design of activated-carbon systems." Chemical Engineering **80**(19): 133-138.

Imaga, C., Abia, A. and Igwe, J. (2015). "Adsorption Isotherm Studies of Ni (II), Cu (II) and Zn (II) Ions on Unmodified and Mercapto-Acetic Acid (MAA) Modified Sorghum Hulls." International Research Journal of Pure and Applied Chemistry **5**(4): 318.

Imam Maarof, H., Hameed, B. H. and Ahmad, A. L. (2003). "Aqueous-Phase Adsorption Of Phenolic Compounds On Activated Carbon."

Iram, M., Guo, C., Guan, Y., Ishfaq, A. and Liu, H. (2010). "Adsorption and magnetic removal of neutral red dye from aqueous solution using Fe3O4 hollow nanospheres." Journal of Hazardous Materials **181**(1): 1039-1050.

Ivanov, K., Gruber, E., Schempp, W. and Kirov, D. (1996). "Possibilities of using zeolite as filler and carrier for dyestuffs in paper." Papier-Zeitschrift fur die Erzeugung von Holzstoff Zellstoff Papier und Pappe **50**(7): 456-459.

Jain, S. and Jayaram, R. V. (2010). "Removal of basic dyes from aqueous solution by low-cost adsorbent: Wood apple shell (< i> Feronia acidissima</i>)." Desalination **250**(3): 921-927.

Jiang, K., Sun, T.-h., Sun, L.-n. and Li, H.-b. (2006). "Adsorption characteristics of copper, lead, zinc and cadmium ions by tourmaline." Journal of Environmental Sciences **18**(6): 1221-1225.

Kabdaşli, I., Tünay, O. and Orhon, D. (1999). "Wastewater control and management in a leather tanning district." Water Science and Technology **40**(1): 261-267.

Kang, S.-Y., Lee, J.-U., Moon, S.-H. and Kim, K.-W. (2004). "Competitive adsorption characteristics of Co 2+, Ni 2+, and Cr 3+ by IRN-77 cation exchange resin in synthesized wastewater." Chemosphere **56**(2): 141-147.

Kannan, N. and Sundaram, M. M. (2001). "Kinetics and mechanism of removal of methylene blue by adsorption on various carbons—a comparative study." Dyes and Pigments **51**(1): 25-40.

Karami, H. (2013). "Heavy metal removal from water by magnetite nanorods." Chemical Engineering Journal **219**: 209-216.

Kavitha, D. and Namasivayam, C. (2007). "Experimental and kinetic studies on methylene blue adsorption by coir pith carbon." Bioresource Technology **98**(1): 14-21.

Kazemipour, M., Ansari, M., Tajrobehkar, S., Majdzadeh, M. and Kermani, H. R. (2008). "Removal of lead, cadmium, zinc, and copper from industrial wastewater by carbon developed from walnut, hazelnut, almond, pistachio shell, and apricot stone." Journal of Hazardous Materials **150**(2): 322-327.

Khalid, K., Ngah, W. S., Hanafiah, M. A., Malek, N. S. and Khazaai, S. N. (2015). "Acid Blue 25 Adsorption onto Phosphoric Acid Treated Rubber Leaf Powder." American Journal of Environmental Engineering **5**(3A): 19-25.

Khan, T. A. and Khan, E. A. (2015). "Removal of basic dyes from aqueous solution by adsorption onto binary iron-manganese oxide coated kaolinite: Non-linear isotherm and kinetics modeling." Applied Clay Science **107**: 70-77.

Khangarot, B. and Ray, P. (1989). "Investigation of correlation between physicochemical properties of metals and their toxicity to the water flea Daphnia magna Straus." Ecotoxicology and environmental safety **18**(2): 109-120.

Kharat, D. (2015). "Preparing agricultural residue based adsorbents for removal of dyes from effluents - a review." Brazilian Journal of Chemical Engineering **32**(1): 1-12.

Khokhar, A. and Siddique, Z. (2015). "Removal of heavy metal ions by chemically treated Melia azedarach L. leaves." Journal of Environmental Chemical Engineering **3**(2): 944-952.

Khosla, E., Kaur, S. and Dave, P. N. (2013). "Tea waste as adsorbent for ionic dyes." Desalination and Water Treatment **51**(34-36): 6552-6561.

Kim, S. Y., Jin, M. R., Chung, C. H., Yun, Y.-S., Jahng, K. Y. and Yu, K.-Y. (2015). "Biosorption of cationic basic dye and cadmium by the novel biosorbent Bacillus catenulatus JB-022 strain." Journal of Bioscience and Bioengineering **119**(4): 433-439.

Koçer, O. and Acemioğlu, B. (2015). "Adsorption of Basic green 4 from aqueous solution by olive pomace and commercial activated carbon: process design, isotherm, kinetic and thermodynamic studies." Desalination and Water Treatment: 1-17.

Kochher, M. S. and Kumar, S. (2012). "Screening For Potential Textile Dye Decolorizing Bacteria." International Journal for Science and Emerging Technologies with Latest Trends **2**(1): 36-48.

Kratochvil, D. and Volesky, B. (1998). "Advances in the biosorption of heavy metals." Trends in Biotechnology **16**(7): 291-300.

Krishnan, K. A., Sreejalekshmi, K., Vimexen, V. and Dev, V. V. (2016). "Evaluation of adsorption properties of sulphurised activated carbon for the effective and economically viable removal of Zn (II) from aqueous solutions." Ecotoxicology and Environmental Safety **124**: 418-425.

Kross, B. C., Nicholson, H. F. and Ogilvie, L. K. (1996). "Methods development study for measuring pesticide exposure to golf course workers using video imaging techniques." Applied Occupational and Environmental Hygiene **11**(11): 1346-1350.

Krysztafkiewicz, A., Binkowski, S. and Jesionowski, T. (2002). "Adsorption of dyes on a silica surface." Applied Surface Science **199**(1): 31-39.

Kumar, K. Y., Muralidhara, H., Nayaka, Y. A., Balasubramanyam, J. and Hanumanthappa, H. (2013). "Low-cost synthesis of metal oxide nanoparticles and their application in adsorption of commercial dye and heavy metal ion in aqueous solution." Powder Technology **246**: 125-136.

Kuo, C.-Y., Wu, C.-H. and Wu, J.-Y. (2008). "Adsorption of direct dyes from aqueous solutions by carbon nanotubes: Determination of equilibrium, kinetics and thermodynamics parameters." Journal of Colloid and Interface Science **327**(2): 308-315.

Kurniawan, T. A., Chan, G. Y., Lo, W.-H. and Babel, S. (2006). "Physico–chemical treatment techniques for wastewater laden with heavy metals." Chemical Engineering Journal **118**(1): 83-98.

Kyzas, G. Z., Lazaridis, N. K. and Mitropoulos, A. C. (2012). "Removal of dyes from aqueous solutions with untreated coffee residues as potential low-cost adsorbents: Equilibrium, reuse and thermodynamic approach." Chemical Engineering Journal **189-190**: 148-159.

Kyzas, G. Z., Siafaka, P. I., Pavlidou, E. G., Chrissafis, K. J. and Bikiaris, D. N. (2015). "Synthesis and adsorption application of succinyl-grafted chitosan for the

simultaneous removal of zinc and cationic dye from binary hazardous mixtures." Chemical Engineering Journal **259**: 438-448.

Lafi, R., ben Fradj, A., Hafiane, A. and Hameed, B. (2014). "Coffee waste as potential adsorbent for the removal of basic dyes from aqueous solution." Korean Journal of Chemical Engineering: 1-9.

Lagergren, S. (1898). "About the theory of so-called adsorption

of soluble substances

" Kungliga Svenska Vetenskapsakad

Handlinger **24**(4): 1-39.

Lalhruaitluanga, H., Jayaram, K., Prasad, M. and Kumar, K. (2010). "Lead (II) adsorption from aqueous solutions by raw and activated charcoals of Melocanna baccifera Roxburgh (bamboo)—a comparative study." Journal of Hazardous Materials **175**(1): 311-318.

Langmuir, I. (1918). "The adsorption of gases on plane surfaces of glass, mica and platinum." Journal of the American Chemical Society **40**(9): 1361-1403.

Li, Z., Imaizumi, S., Katsumi, T., Inui, T., Tang, X. and Tang, Q. (2010). "Manganese removal from aqueous solution using a thermally decomposed leaf." Journal of Hazardous Materials **177**(1): 501-507.

Lin, S. H. and Chang, C. C. (2000). "Treatment of landfill leachate by combined electro-Fenton oxidation and sequencing batch reactor method." Water Research **34**(17): 4243-4249.

Liu, W., Yao, C., Wang, M., Ji, J., Ying, L. and Fu, C. (2012). "Kinetics and thermodynamics characteristics of cationic yellow X-GL adsorption on attapulgite/rice hull-based activated carbon nanocomposites." Environmental Progress & Sustainable Energy **32**(3): 655-662.

Lorenc-Grabowska, E. and Gryglewicz, G. (2007). "Adsorption characteristics of Congo Red on coal-based mesoporous activated carbon." Dyes and Pigments **74**(1): 34-40.

Low, L. W., Teng, T. T., Rafatullah, M., Morad, N. and Azahari, B. (2013). "Adsorption studies of methylene blue and malachite green from aqueous solutions by pretreated lignocellulosic materials." Separation Science and Technology **48**(11): 1688-1698.

Ma, Q., Shen, F., Lu, X., Bao, W. and Ma, H. (2013). "Studies on the adsorption behavior of methyl orange from dye wastewater onto activated clay." Desalination and Water Treatment **51**(19-21): 3700-3709.

Madala, S., Mudumala, V. N. R., Vudagandla, S. and Abburi, K. (2015). "Modified leaf biomass for Pb (II) removal from aqueous solution: Application of response surface methodology." Ecological Engineering **83**: 218-226.

Mall, I. D., Srivastava, V. C., Agarwal, N. K. and Mishra, I. M. (2005). "Adsorptive removal of malachite green dye from aqueous solution by bagasse fly ash and activated carbon-kinetic study and equilibrium isotherm analyses." Colloids and Surfaces A: Physicochemical and Engineering Aspects **264**(1): 17-28.

Mane, V. S. and Babu, P. (2011). "Studies on the adsorption of Brilliant Green dye from aqueous solution onto low-cost NaOH treated saw dust." Desalination **273**(2): 321-329.

Maneerung, T., Liew, J., Dai, Y., Kawi, S., Chong, C. and Wang, C.-H. (2016). "Activated carbon derived from carbon residue from biomass gasification and its application for dye adsorption: Kinetics, isotherms and thermodynamic studies." Bioresource Technology **200**: 350-359.

Maurya, N. S., Mittal, A. K., Cornel, P. and Rother, E. (2006). "Biosorption of dyes using dead macro fungi: Effect of dye structure, ionic strength and pH." Bioresource Technology **97**(3): 512-521.

McCabe, W. L., Smith, J. C. and Harriott, P. (1993). Unit operations of chemical engineering, McGraw-Hill New York.

McKay, G., Guendi, M. E. and Nassar, M. (1997). "Adsorption model for the removal of acids dyes from effluent by bagasse pith using a simplified isotherm." Adsorption Science and Technology **15**(10): 737-752.

Merzouk, B., Gourich, B., Madani, K., Vial, C. and Sekki, A. (2011). "Removal of a disperse red dye from synthetic wastewater by chemical coagulation and continuous electrocoagulation. A comparative study." Desalination **272**(1): 246-253.

Mobasherpour, I., Salahi, E. and Asjodi, A. (2014). "Research on the Batch and Fixed-Bed Column Performance of Red Mud Adsorbents for Lead Removal." Soil and Water **4**: 5.

Mortaheb, H. R., Kosuge, H., Mokhtarani, B., Amini, M. H. and Banihashemi, H. R. (2009). "Study on removal of cadmium from wastewater by emulsion liquid membrane." Journal of Hazardous Materials **165**(1): 630-636.

Najafi, H., Pajootan, E., Ebrahimi, A. and Arami, M. (2015). "The potential application of tomato seeds as low-cost industrial waste in the adsorption of organic dye molecules from colored effluents." Desalination and Water Treatment: 1-11.

Nassar, N. N. (2010). "Kinetics, mechanistic, equilibrium, and thermodynamic studies on the adsorption of acid red dye from wastewater by γ-Fe2O3 nanoadsorbents." Separation Science and Technology **45**(8): 1092-1103.

Nausheen, S., Bhatti, H. N., Furrukh, Z., Sadaf, S. and Noreen, S. (2014). "Adsorptive removal of Drimarine Red HF-3D dye from aqueous solution using low-cost agricultural waste: batch and column study." Chemistry and Ecology **30**(4): 376-392.

Nawaz, S., Bhatti, H. N., Bokhari, T. H. and Sadaf, S. (2014). "Removal of Novacron Golden Yellow dye from aqueous solutions by low-cost agricultural waste: Batch and fixed bed study." Chemistry and Ecology **30**(1): 52-65.

Nieboer, E. and Richardson, D. H. (1980). "The replacement of the nondescript term 'heavy metals' by a biologically and chemically significant classification of metal ions." Environmental Pollution Series B, Chemical and Physical **1**(1): 3-26.

Niemi, H., Lahti, J., Hatakka, H., Kärki, S., Rovio, S., Kallioinen, M., Mänttäri, M. and Louhi-Kultanen, M. (2011). "Fractionation of organic and inorganic compounds from black liquor by combining membrane separation and crystallization." Chemical Engineering & Technology **34**(4): 593-598.

O'Mahony, T., Guibal, E. and Tobin, J. (2002). "Reactive dye biosorption by Rhizopus arrhizus biomass." Enzyme and Microbial Technology **31**(4): 456-463.

Oberlander, D. H.-E. and Roth, K. (1978). "Effect of the heavy metals chromium, nickel, copper, zinc, cadmium, mercury and lead on uptake and translocation of K and P by young barley plants." Journal of Plant Nutrition and Soil Science **141**(1): 107-116.

Ofomaja, A. and Naidoo, E. (2011). "Biosorption of copper from aqueous solution by chemically activated pine cone: a kinetic study." Chemical Engineering Journal **175**: 260-270.

Ofomaja, A., Naidoo, E. and Modise, S. (2009). "Removal of copper (II) from aqueous solution by pine and base modified pine cone powder as biosorbent." Journal of Hazardous Materials **168**(2): 909-917.

Oladoja, N., Aboluwoye, C., Oladimeji, Y., Ashogbon, A. and Otemuyiwa, I. (2008). "Studies on castor seed shell as a sorbent in basic dye contaminated wastewater remediation." Desalination **227**(1-3): 190-203.

Oliveira, L. S., Franca, A. S., Alves, T. M. and Rocha, S. D. F. (2008). "Evaluation of untreated coffee husks as potential biosorbents for treatment of dye contaminated waters." Journal of Hazardous Materials **155**(3): 507-512.

Önal, E., Özbay, N., Yargıç, A. Ş., Şahin, R. Z. Y. and Gök, Ö. (2014). Performance Evaluation of the Bio-char Heavy Metal Removal Produced from Tomato Factory Waste. Progress in Exergy, Energy, and the Environment, Springer**:** 733-740.

Ong, S.-A., Ho, L.-N., Wong, Y.-S. and Zainuddin, A. (2013). "Adsorption behavior of cationic and anionic dyes onto acid treated coconut coir." Separation Science and Technology **48**(14): 2125-2131.

Ong, S., Lee, C. and Zainal, Z. (2007). "Removal of basic and reactive dyes using ethylenediamine modified rice hull." Bioresource Technology **98**(15): 2792-2799.

Ozacar, M. and Sengil, I. A. (2005). "Adsorption of metal complex dyes from aqueous solutions by pine sawdust." Bioresource Technology **96**(7): 791-795.

Ozer, C., Imamoglu, M., Turhan, Y. and Boysan, F. (2012). "Removal of methylene blue from aqueous solutions using phosphoric acid activated carbon produced from hazelnut husks." Toxicological & Environmental Chemistry **94**(7): 1283-1293.

Öztürk, A. and Malkoc, E. (2015). "Cationic Basic Yellow 2 (BY2) adsorption onto manure ash: surface properties and adsorption mechanism." Desalination and Water Treatment **54**(1): 209-226.

Pandharipande, S. and Kalnake, R. P. (2013). "Tamarind fruit shell adsorbent synthesis, characterization and adsorption studies for Cr(VI) & Ni(II) ions from aqueous solution." International Journal of Engineering Sciences & Emerging Technologies **4**(2): 83-89.

Pang, Y. L. and Abdullah, A. Z. (2013). "Current status of textile industry wastewater management and research progress in Malaysia: a review." Clean–Soil, Air, Water **41**(8): 751-764.

Pavan, F. A., Camacho, E. S., Lima, E. C., Dotto, G. L., Branco, V. T. and Dias, S. L. (2014). "Formosa papaya seed powder (FPSP): Preparation, characterization and application as an alternative adsorbent for the removal of crystal violet from aqueous phase." Journal of Environmental Chemical Engineering **2**(1): 230-238.

Pavan, F. A., Lima, E. C., Dias, S. L. P. and Mazzocato, A. C. (2008). "Methylene blue biosorption from aqueous solutions by yellow passion fruit waste." Journal of Hazardous Materials **150**(3): 703-712.

Phalakornkule, C., Polgumhang, S., Tongdaung, W., Karakat, B. and Nuyut, T. (2010). "Electrocoagulation of blue reactive, red disperse and mixed dyes, and application in treating textile effluent." Journal of Environmental Management **91**(4): 918-926.

Prithviraj, D., Deboleena, K., Neelu, N., Noor, N., Aminur, R., Balasaheb, K. and Abul, M. (2014). "Biosorption of nickel by Lysinibacillus sp. BA2 native to bauxite mine." Ecotoxicology and Environmental Safety **107**: 260-268.

Putra, W. P., Kamari, A., Yusoff, S. N. M., Ishak, C. F., Mohamed, A., Hashim, N. and Isa, I. M. (2014). "Biosorption of Cu (II), Pb (II) and Zn (II) ions from aqueous solutions using selected waste materials: Adsorption and characterisation studies." Journal of Encapsulation and Adsorption Sciences **4**(1).

Puyen, Z. M., Villagrasa, E., Maldonado, J., Diestra, E., Esteve, I. and Solé, A. (2012). "Biosorption of lead and copper by heavy-metal tolerant Micrococcus luteus DE2008." Bioresource Technology **126**: 233-237.

Qiu, G., Xie, Q., Liu, H., Chen, T., Xie, J. and Li, H. (2015). "Removal of Cu (II) from aqueous solutions using dolomite–palygorskite clay: Performance and mechanisms." Applied Clay Science **118**: 107-115.

Qu, J., Zhang, Q., Xia, Y., Cong, Q. and Luo, C. (2015). "Synthesis of carbon nanospheres using fallen willow leaves and adsorption of Rhodamine B and heavy metals by them." Environmental Science and Pollution Research **22**(2): 1408-1419.

Rafatullah, M., Sulaiman, O., Hashim, R. and Ahmad, A. (2010). "Adsorption of methylene blue on low-cost adsorbents: A review." Journal of Hazardous Materials **177**(1-3): 70-80.

Ramaraju, B., Manoj Kumar Reddy, P. and Subrahmanyam, C. (2013). "Low cost adsorbents from agricultural waste for removal of dyes." Environmental Progress & Sustainable Energy **13**: 1-9.

Rana, K., Shah, M. and Limbachiya, N. (2014). "Adsorption of copper Cu (2+) metal ion from waste water using sulphuric acid treated sugarcane bagasse as adsorbent." International Journal of Advanced Engineering Research and Science **1**(1): 55-59.

Rashed, M. (2015). Photocatalytic Degradation of Divalent Metals under Sunlight Irradiation Using Nanoparticle TiO2 Modified Concrete Materials (Recycled Glass Cullet). Recent Progress in Desalination, Environmental and Marine Outfall Systems, Springer**:** 93-108.

Ravikumar, K., Deebika, B. and Balu, K. (2005). "Decolourization of aqueous dye solutions by a novel adsorbent: application of statistical designs and surface plots for the optimization and regression analysis." Journal of Hazardous Materials **122**(1): 75-83.

Reish, D., Martin, J., Piltz, F. and Word, J. (1976). "The effect of heavy metals on laboratory populations of two polychaetes with comparisons to the water quality conditions and standards in southern California marine waters." Water Research **10**(4): 299-302.

Ren, X., Xiao, W., Zhang, R., Shang, Y. and Han, R. (2015). "Adsorption of crystal violet from aqueous solution by chemically modified phoenix tree leaves in batch mode." Desalination and Water Treatment **53**(5): 1324-1334.

Rezaei, H. (2013). "Biosorption of chromium by using Spirulina sp." Arabian Journal of Chemistry.

Robinson, T., McMullan, G., Marchant, R. and Nigam, P. (2001). "Remediation of dyes in textile effluent: a critical review on current treatment technologies with a proposed alternative." Bioresource Technology **77**(3): 247-255.

Royer, B., Cardoso, N. F., Lima, E. C., Vaghetti, J. C. P., Simon, N. M., Calvete, T. and Veses, R. C. (2009). "Applications of Brazilian pine-fruit shell in natural and carbonized forms as adsorbents to removal of methylene blue from aqueous solutions—Kinetic and equilibrium study." Journal of Hazardous Materials **164**(2): 1213-1222.

Saeed, A., Akhter, M. W. and Iqbal, M. (2005). "Removal and recovery of heavy metals from aqueous solution using papaya wood as a new biosorbent." Separation and Purification Technology **45**(1): 25-31.

Saeed, A., Sharif, M. and Iqbal, M. (2010). "Application potential of grapefruit peel as dye sorbent: Kinetics, equilibrium and mechanism of crystal violet adsorption." Journal of Hazardous Materials **179**(1): 564-572.

Saifuddin, M. and Kumaran, P. (2005). "Removal of heavy metal from industrial wastewater using chitosan coated oil palm shell charcoal." Electronic Journal of Biotechnology **8**(1): 43-53.

Sakaguchi, T., Horikoshi, T. and Nakajima, A. (1977). "Uptake of copper ion by Chlorella regularis." Journal of the Agricultural Chemical Society of Japan **51**(8): 497-505.

Salleh, M. A. M., Mahmoud, D. K., Karim, W. A. W. A. and Idris, A. (2011). "Cationic and anionic dye adsorption by agricultural solid wastes: A comprehensive review." Desalination **280**(1): 1-13.

Sangi, M. R., Shahmoradi, A., Zolgharnein, J., Azimi, G. H. and Ghorbandoost, M. (2008). "Removal and recovery of heavy metals from aqueous solution using Ulmus carpinifolia and Fraxinus excelsior tree leaves." Journal of Hazardous Materials **155**(3): 513-522.

Sargın, İ., Arslan, G. and Kaya, M. (2016). "Efficiency of chitosan-algal biomass composite microbeads at heavy metal removal." Reactive and Functional Polymers **98**: 38-47.

Sarin, V. and Pant, K. K. (2006). "Removal of chromium from industrial waste by using eucalyptus bark." Bioresource Technology **97**(1): 15-20.

Scarpi, C., Ninci, F., Centini, M. and Anselmi, C. (1998). "High-performance liquid chromatography determination of dir Schuler, CA, Anthony RG, and Ohlendorf. HM 1990. Selenium in Wetlands and Waterfowl Foods and Kesterson Reservoir, California, 1984." Archives of Environmental Contamination and Toxicology **29**: 845-853.

Sen, T. K., Afroze, S. and Ang, H. (2011). "Equilibrium, Kinetics and Mechanism of Removal of Methylene Blue from Aqueous Solution by Adsorption onto Pine Cone Biomass of Pinus radiata." Water, Air, & Soil Pollution **218**: 499-515.

Sen, T. K. and Gomez, D. (2011). "Adsorption of zinc (Zn 2+) from aqueous solution on natural bentonite." Desalination **267**(2): 286-294.

Senthil Kumar, P., Palaniyappan, M., Priyadharshini, M., Vignesh, A., Thanjiappan, A., Sebastina Anne Fernando, P., Tanvir Ahmed, R. and Srinath, R. (2013). "Adsorption of basic dye onto raw and surface-modified agricultural waste." Environmental Progress & Sustainable Energy.

Senthil Kumar, P., Palaniyappan, M., Priyadharshini, M., Vignesh, A., Thanjiappan, A., Sebastina Anne Fernando, P., Tanvir Ahmed, R. and Srinath, R. (2014). "Adsorption of basic dye onto raw and surface-modified agricultural waste." Environmental Progress & Sustainable Energy **33**(1): 87-98.

Sharma, N., Tiwari, D. and Singh, S. (2014). "The Efficiency Appraisal for Removal of Malachite Green by Potato peel and Neem Bark: Isotherm and Kinetic Studies." International Journal of Chemical & Environmental Engineering **5**(2).

Sharma, P., Kaur, H., Sharma, M. and Sahore, V. (2011). "A review on applicability of naturally available adsorbents for the removal of hazardous dyes from aqueous waste." Environmental Monitoring and Assessment **183**(1-4): 151-195.

Sharma, S. K. (2014). Heavy Metals in Water: Presence, Removal and Safety, Royal Society of Chemistry.

Shaw, W. H. R. (1954). "Toxicity of cations towards living systems." Science, N.Y. **120**: 361-363.

Shirkhodaie, M., Hossein Beyki, M. and Shemirani, F. (2016). "Biogenic synthesis of magnetic perlite@ iron oxide composite: application as a green support for dye removal." Desalination and Water Treatment **57**(25): 11859-11871.

Sing, K. S. (1985). "Reporting physisorption data for gas/solid systems with special reference to the determination of surface area and porosity (Recommendations 1984)." Pure and Applied Chemistry **57**(4): 603-619.

Singha, A. S. and Guleria, A. (2015). "Utility of chemically modified agricultural waste okra biomass for removal of toxic heavy metal ions from aqueous solution." Engineering in Agriculture, Environment and Food **8**(1): 52-60.

Sinha, A., Pant, K. K. and Khare, S. K. (2012). "Studies on mercury bioremediation by alginate immobilized mercury tolerant Bacillus cereus cells." International Biodeterioration & Biodegradation **71**: 1-8.

Smith, B., Koonce, T. and Hudson, S. (1993). "Decolorizing dye wastewater using chitosan." American Dyestuff Reporter **82**(10): 18-36.

Sokolowska-Gajda, J., Freeman, H. S. and Reife, A. (1996). "Synthetic dyes based on environmental considerations. Part 2: Iron complexes formazan dyes." Dyes and pigments **30**(1): 1-20.

Srivastava, N. and Majumder, C. (2008). "Novel biofiltration methods for the treatment of heavy metals from industrial wastewater." Journal of Hazardous Materials **151**(1): 1-8.

Srivastava, P., Goyal, S. and Tayade, R. (2013). "Ultrasound-assisted adsorption of reactive blue 21 dye on TiO2 in the presence of some rare earths (La, Ce, Pr & Gd)." The Canadian Journal of Chemical Engineering **99**: 1-11.

Stavropoulos, G., Skodras, G. and Papadimitriou, K. (2015). "Effect of solution chemistry on cyanide adsorption in activated carbon." Applied Thermal Engineering **74**: 182-185.

Suteu, D. and Bilba, D. (2005). "Equilibrium and kinetic study of reactive dye brilliant red HE-3B adsorption by activated charcoal." Acta Chimica Slovenica **52**(1): 73-79.

Tan, I., Ahmad, A. and Hameed, B. (2008). "Adsorption of basic dye using activated carbon prepared from oil palm shell: batch and fixed bed studies." Desalination **225**(1): 13-28.

Tan, J., Zhang, X., Wei, X. and Wang, L. (2012). "Removal of malachite green from aqueous solution using waste newspaper fiber." BioResources **7**(3): 4307-4320.

Tanyildizi, M. Ş. (2011). "Modeling of adsorption isotherms and kinetics of reactive dye from aqueous solution by peanut hull." Chemical Engineering Journal **168**(3): 1234-1240.

Taşar, Ş., Kaya, F. and Özer, A. (2014). "Biosorption of lead (II) ions from aqueous solution by peanut shells: Equilibrium, thermodynamic and kinetic studies." Journal of Environmental Chemical Engineering **2**(2): 1018-1026.

Tehrani-Bagha, A., Nikkar, H., Mahmoodi, N., Markazi, M. and Menger, F. (2011). "The sorption of cationic dyes onto kaolin: Kinetic, isotherm and thermodynamic studies." Desalination **266**(1): 274-280.

Thomas, H. C. (1944). "Heterogeneous ion exchange in a flowing system." Journal of the American Chemical Society **66**(10): 1664-1666.

Tovar-Gómez, R., del Rosario Moreno-Virgen, M., Moreno-Pérez, J., Bonilla-Petriciolet, A., Hernández-Montoya, V. and Durán-Valle, C. J. (2015). "Analysis of synergistic and antagonistic adsorption of heavy metals and acid blue 25 on activated carbon from ternary systems." Chemical Engineering Research and Design **93**: 755-772.

Tseng, R. L., Wu, F. C. and Juang, R. S. (2003). "Liquid-phase adsorption of dyes and phenols using pinewood-based activated carbons." Carbon **41**(3): 487-495.

Tünay, O., Kabdaşli, I., Orhon, D. and Cansever, G. (1999). "Use and minimization of water in leather tanning processes." Water Science and Technology **40**(1): 237-244.

Urgun-Demirtas, M., Benda, P. L., Gillenwater, P. S., Negri, M. C., Xiong, H. and Snyder, S. W. (2012). "Achieving very low mercury levels in refinery wastewater by membrane filtration." Journal of Hazardous Materials **215**: 98-107.

Vadivelan, V. and Kumar, K. V. (2005). "Equilibrium, kinetics, mechanism, and process design for the sorption of methylene blue onto rice husk." Journal of Colloid and Interface Science **286**(1): 90-100.

Vaġzoğullar, A. Ġ., Uğurlu, M. and Kula, Ġ. (2015). "Comparing adsorption activity of raw Sepiolite and CTAB modified Sepiolite: kinetic and adsorption study for removal of Hg+." International Journal of Environment **4**(4): 19-31.

Vakili, M., Rafatullah, M., Ibrahim, M. H., Abdullah, A. Z., Salamatinia, B. and Gholami, Z. (2014). Oil palm biomass as an adsorbent for heavy metals. Reviews of Environmental Contamination and Toxicology Springer. **232:** 61-88.

Valix, M., Cheung, W. and McKay, G. (2004). "Preparation of activated carbon using low temperature carbonisation and physical activation of high ash raw bagasse for acid dye adsorption." Chemosphere **56**(5): 493-501.

Venugopal, B. and Luckey, T. (1975). "Toxicology of non-radioactive heavy metals and their salts." Environmental quality and safety. Supplement **1**: 4.

Vijayaraghavan, J., Bhagavathi Pushpa, T., Sardhar Basha, S., Vijayaraghavan, K. and Jegan, J. (2015). "Evaluation of Red Marine Alga Kappaphycus alvarezii as Biosorbent for Methylene Blue: Isotherm, Kinetic, and Mechanism Studies." Separation Science and Technology **50**(8): 1120-1126.

Vilar, V. J. P., Botelho, C. and Boaventura, R. A. R. (2007). "Methylene blue adsorption by algal biomass based materials: Biosorbents characterization and process behaviour." Journal of Hazardous Materials **147**(1): 120-132.

Vimonses, V., Lei, S., Jin, B., Chow, C. W. K. and Saint, C. (2009). "Kinetic study and equilibrium isotherm analysis of Congo Red adsorption by clay materials." Chemical Engineering Journal **148**(2): 354-364.

Walker, G., Hansen, L., Hanna, J. A. and Allen, S. (2003). "Kinetics of a reactive dye adsorption onto dolomitic sorbents." Water Research **37**(9): 2081-2089.

Wang, H., Yuan, X., Wu, Z., Wang, L., Peng, X., Leng, L. and Zeng, G. (2014). "Removal of basic dye from aqueous solution using Cinnamomum camphora sawdust: kinetics, isotherms, thermodynamics and mass-transfer processes." Separation Science and Technology **49**(17): 2689-2699.

Wang, L., Chen, Z., Yang, J. and Ma, F. (2015). "Pb (II) biosorption by compound bioflocculant: performance and mechanism." Desalination and Water Treatment **53**(2): 421-429.

Wang, P., Ma, Q., Hu, D. and Wang, L. (2016). "Adsorption of methylene blue by a low-cost biosorbent: citric acid modified peanut shell." Desalination and Water Treatment **57**(22): 10261-10269.

Waranusantigul, P., Pokethitiyook, P., Kruatrachue, M. and Upatham, E. (2003). "Kinetics of basic dye (methylene blue) biosorption by giant duckweed (Spirodela polyrrhiza)." Environmental pollution **125**(3): 385-392.

Weber, W. and Morris, J. (1963). "Kinetics of adsorption on carbon from solution." Journal of the Sanitary Engineering Division, Proceeding of the American Society of Civil Engineers **89**(17): 31-60.

Weng, C. H. and Pan, Y. F. (2007). "Adsorption of a cationic dye (methylene blue) onto spent activated clay." Journal of Hazardous Materials **144**(1): 355-362.

Wong, Y., et al. (2004). "Adsorption of acid dyes on chitosan—equilibrium isotherm analyses." Process Biochemistry **39**(6): 695-704.

Wróbel, D., Boguta, A. and Ion, R. M. (2001). "Mixtures of synthetic organic dyes in a photoelectrochemical cell." Journal of Photochemistry and Photobiology A: Chemistry **138**(1): 7-22.

Wu, C.-H., Kuo, C.-Y. and Guan, S.-S. (2015). "Adsorption Kinetics of Lead and Zinc Ions by Coffee Residues." Polish Journal of Environmental Studies **24**(2): 761-767.

Yagub, M. T., Sen, T. K., Afroze, S. and Ang, H. (2014). "Dye and its removal from aqueous solution by adsorption: A review." Advances in Colloid and Interface Science **209**: 172-184.

Yagub, M. T., Sen, T. K., Afroze, S. and Ang, H. M. (2014). "Fixed-bed dynamic column adsorption study of methylene blue (MB) onto pine cone." Desalination and Water Treatment: 1-14.

Yagub, M. T., Sen, T. K. and Ang, H. (2012). "Equilibrium, Kinetics, and Thermodynamics of Methylene Blue Adsorption by Pine Tree Leaves." Water, Air, & Soil Pollution **223**(8): 5267-5282.

Yagub, M. T., Sen, T. K. and Ang, M. (2013). "Removal of cationic dye methylene blue (MB) from aqueous solution by ground raw and base modified pine cone powder." Environmental Earth Sciences **13**: 1-13.

Yaneva, Z. L. and Georgieva, N. V. (2012). "Insights into Congo Red Adsorption on Agro-Industrial Materials- Spectral, Equilibrium, Kinetic, Thermodynamic, Dynamic and Desorption Studies. A Review." International Review of Chemical Engineering **4**(2): 127-146.

Yang, J. and Qiu, K. (2010). "Preparation of activated carbons from walnut shells via vacuum chemical activation and their application for methylene blue removal." Chemical Engineering Journal **165**(1): 209-217.

Yang, Y., Lin, X., Wei, B., Zhao, Y. and Wang, J. (2014). "Evaluation of adsorption potential of bamboo biochar for metal-complex dye: equilibrium, kinetics and artificial neural network modeling." International Journal of Environmental Science and Technology **11**(4): 1093-1100.

Yargıç, A., Şahin, R. Y., Özbay, N. and Önal, E. (2015). "Assessment of toxic copper (II) biosorption from aqueous solution by chemically-treated tomato waste." Journal of Cleaner Production **88**: 152-159.

Yoon, Y. H. and NELSON, J. H. (1984). "Application of gas adsorption kinetics I. A theoretical model for respirator cartridge service life." The American Industrial Hygiene Association Journal **45**(8): 509-516.

You, S.-J. and Teng, J.-Y. (2009). "Anaerobic decolorization bacteria for the treatment of azo dye in a sequential anaerobic and aerobic membrane bioreactor." Journal of the Taiwan Institute of Chemical Engineers **40**(5): 500-504.

Zhang, J., Zhou, Q. and Ou, L. (2012). "Kinetic, Isotherm, and Thermodynamic Studies of the Adsorption of Methyl Orange from Aqueous Solution by Chitosan/Alumina Composite." Journal of Chemical & Engineering Data **67**: 412-419.

Zhang, Z., O'Hara, I. M., Kent, G. A. and Doherty, W. O. (2013). "Comparative study on adsorption of two cationic dyes by milled sugarcane bagasse." Industrial Crops and Products **42**: 41-49.

Zhao, B., Shang, Y., Xiao, W., Dou, C. and Han, R. (2014). "Adsorption of Congo red from solution using cationic surfactant modified wheat straw in column model." Journal of Environmental Chemical Engineering **2**(1): 40-45.

Zhao, B., Xiao, W., Shang, Y., Zhu, H. and Han, R. (2014). "Adsorption of light green anionic dye using cationic surfactant-modified peanut husk in batch mode." Arabian Journal of Chemistry.

Zhao, Y., Xia, Y., Yang, H., Wang, Y. and Zhao, M. (2014). "Synthesis of glutamic acid-modified magnetic corn straw: equilibrium and kinetic studies on methylene blue adsorption." Desalination and Water Treatment **52**(1-3): 199-207.

Zhou, L., Huang, J., He, B., Zhang, F. and Li, H. (2014). "Peach gum for efficient removal of methylene blue and methyl violet dyes from aqueous solution." Carbohydrate Polymers **101**: 574-581.

Zou, W., Bai, H., Gao, S. and Li, K. (2013). "Characterization of modified sawdust, kinetic and equilibrium study about methylene blue adsorption in batch mode." Korean Journal of Chemical Engineering **30**(1): 111-122.

Every reasonable effort has been made to acknowledge the owners of copyright material. I would be pleased to hear from any copyright owner who has been omitted or incorrectly acknowledged.

CHAPTER 3

MATERIALS, METHODS AND CHARACTERISATION

3.1 Introduction

This chapter describes the research design adopted to achieve the aims and objectives of the research study together with the characterisation of raw and modified eucalyptus bark materials. The ability of adsorption depends on the chemical reactivity as well as porosity, available surface area and surface functional groups of adsorbent materials. Therefore, it is necessary to have an in-depth understanding of the sorbent characteristics to know the affinity of sorbent–sorbate materials to achieve the desired removal of organic/inorganic ions. For this purpose, a number of analytical techniques and instruments were used here to characterise both raw and modified sorbents to ascertain the presence of adsorption sites and to study the influence of modification to the eucalyptus bark properties for the sorption which is discussed in this chapter.

3.2 Research Methodology

3.2.1 Materials

3.2.1.1 Collection and Preparation of Adsorbents

A) Eucalyptus Bark (*Eucalyputus Sheathiana*)

Eucalyptus sheathiana (family name: Myrtaceae) trees are evergreen and form about three-quarters of the tree flora of Australia. They are fast growing and abundantly available worldwide. The trees are usually 3-15 m high with smooth barks throughout, prickly, grey or grey-brown or brown [Fig. 3.1 (a)]. The barks in the tree are often hanging in long ribbons. Due to the high number of eucalyptus trees in Australia, massive amounts of barks (as waste) are disposed each year [Fig. 3.1 (b)].

Figure 3.1(a) Eucalyptus *sheathiana* tree and (b) bark from eucalyptus *sheathiana* tree

Eucalyptus sheathiana barks were collected from Curtin University – Bentley campus, Western Australia. The barks were washed repeatedly with distilled water to remove impurities such as sand and leaves, and then dried at 105˚C for 24 h in an oven. The dried biomass was ground using a mechanical grinder supplied by RETSCH, GmbH & Co. KG, West Germany. The resultant powders were passed through British Standard Sieves (BSS) of 106 µm and stored in an airtight plastic container for analysis as well as for conducting adsorption experiments.

B) Modification of Raw Eucalyptus Bark by Chemical Treatment

A weighed amount (50 g) of raw eucalyptus bark powder was contacted with 500 mL of 0.1 M sodium hydroxide (NaOH) solution to prepare base modified eucalyptus bark powder. The whole slurry was stirred overnight with a magnetic stirrer and then the powder was filtered and repeatedly rinsed with distilled water. The washed powders were then dried overnight at 90˚C and used for adsorption experiments.

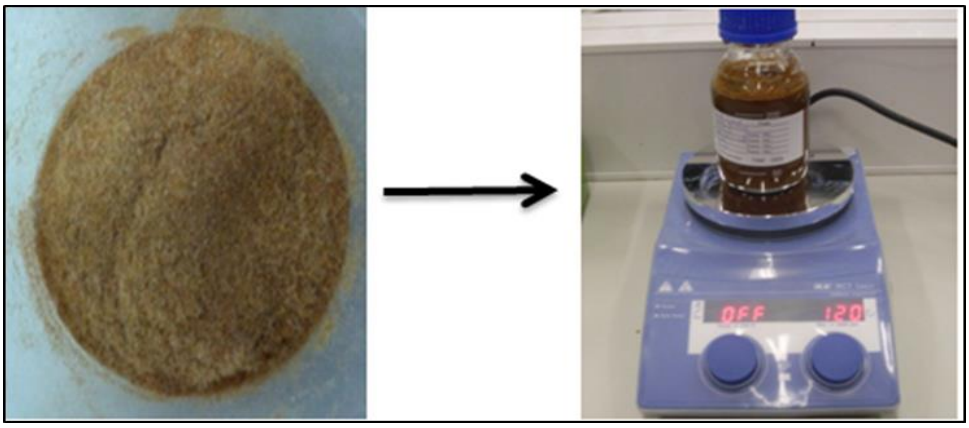

Figure 3.2 Preparation of base modified eucalyptus bark powder

C) Chemicals and Contaminant Adsorbate

All chemicals used were of analytical grade. The basic cationic dye, Methylene Blue (MB), was selected as the model organic dye and solution of Zn^{2+} metal ions as inorganic adsorbate in this study. The formula of MB dye is $C_{16}H_{18}N_3SCl.3H_2O$ with a molecular weight of 319.86 g/mol was supplied by Sigma-Aldrich Pty. Ltd., NSW, Australia. It was used without further purification. The stock solution of 1000 ppm MB dye was prepared by dissolving the appropriate amount (1000 mg) of MB dye in a litre of ultra-pure water. The experimental solutions of varying concentrations were prepared by diluting the stock solution with ultra-pure water. The standard stock solution of Zn^{2+} of 1000 ppm was prepared by dissolving an accurately weighed amount of $Zn(NO_3)_2{\cdot}6H_2O$ salt (supplied by Sigma-Aldrich Pty. Ltd., NSW, Australia) in ultra-pure water. The working solutions were then prepared by diluting the stock solution with ultra-pure water to give the specific concentration of the working solutions. Similarly, salt solutions of 100 ppm, 200 ppm and 300 ppm were prepared by dissolving the appropriate amount of laboratory grade sodium chloride (NaCl), calcium chloride ($CaCl_2$) and ferric chloride ($FeCl_3$) separately in a litre of ultra-pure water to perform experiments with salt effects. All these salts were procured from Rowe Scientific, Perth, Western Australia. Triton X-100 (Average Mol. wt. 625, purity < = 100%) was used as non-ionic surfactant and was procured from Sigma-Aldrich Pty. Ltd., NSW, Australia. The pH of the solutions was adjusted by additing either 0.1 M HCl or 0.1 M NaOH solutions, respectively.

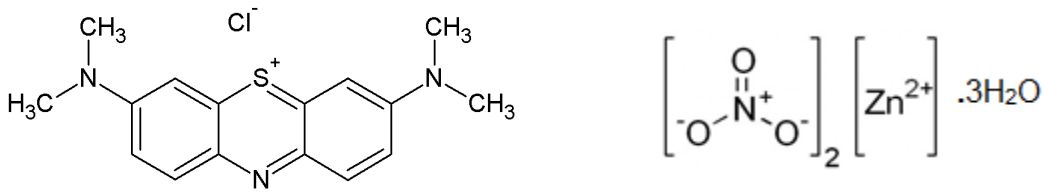

(a) (b)

Figure 3.3 Chemical structure of (a) Methylene Blue (MB) dye and (b) Zine Nitrate Hexahydrate

The SP-8001 UV/VIS spectrophotometer was used to measure the concentrations of methylene blue (MB) dye in solution. The concentration of the residual dye was

measured using UV/visible spectrophotometer (Fig. 3.4) at a λmax corresponding to the maximum adsorption for the dye solution (λmax = 665 nm). The calibration curve (1-5 ppm) was plotted between absorbance and concentration of the MB dye solution to obtain absorbance–concentration profile as shown in Fig. 3.5. After performing every single adsorption experiment, the samples were withdrawn from the shaker at fixed time intervals, centrifuged and then serials of diluted samples were prepared for highly concentrated MB solutions. The absorbance of the diluted samples were obtained using the spectrophotometer and the final residual unknown MB dye concentrations were measured by fitting those data into the calibration curve via calculation. The concentration of Zn^{2+} was measured using Shimadzu AA-7000 Atomic Absorption Spectrophotometer (AAS) at a wavelength of 213.9 nm and with 1.0 nm slit width by standard procedure followed in AAS. pH measurements were done using WP-81 pH-Cond-Salinity meter (Fig. 3.6). All these instruments were calibrated and optimized before use.

Figure 3.4 SP-8001 UV/VIS Spectrophotometer

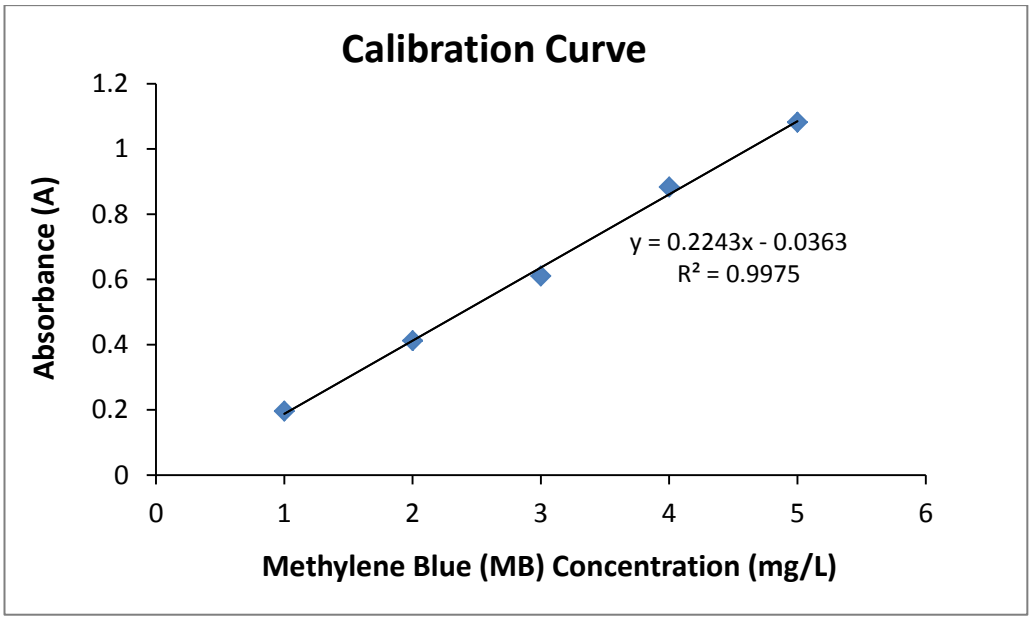

Figure 3.5 Calibration curve of initial Methylene Blue (MB) dye concentrations

Figure 3.6 Measuring pH of solution using pH Meter: WP 81

3.2.1.2 Adsorbent Characterisation

In this study, the raw and modified eucalyptus bark samples were characterized by Scanning electron microscopy (SEM) to examine the surface micro-morphology of materials and Electron diffraction spectrum (EDS) was used for elemental analysis of adsorbents. Characterisation of the attached functional groups on the adsorbent for both raw and modified, was done by using Fourier transform infrared spectroscopy (FTIR) and the presence of minerals in the biomass adsorbents was investigated by X-ray diffractometer (XRD). The elemental percentage composition of carbon, nitrogen and hydrogen in the research materials were established with the help of a

CHNS elemental analyser. Bulk density, particle size, pH_{zpc} (zero point charge), and surface area of the raw and modified adsorbents were also determined.

3.2.2 Experimental Methods

As identified in the literature review, the mechanisms employed by the sorbents for the removal of organic/inorganic ions are defined based on the kinetics, thermodynamics and isotherm behaviour. The data required for the kinetics, isotherm and thermodynamics investigation of sorption mechanisms were generated using batch experiments below. Furthermore, it was identified from the literature review that pH, initial sorbate concentration, temperature, sorbent dose, presence of salts are the primary influencing experimental parameters for adsorption process. Therefore, these parameters were controlled throughout the batch experiments.

3.2.2.1 Batch Adsorption Kinetic Studies

Batch adsorption experiments on raw eucalyptus bark were conducted by using a known amount of the adsorbent sample with 50 mL of aqueous MB adsorbate solutions in a series of 250 mL plastic bottles. The dye mixture was shaken at a constant temperature of 30^0C using Thermo Line Scientific Orbital Shaker Incubator at a speed of 120 rpm (Fig. 3.7). This moderate level of agitation speed (120 rpm) was chosen to increase the degree of mixing of adsorbate MB dye and eucalyptus bark adsorbent particles to enhance adsorption. At predetermined time, the bottles were withdrawn from the shaker and the residual dye solution was separated from the mixture by centrifuging in MULTIFUGE 1 s (Fig. 3.8). The absorbance of the supernatant was measured at the wavelength that corresponds to the maximum absorbance of the sample and the dye concentration was calculated from the linear equation of the calibration curve (Fig. 3.5). The effects of various physicochemical process parameters such as solution pH, adsorbate concentration, temperature, adsorbent dose, salt concentration, etc. on adsorption kinetics are also determined. This was carried out by varying one parameter, keeping other parameters constant.

Figure 3.7 Thermo Line Scientific Orbital Shaker Incubator

Figure 3.8 Centrifugal Analyser (MULTIFUGE 1 s)

To perform Zn^{2+} metal ions batch adsorption experiments on raw and base modified eucalyptus bark, 1000 mg/L of standard Zn^{2+} solution (provided by ChemSupply, South Australia, Australia) was used to obtain calibration curve using AAS instrument. Then a known amount of adsorbent was mixed with 50 mL of aqueous Zn^{2+} adsorbate solution in a series of 250 mL plastic bottles. The contents in the bottles were stirred in Thermo Line Scientific Orbital Shaker Incubator at 120 rpm and at a temperature of 30^0C for adsorption to proceed. As mentioned earlier, agitation speed of 120 rpm was used to influence the adsorption phenomenon by increasing the degree of mixing between adsorbate Zn^{2+} ions and adsorbent particles. The suspensions were collected from the shaker at predetermined time intervals and

resulting mixture was then filtered using micro filter of pore size 0.47 µm. The residual Zn^{2+} concentrations of the solution were determined by using atomic absorption spectrophotometer (Shimadzu AA-7000) with air–acetylene flame at a wavelength of 213.9 nm (Fig. 3.9). The slit width used was 1.0 nm (for the adjustment of the current to avoid high voltage) for zinc adsorption. Several experiments were carried out by varying solution pH, initial adsorbate solution concentration, mass of adsorbent, temperature, and with the addition of salts. For organic methylene blue dye, two additional batch experiments were conducted to investigate mixed dye effect and effect of surfactant.

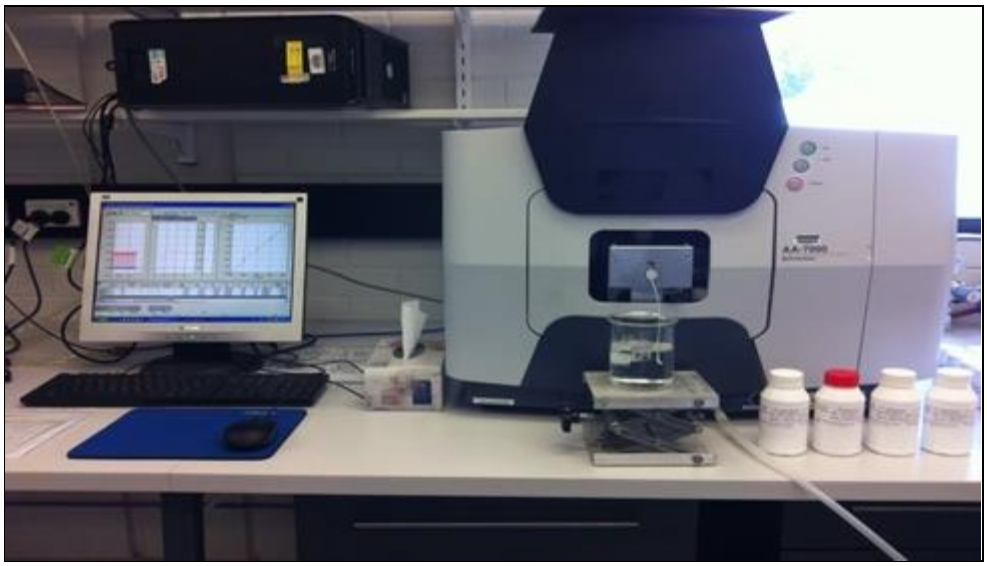

Figure 3.9 Shimadzu AA-7000 atomic absorption spectrophotometer (AAS)

The amount of adsorbate adsorbed onto adsorbent (raw and modified eucalyptus bark) at time *t*, q_t (milligrams per gram) and % adsorption are calculated from Eqs. (3.1) and (3.2) respectively:

$$q_t = \frac{(C_o - C_t)V}{m} \tag{3.1}$$

and adsorbate removal efficiency, i.e. % of adsorption was calculated as:

$$\% \text{ adsorption} = \frac{C_o - C_t}{C_o} \times 100 \tag{3.2}$$

where C_0 is the initial adsorbate concentration (milligrams per litre), C_t is the concentration of adsorbate at any time *t* (min), *V* is the volume of adsorbate solution (litres) and *m* is the mass of adsorbent (grams). All experimental measurements are within ±10 % accuracy.

3.2.2.2 Isotherm Studies

Equilibrium adsorption studies were conducted by contacting 50 mL of MB dye solutions of different initial concentration of 20, 30, 40, 50, 60 and 70 ppm with 20 mg of eucalyptus bark powder in a series of 250 mL plastic bottles for a period of 4 h which was more than sufficient to achieve equilibrium time. For Zn^{2+} metal ions, isotherm studies were conducted using the same volume of metal solution having different initial concentration (range 20 – 70 ppm) for both raw and NaOH modified eucalyptus bark adsorbents at a fixed pH 5.1 for a period of 2 h following the same procedure as for MB dye. The bottles were then shaken at a constant speed of 120 rpm in the Thermo Line Scientific Orbital Shaker Incubator at 30^0C and after the designated period of shaking, the samples were separated as per the method described in Section 3.2.2.1. The concentration of MB dye residue was analysed by SP-8001 UV/VIS spectrophotometer and the remaining Zn^{2+} concentration by Shimadzu AA-7000 atomic absorption spectrophotometer (AAS). Equations (3.1) and (3.2) were used to calculate the equilibrium adsorption capacity, q_e (mg/g) and percentage of adsorption respectively.

3.2.2.3 Desorption Studies

Desorption is important for identification of adsorption mechanism, reusability of adsorbents, recovery of contaminants and reduction of secondary wastes. In desorption studies, the MB loaded adsorbent was separated from solution by centrifugation and then dried in the oven. The dried MB-loaded adsorbent was then agitated with 50 mL of different desorbing agent solutions for the predetermined equilibrium time of the adsorption process and the desorbed MB dye concentration was then measured by UV spectrophotometer. Four different eluting solvents were used: water, HNO_3 (0.1 M), CH_3COOH (0.1 M) and NaOH (0.1M).

To study metal desorption, zinc-loaded adsorbent biomass at different concentrations was separated and gently washed with distilled deionized water to remove any unadsorbed Zn^{2+} ions. The biomass was then agitated in 50 mL of 0.1 M HCl for 100 min and the amount of desorbed Zn^{2+} estimated using AAS as described earlier in Section 3.2.2.1.

3.2.2.4 Column Studies

Since batch processes are usually limited to the treatment of small amounts of wastewater, a more practical alternative to eliminate dye from aqueous solution on a larger scale is required. Therefore, column experiments were performed in order to evaluate the removal and recovery of MB dye under various process conditions such as inlet dye flow rate, adsorbent bed height and initial dye concentration. Breakthrough plots were determined under various conditions. Detailed column experimental procedure is described in respective proceeding Section 5.3.

3.3 Characterisation of Raw and Modified Eucalyptus *Sheathiana* Bark Biomass

3.3.1 Surface Morphology

Raw and modified eucalyptus bark was examined by scanning electron microscopy (SEM) to get the information of surface morphology. The SEM images of all the prepared adsorbents illustrated the highly irregular sizes and shapes [Figs. (3.10a-b)]. It is clear from the SEM pictures that eucalyptus bark (EB) is amorphous carbon with non-crystalline structures. The surface morphology of raw eucalyptus bark is different from sodium hydroxide (NaOH) modified eucalyptus bark as the treatment may significantly alter physicochemical properties and porosity of the materials. After treatment with sodium hydroxide (NaOH), eucalyptus bark has got more irregular shape and porous structure than that of raw eucalyptus bark, and hence more specific surface area is exposed. The treatment with alkali was expected to partially remove protective thin wax on biomass surface and due to the leaching of structural materials; more active sites might have been exposed on the modified bark material which can be observed in Fig. 3.10(b).

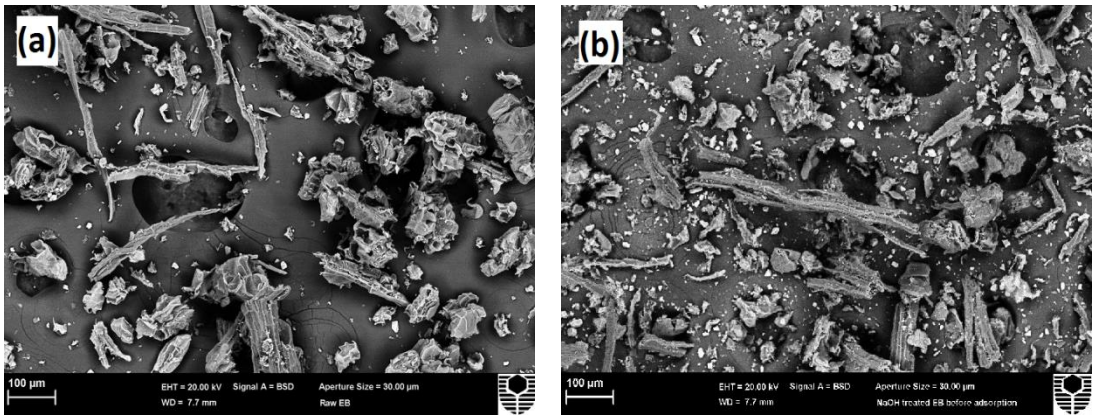

Figure 3.10(a) Raw eucalyptus bark and (b) NaOH modified eucalyptus bark before adsorption

The availability of pores and internal surface is clearly displayed in the SEM image of the eucalyptus bark biomass before adsorption [Fig. 3.10(a)] and the coverage of the surface and the pores by the adsorbed methylene blue is shown in Fig. 3.11(a). Basically, the porous structure that appears in Fig. 3.10(a) were filled by the MB dye molecules, showing the adherence to the surface of the adsorbent [Fig. 3.11(a)] and therefore MB loaded raw EB displayed a dense surface texture. Further, there are significant changes to the surface morphology of the adsorbents, as well as the formation of discrete aggregates on their surfaces following metal ion adsorption. Interaction of raw EB with Zn^{2+} has changed the surface texture of raw EB to fractured and fragmented walls of the pores on its surface [Fig. 3.11(b)]. The higher porous and fibrous texture of the modified EB adsorbent observed in the secondary SEM image of Fig. 3.10(b) indicates high heterogeneity which may contribute to the higher adsorption of Zn^{2+} ions. The greater the number of pores, the greater will be the adsorption of metal Zn^{2+} ions onto the adsorbent surface. The porous texture of modified EB disappeared and lump-like deposits were formed after contact with Zn^{2+} [Fig. 3.11(c)].

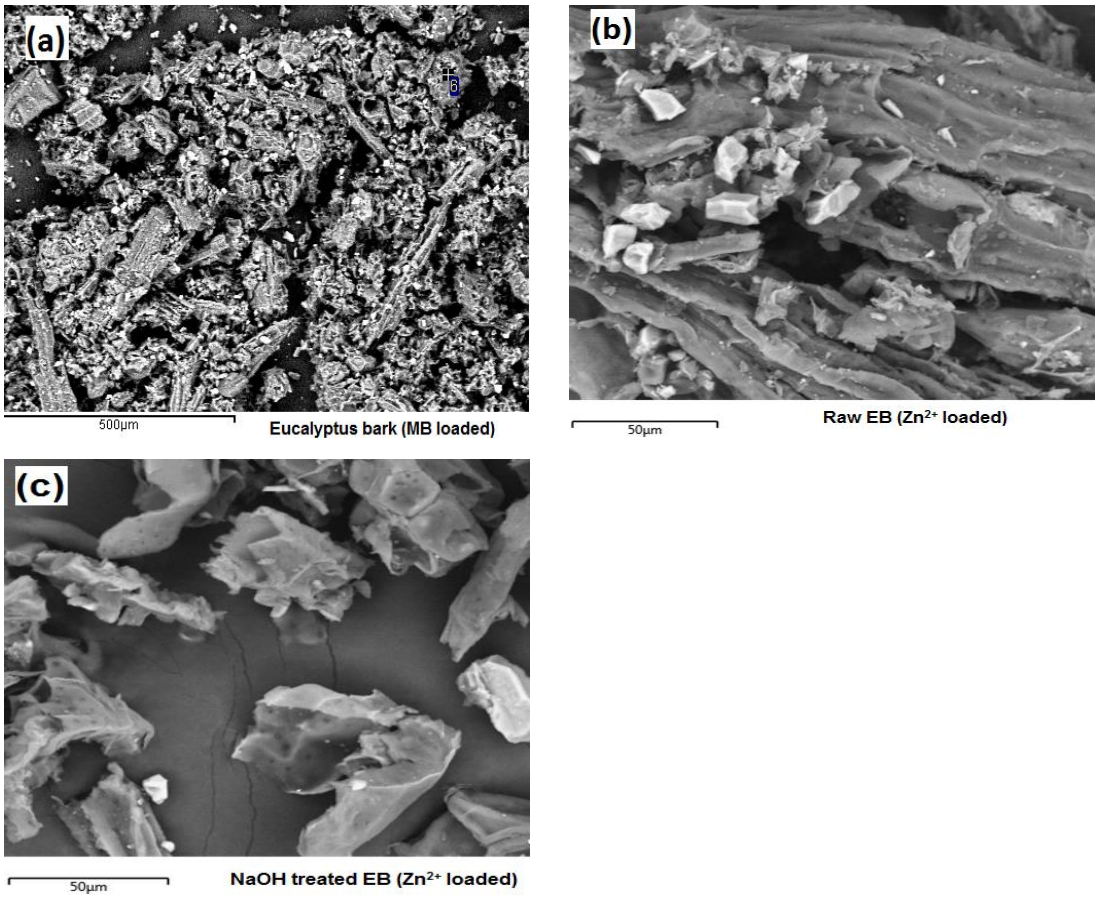

Figure 3.11(a) Raw eucalyptus bark after MB dye adsorption, (b) raw eucalyptus bark after Zn^{2+} adsorption and (c) NaOH modified eucalyptus bark after Zn^{2+} adsorption

3.3.2 EDS Observation

To describe a material uniquely, information about the elements present in the material is required which can usually be found by undertaking Electron Diffraction Spectrum (EDS) analysis. In order to examine the components of the eucalyptus bark adsorbent, Electron Diffraction Spectrum (EDS) of eucalyptus bark biomass was taken and presented in Fig. 3.12. As shown in Fig. 3.12, it has been confirmed that calcium is the major element where oxygen, hydrogen, nitrogen, sodium, magnesium and chloride are homogeneously distributed all over the adsorbent surface.

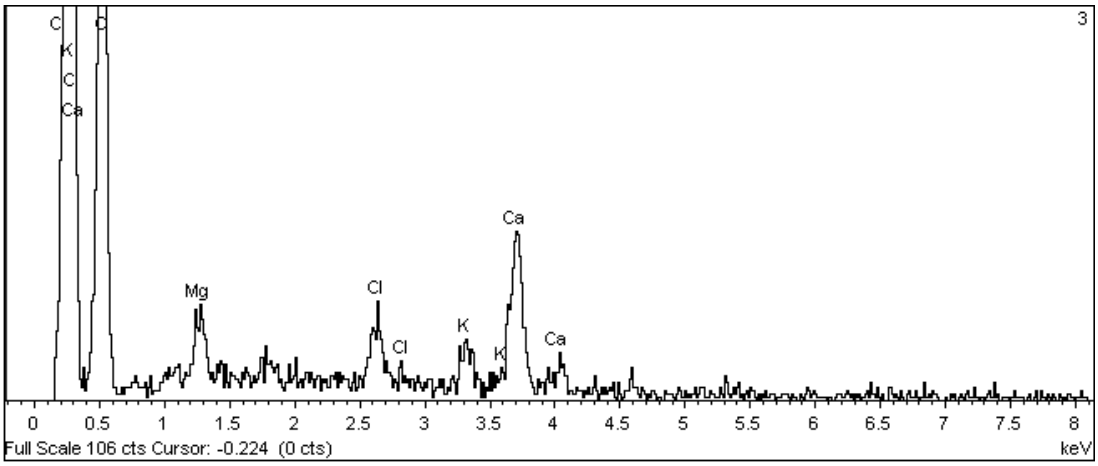

Figure 3.12 EDS surface chemical properties of raw eucalyptus bark (106 µ)

3.3.3 X-Ray Diffraction Spectrum Study

For adequate adsorption, it is significantly important to investigate and quantify the crystalline nature of adsorbent materials. Powder x-ray diffraction (XRD) is used to measure the crystalline content of adsorbent materials, to identify the crystalline phases present, to determine the spacing between lattice planes and to study the preferential ordering and epitaxial growth of crystallites within the material. In this study, chemical analysis of raw and NaOH modified eucalyptus bark was determined by using XRD technique which is presented in Fig. 3.13. The phases present were analysed using powder X-ray diffraction in the 2θ region of 10-90^0 at 25^{0}C by using Cu Kα radiation (λ=1.54 A^0). Major peaks obtained during XRD were identified using EVA software. Fig. 3.13 illustrates the presence of a significant amount of amorphous material due to lignin and tannin in the samples and structure of eucalyptus bark remained unaltered even after treatment with NaOH. The results in Fig. 3.13 showed the XRD pattern of raw and NaOH modified eucalyptus bark where the characteristic main peaks obtained at 2θ values of 14.9^0, 24.36^0, 30.07^0, 38.26^0, 43.4^0, 52.5^{0}and 57.55^0 of the two samples were exactly the same. These peaks are indicative of highly organized crystalline cellulose which are responsible for adsorption.

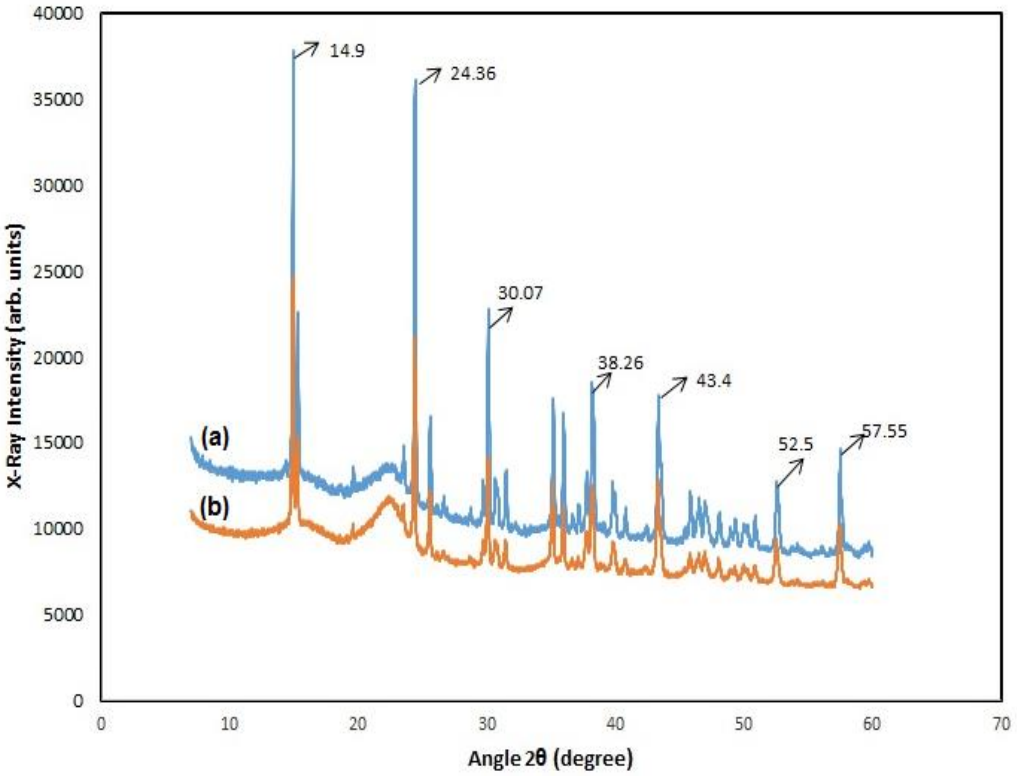

Figure 3.13 X-ray diffraction spectra's of (a) raw and (b) NaOH modified eucalyptus bark (EB) powder

3.3.4 FTIR Spectrum Study

Surface functional groups present in the adsorbent are very essential for the investigation of adsorption characteristic of adsorbent which is largely characterised by the FTIR spectroscopy method. FTIR provides information of the interaction of light and vibrational motion of the covalent chemical bonding of the molecules and lattice vibrations of ionic crystals (Ofomaja, Naidoo et al. 2009). As each substance is a unique grouping of atoms, no two compounds produce the same infrared spectrum. Therefore, infrared spectroscopy can result in a positive classification of different kinds of functional groups present in materials.

The Spectrum 100 FT-IR Spectrometer with a Universal ATR Sampling Accessory with MIR detector and SPECTRUM Version 6.3.4 software from Perkin Elmer (Fig. 3.14) was used to determine the functional groups present in raw and modified

eucalyptus bark adsorbent. This instrument provides reliable and delivers the highest sensitivity and stability in its class, providing accurate data every time.

Figure 3.14 Spectrum 100 FT-IR Spectrometer

The FTIR spectra patterns for raw eucalyptus bark and NaOH modified eucalyptus bark powder are shown in Fig. 3.15. The complex nature of the FTIR spectrum shown in Fig. 3.15 suggests that eucalyptus bark is composed of mixture of functional groups which are responsible for binding of organic dye Methylene Blue and inorganic heavy metal Zn^{2+} ions. Based on Fig. 3.15(a); to detect the surface functional groups observed in raw eucalyptus bark, –OH functional group can be easily recognized by the bands at 3314.9 cm^{-1} and the peak representing C═O stretch appears at 1617.4 cm^{-1} while the nitro group N═O is indicated by 1317.8 cm^{-1} (University of Colorado 1985). The peaks between 1033.8 and 784.5 cm^{-1} may be assigned to the C–O and C–Cl stretching respectively (University of Colorado 1985).

The spectra for modified eucalyptus bark did not show any radical change indicating that treatment with base solution did not significantly alter the chemical properties of raw eucalyptus bark. The spectra of NaOH treated eucalyptus bark sample in Fig. 3.15(b) showed the formation of new adsorption bands with some slight changes in the intensity of the peak at 1617.4 cm^{-1}, 1317.8 cm^{-1}, 1033.8 cm^{-1} and 784.5 cm^{-1}. All these peaks tend to decrease slightly after the treatment with NaOH. The appearance of new shoulder peaks at 2922.5 cm^{-1} represents the aliphatic group C–H while two sharp peaks at 1423.1 cm^{-1} and 1369.9 cm^{-1} are indicating nitro group N═O and the

observed peak at 1157.2 cm^{-1} is attributed for C–O stretching (University of Colorado 1985).

From FTIR study, the formation of new absorption bands, the change in absorption intensity and the shift in wavenumber of functional groups could be due to the changed pore structure and increased surface area of eucalyptus bark modified by NaOH treatment.

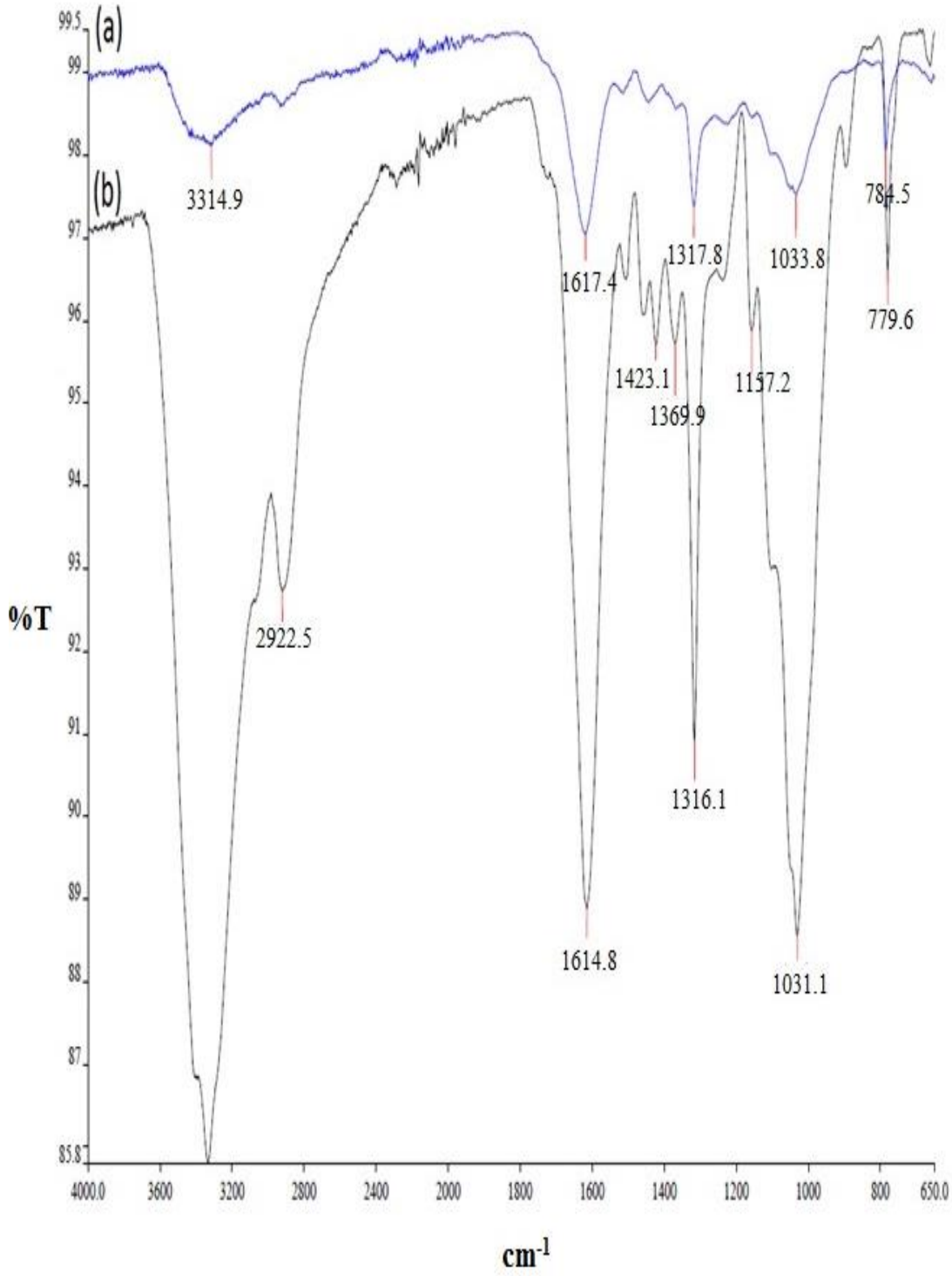

Figure 3.15 FTIR spectrum of (a) raw and (b) NaOH modified eucalyptus bark powder

3.3.5 Particle Size Distribution

For adsorption process; the particle size and its shape and surface area, all are very significant to know because adsorbent particle size affects the surface area, which is an important parameter in adsorption. Larger surface area can give higher adsorption efficiency when lower surface area reduces adsorption. Particle size influences many properties of particulate materials and is a valuable indicator of critical characteristics including content uniformity, dissolution and more importantly quality and performance of absorption rates. Therefore, adsorbent particle size distribution (PSD) is an important consideration in designing water treatment practices.

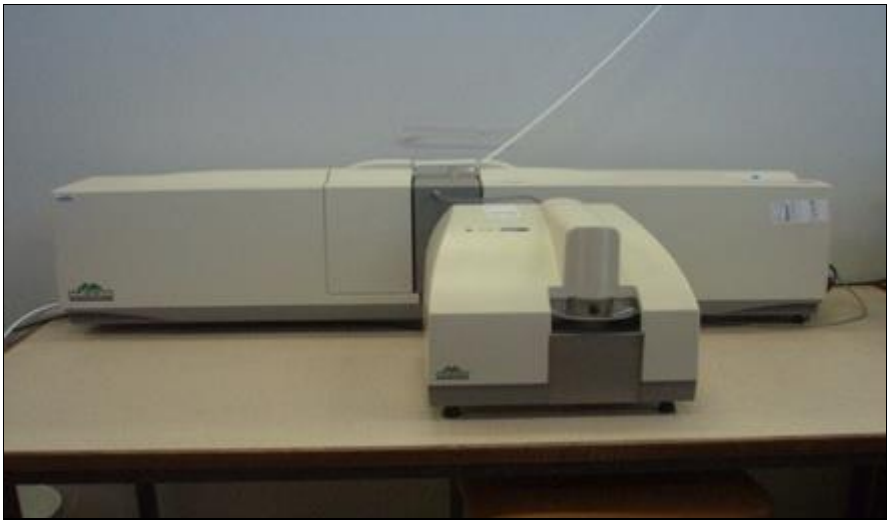

Figure 3.16 Malvern MasterSizer 2000S

The particle size distribution of raw eucalyptus bark biomass was determined by using the Malvern MasterSizer 2000S with the Hydro 2000S (A) Sampler which is presented in Fig. 3.16. The results of surface weighted mean, volume weighted mean and specific surface area were found to be 25.26 µm, 79.67 µm and 0.238 m^2/g respectively for raw eucalyptus bark powder prior to use it as an adsorbent.

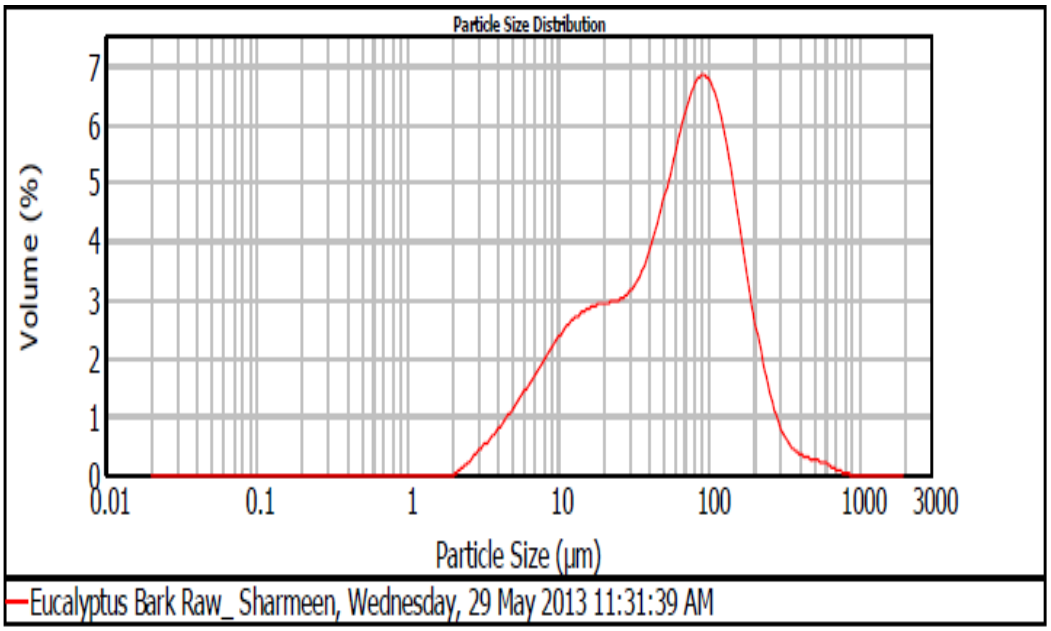

Figure 3.17 Particle size distribution of raw eucalyptus bark

3.3.6 BET Analysis

Adsorption is a surface phenomenon and it depends on adsorbent, adsorbate characteristics under various physicochemical process parameters. An adsorbent characteristic such as BET surface area of adsorbents is vital to know because larger surface area can provide higher interaction between the adsorbate and adsorbent materials for adsorption process. The micromeritics Tristar II 3020 is used to measure the surface area and pore volume of adsorbents (Fig. 3.18). Brunauer–Emmett–Teller (BET) equation is used to calculate the specific surface area while the total pore volume (V_T) is evaluated by converting the adsorption volume of nitrogen at relative pressure 0.95 to equivalent liquid volume of the adsorbate (Lippens and De Boer 1965).

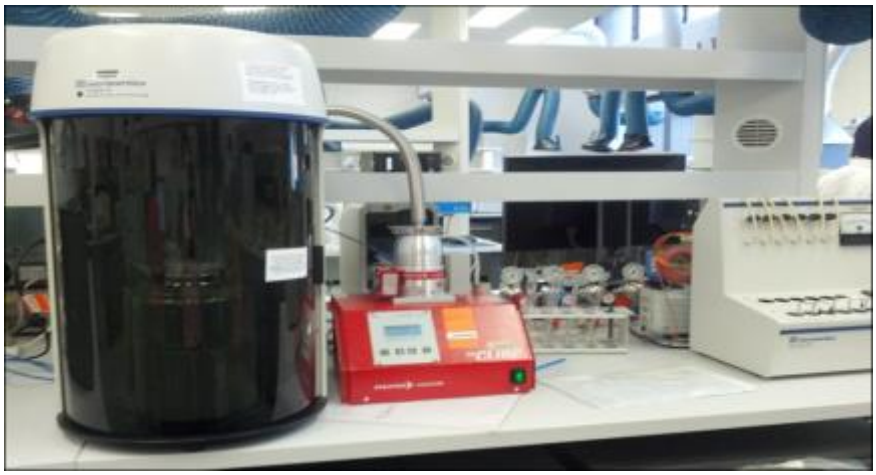

Figure 3.18 Micromeritics Tristar II 3020 and degassing chambers

Surface chemistry of raw and NaOH modified eucalyptus bark such as BET surface area and pore volume distribution were measured using BET method. Prior to analysis, the samples were degassed to eliminate any trace of volatile elements at room temperature for 1 hour then increasing the temperature to 120°C for 6 hours. The samples were then transferred into the Tristar nitrogen adsorption chamber analysis system where thet were cooled in liquid nitrogen. The calculated results for both the adsorbents are presented in Table 3.1.

Table 3.1: BET surface area for raw and NaOH modified eucalyptus bark (EB)

Adsorbent biomass	***BET Surface Area (m^2/g)***	***Pore volume (cm^3/g)***
Raw eucalyptus bark	6.55	0.003432
NaOH modified eucalyptus bark	20.13	0.011532

Table 3.1 compares the values of BET surface area (m^2/g) for the raw and modified eucalyptus bark as well as the total pore volume measurements for the individual adsorbent samples obtained by BET adsorption model. The results in Table 3.1 reveal that BET surface area of raw eucalyptus bark (6.55 m^2/g) is much less than the surface area obtained for NaOH treated eucalyptus bark biomass (20.13 m^2/g) indicating the treatment of eucalyptus bark with NaOH produced significant increase in surface area. Increase in surface area with base treatment has been attributed to extraction of plant components such as sugars, cementing materials and lignin which

usually block pores on adsorbent materials (Marshall, Wartelle et al. 1999, Wartelle and Marshall 2000) leading to further exposure of the adsorbent surface of plant based materials. Studies have shown that some plant based materials applied as adsorbent are porous in nature (Elizalde-González, Mattusch et al. 2007, Zvinowanda, Okonkwo et al. 2009). Table 3.1 shows the values of total pore volume for raw and NaOH modified EB. As explained earlier, the increase in total pore volume can be related to extraction of plant components which may have blocked existing pores and also the creation of new pores due to decrease in crystallinity, separation of structural linkages between lignin and carbohydrates and disruption of the lignin structure (Ofomaja, Naidoo et al. 2009). This observation suggests that base treatment leads to creation of new pores and that mesopore formation predominates with the base treatment in the order NaOH modified EB > raw EB. Most of the commercial adsorbents such as activated carbon, zeolite, silica gel, etc; show high adsorption capacity. However process is not cost effective due to high cost of activated carbon and difficulty in regeneration. Therefore current research was focused on the need to alternative to commercial activated carbon with cost effective but potential adsorbent. Hence the higher BET surface area of NaOH treated EB than raw EB which already gave the prior indication to achieve better adsorption performance for this NaOH treated biomass.

3.3.7 Bulk Density Measurement

The information of bulk density is significant for designing of adsorption towers in real industrial situation. It affects the overall performance of the adsorption process and it is inversely proportional to the particle size (Dawood, Sen et al. 2014). Bulk density is defined as the mass of particles of the material divided by the total volume they occupy (Eq. 3.3). It is used to measure the bulk density of the adsorbent by placing the adsorbent powder into a known volume of 2 mL volumetric cylinder and weight it. It is a property that characterises powders, granules and other solids and is used in reference to mineral components, chemical substances, ingredients, foodstuff or any other masses of particulate matter. As per American Water Work Association, bulk density should be greater than 0.25 g/cm^3 for practical purposes. Plant components such as sugars, tannins and pigments occupy void spaces and contribute largely to their bulk densities and therefore extraction of these plant components with

dilute base solution reduces their bulk densities (Wartelle and Marshall 2000). Hence, NaOH modified eucalyptus bark showed a reduction in bulk density over the raw eucalyptus bark (Table 3.2). Reduction in bulk density of some agricultural solid wastes after washing with 0.1 M of NaOH has also been observed for pine cone (Ofomaja and Naidoo 2011) and sugarcane bagasse (Wartelle and Marshall 2000).

The samples of raw and base modified eucalyptus bark were added in a 2 mL volumetric cylinder and the mass of the used samples were recorded separately. Then the bulk density of raw and base modified eucalyptus bark was measured as per Eq. (3.3) (Dawood, Sen et al. 2014).

$$Bulk\ Density = \frac{\text{Mass of dry sample (g)}}{\text{Total volume used (mL)}} \tag{3.3}$$

Table 3.2: Bulk density of raw and NaOH modified eucalyptus bark (EB)

Adsorbent biomass	***Bulk density (gm/cm^3)***
Raw eucalyptus bark	0.39
NaOH modified eucalyptus bark	0.27

3.3.8 C-H-N Analysis

CHN analysis was performed by Perkin Elmer 2400 Series II CHNS/O analyser as shown in Fig. 3.19. It is used to the simultaneous determination of the percentage amount of carbon, hydrogen and nitrogen in the organic and inorganic substances. The adsorbent of less than two milligrams in weight is placed into an aluminium capsule and dropped into a quartz tube at 1020^{0}C with constant carrier gas flow. During the combustion process, the sample is exposed to strong oxidizing environment to produce N_2, CO_2 and H_2O which can be detected by Thermal Conductivity detector.

Figure 3.19 CHNS/O analyser 2400 Series II by Perkin Elmer

All the results of percentage of elemental analysis (nitrogen, carbon and hydrogen) for raw eucalyptus bark adsorbent done by 2400 Series II CHNS/O analyser by Perkin Elmer are presented in Table 3.3.

Table 3.3: Elemental analysis of raw eucalyptus bark (EB)

Parameters	***Values (Mass %)***
Carbon, C	42.32
Hydrogen, H	5.69
Nitrogen, N	0.24

3.3.9 Point of Zero Charge (pH_{pzc}) Study

Point of zero charge is of fundamental importance in physical chemistry. The point of zero charge (pzc) is a concept relating to the adsorption phenomenon which is discussed in Section 2.4.1.1. Point of zero charge is used to understand the mechanism of adsorption process under varying pH. Adsorption of cations is favoured at pH > pHpzc while adsorption of anions is favoured at pH < pHpzc (Sadaf and Bhatti 2014). In the present study, the point of zero charge (pHpzc) was determined by solid addition method (Mall, Srivastava et al. 2006). This technique is

based on estimating the concentrations of H^+ and OH^- ions, which determine the electric potential. A series of 0.1 M KNO_3 solutions (50 mL each) were prepared and their initial pH was set at 2–12 by addition of 0.1 M HCl or NaOH. To each solution, 0.1 g of adsorbent was added and the suspensions were shaken manually and solution was kept for a period of 48 h with intermittent manual shaking. The final pH of each solution was recorded with a pH meter and difference between initial and final pH (ΔpH) (Y-axis) was plotted against initial pH values (X-axis). The point of intersection of this curve yielded point of zero charge.

The experimental curve for PZC determination of untreated and modified eucalyptus bark is presented in Fig. 3.20 (a) and Fig. 3.20 (b) respectively. The results shown in Fig 3.20 (a-b) indicate that pHpzc of raw eucalyptus bark was around 5.0. Surface modification reduced pHpzc and therefore pHpzc of base treated biomass was found to be 4.5 in this study. This indicates that pH values should be maintained above 5.0 to ensure a predominant negatively charged surface resulting in electrostatic attraction between adsorbate molecules and bark biomass. Below this pH, the surface charge of eucalyptus bark biomass acquires positively charged due to protonation of functional groups which making H^+ ions compete effectively with the MB dye or Zn^{2+} cations and thus a decrease in the amount of adsorbate adsorbed is expected (Oliveira, Franca et al. 2008).

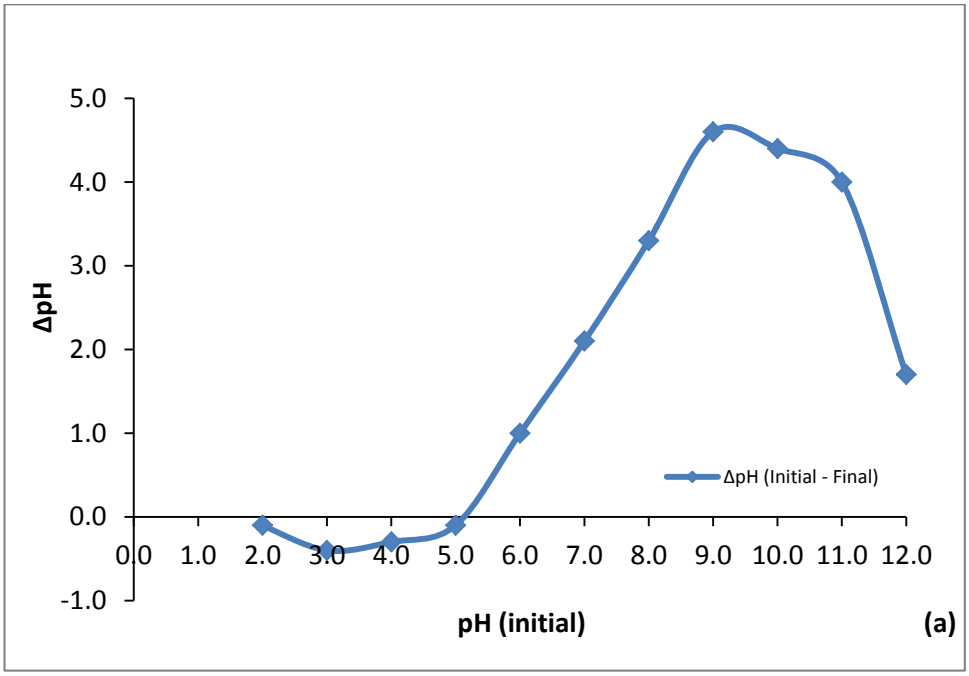

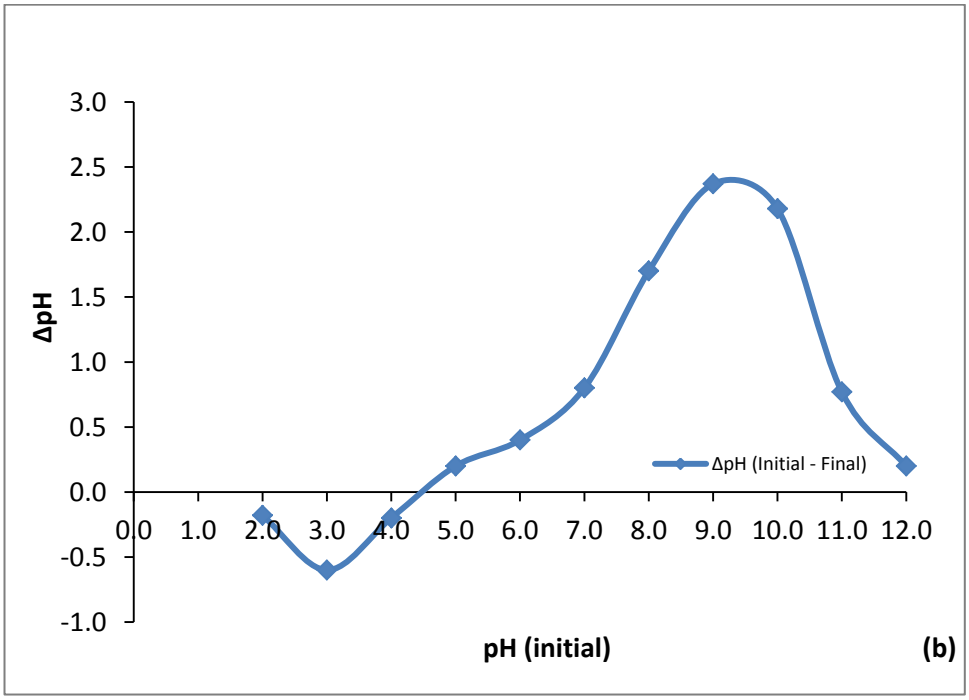

Figure 3.20 Point of zero charge (pHpzc) of (a) raw eucalyptus bark and (b) NaOH modified eucalyptus bark

3.4 Summary

In this chapter, research methods consisted of selection of sorbents for the research project, development of experimental procedures to generate data to test the research hypotheses and the characterisation of raw and NaOH treated eucalyptus bark were presented in details. The study of physico-chemical characterisation helps in understanding adsorption behaviour and mechanism for combining adsorbate-adsorbent interaction for adsorption process and the outcomes based on the results of the characterisation of prepared raw and modified eucalyptus bark are as follows:

- The scanning electron microscopy (SEM) of prepared raw and modified eucalyptus bark materials showed the surface morphology of untreated bark material is different from that of treated bark material and EDS study exposed the components present in adsorbent biomass.
- The chemical analysis using XRD technique identifies that there is no significant changes in the characteristic XRD patterns of raw and NaOH treated eucalyptus bark indicating that the chemical elements present on the surface of raw and NaOH treated eucalyptus bark are same. The peaks obtained also gave good indication of highly organized crystalline cellulose on the adsorbent biomass.
- The FTIR of modified bark revealed a new peak at 2922.5 cm^{-1} which allocates the aliphatic group C–H stretching vibrations. This shows that the treatment of biomass with alkali resulted in the exposure of buried aliphatic groups of the surface of adsorbent which leads to higher adsorption capacity of base treated biomass.
- Surface area was higher for chemically treated bark material compared to untreated bark adsorbent, which also enhances adsorption potential of base treated eucalyptus bark.
- The study of bulk density for raw and modified eucalyptus bark showed lower bulk density for treated eucalyptus bark material. The bulk density for eucalyptus bark was 0.39 gm/cm^3, whereas 0.27 gm/cm^3 bulk density was found for NaOH treated modified eucalyptus bark.

- The study of pH_{zpc} for raw and modified eucalyptus bark showed a decrease of the point of zero charge for modified adsorbent compared to unmodified one. The point of zero charge for modified eucalyptus bark is 4.5 whereas for raw bark, it was observed at 5.0.

3.5 References

Dawood, S., Sen, T. K. and Phan, C. (2014). "Synthesis and characterisation of novel-activated carbon from waste biomass pine cone and its application in the removal of congo red dye from aqueous solution by adsorption." Water, Air, & Soil Pollution **225**(1): 1-16.

Elizalde-González, M. P., Mattusch, J., Peláez-Cid, A. A. and Wennrich, R. (2007). "Characterization of adsorbent materials prepared from avocado kernel seeds: Natural, activated and carbonized forms." Journal of Analytical and Applied Pyrolysis **78**(1): 185-193.

Lippens, B. C. and De Boer, J. (1965). "Studies on pore systems in catalysts: V. The t method." Journal of Catalysis **4**(3): 319-323.

Mall, I., Srivastava, V., Kumar, G. and Mishra, I. (2006). "Characterization and utilization of mesoporous fertilizer plant waste carbon for adsorptive removal of dyes from aqueous solution." Colloids and Surfaces A: Physicochemical and Engineering Aspects **278**(1): 175-187.

Marshall, W., Wartelle, L., Boler, D., Johns, M. and Toles, C. (1999). "Enhanced metal adsorption by soybean hulls modified with citric acid." Bioresource Technology **69**(3): 263-268.

Ofomaja, A. and Naidoo, E. (2011). "Biosorption of copper from aqueous solution by chemically activated pine cone: a kinetic study." Chemical Engineering Journal **175**: 260-270.

Ofomaja, A., Naidoo, E. and Modise, S. (2009). "Removal of copper (II) from aqueous solution by pine and base modified pine cone powder as biosorbent." Journal of Hazardous Materials **168**(2): 909-917.

Oliveira, L. S., Franca, A. S., Alves, T. M. and Rocha, S. D. (2008). "Evaluation of untreated coffee husks as potential biosorbents for treatment of dye contaminated waters." Journal of Hazardous Materials **155**(3): 507-512.

Sadaf, S. and Bhatti, H. N. (2014). "Batch and fixed bed column studies for the removal of Indosol Yellow BG dye by peanut husk." Journal of the Taiwan Institute of Chemical Engineers **45**(2): 541-553.

University of Colorado. (1985). "Table of Characteristic IR Absorptions." Retrieved December 27, 2013, from orgchem.colorado.edu/Spectroscopy/specttutor/irchart.pdf.

Wartelle, L. and Marshall, W. (2000). "Citric acid modified agricultural by-products as copper ion adsorbents." Advances in Environmental Research **4**(1): 1-7.

Zvinowanda, C. M., Okonkwo, J. O., Agyei, N. M. and Shabalala, P. N. (2009). "Physicochemical characterization of maize tassel as an adsorbent. I. Surface texture, microstructure, and thermal stability." Journal of Applied Polymer Science **111**(4): 1923-1930.

Every reasonable effort has been made to acknowledge the owners of copyright material. I would be pleased to hear from any copyright owner who has been omitted or incorrectly acknowledged.

CHAPTER 4

BATCH ADSORPTION STUDIES ON THE REMOVAL OF ORGANIC METHELYNE BLUE (MB) DYE BY RAW EUCALYPTUS BARK

ABSTRACT*

This study was undertaken to evaluate the adsorption potential of a naturally available, cost-effective, raw eucalyptus bark (EB) (Eucalyptus sheathiana) biomass, to remove organic methylene blue (MB) dye from its aqueous solutions. Effects of various process parameters such as initial dye concentration, adsorbent loading, solution pH, temperature, presence of salts, mixture of dyes and surfactant onto MB dye adsorption by bark material were studied. Significant effect on adsorption was witnessed on varying the pH of the MB solutions. Results showed that the optimum pH lies between 7.4 and 10.0. The extent (%) of MB adsorption from aqueous solution decreased with the increase in the initial MB dye concentration, but increased with rise in temperature. The extent of MB dye adsorption was found to be enhanced due to increase of salts concentration. This is because of salting-out-effect, which comprises the changes of various short range forces. The overall kinetic studies showed that the MB dye adsorption by EB biomass followed pseudo-second-order kinetics. The mechanism of MB dye adsorption was analysed by intra-particle diffusion model and desorption study. Free energy change of adsorption (ΔG°), enthalpy change (ΔH°) and entropy change (ΔS°) were calculated to predict the nature of adsorption. The Langmuir adsorption isotherm model yields a better correlation coefficient than the Freundlich model and the dimensionless separation factor "R_L" indicated favourable adsorption process. The maximum Langmuir monolayer adsorption capacity of raw EB for MB dye was found to be 204.08 mg/g at 30°C. A single-stage batch adsorber design for MB dye adsorption onto EB biomass has been presented based on the Langmuir isotherm model equation. The results obtained in this study suggest a promising future for inexpensive raw EB biomass as a novel adsorbent and a better alternative to activated carbon adsorbent used for the removal of MB dye from dye bearing effluents.

* This work has been published in Desalination and Water Treatment Journal (Afroze, S., Sen, T.K., Ang M., & Nishioka, H., 2016. Adsorption of methylene blue dye from aqueous solution by novel biomass eucalyptus *sheathiana* bark: equilibrium, kinetics, thermodynamics and mechanism. *Desalination and Water Treatment*, 57(13):5858-5878. DOI: 10.1080/19443994.2015.1004115)

4.1 Introduction

This chapter deals with investigation for the potential use of raw eucalyptus bark biomass as a cost effective and efficient adsorbent for the removal of methylene blue (MB) dye from its aqueous solution. The influence of various physicochemical parameters such as contact time, initial MB dye concentration, initial solution pH, amount of adsorbent and system temperature on the removal of MB dye through batch kinetic experiments were investigated and discussed. Further, large amount of salts and surfactant are utilized in the dyeing process and there should be an effect of dissolved and mixed salt concentration and surfactant combination on the adsorption capacity of biomass. Therefore, mixed salt effect and surfactant effect on MB dye adsorption has also been presented here. As industrial effluents contain several pollutants simultaneously, the effect of mixed dyes on MB dye adsorption was also studied here. To provide better understanding of the adsorption process and mechanism, batch experimental data were analysed with pseudo-first-order, pseudo-second-order and intraparticle diffusion model. To simulate the adsorption isotherm, two commonly used models, Langmuir and Freundlich were selected to explore MB dye-bark interaction and adsorption mechanism. Finally the effectiveness of raw eucalyptus bark adsorbent under various conditions tested here was compared with other published biomass based adsorbents. In addition, thermodynamic parameters were determined for the sorption of MB dye to explain the process feasibility and desorption efficiency was also calculated to investigate the mechanism and recovery of MB dye together with the regeneration and reusable capacity of the biosorbent. In order to gain insight into the dynamics of the process, a single-stage batch adsorber has been designed for the removal of methylene blue (MB) dye by eucalyptus bark based on the equilibrium data obtained.

4.2 Materials and Methods

4.2.1 Adsorbent

Eucalyptus barks (*E. sheathiana*) were obtained locally from Curtin University – Bentley campus, Western Australia between February and March 2013. The barks were washed repeatedly with deionised water to remove dirt and soluble impurities. The barks were placed in the oven to dry at temperature of 105˚C for 24 h. The dried biomass was crushed in a mechanical grinder to fine powders and passed through British Standard Sieves (BSS) of 106 µm. The resultant raw eucalyptus bark powders of size ≤ 106 µm were stored in an airtight plastic container for analysis as well as for conducting adsorption experiments. The characterisation of raw eucalyptus bark material before and after adsorption is presented in Section 3.3.

4.2.2 Adsorbate and Other Chemicals

Methylene blue (supplied by Sigma-Aldrich Pty. Ltd., NSW, Australia) was taken as the model adsorbate in this study. A stock solution of 1000 mg/L MB dye was prepared by dissolving 1000 mg powder of MB dye in 1000 mL of ultra-pure water. Further details of MB dye and other chemicals used for experimental purposes are described in Section 3.2.1.

4.2.3 Adsorption Experiments

The adsorption of Methylene Blue dye on raw eucalyptus bark was carried out in a batch system. Batch adsorption experiments were conducted by varying the process operating parameters such as initial solution pH, adsorbent dose, initial dye concentration, temperature, addition of salts and surfactant and with mixed dye at predetermined time interval under the aspect of adsorption kinetics, adsorption isotherm and thermodynamic study. A known amount of the adsorbent was mixed with 50 mL Methylene Blue solutions of known concentration in a series of 250 mL plastic bottles. The mixture was shaken in a constant temperature using Thermo Line Scientific Orbital Shaker Incubator at a speed of 120 rpm and temperature of 30^0C. At predetermined time intervals, the bottles were withdrawn from the shaker, supernatant MB dye was separated from the adsorbents by centrifuging and the residual dye concentration in the solution was measured by using UV spectrophotometer. The amount of dye adsorbed onto the adsorbent at time t, q_t

(mg/g) and % Adsorption were calculated as per equations (3.1) and (3.2) respectively.

Furthermore, equilibrium isotherm adsorption process was carried out by contacting 50 mL of MB solution having various initial dye concentrations of 20, 30, 40, 50, 60 and 70 ppm (mg/L) with 20 mg raw eucalyptus bark, solution pH of 7.4 and 30^0C temperature in 250 mL plastic bottles for 4 h which was adequate to reach equilibrium time. The bottles were shaken in Thermo Line Scientific Orbital Shaker Incubator at a speed of 120 rpm. Then the bottles were withdrawn from the shaker, centrifuged and the supernatant was analysed for residual MB dye concentration using UV spectrophotometer. The amount of dye adsorbed onto the adsorbent at equilibrium, q_e (mg/g) was calculated from equation (3.1). Detailed methods are described in Section 3.2.2.

4.3 Results and Discussion

4.3.1 Effect of Initial Solution pH on MB Dye Adsorption Kinetics

The efficiency of adsorption depends on the solution pH because variation in pH leads to the variation in the degree of ionization of the adsorptive molecule and may alter the surface properties of adsorbent (Sen, Afroze et al. 2011). Therefore, controlling the pH of the solution is crucial in sorption studies. Fig. 4.1(a) shows the effect of initial solution pH on amount of MB dye adsorption, q_t (mg/g) and Fig. 4.1(b) represents percentage removal of dye with solution pH. Clearly, both the amount adsorbed and the percentage removal of MB increased with time as well as with the increase of aqueous solution pH from 2.5 to 10.0. From Fig. 4.1(a-b), it was also found that the amount of dye adsorbed increased from 28.89 mg/g (57.80% removal efficiency) to 44.73 mg/g (89.45% removal efficiency) due to change in solution pH from acidic (pH = 2.5) to alkaline (pH = 10.0) for a fixed initial dye concentration of 20 ppm at equilibrium. The observed pH trend clearly indicates that the maximum adsorption of MB dye takes place at pH 10.0. With increasing pH values, the adsorption of methylene blue on eucalyptus bark biomass tends to increase, which can be explained by the electrostatic interaction of cationic MB dye with the negatively charged surface of eucalyptus bark (EB). This electrostatic force of attraction is more with increasing negative surface charge of adsorbent. This was

supported by point of zero surface charge, pH_{zpc} (= 5.0) of eucalyptus bark examined and discussed in Section 3.3 which revealed that the observed favorable pH of the solution for better adsorption is greater than pH_{zpc} i.e. solution pH> pH_{zpc}.

Further, in adsorbent-aqueous systems, the potential of the surface is determined by the activity of H^+ ions, which react with the adsorbent surface. Therefore, the high percentage of dye removal at high pH is also due to presence of less H^+ competing for sorption sites on the biomass. Low pH leads to an increase in H^+ ion concentration in the system, and the surface of bark biomass acquires positive charge by protonation of phenolic and amino groups of eucalyptus bark surface (Dave, Kaur et al. 2011) and hence less amount of cationic MB dye adsorption takes place. In this study, the rate of adsorption is high at higher pH. With the increase of pH value, the net negative charge increases on the surface of eucalyptus bark adsorbent, the surface then exhibits a cation exchange capacity and the increased electrostatic force of attraction enhanced MB dye adsorption capacity. Similar trend was reported for adsorption of MB onto rice husk (Vadivelan and Kumar 2005), palm kernel shell activated carbon (Jumasiah, Chuah et al. 2005) and wheat shells (Bulut and Aydın 2006). The complete calculated experimental data on the adsorption capacity, q_t (mg/g) and dye removal percentage on various pH studies is presented in Appendix A1-A6.

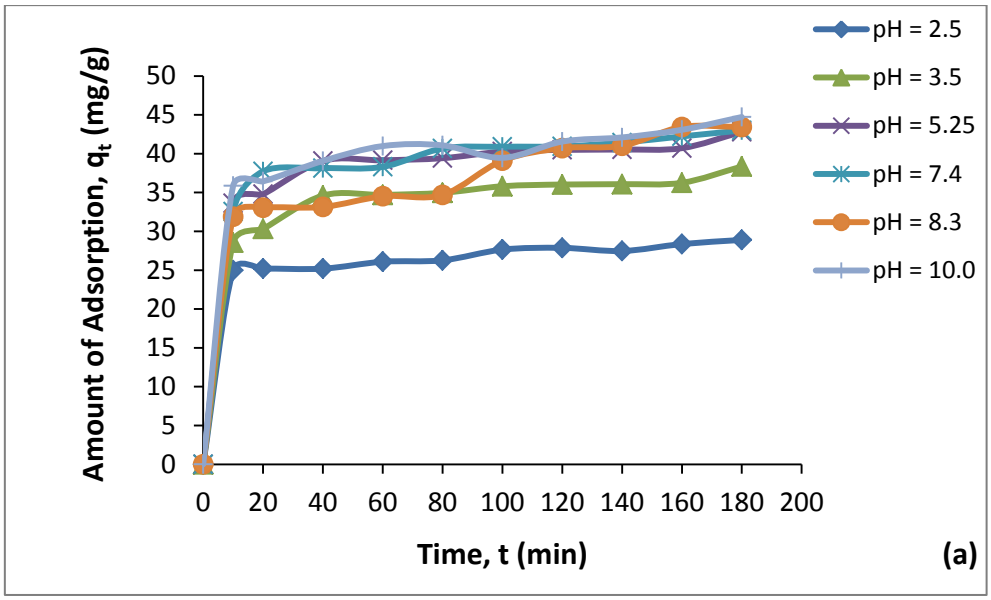

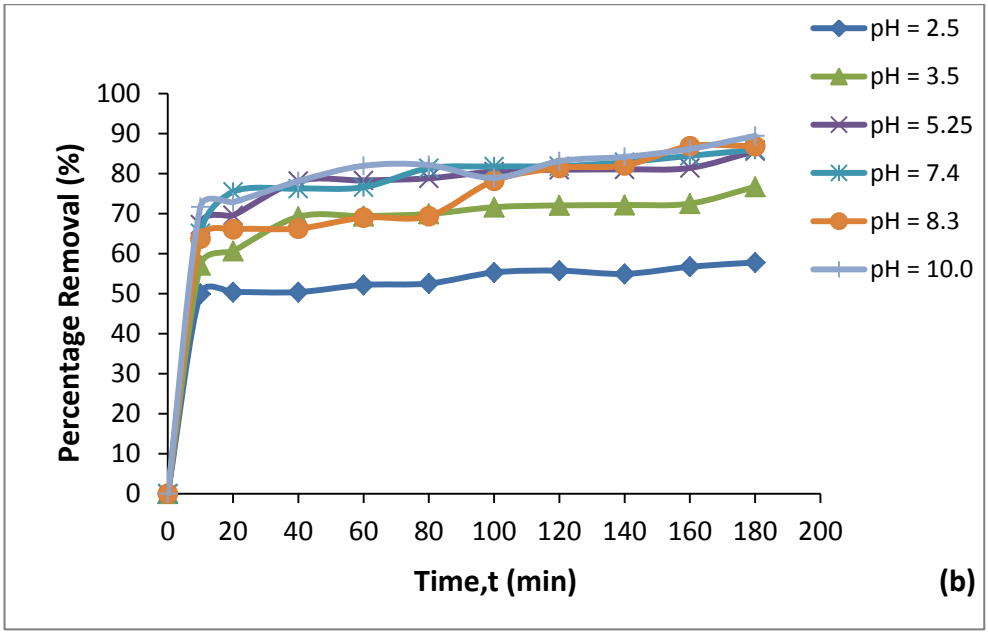

Figure 4.1 Effect of initial solution pH by raw eucalyptus bark on (a) the amount of MB dye adsorption (b) percentage (%) removal of MB dye

(Conditions: Mass of adsorbent = 20 mg, volume of MB solution = 50 mL, initial MB dye concentration = 20 ppm, temp = 30°C, shaker speed = 120 rpm and time of adsorption = 180 min)

4.3.2 Effect of Initial Dye Concentration and Contact Time on MB Dye Adsorption Kinetics

The effect of contact time on the amount of adsorption of methylene blue (MB) dye and its percentage removal were investigated at different initial dye concentration onto eucalyptus bark adsorbent for different contact times, and for which complete

calculated experimental data is presented in Appendix A7-A12 and the obtained results are shown in Fig. 4.2(a) and 4.2(b) respectively. From Fig. 4.2(a), it was observed that the amount of methylene blue (MB) dye adsorption, q_t (milligrams per gram), increased from 43 mg/g to 67.91 mg/g with increase in initial MB dye concentration from 20 ppm to 70 ppm. Further, it was found that the amount of adsorption, i.e. milligrams of adsorbate per gram of adsorbent, increases with increasing contact time at all initial dye concentrations and equilibrium is attained within 140 min. It was also found from Fig. 4.2(b) that the percentage removal of dye increased from 38.81% to 85.95% with decreasing initial concentration of methylene blue dye from 70 to 20 ppm. Basically, from both the Figs. 4.2(a) and 4.2(b), the adsorption percentage decreases and the amount of adsorption increases with increasing initial dye concentration. This is because the initial dye concentration provides the driving force to overcome the resistance to the mass transfer of dye between the aqueous and the solid phase. For constant dosage of adsorbent, at higher initial dye concentration, the available adsorption sites of adsorbent become fewer, and hence, the removal of methylene blue depends upon the initial concentration (Shahryari, Goharrizi et al. 2010). The increase in initial dye concentration also enhances the interaction between adsorbent and dye. Therefore, an increase in initial dye concentration leads to an increase in the adsorption uptake of dye. It is also found from Fig. 4.2(b) that the removal of dye by adsorption onto eucalyptus bark was very fast at the initial period of contact time but slowed down subsequently. These kinetic experiments [Fig. 4.2(a) and 4.2(b)] clearly indicate that adsorption of methylene blue dye on eucalyptus bark is more or less two-step process: a very rapid adsorption of dye to the external surface followed by possible slow intraparticle diffusion in the interior of the adsorbent. The rapid kinetics has significant practical importance, as it facilitates smaller reactor volumes, ensuring high efficiency and economy (Arias and Sen 2009).

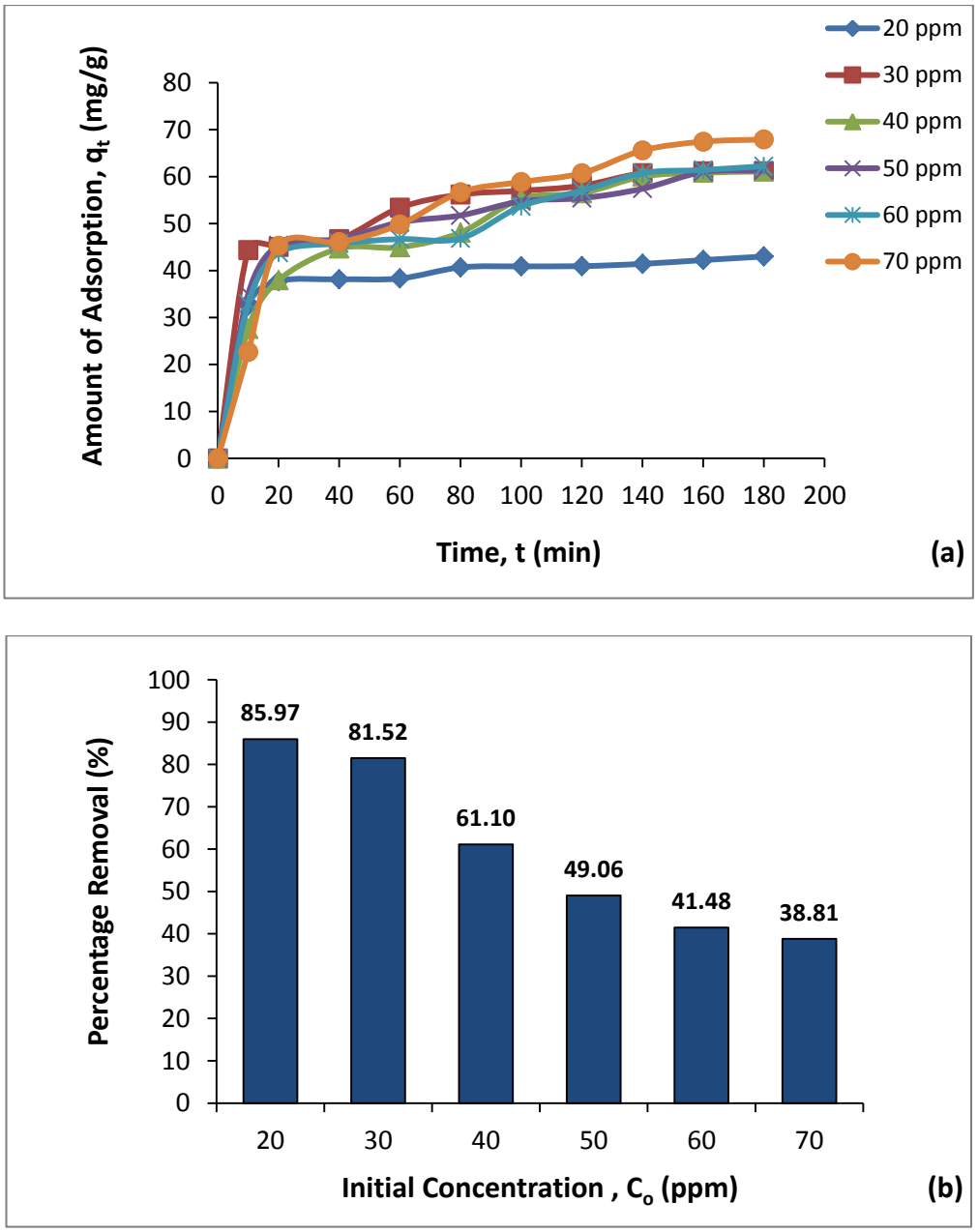

Figure 4.2 Effect of initial solution concentration by raw eucalyptus bark on (a) the amount of MB dye adsorption (b) percentage (%) removal of MB dye

(Conditions: Mass of adsorbent = 20 mg, volume of MB solution = 50 mL, solution pH = 7.4, temp = 30°C, shaker speed = 120 rpm and time of adsorption = 180 min)

4.3.3 Effect of Adsorbent Dosage on MB Dye Adsorption Kinetics

Study of the effect of adsorbent dosage provides an idea of the effectiveness of an adsorbent and the ability of a dye to be adsorbed with a minimum dosage, so as to identify the ability of a dye from an economic point of view (Salleh, Mahmoud et al. 2011). To investigate the effect of eucalyptus bark (EB) dosage for the adsorption of

MB dye, the experiments were conducted with different adsorbent doses (0.01 - 0.03 g/50 mL) while maintaining the initial dye concentration (20 mg/L), temperature (30^0C), pH (7.4) and shaker speed (120 rpm) constant at different contact times. Fig. 4.3(a) shows that the increase in adsorbent dosage from 0.01 to 0.03 g resulted in decrease of amount of adsorbed dye from 72.96 to 31.30 mg/g and at equilibrium, the percentage dye removal was increased from 72.95% to 94% with the increase of adsorbent mass from 0.01 to 0.03 g [Fig. 4.3(b)].

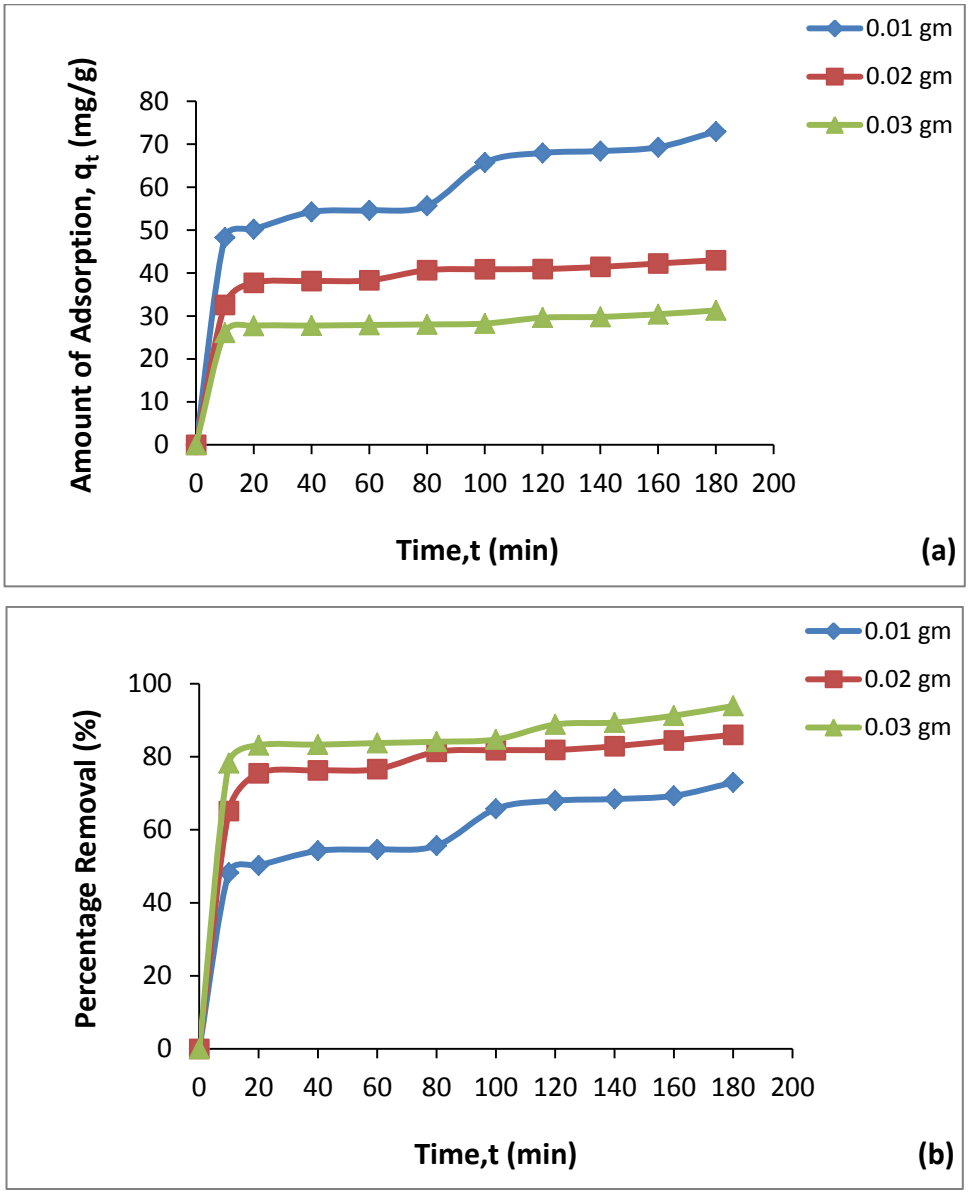

Figure 4.3 Effect of adsorbent dosages by raw eucalyptus bark (a) on the amount of MB dye adsorption (b) percentage (%) removal of MB dye

(Conditions: Volume of MB solution = 50 mL, solution pH = 7.4, initial MB dye concentration = 20 ppm, temp = 30°C, shaker speed = 120 rpm and time of adsorption = 180 min)

At higher eucalyptus bark to methylene blue concentration ratios, there is a very fast superficial sorption onto the eucalyptus bark surface that gives a lower methylene blue concentration in the solution compared to the lower biomass to methylene blue concentration ratio. This is because a fixed mass of eucalyptus bark can only adsorb a fixed amount of dye. Therefore the higher the adsorbent dosage, the larger the volume of effluent that a fixed mass of eucalyptus bark biomass can purify. The decrease in amount of dye adsorbed, q_e (mg/g) with increasing adsorbent mass, is due to the split in the flux or the concentration gradient between solute concentration in the solution and the solute concentration in the surface of the adsorbent (Sen, Afroze et al. 2011). Thus, with increasing adsorbent mass, the amount of dye adsorbed onto unit weight of adsorbent gets reduced and hence causing a decrease in q_e value with increasing adsorbent mass concentration (Vadivelan and Kumar 2005). A similar behaviour was observed for methylene blue adsorption on guava leaf (Ponnusami, Vikram et al. 2008), on gulmohar plant leaf (Ponnusami, Gunasekar et al. 2009) and on cashew nut shell activated carbon (Kumar, Ramalingam et al. 2011). Further, increasing the amount of the adsorbent and keeping fixed adsorbate concentration makes a large number of adsorbent sites available for adsorption, hence increase in percentage (%) of adsorption and decrease in the amount of adsorption, q_e (Oladoja, Aboluwoye et al. 2008). Full calculation on the adsorption capacity, q_t (mg/g) and dye removal percentage for different adsorbent dosages is presented in Appendix A13-A15.

4.3.4 Effect of Temperature and Thermodynamic Parameters Calculation for MB Dye Adsorption Kinetics

Real textile effluents are mostly released at relatively higher temperatures so temperature is also an important design parameter for the real application of biosorption process (Sadaf and Bhatti 2013). There are two major effects of temperature on the adsorption process: increasing the temperature is known to increase the rate of diffusion of the adsorbate molecules across the external boundary layer and in the internal pores of the adsorbent particle, owing to the decrease in the viscosity of the solution (Al-Qodah 2000). In addition, changing the temperature will change the equilibrium capacity of the adsorbent for a particular adsorbate (Al-

Qodah 2000). The effect of temperature on the equilibrium adsorption capacity of raw eucalyptus bark for MB dye was carried out at temperatures of 30, 45 and 60°C.

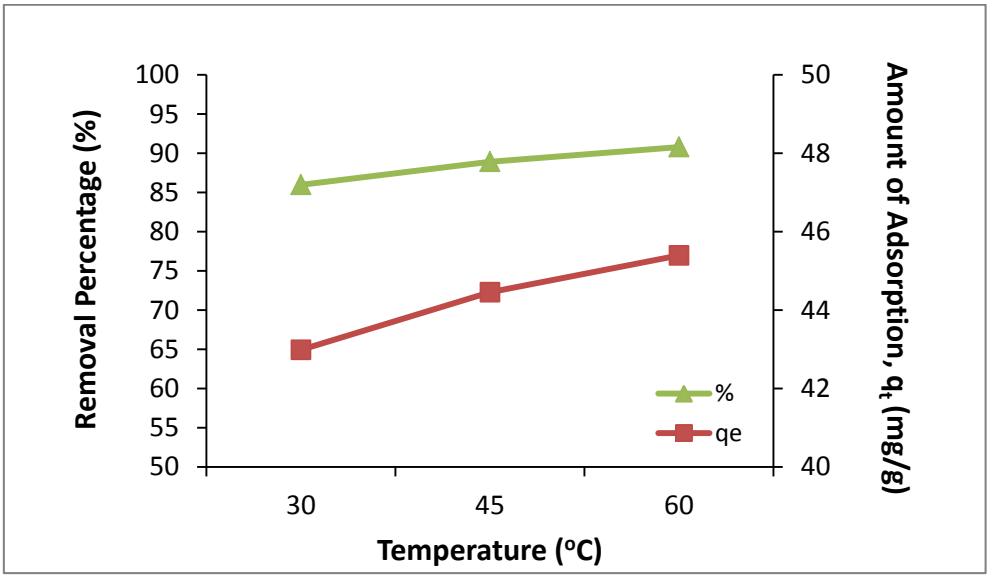

Figure 4.4 Effect of temperature on the adsorption of MB dye onto EB powder

(Conditions: Mass of adsorbent = 20 mg, volume of MB solution = 50 mL, solution pH = 7.4, initial MB dye concentration = 20 ppm, shaker speed = 120 rpm and time of adsorption = 180 min)

Fig. 4.4 depicts the influence of solution temperature on the adsorption of MB dye onto eucalyptus bark (EB) adsorbent where it was observed that the adsorption capacity, q_t (mg/g) increased simultaneously with the increase in reaction temperature from 30-60°C. It was also found that the increase in temperature from 30°C to 60°C resulted in increase in the percentage removal (%) of adsorption from 85.97% to 90.79%. The fact that the adsorption of dye was in favor of temperature indicates that the mobility of the dye molecule increased with increase in temperature and the molecules escape from the liquid phase of dye to solid phase of bark adsorbent with an increase in temperature of the solution. With increasing reaction temperature, the amount of non-protonated functional groups on the adsorbent increases due to the increase in the dissociation constant of the protonated carboxyl groups and increasing temperature can cause a swelling effect within the internal structure of the adsorbent (Zhao, Xia et al. 2014). This effect enabled the MB ions to penetrate further and dye molecules interact more effectively with the adsorbent surface with rise in temperature resulting in enhanced adsorption capacity. The increase in adsorption capacity with increasing temperature suggests that the process

of removal of MB dye by eucalyptus bark biomass is endothermic in nature. Similar types of results were reported by other researchers for methylene blue adsorption on water weeds biomass (Tarawou and Horsfall Jr 2007), cashew nut shell (Senthil Kumar, Ramalingam et al. 2010) and NaOH modified malted sorghum mash (Oyelude and Appiah-Takyi 2012). Complete calculated experimental data on the adsorption capacity, q_t (mg/g) and dye removal percentage at different reaction temperatures is presented in Appendix A16-A18.

The determination of the basic thermodynamic parameters: change in Gibb's free energy of adsorption (ΔG^o), change in enthalpy of adsorption (ΔH^o) and change in entropy of adsorption (ΔS^o), is important to understand the changes in the reaction that can be expected during adsorption process. Therefore, the thermodynamics parameters have been calculated using Eq. (2.11) and Eq. (2.12) illustrated in Section 2.8 from the linear form of the Van't Hoff plot [log (q_e/C_e) vs. $1/T$] in Fig. 4.5. All three thermodynamic parameters are presented in Table 4.1. From Table 4.1, the change in Gibbs free energy (ΔG^0) was found to be negative with values from -6.89 to -8.89 kJ/mol at all the temperatures studied. This negative result of ΔG^0 confirmed the feasibility of the process and the spontaneous nature of physical adsorption with a high preference of MB dye on eucalyptus bark. The ΔG^0 value becomes more negative with increasing temperature supports that MB adsorption on eucalyptus bark is favoured with the increase in temperature. The positive value of ΔH^0 revealed the process to be endothermic and irreversible. The positive value ΔS^0 indicates favourable randomness at the solid/solution interface though its value is small. This suggests the structural changes after adsorption of MB dye takes place on bark (Dave, Kaur et al. 2011).

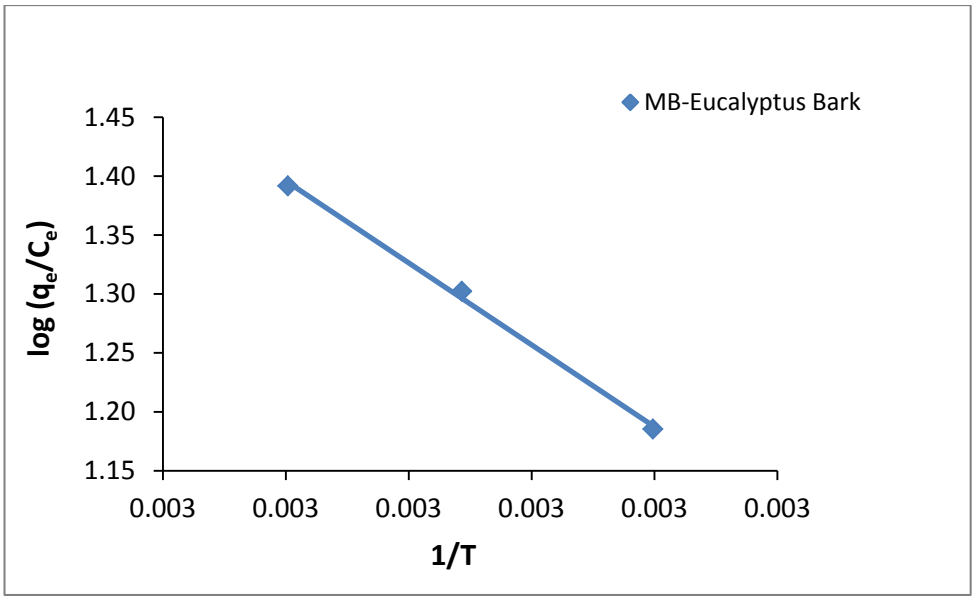

Figure 4.5 Van't Hoff plot for adsorption of MB dye on raw eucalyptus bark

Table 4.1: Thermodynamic parameters for adsorption of MB dye onto raw eucalyptus bark at different temperature

Temp. (K)	*ΔG° (KJ/mole)*	*ΔH°(KJ/mole)*	*ΔS° (KJ /mole.K)*
303.15	-6.89		
318.15	-7.89	13.31	0.067
333.15	-8.89		

4.3.5 Effect of Surfactant on MB Dye Adsorption Kinetics

Surfactants are typically used in the textile industries during different washing processes (Zaheer, Bhatti et al. 2014). Therefore, the effect of their presence on the dye sorption was examined. Surfactant, Triton X-100 was added (1%) to the 50 mL of 20 ppm MB dye solution to check out the effect of surfactant on the MB dye removal from the solution for which experimental data is presented in appendix A19 and in Fig. 4.6. From Fig. 4.6, it is clearly observed that amount of MB dye adsorption in the absence of surfactant was about 43 mg/g whereas the adsorption amount of MB dye decreased by 9.8% in the presence of non-ionic surfactant Triton X-100 and became 38.79 mg/g. This decrease in adsorption of MB dye can be explained due to the competition between dye molecules and surfactants for the attachment to the adsorbent surface in presence of non-ionic TX-100 molecules, ultimately resulting in lower MB dye adsorption. Decrease in MB dye removal in the

presence of non-ionic surfactant was also observed by (Geçgel, Özcan et al. 2012). Similar trend of decrease in biosorption capacity of biosorbent in presence of surfactants was further reported by Brahimi-Horn et al. (Brahimi-Horn MC 1992) and by Sana et al. (Sadaf and Bhatti 2013).

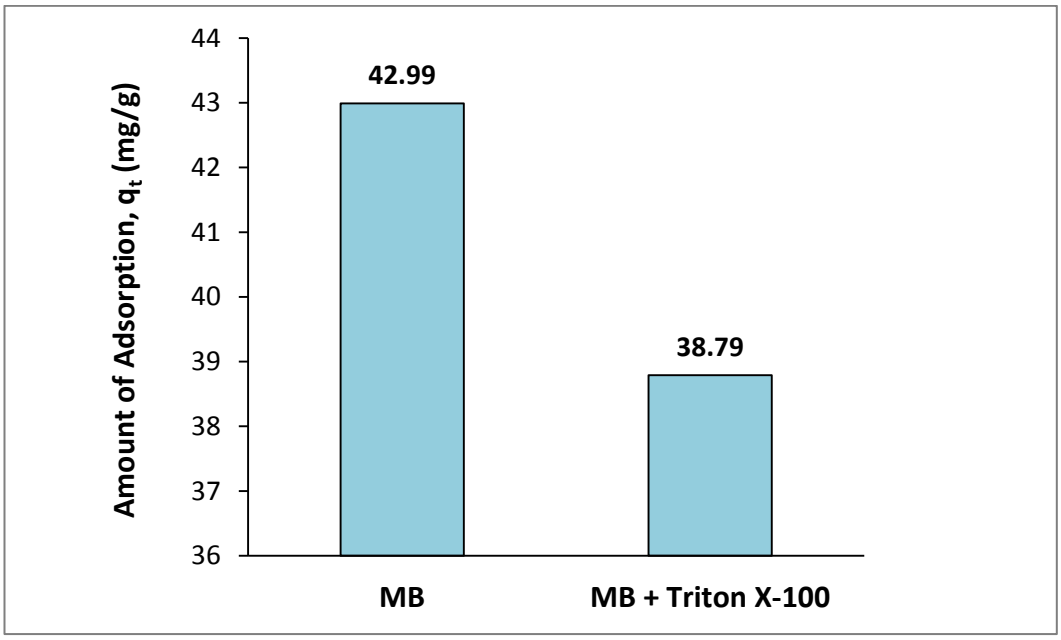

Figure 4.6 Effect of surfactant on the amount of adsorption of MB dye onto EB powder

(Conditions: Mass of adsorbent = 20 mg, volume of MB solution = 50 mL, initial MB dye concentration = 20 ppm, volume of Triton X-100 = 1.0 mL, temp = 30°C, shaker speed = 120 rpm and time of adsorption = 180 min)

4.3.6 Effect of Presence of Mixed Dye

Textile dyeing operations can use different classes of chemical dyes and chemicals depending on the textile, which results in a mixed wastewater. Similar to methylene blue (MB), congo red (CR) is another toxic common dye which is extensively used in several industrial activities. However MB dye is cationic and CR dye is anionic in nature. Therefore, competitive adsorption of mixed dyes; methylene blue (MB) and congo red (CR) dye from their binary solution was investigated at an initial solution pH of 7.4 and 30°C temperature onto raw eucalyptus bark adsorbent.

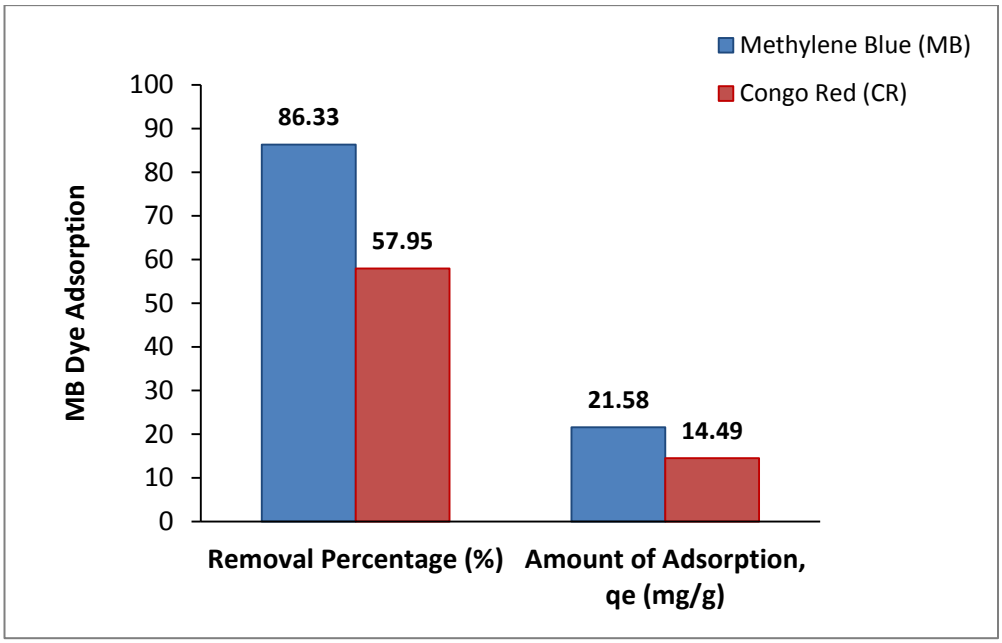

Figure 4.7 Effect of mixture of adsorbents on the adsorption onto EB powder

(Conditions: Mass of adsorbent = 20 mg, volume of MB solution = 25 mL, volume of CR solution = 25 mL, initial MB concentration = 20 ppm, initial CR concentration = 20 ppm, temp = 30°C, shaker speed = 120 rpm and time of adsorption = 180 min)

It was found that the percentage removal and amount of MB dye adsorption was higher (86.33% and 21.58 mg/g respectively) compared to CR removal (57.95% removal efficiency and 14.49 mg/g adsorption capacity) for a particular solution pH of 7.4 (Fig. 4.7). At this solution pH of 7.4, the surface charge is mostly negative in nature and hence large amount of cationic dye MB adsorption took place due to electrostatic force of attraction compared to less amount of anionic dye CR adsorption. However from this study, it is evident that eucalyptus bark material can be used to remove both cationic and anionic dyes from their aqueous solutions. Complete calculation on the adsorption capacity, q_t (mg/g) and dye removal percentage for mixed dye study is presented in Appendix A20.

4.3.7 Effect of Inorganic Mono, Di and Trivalent Ions on MB Dye Adsorption Kinetics

Since large amounts of salts are generally utilized in dyeing processes, the effects of ionic strength on adsorption must be evaluated. To examine how inorganic ions affect adsorption of methylene blue (MB) onto raw eucalyptus bark (EB) biomass, investigation was carried out in this study by adding NaCl, $CaCl_2$ and $FeCl_3$ of

concentrations ranging from 100 – 300 ppm to the MB solution. The complete calculated data on experimental findings is presented in Appendix A21-A23 and the results are shown in Fig. 4.8. From Fig. 4.8, it can be observed that the MB dye removal capacity by eucalyptus bark decreased due to presence of monovalent NaCl salt and it was more significantly decreased with decreasing salt concentration. This may be due to the following reasons: (i) the protonated functional group of MB dye can interact with the chloride ions of the ionic medium by lowering its availability to the potential interaction with negative charges of sorbent material, (ii) the inorganic cations could compete with the MB cations adsorbed on the adsorption sites and reduced the adsorption. Similar trend was observed for divalent $CaCl_2$ salt but comparatively to a lesser extent whereas for trivalent $FeCl_3$ salt, an increase in ionic strength also increased adsorption (Fig. 4.8). This was due to the attractive electrostatic interactions between the adsorbent surface and charged adsorbate ions. When the surface and adsorbate have the same charge and non-electrostatic forces govern adsorption, or for adsorbed amounts where lateral interactions predominate, increased ionic strength will increase adsorption (Stavropoulos, Skodras et al. 2015). Bharathi and Ramesh (Bharathi and Ramesh 2013) also reported that the electrical double layer surrounding the adsorbent surface was compressed due to presence of increasing salt concentration which may lead to a decrease in the electrostatic potential and hence a reduction of coulombic free energy and a decrease in basic dye adsorption as in the case of NaCl-MB and $CaCl_2$-MB system. Further Fig. 4.8 indicates that the adsorption of positively charged MB on negatively charged eucalyptus bark biomass (at this pH) enhanced with the nature of salt in the order of $Na^{+}<Ca^{++}<Fe^{+++}$. Wang et al (Wang, Zhou et al. 2008) reported that the amount of adsorption depends on the nature of electrolytes such as chloride salt of sodium which favours attractive electrostatic forces. The percentage of MB removal was increased with the increase in trivalent $FeCl_3$ salt concentration when compared with the results of MB adsorption without salt. For $FeCl_3$ – MB system, this behaviour may be due to the dye dimerization in solution or formation of dye aggregation induced by the effect of salt ions which is known as “salting-out-effect” (Kuo, Wu et al. 2008, Fedoseeva, Fita et al. 2010). Basically, various types of short range forces such as Vander Waals force, dipole-dipole and ion-dipole force increased with salt concentration during dye dimerization (Fedoseeva, Fita et al. 2010). From Fig. 4.8, it was also observed that the amount of MB adsorption increased more with

divalent/trivalent salt cations compared to monovalent cations. This may be due to increase in surface charge density of Ca^{2+}/Fe^{3+} compared to Na^{+} ions at this medium solution pH range where precipitation was nil.

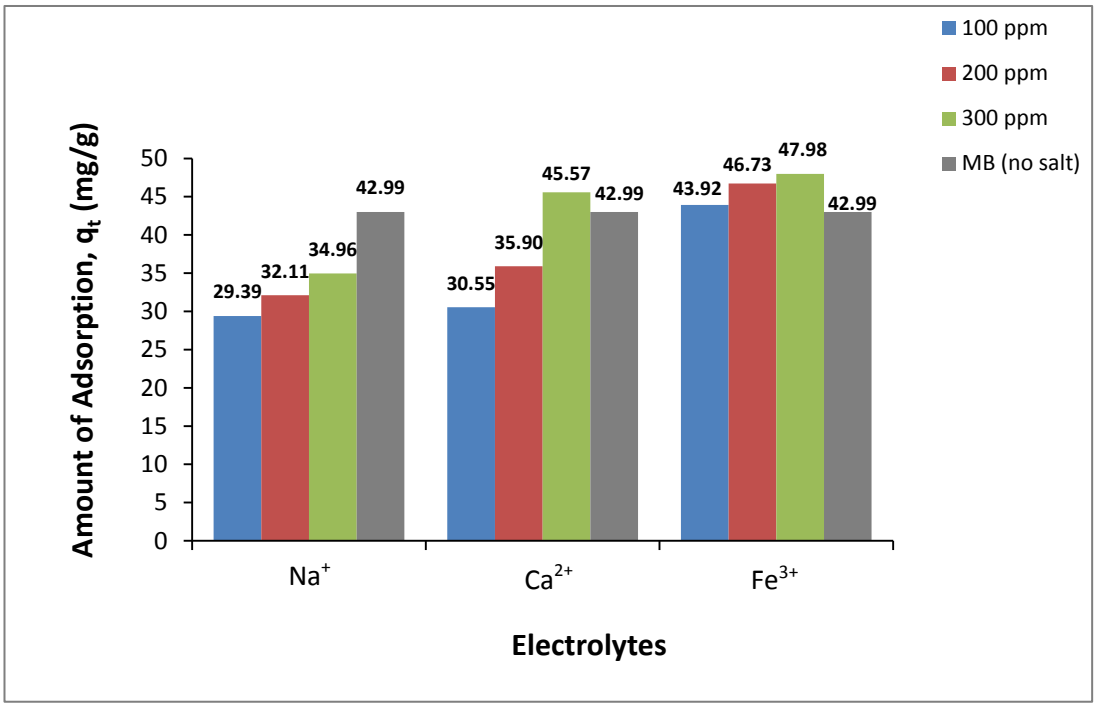

Figure 4.8 Effect of electrolytes on the adsorption of MB dye onto EB powder

(Conditions: Mass of adsorbent = 20 mg, total reaction volume = 50 mL (48 mL of MB solution + 2 mL salt solution), initial MB dye concentration = 20 ppm, solution pH = 7.4, temp = 30°C, shaker speed = 120 rpm and time of adsorption = 180 min)

4.4 Desorption Studies

Adsorption can be made attractive, competent and cost effective if the biomass used can be regenerated after biosorption process. Batch desorption studies were carried out to explore the possibilities of eucalyptus bark regeneration for reuse and the recovery of the sorbed dye. Therefore, MB loaded raw eucalyptus bark adsorbent used for adsorption experiments earlier was separated from solution by centrifugation and then dried in the oven at 60^{0}C overnight. The dried MB-loaded adsorbent was then placed in Erlenmeyer flasks containing 50 mL of the desorbing agent solution. The sample was agitated for 4 h and then filtered. The desorbed MB concentration was quantified using the UV/visible spectrophotometer. Four different

eluting solvents were used: water, HNO_3 (0.1 M), CH_3COOH (0.1 M) and NaOH (0.1M).

Previously, the study on the effect of pH reveals that maximum adsorption occurs at high alkaline pH. So it was obvious that desorption will occur at low pH. From desorption studies, it was revealed that maximum desorption of methylene blue (46.18%) was observed using strong nitric acid (HNO_3) having a pH value of 1.0. This is because at low pH, a positive charge develops on the surface of biomass due to which electrostatic repulsion occurs between the molecules of dye and the biomass, resulting in the detachment of dye cations from the adsorbent surface. Hence, percentage (%) desorption decreased with increase in pH of the desorbing medium and the results obtained are presented in Fig. 4.9.

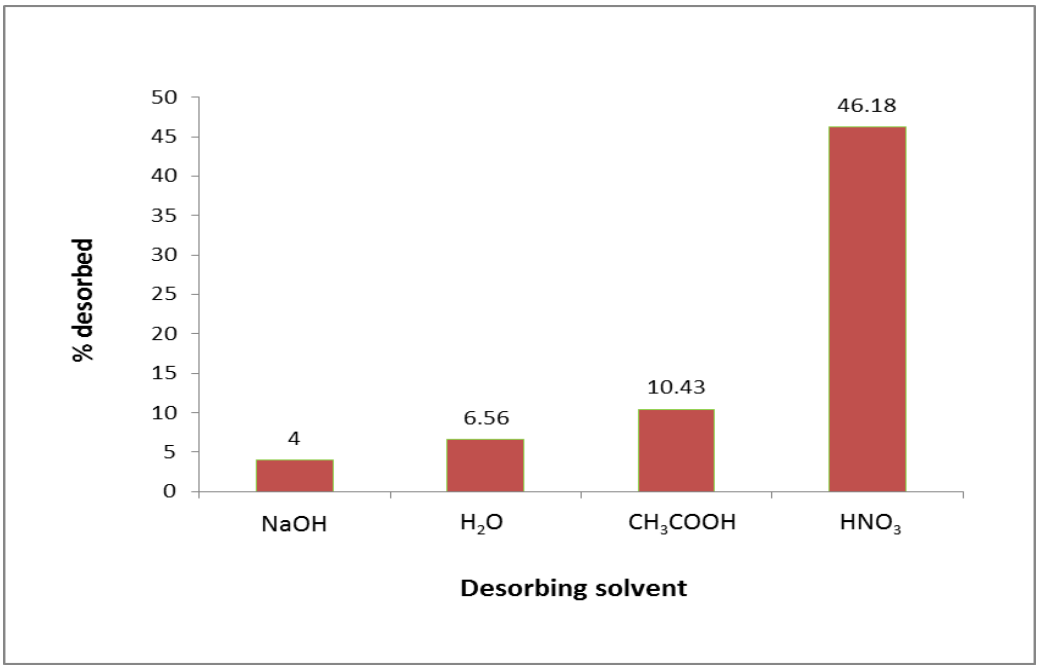

Figure 4.9 Batch desorption of MB dye from raw eucalyptus bark using different solvents

In strong acidic medium such as nitric acid (HNO_3), the protons in solution replaces the MB ions on the biomass surface, while the apparent poor recovery (4%) was observed in basic media such as NaOH, may be due to the coordinating ligands being deprotonated, hence bound-dye ions find it difficult to be detached from the biomass (Horsfall Jnr, Ogban et al. 2006). From Fig. 4.9, it is also noticed that desorption of MB dye was 6.56% in normal water and 10.43% in while highly concentrated acidic

acid (CH_3COOH). Therefore, the desorption study by strong inorganic nitric acid, organic acetic acid and normal water indicates that the adsorption phenomenon of MB dye onto eucalyptus bark material was mainly due to ion-exchange along with chemisorption and partially physical in nature (Ramalakshmi, Muthuchelian et al. 2011).

From the desorption studies, it can be concluded that regeneration of eucalyptus bark adsorbent will not be economical for the treatment process. However, upon the abundance of eucalyptus bark, as an agricultural waste with no great value, except for the cost to be incurred in its collection and transportation, at present, the recovery of MB dye and the regeneration of the adsorbent are not essential. Premised on this fact, the exhausted eucalyptus bark along with the adsorbed dye could be dried and used as a fuel in boilers/incinerators.

4.5 Application of Adsorption Kinetic Models

In order to investigate the mechanism of adsorption, particularly potential rate-controlling step and the transient behaviour of the dye adsorption process, adsorption kinetics is very significant and useful for adsorber design in wastewater treatment. In this study, the applicability of pseudo-first-order, pseudo-second-order and intraparticle diffusion models was tested for the adsorption of MB dye onto raw eucalyptus bark. The theory of all these models is presented in Section 2.6. These models have been evaluated and analysed by fitting experimental data at different physicochemical conditions.

There are several error analysis methods used to predict the best fit of models. In this work, the best fit model was selected based on the linear regression correlation coefficient R^2 values and also by determining sum of squared errors (SSE, %) function. The value of R^2 closest to unity is assumed to provide the best fit meanwhile for the sum of squared errors, the lower value of SSE, % indicates the better fit. The estimation for the sum of squared errors (SSE, %) calculated is given by:

$$\boldsymbol{SSE}, \% = \sqrt{\frac{\sum(q_{e,exp} - q_{e,cal})^2}{N}} \tag{4.1}$$

where N is the number of data points, $q_{e,exp}$ equilibrium capacity obtained from the experimental data (mg/g) and $q_{e,cal}$ equilibrium capacity obtained from model (mg/g).

4.5.1 Pseudo First Order Kinetic Model

Linear plots of log ($q_e - q_t$) vs. t for experimental data at various physico-chemical conditions are fitted for pseudo first order model using equation (2.1), which is presented in Fig. 4.10 where q_e and q_t refer to the amount of MB adsorbed (mg/g) at equilibrium and at time, t (min) respectively. From those plots, the pseudo-first-order rate constant (K_1) and linear regression co-efficient (R^2) have been calculated which gives lower value (Table 4.2). Moreover, pseudo-first-order kinetic model predicts very poor value of the calculated equilibrium adsorption capacity (q_e) than the experimental value and hence it gives the inapplicability of this model.

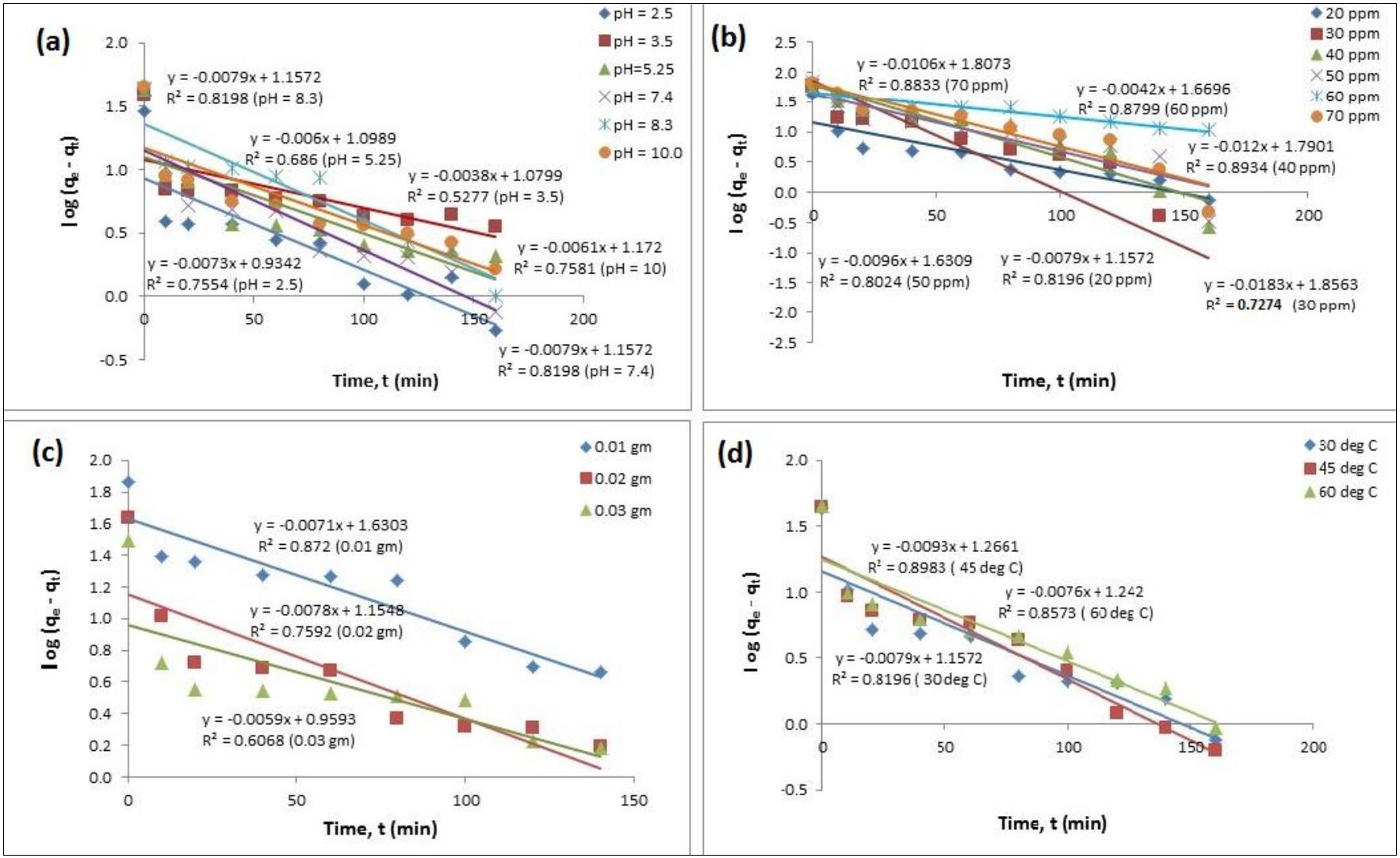

Figure 4.10 Pseudo-first-order kinetic model for the adsorption of MB dye onto raw eucalyptus bark at different (a) initial pH (b) initial concentrations (c) adsorbent dosages and (d) solution temperatures

Table 4.2: Pseudo-first-order kinetic model parameters for adsorption of MB dye on raw eucalyptus bark

Pseudo-first-order kinetic model parameters				
System Parameters	***q_e (mg/g), Experimental***	***K_1 (min^{-1})***	***q_e (mg/g), Calculated***	***R^2***
Adsorbent Dosage (mg)				
10	72.96	0.0164	5.11	0.872
20	42.99	0.0180	3.17	0.7592
30	31.30	0.0136	2.61	0.6068
Initial MB Dye Concentration (ppm)				
20	42.99	0.0182	3.18	0.8196
30	61.14	0.0421	6.40	0.7274
40	61.1	0.0276	5.99	0.8934
50	61.32	0.0221	5.11	0.8024
60	71.98	0.0097	5.31	0.8799
70	67.91	0.0244	6.09	0.8833
pH				
2.5	28.9	0.0168	2.55	0.7554
3.5	38.35	0.0088	2.94	0.5277
5.25	42.81	0.0138	3.00	0.6860
7.4	42.99	0.0182	3.18	0.8198
8.3	43.43	0.0182	3.18	0.8198
10	44.73	0.0140	3.23	0.7581
Temperature (^oC)				
30	42.99	0.0182	3.18	0.8196
45	44.46	0.0214	3.55	0.8983
60	45.39	0.0175	3.46	0.8573
Salt Concentration				
100 mg/L NaCl	29.39	0.0182	4.63	0.7646
200 mg/L NaCl	32.11	0.0203	5.36	0.791
300 mg/L NaCl	34.96	0.0069	4.45	0.9276
100 mg/L $CaCl_2$	30.55	0.0193	3.92	0.9089
200 mg/L $CaCl_2$	35.90	0.0210	4.67	0.8857
300 mg/L $CaCl_2$	45.57	0.0309	2.83	0.8579
100 mg/L $FeCl_3$	43.92	0.0193	5.01	0.907
200 mg/L $FeCl_3$	46.73	0.0242	5.39	0.8824
300 mg/L $FeCl_3$	47.98	0.0341	5.53	0.9443
Surfactant				
Triton X-100	38.80	0.0368	3.82	0.7194

4.5.2 Pseudo Second Order Kinetic Model

To study the pseudo-second-order model, Eq. (2.2) is used to construct plots of t/q_t versus t to fit experimental data at various physico-chemical conditions which plots are presented in Fig. 4.11. The initial sorption rate h, pseudo-second-order-rate constant K_2, amount of dye adsorbed at equilibrium q_e, and the corresponding linear regression correlation coefficient R^2 values are determined from the slope and intercept of plot t/q_t vs. t which are tabulated in Table 4.3. The R^2 values were found to be close to 1. The higher R^2 values confirm that the sorption process follows pseudo-second-order mechanism.

The half-adsorption time of adsorbate, $t_{1/2}$, i.e. the time required for eucalyptus bark to uptake half of the amount adsorbed at equilibrium, is often considered as a measure of the rate of adsorption and is given by the relationship (Sen, Afroze et al. 2011):

$$t_{½} = 1/k_2 q_e \qquad (4.2)$$

The calculated values of $t_{1/2}$ for the methylene blue (MB) dye adsorption onto eucalyptus bark were 3.91 min, 4.03 min, 5.58 min, 9.97 min, 16.33 min and 17.89 min for an initial concentration range of 20, 30, 40, 50, 60 and 70 ppm respectively.

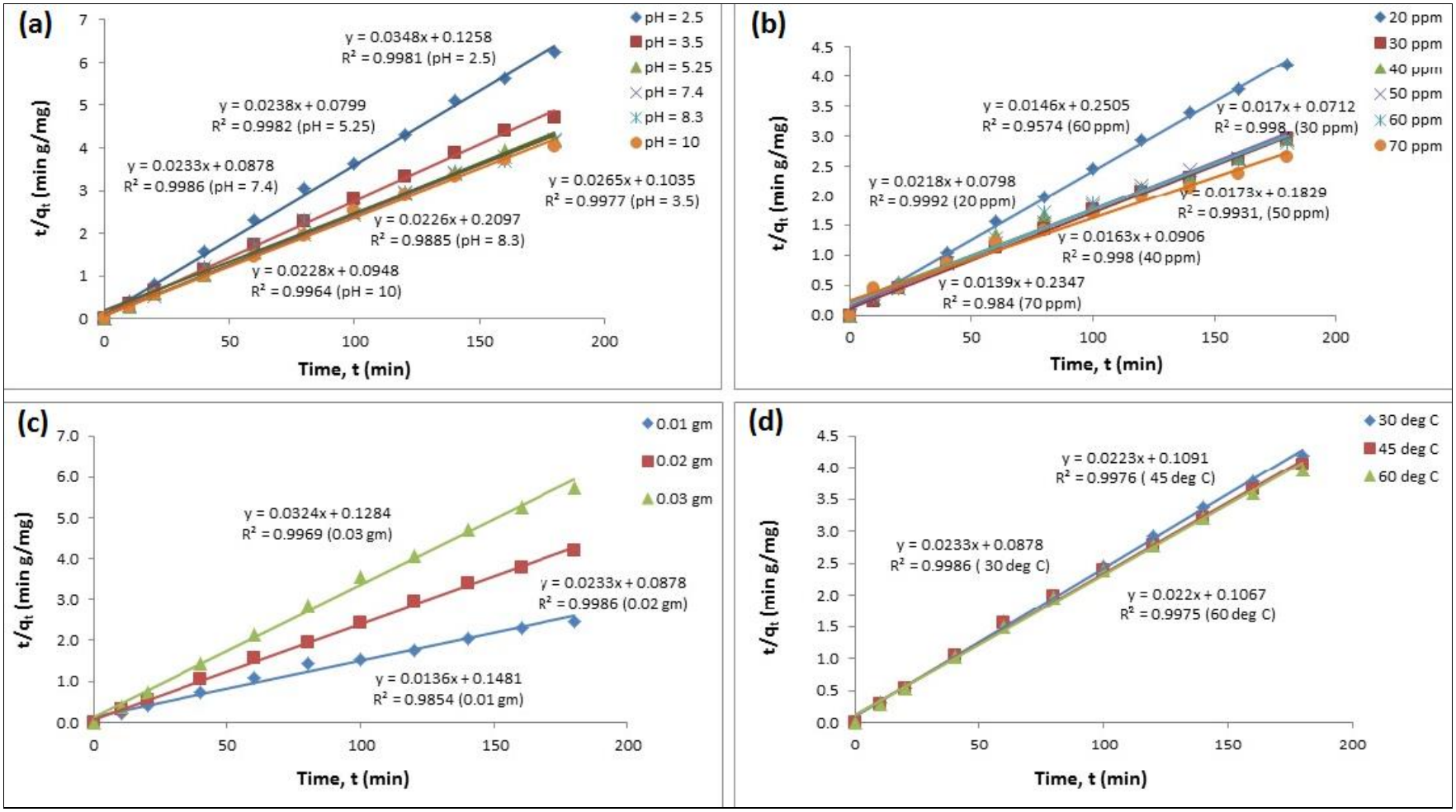

Figure 4.11 Pseudo-second-order kinetic model for the adsorption of MB dye onto raw eucalyptus bark at different (a) initial pH (b) initial concentrations (c) adsorbent dosages and (d) solution temperatures

Table 4.3: Pseudo-second-order kinetic model parameters for adsorption of MB dye on raw eucalyptus bark

Pseudo-second-order kinetic model parameters					
System Parameters	***q_e (mg/g), Experimental***	***K_2 (mg/g-min)***	***q_e (mg/g), Calculated***	***h (mg/g-min)***	***R^2***
Adsorbent Dosage (mg)					
10	72.96	0.0012	73.53	6.75	0.9854
20	42.99	0.0062	42.92	11.39	0.9986
30	31.30	0.0082	30.86	7.79	0.9969
Initial MB Dye Concentration (ppm)					
20	42.99	0.0060	45.87	12.53	0.9992
30	61.14	0.0041	58.82	14.04	0.9980
40	61.10	0.0029	61.35	11.04	0.9980
50	61.32	0.0016	57.80	5.47	0.9931
60	67.91	0.0008	71.94	4.26	0.9931
70	71.98	0.0009	68.49	3.99	0.9574
pH					
2.5	28.90	0.0096	28.74	7.95	0.9981
3.5	38.35	0.0068	37.74	9.66	0.9977
5.25	42.81	0.0071	42.02	12.52	0.9982
7.4	42.99	0.0062	42.92	11.39	0.9986
8.3	43.43	0.0024	44.25	4.77	0.9885
10	44.73	0.0055	43.86	10.55	0.9964
Temperature (^oC)					
30	42.99	0.0062	42.92	11.39	0.9986
45	44.46	0.0046	44.84	9.17	0.9976
60	45.39	0.0045	45.45	9.37	0.9975
Salt Concentration					
100 mg/L NaCl	29.39	0.0007	32.68	0.78	0.8803
200 mg/L NaCl	32.11	0.0002	45.05	0.44	0.5965
300 mg/L NaCl	34.96	0.0006	32.36	0.66	0.7808
100 mg/L $CaCl_2$	30.55	0.0023	31.45	2.28	0.9865
200 mg/L $CaCl_2$	35.90	0.0011	39.22	1.62	0.9398
300 mg/L $CaCl_2$	45.57	0.0158	45.87	33.22	0.9999
100 mg/L $FeCl_3$	43.92	0.0010	46.51	2.14	0.9660
200 mg/L $FeCl_3$	46.73	0.0010	49.75	2.54	0.9712
300 mg/L $FeCl_3$	47.98	0.0015	51.02	4.01	0.9904
Surfactant					
Triton X-100	38.80	0.0060	45.87	12.53	0.9992

4.5.3 Intraparticle Diffusion Model and Mechanism of Adsorption

For a solid/liquid sorption process, the solute transfer is usually described by either external mass transfer (boundary layer diffusion) or intraparticle diffusion or both. The mechanism for the removal of methylene blue from its aqueous phase by adsorption is assumed to consist of four steps: movement of MB dye molecules from the bulk solution to the surface of eucalyptus bark, diffusion through the boundary layer to the surface of eucalyptus bark, adsorption at sites and intraparticle diffusion into the inside of eucalyptus bark. The rate controlling step is the slowest step for adsorption. To understand the underlying adsorption mechanism that results in the apparent dynamic behaviour of the system, the most commonly used technique is by fitting the adsorption experimental data with intra-particle diffusion plot using Eq. (2.4). According to the intra-particle diffusion model, if a plot of the amount of sorbate adsorbed per unit weight of sorbent (q_t) versus square root of contact time ($t^{0.5}$) gives a linear plot, it indicates that intra-particle/pore diffusion is the rate limiting step in the adsorption process and the slope gives the value of rate constant of intraparticle transport, K_{id} (Oladoja, Aboluwoye et al. 2008). The intra-particle diffusion plots of amount sorbed per unit weight of sorbent, q_t (mg/g) versus square root of time, $t^{0.5}$ for various kinetic parameters such as different solution pH, initial MB dye concentrations, adsorbent dosages and temperature are shown here in Fig. 4.12.

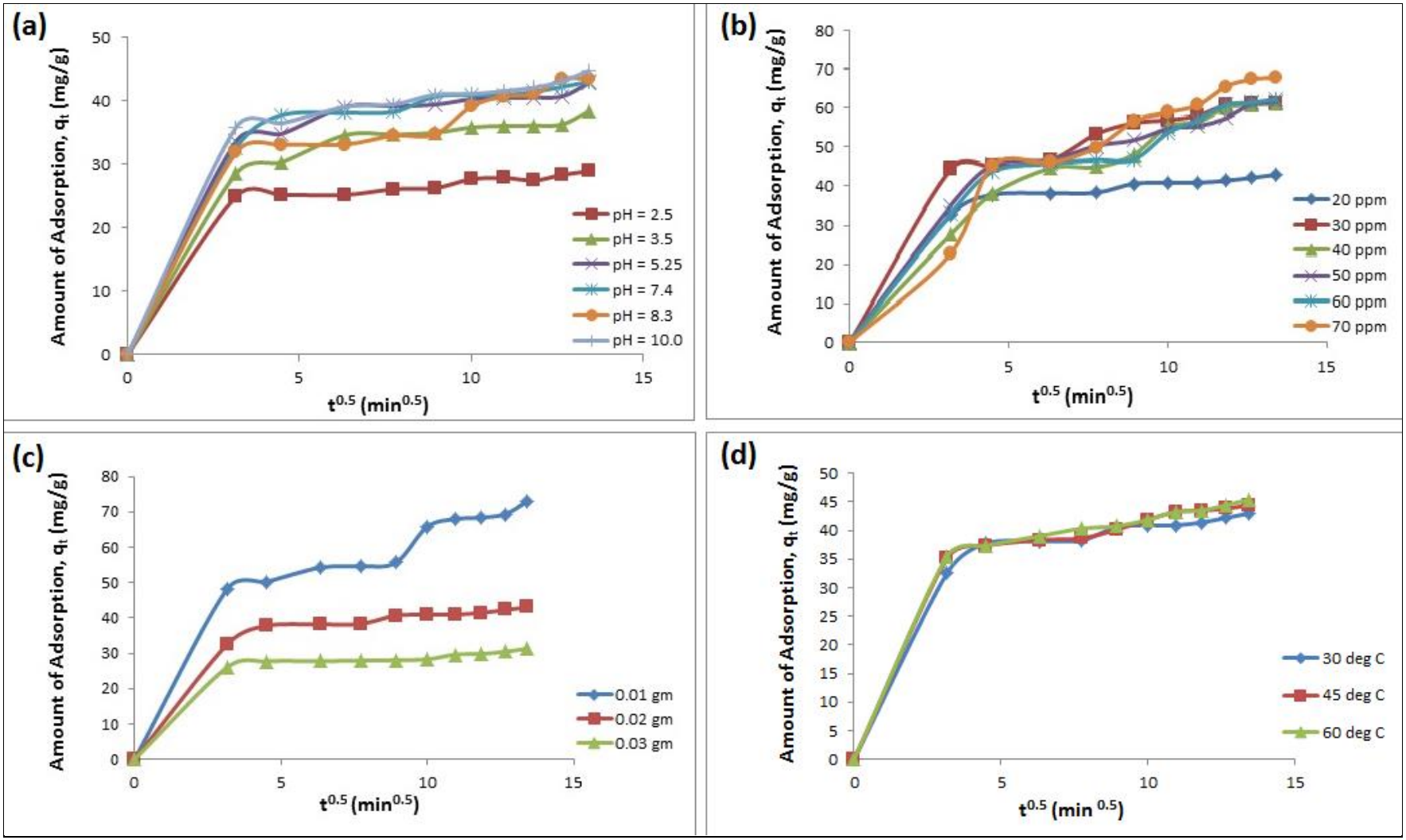

Figure 4.12 Intraparticle diffusion model for the adsorption of MB dye onto raw eucalyptus bark at different (a) initial pH (b) initial concentrations (c) adsorbent dosages and (d) solution temperatures

The plots obtained in Fig. 4.12 contrasted the prediction of the intraparticle diffusion model. Each plot shows that the adsorption of methylene blue by eucalyptus bark was found to be rapid at the initial period of contact time, and then became slow and stagnated with increase in contact time. The presentation of the experimental data for each plot in Fig. 4.12 is not linear over the whole time range and can be signified that the dye molecules were transported to the external surface of the eucalyptus bark through film diffusion and its rate was very fast. After that, MB dye molecules entered into eucalyptus bark particles by intraparticle diffusion through pores. This indicates that the intra-particle diffusion is involved in the adsorption process of MB dye onto eucalyptus bark but not the only rate controlling step. However, the controlling step might be distributed between intraparticle and external transport mechanisms.

The diffusion coefficient, D_p, largely depends on the surface properties of adsorbents. The diffusion coefficient for the intra-particle transport of different MB initial concentrations was also calculated using the following relationship (Sen, Afroze et al. 2011):

$$t_{1/2} = 0.03\, r_0^2 / D_p \qquad (4.3)$$

where $t_{1/2}$ is the half-life in secs as calculated from Eq. (4.2) . To calculate r_o the radius of the adsorbent particle (cm), surface weighted mean diameter of eucalyptus bark particles of 25.26 μm (radius = 12.63μm = 12.63 × 0.0001 cm = 0.001263 cm) was utilised. The diffusion coefficient, D_p (cm^2/sec) was calculated from Eq. (4.3) and the values were found to be 2.04×10^{-10} cm^2/sec, 1.98×10^{-10} cm^2/sec, 1.43×10^{-10} cm^2/sec, 8.0×10^{-11} cm^2/sec, 4.89×10^{-11} cm^2/sec and 4.46×10^{-11} cm^2/sec for an initial methylene blue concentration of 20, 30, 40, 50, 60 and 70 ppm respectively. The D_p values for methylene blue on eucalyptus bark are much lower than those of benzene derivatives. The D_p values of phenol and benzene on carbon are 90.1×10^{-9} and 8×10^{-9} cm^2/s, respectively (Sen, Afroze et al. 2011). This was attributed to the larger molecular size of the present systems, the factor that slows down in diffusion rate (Dawood and Sen 2012). In addition, due to strong interaction between methylene blue and eucalyptus bark, mobility was low.

All kinetic parameters obtained from experimental data fitted into intraparticle diffusion model plots under various process conditions are tabulated in Table 4.4. The observed linear regression coefficient R^2 values are lower with respect to pseudo-second-order kinetic model which makes intraparticle diffusion model incompatible for this system. However, the role and significance of intraparticle diffusion could not be totally neglected.

Table 4.4: Intraparticle diffusion model parameters for adsorption of MB dye on raw eucalyptus bark

Intraparticle diffusion model parameters				
System Parameters	***q_e (mg/g), Experimental***	***q_e (mg/g), Calculated***	***K_{id} (mg/g.min$^{0.5}$)***	***R^2***
Adsorbent Dosage (mg)				
10	72.96	77.46	4.2144	0.7906
20	42.99	47.92	2.2601	0.6158
30	31.30	34.18	1.5342	0.5559
Initial MB Dye Concentration (ppm)				
20	42.99	47.92	2.2601	0.6158
30	61.14	68.23	3.5611	0.7458
40	61.1	66.82	4.1003	0.9092
50	61.32	66.55	3.6692	0.8073
60	71.98	66.89	3.8692	0.8534
70	67.91	73.88	4.6776	0.9073
pH				
2.5	28.90	31.94	1.4358	0.5582
3.5	38.35	42.07	2.0167	0.6353
5.25	42.81	47.14	2.1992	0.6024
7.4	42.99	47.92	2.2601	0.6158
8.3	43.43	46.85	2.4171	0.7267
10.0	44.73	48.81	2.2821	0.6083
Temperature				
30^0C	42.99	48.29	2.2601	0.6158
45^0C	44.46	49.45	2.3639	0.6367
60^0C	45.39	50.03	2.3899	0.6364
Salt Concentration				
100 mg/L NaCl	29.39	28.64	2.1088	0.9774
200 mg/L NaCl	32.11	38.02	2.5484	0.9266
300 mg/L NaCl	34.96	29.11	2.1199	0.9036
100 mg/L $CaCl_2$	30.55	32.78	1.9775	0.8997
200 mg/L $CaCl_2$	35.90	37.87	2.4691	0.9351
300 mg/L $CaCl_2$	45.57	52.06	2.2523	0.5111
100 mg/L $FeCl_3$	43.92	45.77	2.9799	0.958
200 mg/L $FeCl_3$	46.73	49.68	3.1641	0.9447

300 mg/L $FeCl_3$	47.98	53.59	3.2072	0.8922
Surfactant				
Triton X-100	38.80	43.9300	2.01	0.5808

4.5.4 Validity of Kinetic Models

The adsorption kinetics of MB dye onto eucalyptus bark (EB) was further verified at different initial concentrations. The validity of each model was also determined by the sum of squared errors (SSE, %) using Eq. (4.1). It was found that the pseudo-second order kinetic model yielded the lowest SSE value of 3.01% compared to the value of 56.34% for the pseudo-first-order kinetic model and 46.80% for the intraparticle diffusion model. This is also agreement with the R^2 values obtained and proves that the adsorption of MB dye onto the eucalyptus bark biomass could be best described by the pseudo-second-order kinetic model.

4.6 Adsorption Equilibrium Isotherm Models

Equilibrium isotherm studies are important to describe how adsorbate molecules interact with the adsorbent surface. Equilibrium studies determine the capacity of the adsorbent and describe the adsorption mechanism. The experimental data were fitted to the Freundlich and Langmuir isotherm model equations which are presented in Section 2.6 and isotherm parameters were calculated. Linear regression analysis was then used to determine the best fitted isotherm.

The study of the Langmuir isotherm judges the adsorption efficiency of the adsorbent. The Langmuir isotherm model is valid for monolayer adsorption onto a surface containing finite number of identical sites of uniform strategies of adsorption with no transmigration of adsorbate in the plane of surface (Langmuir 1916). This study is also useful in optimizing the operating conditions for effective adsorption. Langmuir isotherms [Eq. (2.6) and Eq. (2.7)] are found to be obeyed by MB dye on eucalyptus bark biomass as shown in Figs. 4.13(a) and 4.13(b). This indicates that the dyes are chemisorbed on the surface of eucalyptus bark. These logarithmic equations for the adsorption studies of MB dye on eucalyptus bark gave high linearity with a range of correlation coefficient between 0.9588 and 0.9822. Hence both the Langmuir isotherms I and II fit the experimental data very well. The

maximum adsorption capacity, q_m (mg/g) and K_L values for Langmuir constants can be obtained from the linear equations of different plots [Figs. 4.13(a-b)].

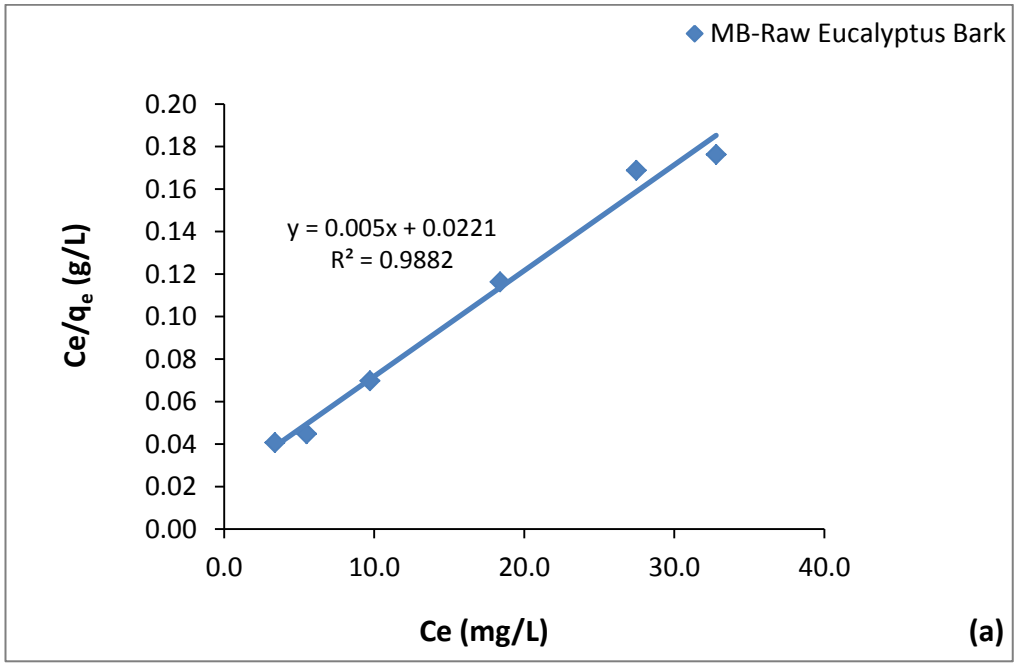

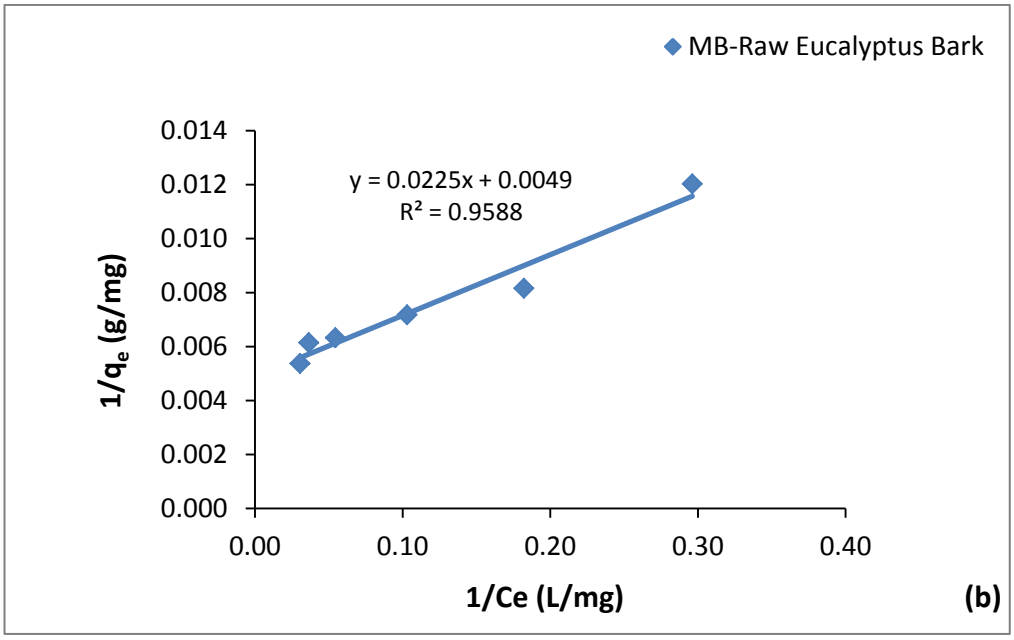

Figure 4.13 (a) Langmuir-I plot and (b) Langmuir-II plot

(Conditions: Amount of adsorbent added = 10 mg; initial MB dye concentration = 20, 30, 40, 50, 60, 70 ppm; soluiton pH = 9.9 ≈ 10.2 ; emperature = 30°C; shaker speed = 120 rpm and time of adsorption = 180 min)

Freundlich model is developed to explain how adsorption takes place on heterogeneous surfaces (Tan, Ahmad et al. 2008). To study the Freundlich isotherm, adsorption equilibrium data were fitted with experimental data which is presented in Fig. 4.14. The value of correlation coefficient, R^2 of the Freundlich isotherm fit is 0.8973. K_f and n are the Freundlich constants with n giving an indication of how favourable the adsorption process is. The values of K_f and n are calculated from the slope and intercept of the plot $\ln q_e$ vs. $\ln C_e$ (Fig. 4.14) using Eq. (2.10). The obtained value of slope $1/n$ is 0.2966 ranging between 0 and 1 which is a measure of adsorption intensity or surface heterogeneity indicating more heterogeneous as its value gets closer to zero (Haghseresht and Lu 1998).

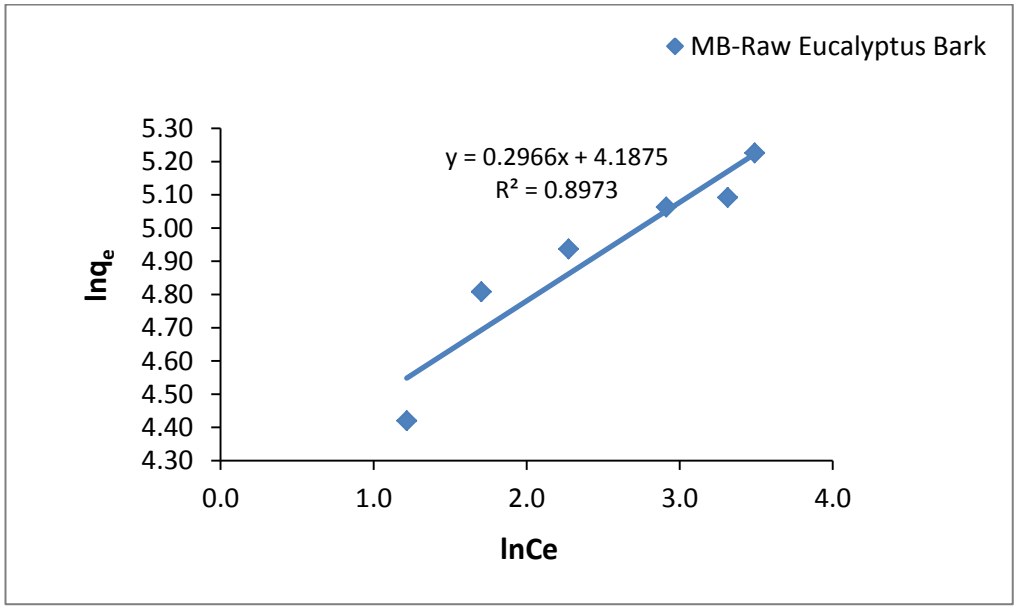

Figure 4.14 Freundlich plot: Amount of adsorbent 10 mg; initial MB concentration = 20, 30, 40, 50, 60 and 70 ppm, soluiton pH = 9.9 ≈ 10.2, temperature = 30°C; Shaker Speed = 120 rpm and time of adsorption = 180 min.

The linear regression coefficient (R^2) for the two types of Langmuir model show much higher values compared to Freundlich model which gives a clear indication that Langmuir model is best fitted with the equilibrium data. The values of Freundlich & Langmuir model parameters are summarised and presented in Table 4.5 below:

Table 4.5: Calculated values of model parameters obtained from Freundlich and Langmuir isotherms

LANGMUIR (TYPE I)		
q_m **(mg/g)**	K_a **(L/mg)**	R^2
204.1	0.2178	0.9588
LANGMUIR (TYPE II)		
q_m **(mg/g)**	K_a **(L/mg)**	R^2
200.0	0.2262	0.9882
FREUNDLICH		
K_f **(L/g)**$^{1/n}$	**1/*n***	R^2
65.9	0.2966	0.8973

The separation factor (R_L) is a dimensionless constant used to investigate the adsorption system feasibility at different initial dye concentration and can be determined from Langmuir plot as per the following relation:

$$R_L = \frac{1}{1+K_a C_0} \tag{4.4}$$

The R_L values, using Eq. (4.4) for the adsorption of MB dye onto eucalyptus bark are in the range of 0.06 to 0.19. The R_L values obtained are found to decrease with the increment of initial MB solution concentration and as $0<R_L<1$, this indicated that MB dye adsorption onto eucalyptus bark is a favorable adsorption process (Baskaralingam, Pulikesi et al. 2006).

Table 4.6 summarises the adsorption capacity of different types of adsorbents for MB dye under more or less similar experimental conditions of adsorbents and it is compared with the present study. From Table 4.6, it can be found that raw eucalyptus bark is effective adsorbent for the removal of MB dye from its aqueous solution and it is much better compared to many other agricultural waste materials and activated carbons.

Table 4.6: Comparison of the adsorption capacity (q_m in mg/g) of different sorbents for the removal of methylene blue (MB) dye

Adsorbent	***Maximum Adsorption Capacity, q_m (mg/g)***	***References***
Durian leaf powder	125	(Hussin, Talib et al. 2015)
Mango seeds	25.36	(Senthil Kumar, Palaniyappan et al. 2014)
Pine cone biomass	109.89	(Sen, Afroze et al. 2011)
Wood apple shell	95.2	(Jain and Jayaram 2010)
Gulmohar plant leaf	186.22	(Ponnusami, Gunasekar et al. 2009)
Powdered activated carbon	91	(Yener, Kopac et al. 2008)
Coffee husk	90.1	(Oliveira, Franca et al. 2008)
Cherry sawdust	39.84	(Ferrero 2007)
Caster seed shell	158.73	(Oladoja, Aboluwoye et al. 2008)
Coconut husk	99	(Oladoja, Aboluwoye et al. 2008)
Rice husk	40.59	(Vadivelan and Kumar 2005)
Eucalyptus bark	204.08	Present study

4.7 Design of Single Stage Batch Adsorber from Isotherm Data

The design of a single-stage batch adsorption system was determined from the Langmuir adsorption isotherm data using the method developed by Vadivelan and Kumar (Vadivelan and Kumar 2005). Due to lack of extensive experimental data, empirical design procedures based on adsorption isotherm studies are the most common method to predict the adsorber size and performance (Dawood, Sen et al. 2014). The design objective was to reduce initial MB dye concentration of C_o (mg/L) to C_t (mg/L) for which total dye solution is V (L). The amount of adsorbent was m (g) and the solute loading changes from q_o (mg/g) to q_t (mg/g). At time $t = 0$, $q_o = 0$ and as time proceeds the mass balance equates the dye removed from the liquid to

the adsorbed by the adsorbent. The mass balance for methylene blue (MB) dye in the single-stage operation under equilibrium is expressed as (Dawood, Sen et al. 2014):

$$V\,(C_0\text{-}Ce) = m\,(q_e\text{-}q_0) = mq_e \tag{4.5}$$

Under equilibrium conditions,

$C_1 \rightarrow C_e$ and $q_1 \rightarrow q_e$

The Langmuir isotherm of Eq. (4.5) can be written and rearranged as:

$$\frac{m}{V} = \frac{C_0 - C_e}{q_e} = \frac{C_0 - C_e}{\frac{q_m K_a C_e}{1 + K_a C_e}} \tag{4.6}$$

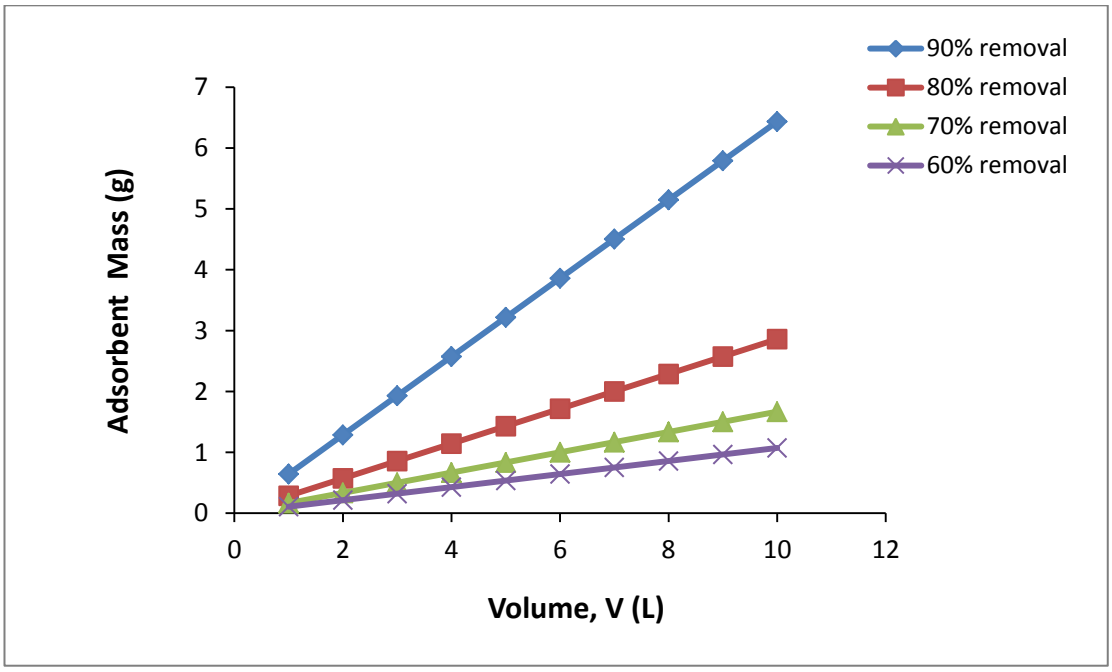

Figure 4.15 Adsorbent mass (g) against volume (litres) of solution treated

Fig. 4.15 shows a series of plots for the predicted amount of eucalyptus bark adsorbent required to remove certain percentage of 100 mg/L MB dye from specific volumes of wastewater solutions in a single-batch adsorber. For example, to remove 90% of MB dye colour from 1, 2, 3, 4, 5, 6, 7, 8, 9 and 10 L aqueous solution at 303 K, requires 0.643, 1.287, 1.930, 2.574, 3.217, 3.861, 4.504, 5.148, 5.791 and 6.435 kg of raw eucalyptus bark adsorbent respectively.

4.8 Summary

In this study, the effectiveness of raw eucalyptus bark (EB) was tested as a low-cost adsorbent for MB removal from aqueous solution. The present study demonstrates that eucalyptus bark, an agro-based waste and inexpensive biomaterial, can be an alternative for many expensive adsorbents used for the removal of methylene blue dye in wastewater treatment. The outcomes of this chapter are as follows:

- The amount of methylene blue (MB) dye uptake on eucalyptus bark was found to increase with an increase in initial solution pH, initial MB dye concentration, contact time, ionic strength and system temperature; but decreased with increase in the amount of adsorbent and non-ionic surfactant.
- From the mixed contaminant study, it has been found that eucalyptus bark has a good adsorption capacity to adsorb both cationic dye methylene blue (MB) and anionic dye Congo red (CR) simultaneously.
- Overall, kinetic studies showed that the process of MB dye adsorption onto eucalyptus bark adsorbent followed pseudo-second order kinetic model and the adsorption was controlled by chemisorption process.
- The experimental data correlated reasonably well by both Langmuir I and Langmuir II adsorption isotherms with an adsorption capacity of 204.08 mg/g. The dimensionless separation factor (R_L) gives an indication of favourable adsorption.
- The results of the batch desorption studies showed that ion-exchange and chemisorption played a prominent role in the sorption process and as the regeneration of eucalyptus bark is not economically viable, the exhausted eucalyptus bark could be used as a fuel in incinerators.
- The thermodynamic analysis indicated that the adsorption process is endothermic, irreversible and spontaneous in nature.

4.9 References

Al-Qodah, Z. (2000). "Adsorption of dyes using shale oil ash." Water Research **34**(17): 4295-4303.

Arias, F. and Sen, T. K. (2009). "Removal of zinc metal ion (Zn< sup> 2+</sup>) from its aqueous solution by kaolin clay mineral: A kinetic and equilibrium study." Colloids and Surfaces A: Physicochemical and Engineering Aspects **348**(1): 100-108.

Baskaralingam, P., Pulikesi, M., Elango, D., Ramamurthi, V. and Sivanesan, S. (2006). "Adsorption of acid dye onto organobentonite." Journal of Hazardous Materials **128**(2): 138-144.

Bharathi, K. and Ramesh, S. (2013). "Removal of dyes using agricultural waste as low-cost adsorbents: a review." Applied Water Science **3**(4): 773-790.

Brahimi-Horn MC, L. K., Liany SL, Mou DG (1992). "Binding of textile azo dyes by Morothecium verrucaria Orange II, 10B (blue) and RS (red) azo dye uptake for textile wastewater decolourization." Journal of Industrial Microbiology **10**: 245-261.

Bulut, Y. and Aydın, H. (2006). "A kinetics and thermodynamics study of methylene blue adsorption on wheat shells." Desalination **194**(1): 259-267.

Dave, P. N., Kaur, S. and Khosla, E. (2011). "Removal of Eriochrome black-T by adsorption on to eucalyptus bark using green technology." Indian Journal of Chemical Technology **18**(1): 53-60.

Dawood, S. and Sen, T. K. (2012). "Removal of anionic dye Congo red from aqueous solution by raw pine and acid-treated pine cone powder as adsorbent: Equilibrium, thermodynamic, kinetics, mechanism and process design." Water Research **46**(6): 1933-1946.

Dawood, S., Sen, T. K. and Phan, C. (2014). "Synthesis and characterisation of novel-activated carbon from waste biomass pine cone and its application in the removal of congo red dye from aqueous solution by adsorption." Water, Air, & Soil Pollution **225**(1): 1-16.

Fedoseeva, M., Fita, P., Punzi, A. and Vauthey, E. (2010). "Salt effect on the formation of dye aggregates at liquid/liquid interfaces studied by time-resolved surface second harmonic generation." The Journal of Physical Chemistry C **114**(32): 13774-13781.

Ferrero, F. (2007). "Dye removal by low cost adsorbents: Hazelnut shells in comparison with wood sawdust." Journal of Hazardous Materials **142**(1): 144-152.

Geçgel, Ü., Özcan, G. and Gürpınar, G. Ç. (2012). "Removal of methylene blue from aqueous solution by activated carbon prepared from pea shells (Pisum sativum)." Journal of Chemistry **2013**.

Haghseresht, F. and Lu, G. (1998). "Adsorption characteristics of phenolic compounds onto coal-reject-derived adsorbents." Energy & Fuels **12**(6): 1100-1107.

Horsfall Jnr, M., Ogban, F. E. and Akporhonor, E. E. (2006). "Recovery of lead and cadmium ions from metal-loaded biomass of wild cocoyam (Caladium bicolor) using acidic, basic and neutral eluent solutions." Electronic Journal of Biotechnology **9**(2).

Hussin, Z. M., Talib, N., Hussin, N. M., Hanafiah, M. A. and Khalir, W. K. (2015). "Methylene Blue Adsorption onto NaOH Modified Durian Leaf Powder: Isotherm and Kinetic Studies." American Journal of Environmental Engineering **5**(3A): 38-43.

Jain, S. and Jayaram, R. V. (2010). "Removal of basic dyes from aqueous solution by low-cost adsorbent: Wood apple shell (< i> Feronia acidissima</i>)." Desalination **250**(3): 921-927.

Jumasiah, A., Chuah, T. G., Gimbon, J., Choong, T. S. Y. and Azni, I. (2005). "Adsorption of basic dye onto palm kernel shell activated carbon: sorption equilibrium and kinetics studies." Desalination **186**(1): 57-64.

Kumar, P. S., Ramalingam, S. and Sathishkumar, K. (2011). "Removal of methylene blue dye from aqueous solution by activated carbon prepared from cashew nut shell as a new low-cost adsorbent." Korean Journal of Chemical Engineering **28**(1): 149-155.

Kuo, C.-Y., Wu, C.-H. and Wu, J.-Y. (2008). "Adsorption of direct dyes from aqueous solutions by carbon nanotubes: Determination of equilibrium, kinetics and thermodynamics parameters." Journal of Colloid and Interface Science **327**(2): 308-315.

Langmuir, I. (1916). "The constitution and fundamental properties of solids and liquids. Part I, solids." Journal of the American Chemical Society **38**(11): 2221-2295.

Oladoja, N., Aboluwoye, C., Oladimeji, Y., Ashogbon, A. and Otemuyiwa, I. (2008). "Studies on castor seed shell as a sorbent in basic dye contaminated wastewater remediation." Desalination **227**(1): 190-203.

Oliveira, L. S., Franca, A. S., Alves, T. M. and Rocha, S. D. F. (2008). "Evaluation of untreated coffee husks as potential biosorbents for treatment of dye contaminated waters." Journal of Hazardous Materials **155**(3): 507-512.

Oyelude, E. O. and Appiah-Takyi, F. (2012). "Removal of methylene blue from aqueous solution using alkali-modified malted sorghum mash." Turkish Journal of Engineering and Environmental Sciences **36**(2): 161-169.

Ponnusami, V., Gunasekar, V. and Srivastava, S. (2009). "Kinetics of methylene blue removal from aqueous solution using gulmohar (< i> Delonix regia</i>) plant leaf powder: Multivariate regression analysis." Journal of Hazardous Materials **169**(1): 119-127.

Ponnusami, V., Vikram, S. and Srivastava, S. (2008). "Guava (< i> Psidium guajava</i>) leaf powder: Novel adsorbent for removal of methylene blue from aqueous solutions." Journal of Hazardous Materials **152**(1): 276-286.

Ramalakshmi, S., Muthuchelian, K. and Swaminathan, K. (2011). "Kinetic and equilibrium studies on biosorption of reactive blacks dye from aqueous solution by native and treated fungi alternaria raphani." Journal of Bioscience Research **2**(4): 239-248.

Sadaf, S. and Bhatti, H. N. (2013). "Batch and fixed bed column studies for the removal of Indosol Yellow BG dye by peanut husk." Journal of the Taiwan Institute of Chemical Engineers.

Salleh, M. A. M., Mahmoud, D. K., Karim, W. A. W. A. and Idris, A. (2011). "Cationic and anionic dye adsorption by agricultural solid wastes: A comprehensive review." Desalination **280**(1): 1-13.

Sen, T. K., Afroze, S. and Ang, H. (2011). "Equilibrium, kinetics and mechanism of removal of methylene blue from aqueous solution by adsorption onto pine cone biomass of Pinus radiata." Water, Air, & Soil Pollution **218**(1-4): 499-515.

Senthil Kumar, P., Palaniyappan, M., Priyadharshini, M., Vignesh, A., Thanjiappan, A., Sebastina Anne Fernando, P., Tanvir Ahmed, R. and Srinath, R. (2014). "Adsorption of basic dye onto raw and surface-modified agricultural waste." Environmental Progress & Sustainable Energy **33**(1): 87-98.

Senthil Kumar, P., Ramalingam, S., Senthamarai, C., Niranjanaa, M., Vijayalakshmi, P. and Sivanesan, S. (2010). "Adsorption of dye from aqueous solution by cashew nut shell: Studies on equilibrium isotherm, kinetics and thermodynamics of interactions." Desalination **261**(1): 52-60.

Shahryari, Z., Goharrizi, A. S. and Azadi, M. (2010). "Experimental study of methylene blue adsorption from aqueous solutions onto carbon nano tubes." International Journal of Water Resources and Environmental Engineering **2**(2): 16-28.

Stavropoulos, G., Skodras, G. and Papadimitriou, K. (2015). "Effect of solution chemistry on cyanide adsorption in activated carbon." Applied Thermal Engineering **74**: 182-185.

Tan, I., Ahmad, A. and Hameed, B. (2008). "Adsorption of basic dye using activated carbon prepared from oil palm shell: batch and fixed bed studies." Desalination **225**(1): 13-28.

Tarawou, T. and Horsfall Jr, M. (2007). "Adsorption of methylene blue dye on pure and carbonized water weeds." Bioremediation Journal **11**(2): 77-84.

Vadivelan, V. and Kumar, K. V. (2005). "Equilibrium, kinetics, mechanism, and process design for the sorption of methylene blue onto rice husk." Journal of Colloid and Interface Science **286**(1): 90-100.

Wang, X. S., Zhou, Y., Jiang, Y. and Sun, C. (2008). "The removal of basic dyes from aqueous solutions using agricultural by-products." Journal of Hazardous Materials **157**(2): 374-385.

Yener, J., Kopac, T., Dogu, G. and Dogu, T. (2008). "Dynamic analysis of sorption of methylene blue dye on granular and powdered activated carbon." Chemical Engineering Journal **144**(3): 400-406.

Zaheer, S., Bhatti, H. N., Sadaf, S., Safa, Y. and Zia-ur-Rehman, M. (2014). "Biosorption characteristics pf sigarcanr bagasse for the removal of foron blue e-el dye from aqueous solutions." The Journal of Animal & Plant Sciences **24**(1): 272-279.

Zhao, Y., Xia, Y., Yang, H., Wang, Y. and Zhao, M. (2014). "Synthesis of glutamic acid-modified magnetic corn straw: equilibrium and kinetic studies on methylene blue adsorption." Desalination and Water Treatment **52**(1-3): 199-207.

Every reasonable effort has been made to acknowledge the owners of copyright material. I would be pleased to hear from any copyright owner who has been omitted or incorrectly acknowledged.

CHAPTER 5

ADSORPTION OF METHYLENE BLUE (MB) DYE THROUGH FIXED BED COLUMN STUDY BY RAW EUCALYPTUS BARK

ABSTRACT*

In this study, the adsorptive effectiveness of sustainable and cost-effective eucalyptus bark biomass in the removal of methylene blue (MB) dye from its aqueous solution has been tested using a packed bed up-flow column experiment. A series of column experiments using raw eucalyptus bark was performed to determine the breakthrough curves with varying inlet MB dye flow rate (10–15 mL min^{-1}), initial MB dye concentration (50–100 mg L^{-1}) and adsorbent bed height (10–15 cm). High bed height, low flow rate and high initial dye concentration were found to be the better conditions for maximum dye adsorption. To predict the breakthrough curves and to determine the characteristic parameters of the column dynamics for industrial applications and for process design, Thomas model, Yoon–Nelson model and bed depth service time model were applied to experimental breakthrough data. All models were found suitable for describing the dynamic behaviour of the column, with respect to MB flow rate, initial dye concentration and adsorbent bed height. The findings revealed that eucalyptus bark biomass has a high adsorption potential for the removal of MB dye from aqueous solutions in a column system, and that it could be used to treat dye-containing effluents.

* This work has been published in Research on Chemical Intermediates Journal (Afroze, S., Sen, T.K. & Ang H. M., 2016. Adsorption performance of continuous fixed bed column for the removal of methylene blue (MB) dye using Eucalyptus *sheathiana* bark biomass. *Research on Chemical Intermediates*, 42(3), 2343-2364. DOI: 10.1007/s11164-015-2153-8)

5.1 Introduction

The aim of this chapter is to evaluate the adsorption capacity of eucalyptus bark biomass for the removal of MB dye from its aqueous solution through the dynamic fixed bed column performance. Basically, adsorption dynamics and modelling are essential because they provide significant information on sorbent capacity and prediction of the time necessary for the effective operation of a fixed bed column (Yaneva and Georgieva 2012). Raw eucalyptus bark was used as adsorbent to remove MB dye from its aqueous solution in a batch mode (Afroze, Sen et al. 2015). It was found that there was higher adsorption capacity for raw eucalyptus bark biomass and it was a function of various physico-chemical process parameters such as initial MB dye concentration, solution pH, adsorbent dose, contact time, ionic strength, and temperature. There are many reported results on the removal of MB dye from aqueous solution by a wide range of adsorbents which has been reviewed by various researchers (Crini 2006, Rafatullah, Sulaiman et al. 2010, Ali, Asim et al. 2012) and (Afroze and Sen 2015). However, the majority of the earlier investigations on MB dye adsorption were mainly focused to batch equilibrium studies. The results obtained from batch adsorption experiments such as adsorption capacity, adsorption mechanism and kinetic parameters under optimum physico-chemical process conditions for maximum adsorption fulfil the fundamental requirements in making more detailed conclusions about the effectiveness of adsorbents whether to be used or not for real industrial applications. However the data may not be applicable to most of the treatment system such as continuous real column operations where contact time is not sufficient to attain equilibrium. Moreover, batch experimental data are often not easy to apply directly to fixed bed column performances because isotherms are unable to give accurate data for scale up since a flow column is not at equilibrium. Hence there is a need to perform adsorption study using fixed bed columns. The reported number of results on column study is limited compared to massive adsorption study on organic/inorganic removal by various adsorbents which is also mentioned in recent review article by Yagub et al (Yagub, Sen et al. 2014). Moreover, in practical industrial water treatment processes, adsorption in fixed-bed columns are preferable, and the experimental data obtained from the laboratory scale fixed-bed columns are helpful for industrial application (Baral, Das et al. 2009). The major characteristics of fixed bed adsorption are the concentration-time curves

commonly referred to as the breakthrough curves (BTC) and the breakthrough time at which the effluent concentration reaches the threshold value. The realistic design of adsorption systems is based on accurate predictions of breakthrough curves (BTC) at specified conditions. Despite the usefulness of fixed bed mode, its analysis is usually complex. Therefore this study was designed to investigate the effects of important process parameters such as inlet MB flow rate (10–15 mL min^{-1}), initial MB dye concentration (50–100 mg L^{-1}) and adsorbent bed depth (10–15 cm) to remove MB dye from its aqueous solution using eucalyptus bark biomass in a laboratory scale dynamic fixed bed column operation. Different dynamic models like Thomas model, Yoon-Nelson model and Bed Depth Service Time (BDST) model, were applied to the experimental column data for better understanding about the mechanism of the process which can be used further to scale up for an actual industrial situation.

5.2 Materials and Methods

Raw eucalyptus bark was selected as adsorbent material and methylene blue (MB) dye as model adsorbate for this study.

5.2.1 Adsorbent and its characterisation

Eucalyptus barks were collected locally from Curtin University, Bentley Campus at Perth, Western Australia between February and March 2013 and they are prepared for column use in the same manner as detailed in Section 4.2.1. The adsorbent characterisation is discussed earlier in Section 3.3.

5.2.2 Adsorbate and Other Chemicals

The MB dye adsorbate used for column experiments is prepared according to Section 3.2.1.1 (part C).

5.3 Fixed Bed Adsorption Column Design and Experimental Procedure

Continuous adsorption study in a fixed-bed column was carried out to evaluate the dynamic behaviour of methylene blue (MB) from aqueous solution by using eucalyptus bark powder as adsorbent. For this purpose, the continuous flow adsorption experiments were conducted in a fixed bed Perspex glass column of 30 cm height with 2.5 cm internal diameter which is shown in Fig. 5.1. Eucalyptus bark material (≤ 106 μ) was packed into the glass column to yield the desired bed height. The top and bottom of the bed was covered by a layer of pre-equilibrated glass wool in order to avoid the loss of adsorbent and also to ensure a closely packed arrangement. Both the ends of the column were connected with circular threaded caps. A porous sheet was attached at the bottom of the column in order to support the adsorbent bed and to ensure uniform inlet flow and a good homogenous liquid distribution into the column (Fig. 5.1). This arrangement of fixed packed bed column allows appropriate contact between the solution of adsorbate and the solid phase of adsorbent where the solid bed does not move normally. Influent MB dye solution was injected into the column at a fixed and controlled discharge rate upward through a peristaltic pump which was placed at the bottom of the vertical column. The solution was pumped upward to avoid channelling due to gravity. The experimental set-up of the fixed-bed column is schematically shown in Fig. 5.1.

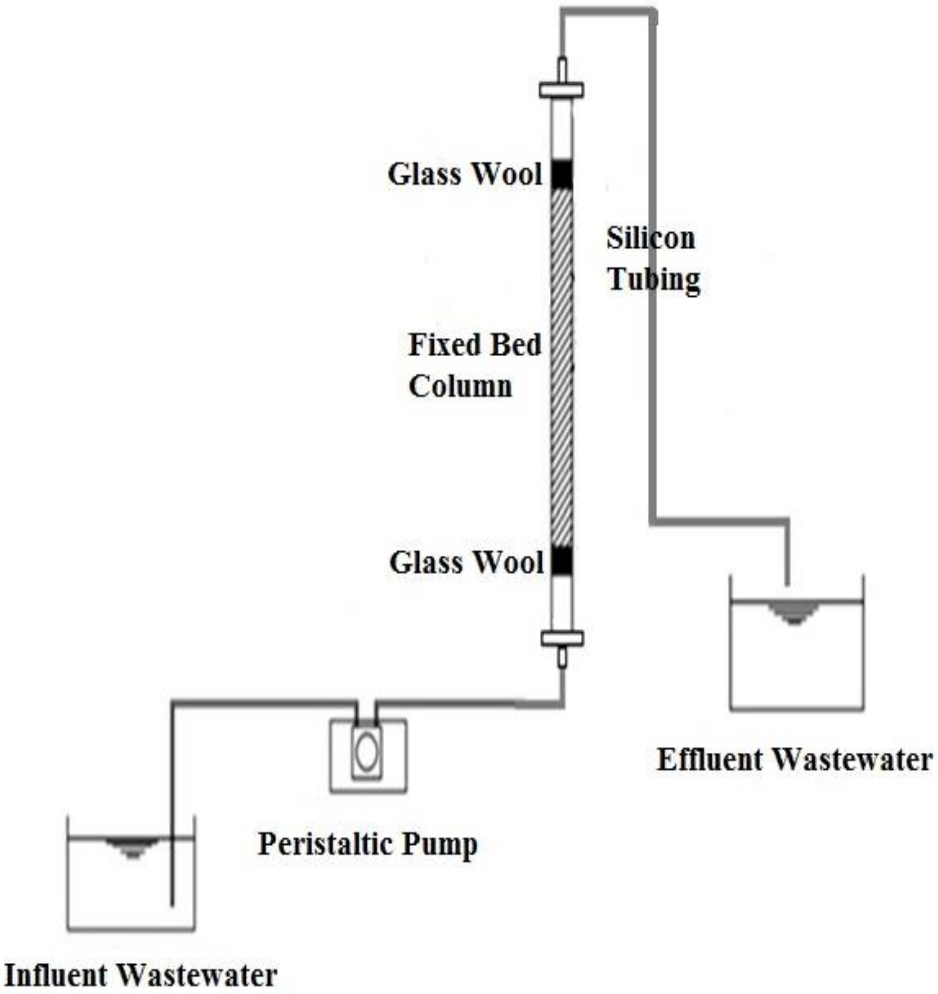

Figure 5.1 Schematic Diagram of Fixed bed Column

The effect of inlet MB dye flow rate, influent MB dye concentration and adsorbent bed height on the adsorption characteristics of adsorbent was investigated at pH 7.4. A series of experiments were conducted to study the effect of inlet MB dye flow rate (10, 12 and 15 mL/min), initial MB dye concentration (50, 75 and 100 mg/L) and adsorbent bed height (10, 12 and 15 cm). All the experiments were carried out at room temperature. Samples were collected at regular time intervals and the concentration of MB in the effluent was analysed using SP-8001 UV/VIS spectrophotometer. Sampling of column effluent was done at certain time intervals in order to study the breakthrough point or column service time and shape of breakthrough curve (BTC). Operation of the column was stopped when the effluent

MB concentration exceeded a value of 99.5% of its initial concentration. The obtained breakthrough curves (BTCs) from column experimental data were applied to the various dynamic column performance models and model parameters were determined under various process operating conditions.

5.4 Modelling and Column Adsorption Process Analysis

The design of a fixed bed column involves the shape assessment of the breakthrough curve and the appearance of the breakpoint is a key factor in accessing the feasibility of using the adsorbent in real applications. In simple words, the performance of a fixed bed column is described through the theory of the breakthrough curve (BTC). For a given column bed height, the plot of exit concentration verses lapse time or volume throughput reacted is known as breakthrough curve (BTC) (Ghorai and Pant 2005). The characteristic shape of the breakthrough curve along with the time axis depends on the inlet flow rates, concentration and other properties such as column diameter and bed height (Ghorai and Pant 2005). For a given concentration, the breakthrough point (the time until the sorbed species are detected in the column effluent) and the breakthrough curve are the leading characteristics for overall performance of flow through columns such as operation, dynamic response and design of an adsorption column which directly affect the economy of the process. Hence successful design of an adsorption column requires prediction of the concentration–time profile from breakthrough curve for the effluent discharged from the column (Baral, Das et al. 2009).

The typical breakthrough curve is usually expressed by plotting $C_{effluent}$ (C_t) or $C_{effluent}/C_{influent}$ (C_o) versus treated volume V or service time t for a given bed height. Fig. 5.2 depicts an ideal breakthrough curve (BTC) where the column capacity is fully utilized (Yagub, Sen et al. 2014). The concentration at breakthrough point is chosen arbitrarily at some low value, C_b. The effluent concentration (C_t) from the column that reaches about 0.1% of the influent concentration (C_0) is the breakthrough point. When the effluent concentration C_t is approaching to 99.5% of C_o (influent adsorbate concentration) then the adsorbent is considered to be essentially exhausted (Faust and Aly 2013). The area under the breakthrough curve gives the total quantity of sorbed adsorbate for a given feed concentration. The

effectiveness of an adsorbent can be obtained from the BTC of effluent concentration where a typical S-shaped breakthrough curve is commonly observed (Cruz-Olivares, Pérez-Alonso et al. 2013).

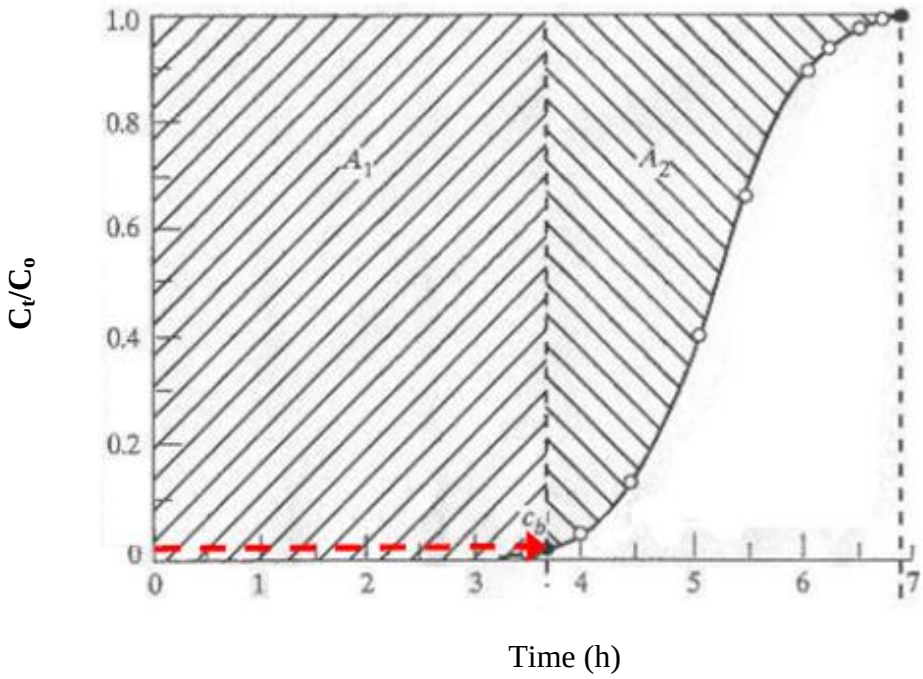

Figure 5.2 Ideal Breakthrough Curve

For column data analysis, the following parameter calculations are appropriate.

Time equivalent to total or Stoichiometric Capacity is (Yagub, Sen et al. 2014):

$$t_t = \int_{t=0}^{t=\infty} \left(1 - \frac{c_t}{c_0}\right) dt = A_1 + A_2 \quad (5.1)$$

Time equivalent to usable capacity is (Yagub, Sen et al. 2014):

$$t_u = \int_{t=o}^{t_b} \left(1 - \frac{c_t}{c_0}\right) dt = A_1 \quad (5.2)$$

Usable capacity of bed up to the breakthrough point time, t_b

$t_u \approx t_b$

Area under the curve $\int_{t=o}^{t=\infty} \left(1 - \frac{c_t}{c_0}\right) dt$, gives t_t value (total time), whereas area under curve $\int_{t=o}^{t_b} \left(1 - \frac{c_t}{c_0}\right) dt$ gives, t_u value t_u/t_t is the fraction of the total bed capacity or length utilized up to break point. Area under the curve can be determined either graphically or by numerical integration.

Also, the unused bed length (H_{UNB}) or Mass Transfer Zone (MTZ) can be calculated as (Yagub, Sen et al. 2014):

$$H_{UNB} = (1 - t_u/t_t)\ H_T = (1 - t_b/t_t)\ H_T \quad (5.3)$$

where H_T is total bed height in cm.

$$MTZ = H_{UNB} \quad (5.4)$$

The used bed length H_B (up to the break point) can be calculated as:

$$H_B = (t_b/t_t)\ H_T \quad (5.5)$$

The total effluent volume (V_{eff}) can be estimated as follows (Al-Degs, Khraisheh et al. 2009):

$$V_{eff} = Q\ t_{total} \quad (5.6)$$

where Q and t_{total} are the volumetric flow rate (mL/min) and the total flow time (min) respectively.

The total adsorbed MB quantity (q_{total}) in mg for a given inlet concentration is equal to the flow rate and the area under the plot of the adsorbed MB dye concentration C_{ads} ($C_{ads} = C_0 - C_t$), where C_0 and C_t (mg L^{-1}) are the influent and effluent dye concentrations, respectively, versus time (min) and is calculated as follows (Cruz-Olivares, Pérez-Alonso et al. 2013):

$$q_{total} = QA/1000 = (QC_o/1000)\int_{t=o}^{t=t_{total}} C_{ads}\, dt \quad (5.7)$$

where Q is the flow rate (mL/min), A is the area under the breakthrough curve and t (min) could be t_{total}, t_{sat} or t_b that represent the total flow time, the saturation time or the breakthrough time, respectively.

The total amount of MB dye sent to column (m_{total}) is as follows (Ghomshe, Mousavi et al. 2011):

$$m_{total} = C_o\, Q\, t_{total}/\ 1000 \quad (5.8)$$

The total percentage (%) removal of MB dye can be found from the ratio of total adsorbed quantity (q_{total}) to the total amount sent (m_{total}) to the column as:

$$\%\ Removal = (q_{total}\ /m_{total}) \times 100 \quad (5.9)$$

5.5 Results and Discussion

5.5.1 Effect of Initial MB Dye Flow Rate

The adsorption of methylene blue (MB) dye onto eucalyptus bark biomass at different flow rates (10, 12 and 15 mL/min) was investigated with an optimised bed height of 12 cm and inlet MB dye adsorbate concentration of 75 mg L^{-1}. The breakthrough curves of comparative normalized dye concentration (C_t/C_o) versus time (t) at various flow rates are shown in Fig. 5.3 for which the experimental data is presented in Appendix B1-B3. It was observed that the higher the flow rate, the faster the occurrence of breakthrough curve (Fig. 5.3). It was found that the maximum uptake was achieved at a flow rate of 10 mL/min. At these examined flow rates (10-15 mL/min), the MB removal percentage (%) decreased with increasing flow rate and maximum 46% MB dye was removed with the lowest flow rate of 10 mL/min.

The breakthrough curves (Fig. 5.3) further showed that initially the adsorption was very rapid for all three different flow rates (10, 12 and 15 mL/min) which may be associated with the availability of reaction sites able to capture dye molecules around or inside the cells. Later, the uptake became less effective due to the gradual occupancy of these sites. The breakthrough occurred faster with higher flow rate and the break point time and adsorbed dye concentration decreased as well. The reason behind this is when the residence time of MB adsorbate in the column was not long enough for adsorption equilibrium to be reached at that flow rate, the front of the adsorption zone quickly reached the top of the column which saturated the column early and the MB solution left the column before equilibrium occurred (Ghorai and Pant 2005). Thus, the contact time of MB dyes with eucalyptus bark was very short at higher flow rate, causing a reduction in removal efficiency. At a low inlet MB dye flow rate, MB dye gets more time to contact with eucalyptus bark that resulted in shallow adsorption zone as well as higher removal of MB dye molecules in column. Therefore from Table 5.1, it was observed that the breakthrough time decreased from 102 to 43 min for the flow rates ranging between 10 and 15 mL/min respectively and dye removal percentage in column decreases with increase in flow rate. The various BTC fittings are also presented in Table 5.1. The variation in the slope of the

breakthrough curve and adsorption capacity may also be explained on the basis of mass transfer fundamentals. As the velocity increases, the rate of mass transfer increased, i.e. the amount of dye adsorbed onto unit bed height (mass transfer zone) increased with increasing flow rate leading to faster saturation at higher flow rate (Ko, Porter et al. 2000). This was further supported by the results of mass transfer zone (MTZ) or unused beds (H_{UNB}) presented in Table 5.1. Similar trend of results was reported by other researchers for MB dye adsorption by melon peels (Djelloul and Hamdaoui 2014), pine cone (Yagub, Sen et al. 2014) and rick husk (Han, Wang et al. 2007). Overall, Table 5.1 indicates that the packed bed column gives better performance in the removal of MB at lower solution flow rate, which is not favourable for large effluent treatment systems.

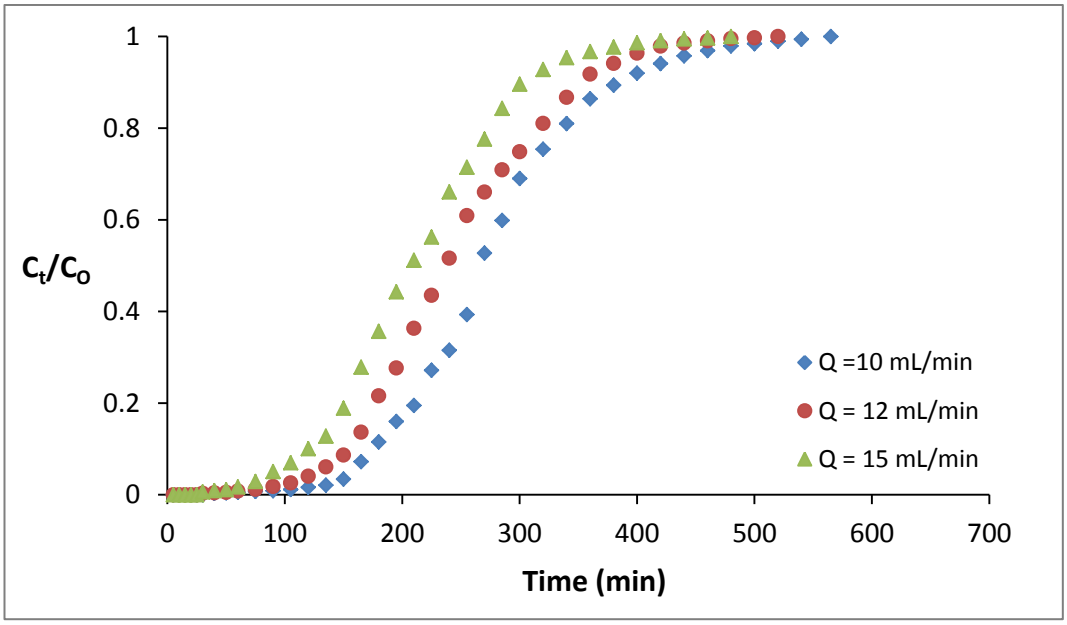

Figure 5.3 Comparison of experimental breakthrough curves (BTC) of MB dye adsorption on raw eucalyptus bark at different flow rates

(Conditions: Initial MB dye concentration = 75 mg/L, bed height = 12 cm, temperature = 25±1°C)

Table 5.1: Breakthrough curves (BTCS) parameters of fixed bed column at different MB dye flow rates for its removal by eucalyptus bark biomass

Q (mL/min)	t_b (min)	V_{eff} (mL)	t_{total} (min)	m_{total} (mg)	q_{total} (mg)	% Removal	MTZ or H_{UNB} (cm)	H_B (cm)
10	102	2590.7	259.1	423.8	194.3	45.9	7.3	4.7
12	63	2750.5	229.2	468	206.3	44.1	8.7	3.3
15	43	2954.8	197	540	221.6	41.0	9.4	2.6

5.5.2 Effect of Initial MB Dye Concentration

The effect of initial dye concentrations was carried out using 50, 75 and 100 mg/L of MB dye, keeping the bed height of 12 cm and the flow rate of 12 mL/min constant. The sorption breakthrough curves obtained for various adsorbate concentrations (50, 75 and 100 mg/L) are illustrated in Fig. 5.4 and experimental data is presented in Appendix B4-B6. The curves have relatively the same shape for all initial MB dye concentrations and resulting more shortened mass transfer zone. All the results of BTCS parameters of fixed bed column for MB dye removal by eucalyptus bark at different initial MB dye concentrations are presented in Table 5.2. Table 5.2 shows that the amount of total sorbed dye, equilibrium dye uptake and MTZ increased whereas the total percentage removal decreased with increasing inlet MB dye concentration.

The study of the effect of adsorbate concentration on the performance of the breakthrough curve is important since a given mass of adsorbent can only adsorb a fixed amount of dye. Therefore, the more concentrated an effluent, the smaller is the volume of effluent that a fixed mass of adsorbent can purify (Markovska, Meshko et al. 2001). As expected, for low inlet concentrations of MB dye, the breakthrough occurred late and surface of the adsorbent was saturated with MB dye after a long time whereas for higher MB concentration, the breakthrough occurred in a short period of time (Fig. 5.4). At lower inlet MB concentration, the breakthrough was flatter indicating a relatively wide mass transfer zone and film controlled process. On

the contrary, the breakthrough curves were sharp at high inlet MB concentration, implying a relatively smaller mass transfer zone and intra-particle diffusion controlled process. Similar results have been reported by other researchers for different systems (Hadi, Samarghandi et al. 2011, Bharathi and Ramesh 2013, Reddy and Nirmala 2014). Fig. 5.4 illustrated that the breakthrough time decreased with increasing influent MB concentration which can be explained by the fact that more adsorption sites were being covered with the increase in MB dye concentration. The larger the influent concentration, the steeper is the slope of breakthrough curve and smaller is the breakthrough time. Decreased inlet MB dye concentrations gave delayed breakthrough curves and the treated volume was also higher, since the lower concentration gradient caused slower transport due to decreased diffusion coefficient (Padmesh, Vijayaraghavan et al. 2005, Han, Wang et al. 2007). At the highest MB concentration (100 mg/L), the binding sites of EB bed saturated more quickly leading to earlier breakthrough and exhaustion time (Table 5.2).

With increase in initial MB dye concentration from 50 to 100 mg/L, the total amount of MB dye adsorbed was found to increase from 160 – 228.1 mg and the percentage (%) MB dye removal decreased from 46% to 43.2% when the inlet MB concentration increased from 50 to 100 mg/L (Table 5.2). The increase in uptake capacity of the adsorbent may be due to high inlet MB concentration providing higher driving force for the transfer process to overcome the mass transfer resistance. Consequently, at lower concentrations, all dye molecules present in the solution interact with the binding sites of the adsorbent, facilitating higher adsorption. Hence at higher concentrations, more dye molecules are left unadsorbed in the solution due to the saturation of available binding sites resulting in decreased adsorption efficiency. The same trend was also observed by other researchers (Goel, Kadirvelu et al. 2005, Baral, Das et al. 2009). However, percentage removal obtained from column study was lower than that obtained from batch study for the same initial dye concentration (Afroze, Sen et al. 2016) which may be insufficient contact time and not full bed being utilized due to channelling. Similar trends were obtained for adsorption of methylene blue onto pine cone (Yagub, Sen et al. 2014) and onto cedar sawdust and crushed brick (Hamdaoui 2006).

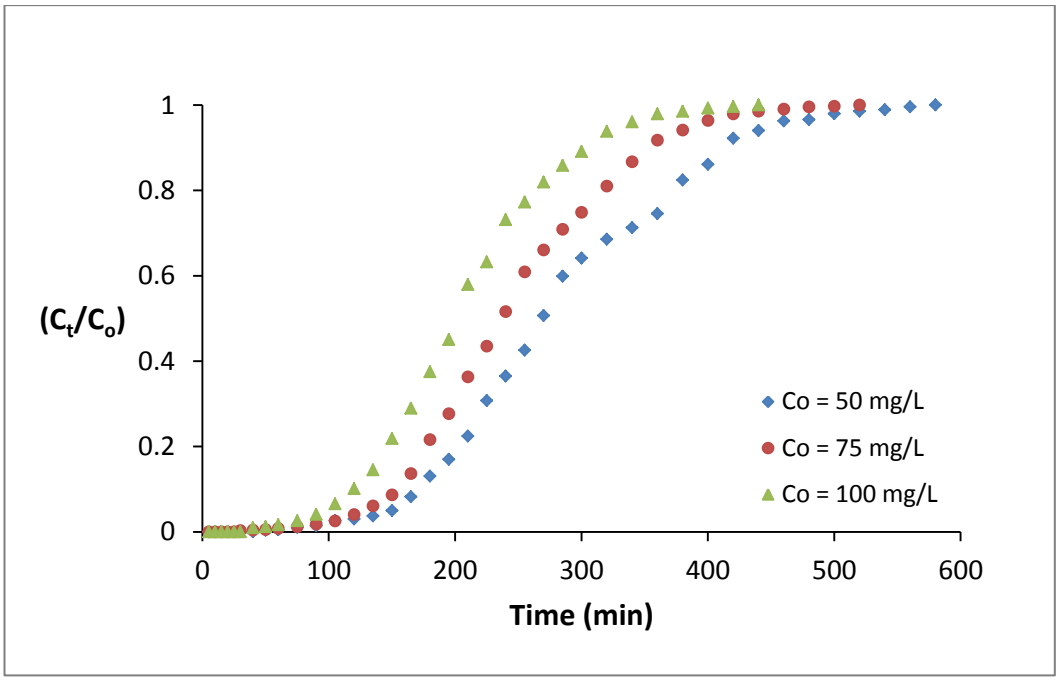

Figure 5.4 Comparison of experimental breakthrough curves (BTC) of MB dye adsorption on raw eucalyptus bark at different initial MB dye concentrations

(Conditions: MB dye flow rate = 12 mL/min, bed height = 12 cm, temperature = 25±1°C)

Table 5.2: Breakthrough curves (BTCS) parameters of fixed bed column at different inlet MB dye concentration for its removal using eucalyptus bark biomass

C_o (mg/L)	t_b (min)	V_{eff} (mL)	t_{total} (min)	m_{total} (mg)	q_{total} (mg)	% Removal	MTZ or H_{UNB} (cm)	H_B (cm)
50	75	3191.6	265.97	348	159.6	46	8.6	3.4
75	63	2750.5	229.21	468	206.3	44.1	8.7	3.3
100	42	2280.8	190.06	528	228.1	43.2	9.3	2.7

5.5.3 Effect of Adsorbent Bed Height

The effect of bed height on the adsorption of methylene blue (MB) dye obtained at 10, 12 and 15 cm and a constant initial dye concentration of 75 mg L^{-1}, solution pH 7.4 and a constant flow rate of 12 mL min^{-1} as presented in Table 5.3. Appendix B7-

B9 elaborates all the results obtained from experimental data for which Fig. 5.5 represents the performance of breakthrough curves plotted between time and ratio of final (outlet) and initial (inlet) MB dye concentrations (C_t/C_o) for different bed heights of 10, 12 and 15 cm.

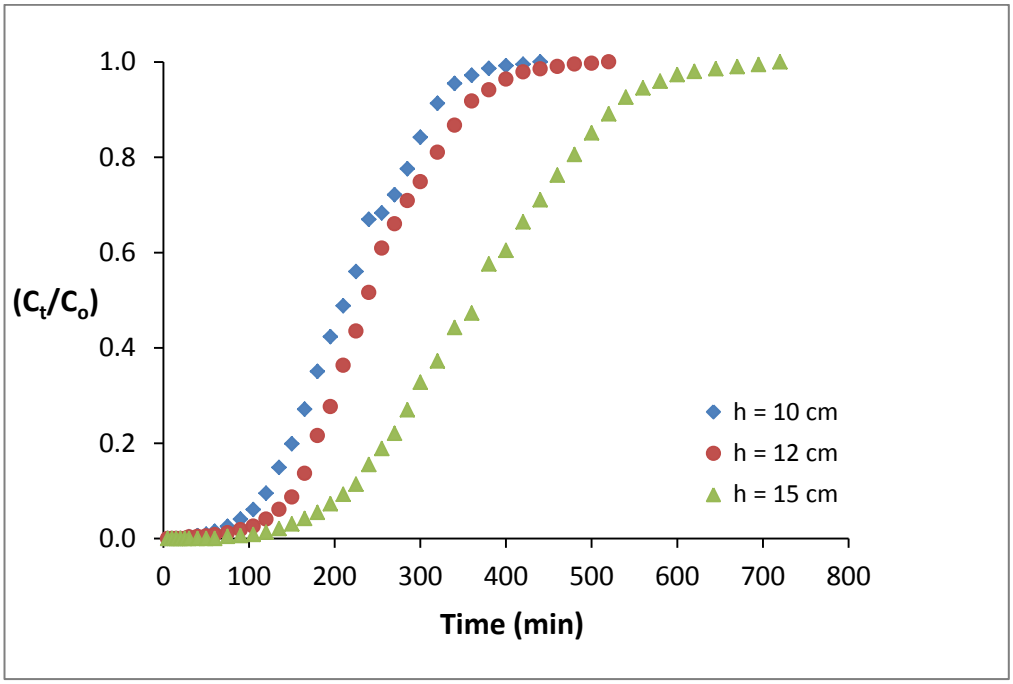

Figure 5.5 Comparison of experimental breakthrough curves (BTC) for MB dye adsorption on raw eucalyptus bark at different bed heights

(Conditions: Initial MB dye concentration = 75 mg/L, MB dye flow rate = 12 cm, temperature = 25±1°C)

The results in Fig. 5.5 revealed that an increase in the bed height increased both the breakthrough time and the saturation/exhaustion time. By increasing bed height from 10 to 15 cm, the breakthrough time increased from 50 min to 105 min and the percentage dye removal also increased from 43.6 to 48% (Table 5.3). With the increased bed height, the adsorbent eucalyptus bark load also increased. Consequently, the residence time of MB solution inside the adsorbent bed was increased, allowing the dye molecules to diffuse deeper into the eucalyptus bark which in turn resulting in increased used bed height (H_B) and higher dye removal efficiency. Higher MB uptake and more treated volume of effluents observed at the highest bed height was due to the availability of increased surface area of the biomass, which provided a greater number of available binding sites for the attachment of MB dye molecules for adsorption process. Hence the MB solute

particles got enough time to get diffused into the adsorbent, remained into the adsorbent biomass for long time and thus volume of treated solution was increased during column operation (Table 5.3). Further, higher breakthrough time gives better intra-particle diffusion phenomenon and hence more adsorption capacity of column bed (Sadaf and Bhatti 2014). Various researchers were also reported similar observation (Saha, Chakraborty et al. 2012, Mobasherpour, Salahi et al. 2014, Sadaf and Bhatti 2014).

Table 5.3: Breakthrough curves (BTCS) parameters of fixed bed column at different bed height of eucalyptus bark biomass for the removal of MB dye

h (cm)	t_b (min)	V_{eff} (mL)	t_{total} (min)	m_{total} (mg)	q_{total} (mg)	% Removal	MTZ or H_{UNB} (cm)	H_B (cm)
10	50	2405.7	200.47	414	180.4	43.6	9.0	3.0
12	63	2750.5	229.21	468	206.3	44.1	8.7	3.3
15	105	4183.5	348.63	648	313.8	48	8.4	3.6

5.6 Kinetic Modelling of Fixed Bed Column Studies

Three kinetic models, Thomas, Yoon-Nelson and BDST, were applied to the experimental data in the continuous mode study which are discussed below.

5.6.1 Application of Thomas Model

This model is suitable for determining the maximum concentration (q_o) of the solid phase of MB sorbate on adsorbent biomass and the rate constant (K_{Th}) of the MB sorbate in continuous mode studies. The K_{Th} and q_o were obtained from the slope and intercepts of linear plots of ln $[(C_o/C_t) - 1]$ against t using values of BTC column experimental data fitted into the Thomas model according to Eq.(2.13).

The predicted breakthrough curves at different experimental conditions (different flow rate, different inlet MB dye concentration and different bed height) according to Thomas model are shown in Figs. 9(a-c). The results of K_{Th}, q_o and R^2 are listed in Table 5.4. From the regression coefficient (R^2) and other parameters in Table 5.4, it can be concluded that Thomas model fitted the experimental data well.

As observed in Table 5.4, when the flow rate increased from 10 mL min^{-1} to 15 mL min^{-1}; the value of Thomas rate constant (K_{Th}) increased but the value of q_o decreased from 45.24 to 38.76 mg/g. Higher flow rate reduces the adsorption capacity due to inadequate residence time of the solute particles in the column and diffuse the solute into the pores of the adsorbent which forced the solute molecules to leave the column before attaining equilibrium (Tan, Ahmad et al. 2008). Further, shown in Table 5.4, with the increase in inlet MB dye concentration, the amount of maximum solid-phase concentration (q_o) increased whereas the value of Thomas rate constant (K_{Th}) decreased. This is because the driving force for adsorption is the concentration difference between the dye in the solution and the dye on the adsorbent (Han, Wang et al. 2007). Thus the higher driving force due to the higher MB dye concentration resulted in better column performance. Hence, with the increased bed depth, the values of maximum solid-phase concentration (q_o) increased and Thomas rate constant (K_{Th}) decreased. Therefore lower MB dye flow rate, higher initial MB dye concentration, and higher adsorbent bed depth would increase the adsorption of MB onto eucalyptus bark loaded column. Similar type of Thomas constants for different systems was reported by Yagub et al. (Yagub, Sen et al. 2014) and by Bharathi and Ramesh (Bharathi and Ramesh 2013).

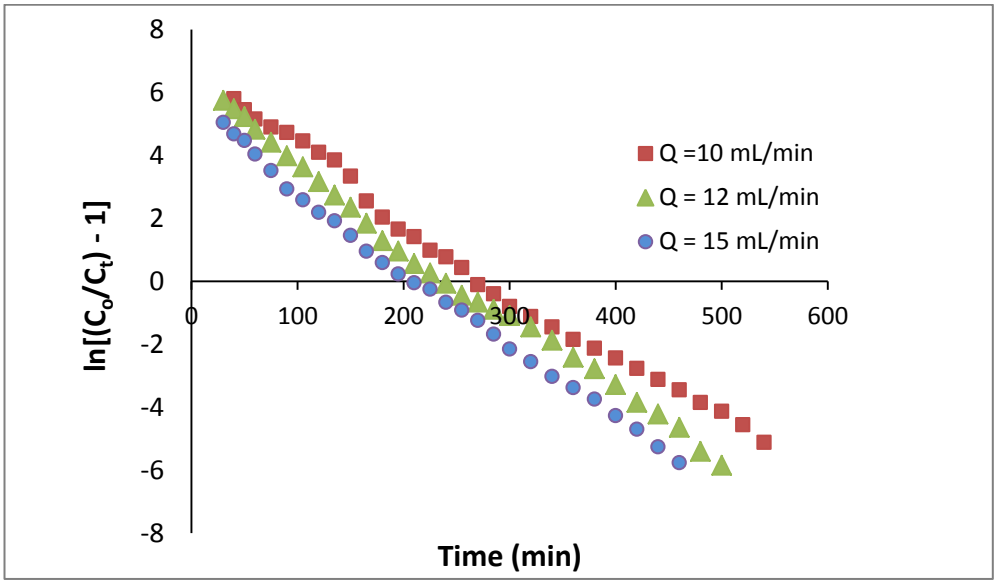

Figure 5.6 Thomas kinetic plot for the adsorption of MB on eucalyptus bark: Effect of flow rate

(Conditions: Inlet MB dye concentration = 75 mg/L, bed height = 12 cm, temperature = 25±1 ^{o}C)

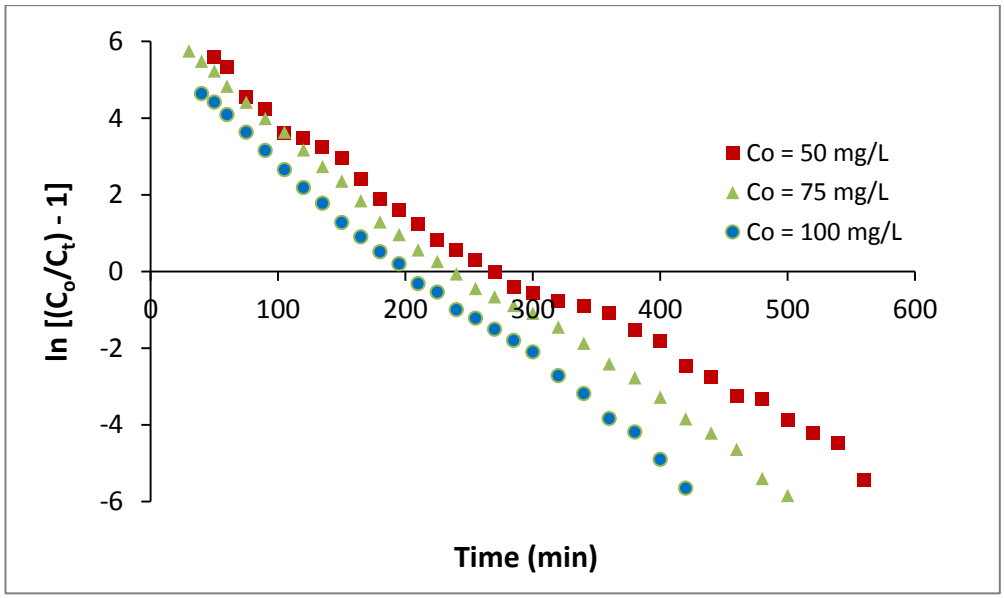

Figure 5.7 Thomas kinetic plot for the adsorption of MB on eucalyptus bark: Effect of inlet MB dye concentration

(Conditions: MB dye flow rate = 12 mL/min, bed height = 12 cm, temperature = 25±1 ^{o}C)

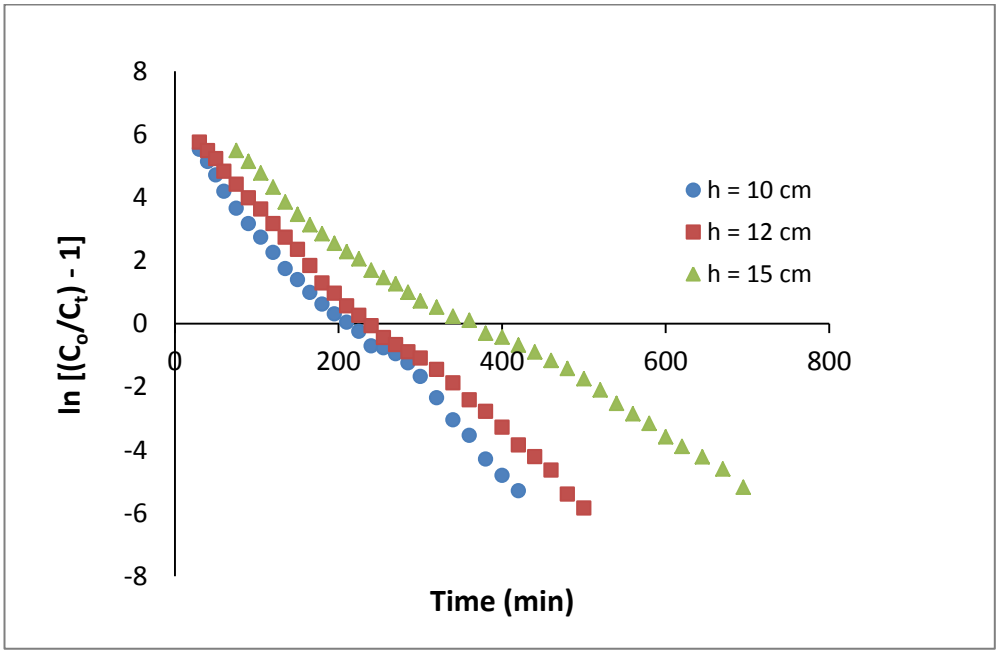

Figure 5.8 Thomas kinetic plot for the adsorption of MB on eucalyptus bark: Effect of adsorbent bed height

(Conditions: Inlet MB dye concentration = 75 mg/L, MB dye flow rate = 12 mL/min, temperature = 25±1 ^{o}C)

Table 5.4: Thomas kinetic model parameters at different experimental conditions by non-linear regression analysis

Thomas Parameters	***Flow Rate (mL/min)***			***Initial MB dye Concentration (mg/L)***			***Bed Height (cm)***		
	10	**12**	**15**	**50**	**75**	**100**	**10**	**12**	**15**
K_{Th} **(mL/min mg)**	0.29	0.33	0.37	0.39	0.33	0.26	0.35	0.33	0.21
q_o **(mg/g)**	45.24	43.93	38.76	33.74	43.93	48.29	41.83	43.93	49.55
R^2	0.99	0.99	0.84	0.99	0.99	0.99	0.99	0.99	0.99

5.6.2 Application of Yoon-Nelson Model

Yoon–Nelson model was also applied to study the breakthrough curve behaviour of MB dye on eucalyptus bark biomass. According to Eq. (2.14), the values of the model parameters such as Yoon–Nelson constant (K_{YN}) and τ (the time required for 50 % sorbate breakthrough) were calculated from the plot of ln $[C_t/(C_0-C_t)]$ versus t (time) at different flow rates (10, 12 and 15 mL min^{-1}), different initial MB dye concentrations (50, 75 and 100 mg/L) and also at different bed heights (10, 12 and 15 cm). This plot will result in a straight line with slope of K_{YN} and intercept of τK_{YN} which are presented in Figs. 5.9-5.11. The values of all determined parameters are listed in Table 5.5. Table 5.5 shows that the rate constant K_{YN} increased and the 50% breakthrough time τ decreased with increasing both flow rate and MB inlet concentration. With the increasing bed heights, the values of τ increased while the values of K_{YN} decreased. This can be attributed to the fact that increase in initial dye concentration increases the competition between adsorbate molecules for the adsorption site, which ultimately results in increased uptake rate (Hamdaoui 2006). Similar trend was also observed for the adsorption of MB dye by melon peel (Djelloul and Hamdaoui 2014).

It was also found in Table 5.5 that the time required to achieve 50% of adsorbate breakthrough time τ from the Yoon–Nelson model seemed to agree with the experimental data ($\tau_{50\%\ exp}$) in the entire column adsorption system, thus indicating the suitability of the Yoon–Nelson model for the proposed system.

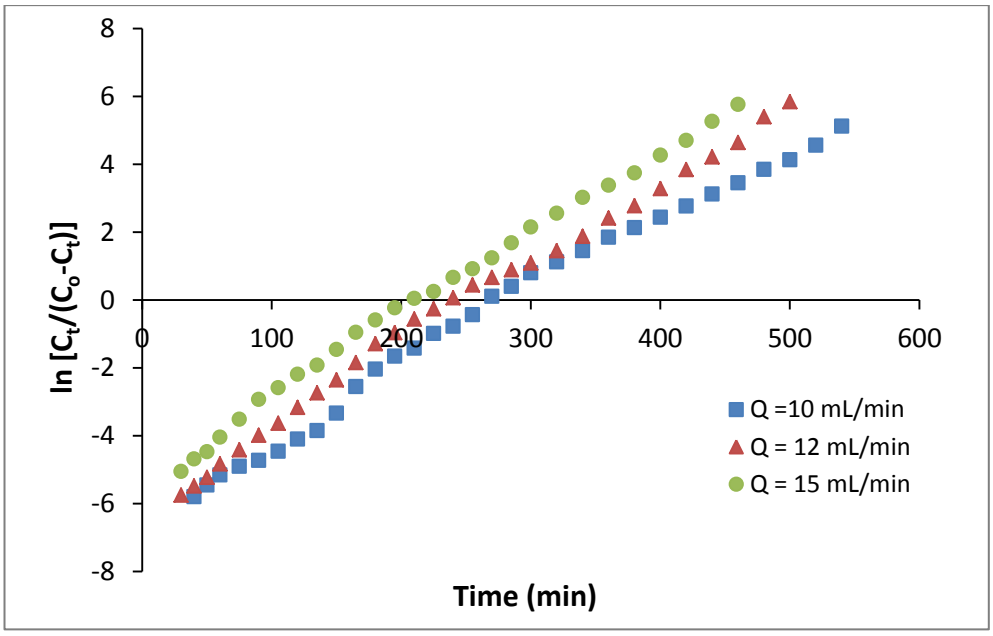

Figure 5.9 Yoon–Nelson kinetic plot for the adsorption of MB on eucalyptus bark: Effect of flow rate

(Conditions: Inlet MB dye concentration = 75 mg/L, bed height = 12 cm, temperature = 25±1 ^{o}C)

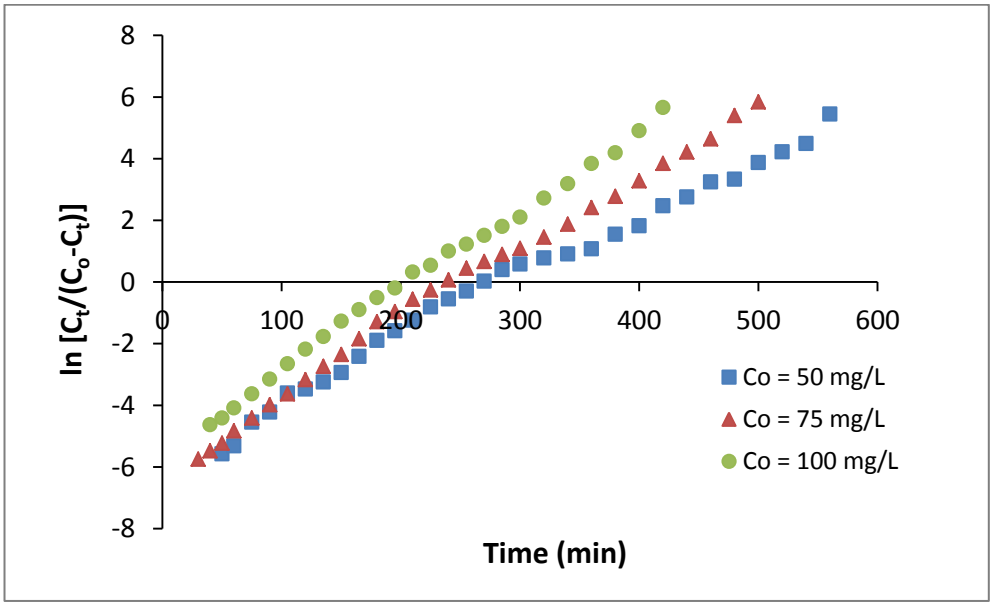

Figure 5.10 Yoon–Nelson kinetic plot for the adsorption of MB on eucalyptus bark: Effect of inlet MB dye concentration

(Conditions: MB dye flow rate = 12 mL/min, bed height = 12 cm, temperature = 25±1 ^{o}C)

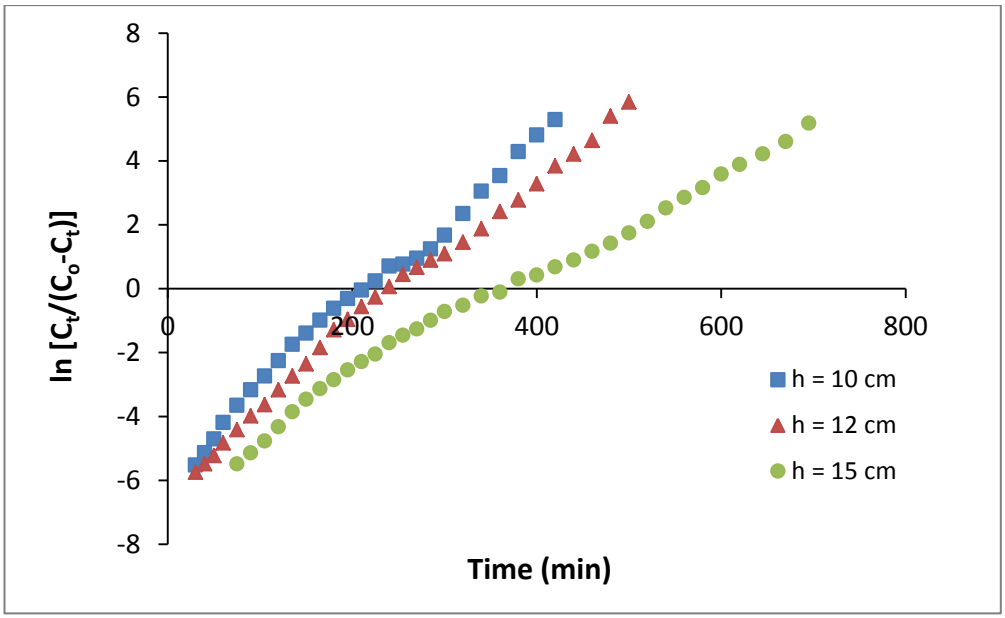

Figure 5.11 Yoon–Nelson kinetic plot for the adsorption of MB on eucalyptus bark: Effect of adsorbent bed height

(Conditions: Inlet MB dye concentration = 70 mg/L, MB dye flow rate = 12 mL/min, temperature = 25±1 ^{o}C)

Table 5.5: Yoon–Nelson kinetic model parameters at different experimental conditions by non-linear regression analysis

Yoon-Nelson Parameters	***Flow Rate (mL/min)***			***Initial MB dye Concentration (mg/L)***			***Bed Height (cm)***		
	10	**12**	**15**	**50**	**75**	**100**	**10**	**12**	**15**
K_{YN} **(min^{-1})**	0.021	0.024	0.027	0.02	0.024	0.026	0.026	0.024	0.016
τ (min)	295.43	251.41	206.60	288.09	251.41	208.47	218.07	251.41	368.35
$\tau_{50\%exp.}$**(min)**	265	238	208	268	238	200	212	238	362
R^2	0.989	0.994	0.996	0.986	0.994	0.996	0.99	0.994	0.99

5.6.3 Application of Bed Depth Service Time (BDST) Model

The Bed Depth Service Time (BDST) model was used to express the effect of bed depth on the mode of the breakthrough curves. Therefore, the data obtained from the experimental column studies between MB dye and eucalyptus bark also fitted to the BDST model at different bed heights (10, 12 and 15 cm) according to Eq. (2.15). Hence the BDST plot of service time against bed height at a flow rate of 12 mL/min

and with inlet MB dye concentration of 75 mg/L (Fig. 5.12) was linear (R^2 = 0.9983) which indicated a good fit of BDST model from the experimental results. The value of the sorption capacity of the bed per unit bed volume (N_o) was calculated from the slope of BDST plot, assuming initial concentration (C_o) and linear velocity (v) as constant during the column operation. The rate constant (K_a), calculated from the intercept of BDST plot, characterizes the rate of solute transfer from the fluid phase to the solid phase. The computed N_o and K_a were 10113 mg L^{-1} and 0.539 L mg^{-1} min^{-1}, respectively. These results confirm that the BDST model can be used to predict the adsorption performance at other operation conditions for adsorption of MB dye onto eucalyptus bark biomass to scale up the process without further experimental runs.

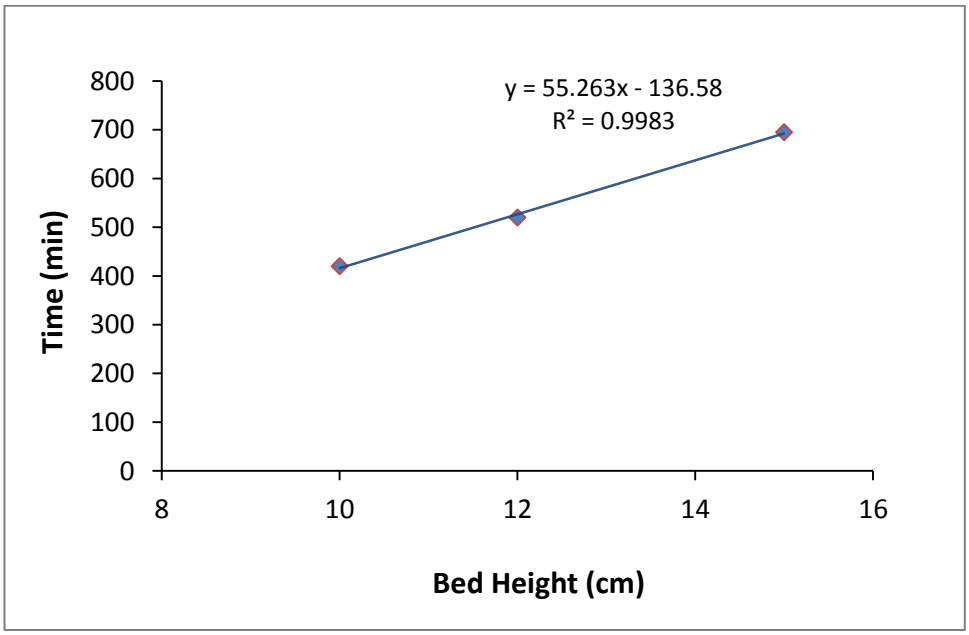

Figure 5.12 Bed Depth Service Time (BDST) kinetic plot for the adsorption of MB on eucalyptus bark

(Conditions: Inlet MB dye concentration = 75 mg/L, MB dye flow rate = 12 mL/min, temperature = 25±1 ^oC)

5.7 Summary

Adsorption dynamics study of a fixed bed column for the removal of methylene blue (MB) dye on raw eucalyptus bark adsorbent biomass was applied. The obtained results from the breakthrough curves determined at various flow rates, initial dye concentrations and bed depths showed the following outcomes in this chapter:

- Adsorption of MB dye was strongly dependent on adsorbate flow rate, initial MB dye concentration and adsorbent bed height. As the flow rate increased, the uptake capacity was found to decrease. The increase in initial dye concentration resulted in higher adsorption. An increase in bed height resulted in improved sorption performance.
- The application of Thomas model showed that the value of maximum solid-phase concentration (q_o) decreased when the flow rate increased but increased with the increased adsorbent bed height and increasing inlet MB dye concentration. The value of Thomas rate constant (K_{Th}) increased with increase in flow rate but decreased with increasing initial MB dye concentration and the height of the bed.
- The results from Yoon–Nelson model showed that the time required to achieve 50% adsorbate breakthrough $\boldsymbol{\tau}$ seemed to agree well with the experimental data ($\boldsymbol{\tau}_{50\%\ exp.}$) and also the results showed that the rate constant K_{YN} increased with both increasing flow rate and initial MB dye concentration but decreased with increasing the bed height.
- From Bed Depth Service Time (BDST) model, the bed sorption capacity N_o was found to be 10113 mg L^{-1} for MB adsorption by bark material.
- From the results, it can be stated that the regression coefficient R^2 values are very close for all the three models (Thomas, Yoon-Nelson and BDST), and hence all these three models can be applied to describe the experimental data.
- The comparative analysis of the experimental modes as well as Thomas and Yoon-Nelson model breakthrough curves together with the values of the model parameters proved satisfactory correlations with the experimental data. The results such as sorption capacity and prediction of the time necessary for the effective column operation indicates that the external mass transfer resistance plays a dominating role for the mechanism of the process whereas the effect of axial dispersion could not also be neglected.

5.8 References

Afroze, S. and Sen, T. K. (2015). Agricultural Solid Wastes in Aqueous Phase Dye Adsorption: A Review. Agricultural Wastes Characteristics, Types and Management. C. N. Foster. New York, NOVA Publishers. **1:** 169-214.

Afroze, S., Sen, T. K., Ang, M. and Nishioka, H. (2015). "Adsorption of methylene blue dye from aqueous solution by novel biomass Eucalyptus sheathiana bark: equilibrium, kinetics, thermodynamics and mechanism." Desalination and Water Treatment **57**(13): 5858-5878.

Afroze, S., Sen, T. K., Ang, M. and Nishioka, H. (2016). "Adsorption of methylene blue dye from aqueous solution by novel biomass eucalyptus *sheathiana* bark: equilibrium, kinetics, thermodynamics and mechanism." Desalination and Water Treatment **57**(13): 5858-5878.

Al-Degs, Y., Khraisheh, M., Allen, S. and Ahmad, M. (2009). "Adsorption characteristics of reactive dyes in columns of activated carbon." Journal of Hazardous Materials **165**(1): 944-949.

Ali, I., Asim, M. and Khan, T. A. (2012). "Low cost adsorbents for the removal of organic pollutants from wastewater." Journal of Environmental Management **113**: 170-183.

Baral, S., Das, N., Ramulu, T., Sahoo, S., Das, S. and Chaudhury, G. R. (2009). "Removal of Cr (VI) by thermally activated weed Salvinia cucullata in a fixed-bed column." Journal of Hazardous Materials **161**(2): 1427-1435.

Bharathi, K. S. and Ramesh, S. P. T. (2013). "Fixed-bed column studies on biosorption of crystal violet from aqueous solution by Citrullus lanatus rind and Cyperus rotundus." Applied Water Science **3**(4): 673-687.

Crini, G. (2006). "Non-conventional low-cost adsorbents for dye removal: a review." Bioresource Technology **97**(9): 1061-1085.

Cruz-Olivares, J., Pérez-Alonso, C., Barrera-Díaz, C., Ureña-Nuñez, F., Chaparro-Mercado, M. and Bilyeu, B. (2013). "Modeling of lead (II) biosorption by residue of allspice in a fixed-bed column." Chemical Engineering Journal **228**: 21-27.

Djelloul, C. and Hamdaoui, O. (2014). "Dynamic adsorption of methylene blue by melon peel in fixed-bed columns." Desalination and Water Treatment: 1-10.

Faust, S. D. and Aly, O. M. (2013). Adsorption processes for water treatment, Elsevier.

Ghomshe, S. T., Mousavi, S., Soltanieh, M. and Kordi, A. S. (2011). "Batch and column study of haloacetic acids adsorption onto granular activated carbon." Scientific Research and Essays **6**(16): 3553-3560.

Ghorai, S. and Pant, K. (2005). "Equilibrium, kinetics and breakthrough studies for adsorption of fluoride on activated alumina." Separation and Purification Technology **42**(3): 265-271.

Goel, J., Kadirvelu, K., Rajagopal, C. and Garg, V. K. (2005). "Removal of lead (II) by adsorption using treated granular activated carbon: batch and column studies." Journal of Hazardous Materials **125**(1): 211-220.

Hadi, M., Samarghandi, M. R. and McKay, G. (2011). "Simplified fixed bed design models for the adsorption of acid dyes on novel pine cone derived activated carbon." Water, Air, & Soil Pollution **218**(1-4): 197-212.

Hamdaoui, O. (2006). "Dynamic sorption of methylene blue by cedar sawdust and crushed brick in fixed bed columns." Journal of Hazardous Materials **138**(2): 293-303.

Han, R., Wang, Y., Yu, W., Zou, W., Shi, J. and Liu, H. (2007). "Biosorption of methylene blue from aqueous solution by rice husk in a fixed-bed column." Journal of Hazardous Materials **141**(3): 713-718.

Ko, D. C., Porter, J. F. and McKay, G. (2000). "Optimised correlations for the fixed-bed adsorption of metal ions on bone char." Chemical Engineering Science **55**(23): 5819-5829.

Markovska, L., Meshko, V. and Noveski, V. (2001). "Adsorption of basic dyes in a fixed bed column." Korean Journal of Chemical Engineering **18**(2): 190-195.

Mobasherpour, I., Salahi, E. and Asjodi, A. (2014). "Research on the Batch and Fixed-Bed Column Performance of Red Mud Adsorbents for Lead Removal." Soil and Water **4**: 5.

Padmesh, T., Vijayaraghavan, K., Sekaran, G. and Velan, M. (2005). "Batch and column studies on biosorption of acid dyes on fresh water macro alga Azolla filiculoides." Journal of Hazardous Materials **125**(1): 121-129.

Rafatullah, M., Sulaiman, O., Hashim, R. and Ahmad, A. (2010). "Adsorption of methylene blue on low-cost adsorbents: A review." Journal of hazardous materials **177**(1-3): 70-80.

Reddy, M. S. and Nirmala, V. (2014). "Bengal gram seed husk as an adsorbent for the removal of dyes from aqueous solutions–Column studies." Arabian Journal of Chemistry.

Sadaf, S. and Bhatti, H. N. (2014). "Evaluation of peanut husk as a novel, low cost biosorbent for the removal of Indosol Orange RSN dye from aqueous solutions: batch and fixed bed studies." Clean Technologies and Environmental Policy **16**(3): 527-544.

Saha, P. D., Chakraborty, S. and Chowdhury, S. (2012). "Batch and continuous (fixed-bed column) biosorption of crystal violet by Artocarpus heterophyllus (jackfruit) leaf powder." Colloids and Surfaces B: Biointerfaces **92**: 262-270.

Tan, I., Ahmad, A. and Hameed, B. (2008). "Adsorption of basic dye using activated carbon prepared from oil palm shell: batch and fixed bed studies." Desalination **225**(1): 13-28.

Yagub, M. T., Sen, T. K., Afroze, S. and Ang, H. (2014). "Dye and its removal from aqueous solution by adsorption: A review." Advances in Colloid and Interface Science **209**: 172-184.

Yagub, M. T., Sen, T. K., Afroze, S. and Ang, H. M. (2014). "Fixed-bed dynamic column adsorption study of methylene blue (MB) onto pine cone." Desalination and Water Treatment: 1-14.

Yaneva, Z. L. and Georgieva, N. V. (2012). "Insights into Congo Red Adsorption on Agro-Industrial Materials- Spectral, Equilibrium, Kinetic, Thermodynamic, Dynamic and Desorption Studies. A Review." International Review of Chemical Engineering **4**(2): 127-146.

Every reasonable effort has been made to acknowledge the owners of copyright material. I would be pleased to hear from any copyright owner who has been omitted or incorrectly acknowledged.

CHAPTER 6

BATCH ADSORPTION STUDIES ON THE REMOVAL OF ZINC (II) METAL IONS BY RAW AND MODIFIED EUCALYPTUS BARK*

ABSTRACT*

In this study, potential application of abundantly available agricultural by-product Eucalyptus sheathiana bark in its raw and sodium hydroxide (NaOH) modified form to remove Zn^{2+} from its aqueous solutions was investigated by considering parameter identification and optimization, reusability, equilibrium, kinetic and thermodynamic studies. The adsorbent was characterized by SEM-EDX, FTIR, XRD, BET surface area and bulk density and point of zero charge were also determined. The process was strongly pH dependent and the adsorption percentage of Zn^{2+} was increased with an increase in solution pH from 2.5 to 5.1. Conversely, the adsorption percentage of Zn^{2+} decreased with the increase in adsorbent dosage, initial metal concentration, temperature and ionic strength. Kinetic measurements showed that the process was multistep, rapid and diffusion controlled. It was found to follow the pseudo-second-order rate equation. Equilibrium adsorption studies showed that both Freundlich and Langmuir models are applicable for both raw and base modified eucalyptus bark. MPSD error function was used to treat the equilibrium data using non-linear optimization technique for evaluating the fit of the isotherm equations. The maximum sorption capacity of modified eucalyptus bark was 250.00 mg/g at 30°C which was comparative to other adsorbents. Various thermodynamic parameters indicate that the process was spontaneous and physical in nature. Desorption studies were also performed to determine possible recovery potential of Zn^{2+} and the re-usability of the biomass and to identify the mechanism of adsorption.

*This work is in Press of Process Safety and Environmental Protection Journal (Afroze, S., Sen, T.K. & Ang H. M., 2016. Adsorption removal of Zinc (II) from Aqueous Phase by Raw and Base Modified Eucalyptus *Sheathiana* Bark: kinetics, mechanism and equilibrium study. *Process Safety and Environmental Protection Journal*, doi:10.1016/j.psep.2016.04.009)

6.1 Introduction

This chapter deals with the adsorptive characteristics of raw and chemically modified eucalyptus bark as adsorbents for the removal of zinc (II) metal ions from its aqueous solution. Batch adsorption experiments were conducted to evaluate the effectiveness of the prepared adsorbents; raw and chemically NaOH treated eucalyptus bark at various process conditions. The effects of different physicochemical process parameters such as contact time, initial Zn^{2+} concentration, solution pH, amount of adsorbent, system temperature and salt concentration on the removal of Zn^{2+} were studied through batch kinetic experiments and analysed. The obtained batch experimental data were analysed with three commonly used kinetic models; pseudo-first-order, pseudo-second-order and intraparticle diffusion model to provide better understanding of the adsorption process and mechanism. Consequently, two commonly used isotherm models, Langmuir and Freundlich models were selected to explain the interaction between Zn^{2+}- eucalyptus bark (raw and base modified) and to investigate the mechanism of adsorption. To assess the reusability and applicability of raw and modified eucalyptus bark adsorbent, % desorption was studied. Thermodynamic parameters, standard Gibbs free energy change (ΔG^o), enthalpy change (ΔH^o) and entropy change (ΔS^o) were also calculated to study the nature of adsorption. Finally, the adsorption efficiency of raw and base modified eucalyptus bark adsorbents tested here was compared with other published biomass based adsorbents. In order to gain insight into the process dynamics, a single-stage batch adsorber has been designed for the removal of Zn^{2+} by raw and modified eucalyptus bark based on the equilibrium data obtained.

6.2 Materials and Methods

6.2.1 Adsorbent

Eucalyptus barks (*E. sheathiana*) were collected locally from Curtin University – Bentley campus, Western Australia between February and March 2013. The barks were washed several times with deionised water to remove dust, dirt and soluble impurities. The barks were placed in the oven to dry at 105˚C for 24 h. The dried biomass was crushed into fine powders using a mechanical grinder. The resultant

powders were passed through British Standard Sieves (BSS) of 106 µm and powders of size ≤ 106 µm were collected in an airtight plastic container and used as adsorbent for adsorption experiments.

Base modified eucalyptus bark was prepared by mixing 50 g of raw eucalyptus bark powder with 500 mL of 0.1 M sodium hydroxide (NaOH) solution. The whole mixture was stirred with a magnetic stirrer set at 120 rpm for a period of 24 h at room temperature. The treated powder was filtered and repeatedly rinsed with distilled water to ensure the removal of excess NaOH from the powder. The washed powders were then dried overnight at 90˚C and used for adsorption experiments. The characterisation of raw and modified eucalyptus bark before and after adsorption were studied which are presented in Section 3.3.

6.2.2 Adsorbate and Other Chemicals

All chemicals used were of analytical grade. The Zn^{2+} solution was selected as the model inorganic adsorbate for this study. The standard stock solution of Zn^{2+} of 1000 ppm was prepared by dissolving an accurately weighed amount of $Zn(NO_3)_2{\cdot}6H_2O$ salt (supplied by Sigma-Aldrich Pty. Ltd., NSW, Australia) in ultra-pure water. The working solutions were then prepared by diluting the stock solution with ultra-pure water to give the specific concentration of the working solutions. Further details of other chemicals used for experimental purposes are presented in Section 3.2.1.

6.2.3 Adsorption Experiments

The adsorption of Zn^{2+} on raw and modified eucalyptus bark was carried out in a batch system. 1000 mg/L of standard Zn^{2+} solution was used to obtain calibration curve using atomic absorption spectrophotometer (AAS) where the slit width used was 1.0 nm with a wavelength of 213.9 nm for Zn^{2+} adsorption. Batch adsorption experiments were conducted by varying the process operating parameters such as initial solution pH, initial Zn^{2+} concentration, adsorbent dose, temperature and salt concentrations at predetermined time interval under the aspect of adsorption kinetics, adsorption isotherm and thermodynamic study. A known amount of the adsorbent was mixed with 50 mL of Zn^{2+} solutions of known concentration in a series of 250 mL plastic bottles. The mixture was then shaken in a constant temperature using Thermo Line Scientific Orbital Shaker Incubator at a speed of 120 rpm and

temperature of 30^0C. At predetermined time intervals, the plastic bottles were withdrawn from the shaker, supernatant Zn^{2+} was separated from the adsorbents through filtration and the residual Zn^{2+} concentration in the solution was measured by using AAS. Further details of the experiments conducted for Zn^{2+} adsorption are mentioned in Section 3.2.2. The amount of Zn^{2+} adsorbed onto the adsorbent, q_t (mg/g) at time t and % Adsorption were calculated as per equations (3.1) and (3.2) respectively.

Further, equilibrium adsorption studies were conducted in a series of 250 mL plastic bottles where 50 mL Zn^{2+} solution of concentrations ranging from 20 to 70 ppm was mixed with 20 mg of raw and modified eucalyptus bark separately. The isotherm experiments were carried out for 2 h which was sufficient enough to attain equilibrium time for this study. The mixture was shaken in Thermo Line Scientific Orbital Shaker Incubator at a speed of 120 rpm. The solution pH of 5.1 and 30^0C temperature was maintained at all times. The bottles were then withdrawn from the shaker, filtered and the filtrates were analysed for residual Zn^{2+} concentration using AAS. The amount of Zn^{2+} adsorbed onto the adsorbent at equilibrium, q_e (mg/g) was calculated from Eq. (3.1). Detailed methods are described in Section 3.2.2 as well.

6.3 Results and Discussion

At various physico-chemical process conditions, full experimental data for the adsorption of Zn^{2+} onto raw and modified eucalyptus bark are tabulated in Appendix C1-C24.

6.3.1 Effect of Initial Solution pH on Zn^{2+} Adsorption Kinetics

The initial solution pH plays a significant role in the adsorption process, as the variation in pH leads to the variation in the degree of ionization of the adsorptive molecules and the surface properties of the adsorbent (Nandi, Goswami et al. 2009). The effect of initial solution pH on Zn^{2+} adsorption from aqueous solution by raw and modified eucalyptus bark (EB) was investigated over an initial solution pH range of 2.5–5.6 which is presented in Fig. 6.1. It was found that the amount of Zn^{2+} adsorbed, q_t (mg/g) increased with the increase in initial solution pH for both the systems. The increase in Zn^{2+} sorption is due to the electrostatic interaction of

cationic Zn^{2+} metal ions with the negatively charged surface of the eucalyptus bark material.

According to Surface Complexation Model (SCM), cations with the hydroxyl group on the surface of adsorbent forms a surface complex as per equations (6.1) and (6.2) respectively. Adsorption of metal ions may result in the formation of more than one type of surface complex which attributes the following reactions for Zn^{2+} with an oxide surface site where S in the symbol of adsorbent hydroxyl surface (Davis and Leckie 1978), i.e.,

$$\equiv SOH + Zn^{2+} \leftrightarrow SO^{-}-Zn^{2+} + H^{+} \quad (6.1)$$

$$\equiv SOH + Zn^{2+} + H_2O \leftrightarrow [SO^{-}-ZnOH^{+}] + 2H^{+} \quad (6.2)$$

As pH influences the sorbent surface charge and with the increase in pH, less competition from protons to reaction sites increases the concentration of $Zn(OH)^{+}$ species, and therefore higher amount of Zn^{2+} adsorption was observed up to solution pH 5.1. The total adsorption density of Zn^{2+} is a sum of the surface concentrations of $[SO^{-}-Zn^{2+}]$ and $[SO^{-}-ZnOH^{+}]$. $[SO^{-}-ZnOH^{+}]$ is the predominant Zn^{2+} surface species for pH ≥ 5. This was also supported by point of zero surface charge (pH_{zpc}) of eucalyptus bark (= 5.0) examined and discussed in Section 3.3 which influences adsorbent surface charge. Hence, with the increase in solution pH, the negative surface charges of the adsorbents also increase. As solution pH rises towards and above pH_{PZC}, the formation of dissociated surface sites, SO^{-}, is favoured with the reduction of H^{+} ions in solution which basically competes with Zn^{2+} for sorption sites. For this study, after solution pH 5.1, the sorption capacity for all raw and modified samples was found to decrease at pH 5.6 [Fig. 6.1(a)], due to the decreasing concentration of Zn^{2+} and $Zn(OH)^{+}$ at higher pH and the appearance of $Zn(OH)_2$ species in solution. Higher initial solution pH were not examined further to avoid Zn^{2+} precipitation as $Zn(OH)_2$ at pH above 5.5. Ofamaja and Naidoo (Ofomaja and Naidoo 2011) also reported similar results in their previous work for Cu(II) adsorption on chemically activated pine cone.

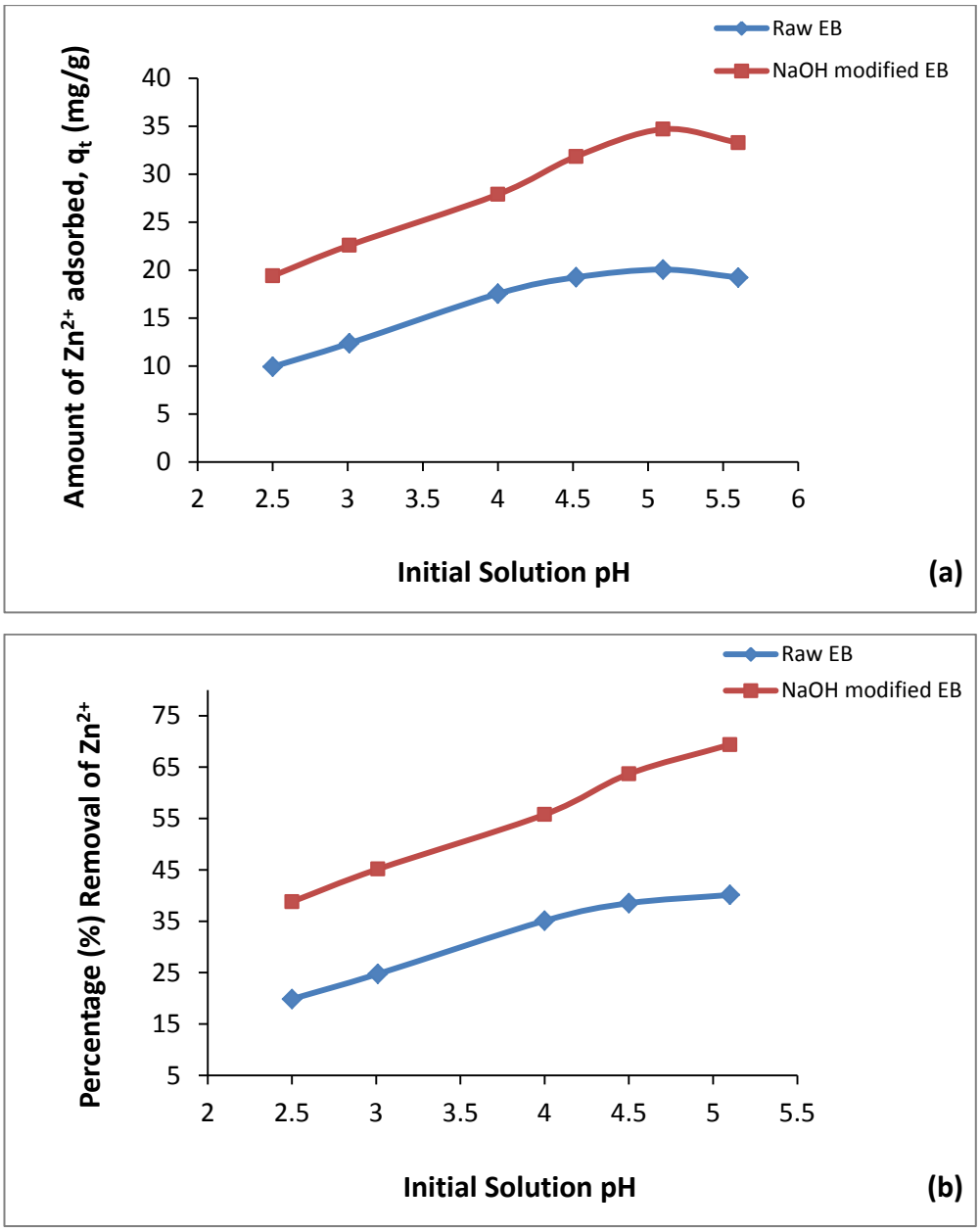

Figure 6.1 Effect of initial solution pH by raw and NaOH modified EB powder on (a) the amount of Zn^{2+}adsorption (b) percentage (%) removal of Zn^{2+}

(Conditions: Mass of Adsorbent = 20 mg, volume of Zn^{2+} solution = 50 mL, Initial Zn^{2+} solution concentration = 20 ppm, temp = 30°C, shaker speed = 120 rpm and time of adsorption = 100 min)

Further, Fig. 6.1(b) shows higher percentage of Zn^{2+} removal occurred at higher pH due to presence of less H^+ competing for sorption sites on the modified biomass. Hence, at pH 5.1, 69.38% of Zn^{2+} was removed using modified bark where 40.12% removal efficiency was achieved for raw adsorbent. From BET analysis in Section 3.3, it was also observed that the results of total pore volume for the modified samples are higher than the raw sample. Therefore, the internal surface area of the

modified samples is larger than that of the raw ones which leads to increased adsorption of Zn^{2+} for the modified biomass over the raw adsorbent material. Similar trend was reported for adsorption of Zn(II) ions by coconut tree sawdust (Putra, Kamari et al. 2014), neem bark (Bhattacharya, Mandal et al. 2006) and by carrot residues (Nasernejad, Zadeh et al. 2005).

6.3.2 Effect of Initial Metal Concentration and Contact Time on Zn^{2+} Adsorption Kinetics

The adsorptive metal removal mechanism is of great significance for developing sorbent-based water technology and is particularly dependent on the initial heavy metal ions concentration. Therefore, the initial metal concentration has strong effect on its removal from aqueous solution. In order to establish equilibration time for maximum adsorption and to know the kinetics of adsorption process, the effects of initial metal concentration with time on the adsorption of Zn^{2+} ions were investigated onto raw and modified eucalyptus bark, and the results are presented in Figs. 6.2(a) and 6.2(b) respectively.

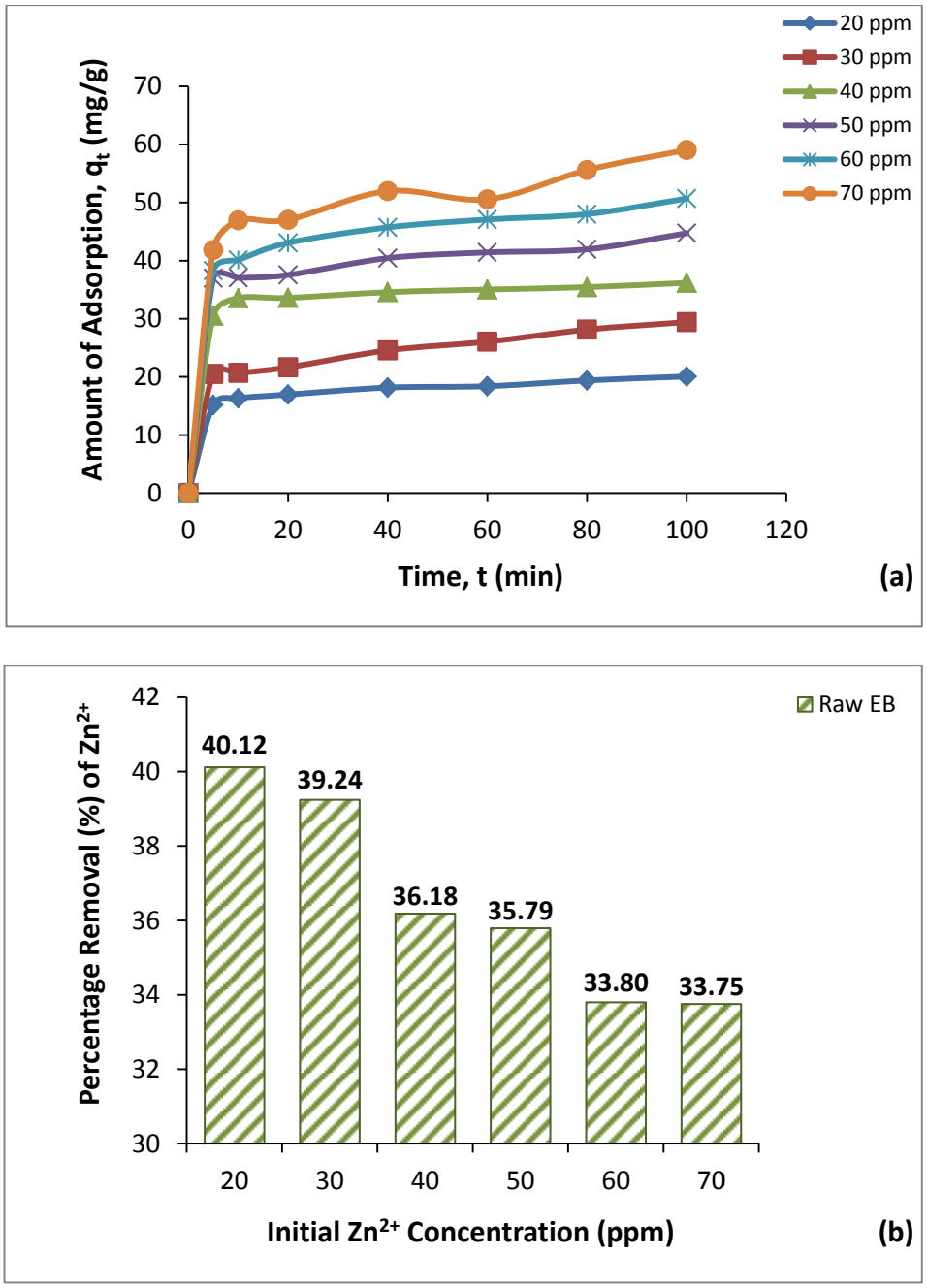

Figure 6.2 Effect of initial metal concentration by raw EB powder on (a) the amount of Zn^{2+} adsorption (b) percentage (%) removal of Zn^{2+}

(Conditions: Mass of adsorbent = 20 mg, volume of Zn^{2+} solution = 50 mL, solution pH = 5.1, temp = 30°C and shaker speed = 120 rpm)

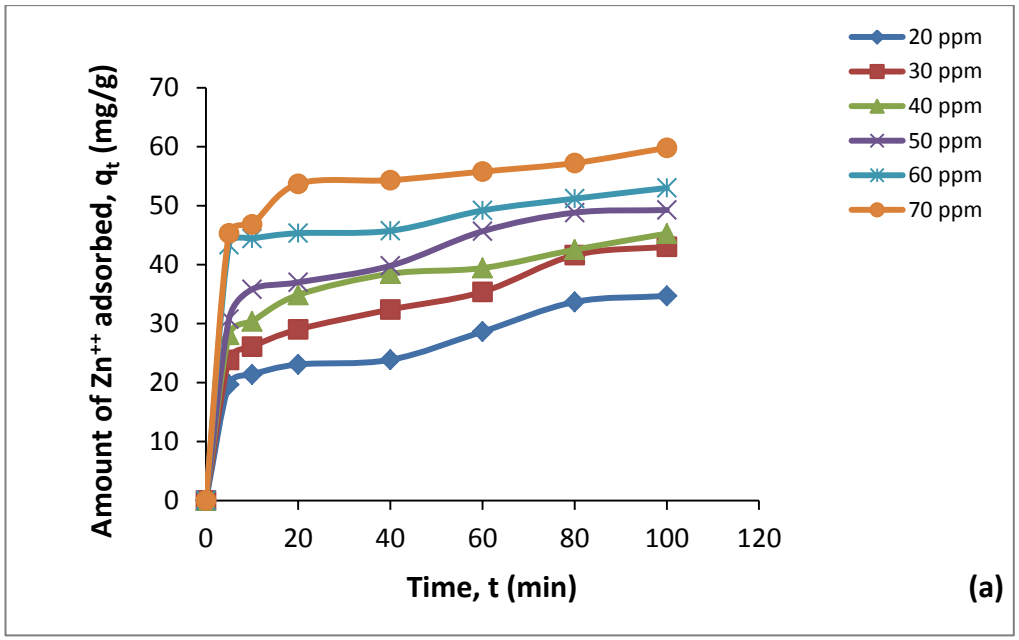

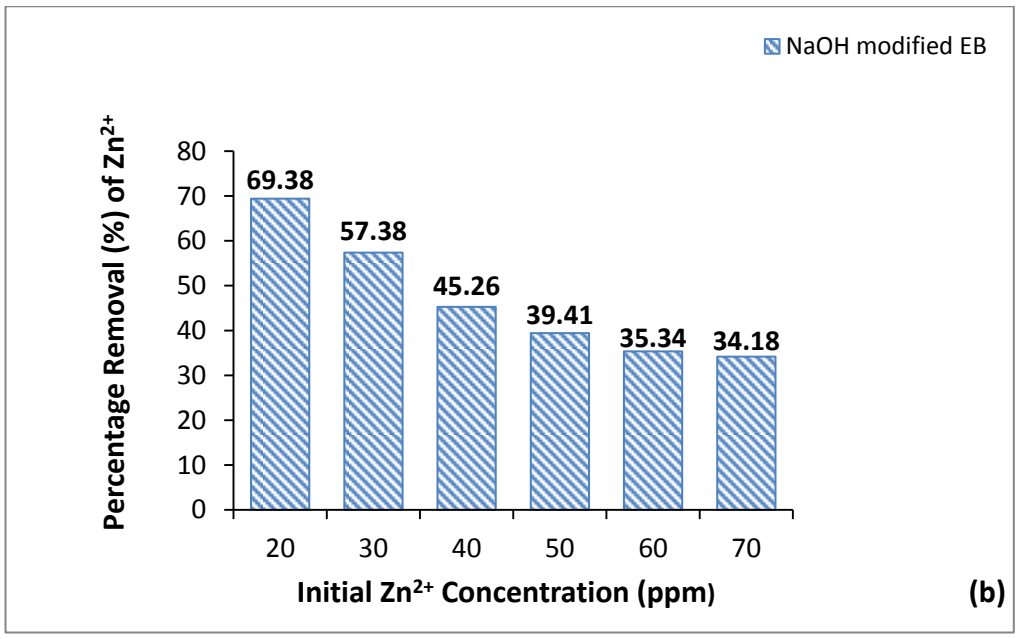

Figure 6.3 Effect of initial metal concentration by NaOH modified EB powder on (a) the amount of Zn^{2+}adsorption (b) percentage (%) removal of Zn^{2+}

(Conditions: Mass of adsorbent = 20 mg, volume of Zn^{2+} solution = 50 mL, solution pH = 5.1, temp = 30°C and shaker speed = 120 rpm)

From Figs. 6.2(a-b) and 6.3(a-b), it was found that metal sorption occurred rapidly and an increase in initial Zn^{2+} concentration leads to an increase in the sorption capacity of Zn^{2+} by both raw and modified eucalyptus barks. The equilibrium uptake increased with higher initial metal ions concentration at the range of experimental initial metal concentrations and equilibrium is attained within 100 min. From Fig.

6.3(a), the amount of Zn^{2+} adsorption, q_t (mg/g) onto modified eucalyptus bark, was observed to increase from 34.69 mg/g to 59.82 mg/g with an increase in initial Zn^{2+} concentration from 20 ppm (mg/L) to 70 ppm (mg/L) which is higher than the amount of Zn^{2+} adsorbed q_t (mg/g) by untreated raw bark adsorbent (20.06 mg/g to 59.06 mg/g). Further, it was witnessed from Fig. 6.2(b) that the percentage removal of Zn^{2+} increased from 33.75% to 40.12% for raw biomass and 34.18% to 69.38% for modified biomass [Fig. 6.3(b)] with decreasing initial concentration of Zn^{2+} from 70 to 20 ppm (mg/L). In general, it can be concluded that the amount of adsorption increases and removal percentage (%) decreases with increasing initial metal ion concentration [Figs. 6.2(a-b) and 6.3(a-b)] for both the systems.

As discussed by Wang et al. (Wang, Chen et al. 2015), high initial metal concentration accelerates the driving force and reduces the mass transfer resistance and hence increase adsorption. It was also found from Fig. 6.3(b) that the percentage (%) removal of Zn^{2+} ions by modified EB is very fast at the initial period of contact but slowed down with time. This kinetic experiment clearly indicated that adsorption of Zn^{2+} metal ions on modified eucalyptus bark is more or less two-step process: a very rapid adsorption of Zn^{2+} metal ions to the external surface followed by possible slow intraparticle diffusion in the interior of the adsorbent. The rapid kinetics has significant practical importance, as it facilitates smaller reactor volumes, ensuring high efficiency and economy (Arias and Sen 2009, Sen, Afroze et al. 2011). These findings are in agreement with the observation of other researchers for the removal of Zn(II) by eggshell (Putra, Kamari et al. 2014) and adsorption of lead(II) onto raw and NaOH modified pine cone powder (Ofomaja and Naidoo 2010).

6.3.3 Effect of Adsorbent Dosage on Zn^{2+} Adsorption Kinetics

Adsorbent dosage is one of the important parameters in adsorption processes because it determines the capacity of an adsorbent for a given initial concentration of the adsorbate under a given set of operating conditions. Adsorbent loading is also significant for the design of an adsorber for the optimisation of the process. The adsorption of Zn^{2+} by raw and modified eucalyptus bark by NaOH were conducted with different adsorbent doses (0.01 - 0.03 g) in the solution while maintaining the initial metal ions concentration (20 mg/L), temperature (30^0C), stirring speed (120 rpm), contact time (100 min), and pH (5.1) constant. The effect of sorbent dosage on

the adsorption of Zn^{2+} at equilibrium is shown in Figs. 6.4(a-b). At equilibrium, Figs. 6.4(a-b) showed that increasing the dose of adsorbent from 0.01 to 0.03 g, decreased the amount of Zn^{2+} adsorbed per unit mass of adsorbent as well as decreased percentage (%) removal of Zn^{2+} for both raw and modified eucalyptus barks. This is a common phenomenon observed for many systems.

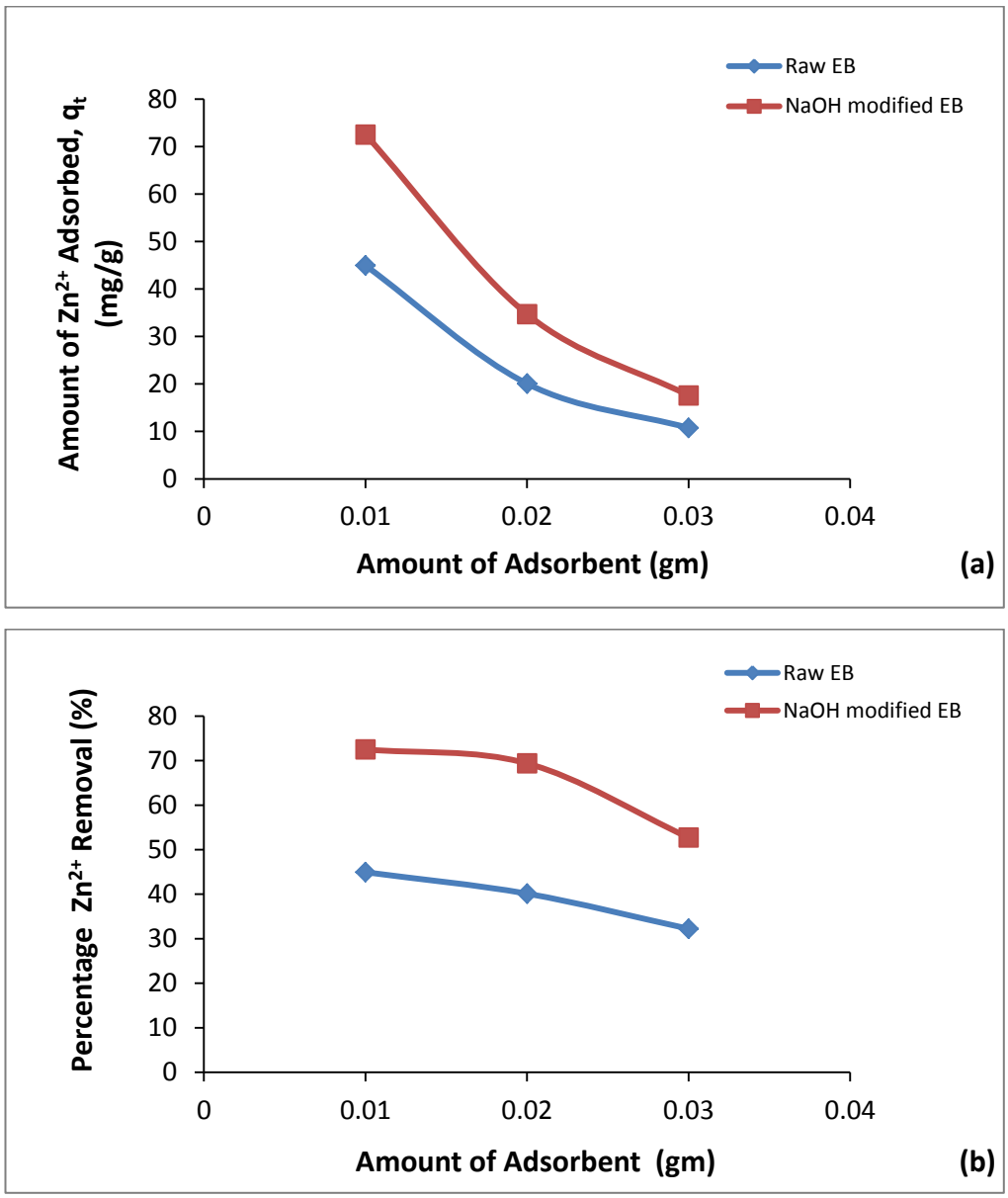

Figure 6.4 Effect of adsorbent dosages by raw and NaOH modified EB powder on (a) the amount of Zn^{2+}adsorption (b) percentage (%) removal of Zn^{2+}

(Conditions: Volume of Zn^{2+} Solution = 50 mL, Solution pH = 5.1, Initial Zn^{2+} Concentration = 20 ppm, Temp = 30°C, Shaker Speed = 120 rpm and Time of Adsorption = 100 min)

The number of adsorption sites per unit mass of an adsorbent should remain constant, independent of the total adsorbent mass; increasing the adsorbent amount in a fixed volume reduces the number of available sites as the effective surface area is likely to be decreased (Sen and Gomez 2011). Therefore the higher the adsorbent dosage, the larger the volume of effluent that a fixed mass of eucalyptus bark biomass can purify. The decrease in amount of Zn^{2+} adsorbed, q_e (mg/g) with increasing adsorbent mass, is due to the split in the flux or the concentration gradient between solute concentration in the solution and the solute concentration in the surface of the adsorbent (Afroze, Sen et al. 2015). Thus, with increasing adsorbent mass, the amount of Zn^{2+} adsorbed onto unit weight of adsorbent gets reduced and hence causing a decrease in q_e value with increasing adsorbent mass concentration. Various researchers also explained this phenomenon by particle-particle interactions. For the system with higher solid content, these interactions may physically block some adsorption sites from the adsorbing solutes and thus, causing decreased adsorption, or the electrical surface charges on the closely packed particles reduce attractions between the adsorbing solutes and surfaces of individual adsorbent particles by creating electrostatic interferences (Sen and Gomez 2011). A similar behaviour was also reported for Zn (II) removal on natural bentonite (Sen and Gomez 2011) and by horseradish tree biomass (Bhatti, Mumtaz et al. 2007). Another observation from the pattern in the results of Fig. 6.4(a) is that even though the trend of adsorbed amount of Zn^{2+} was decreased with increasing adsorbent concentration for both the systems whereas Zn^{2+} adsorption capacity was lower for raw EB compared to NaOH treated bark material. The interpretation is also due to higher available surface sites for modified EB compared to unmodified ones. Similar observation was also observed for the removal of Cu(II) by raw and base modified pine cone (Ofomaja, Naidoo et al. 2009).

6.3.4 Effect of Temperature on Zn^{2+} Adsorption Kinetics and Thermodynamic Studies

To observe the effect of temperature on the adsorption capacity, experiments were carried out at three different temperatures of 30, 45 and 60°C for a fixed initial Zn^{2+} metal ions concentration of 20 ppm (mg/L). Fig. 6.6 illustrates the influence of temperature on the adsorption of Zn^{2+} onto raw and NaOH modified eucalyptus bark

(EB) where the results showed that the equilibrium amount of adsorption, q_e (mg/g) for base modified adsorbent is higher compared to untreated raw adsorbent. With an increase in temperature from 30°C to 60°C; equilibrium adsorption capacity (q_e) was decreased from 20.06 mg/g to 17.47 mg/g for raw eucalyptus bark. Consequently, the amount of adsorption was found to be reduced from 34.69 mg/g (at 30°C) to 20.84 mg/g (at 60°C) for the modified biomass material (Fig. 6.5).

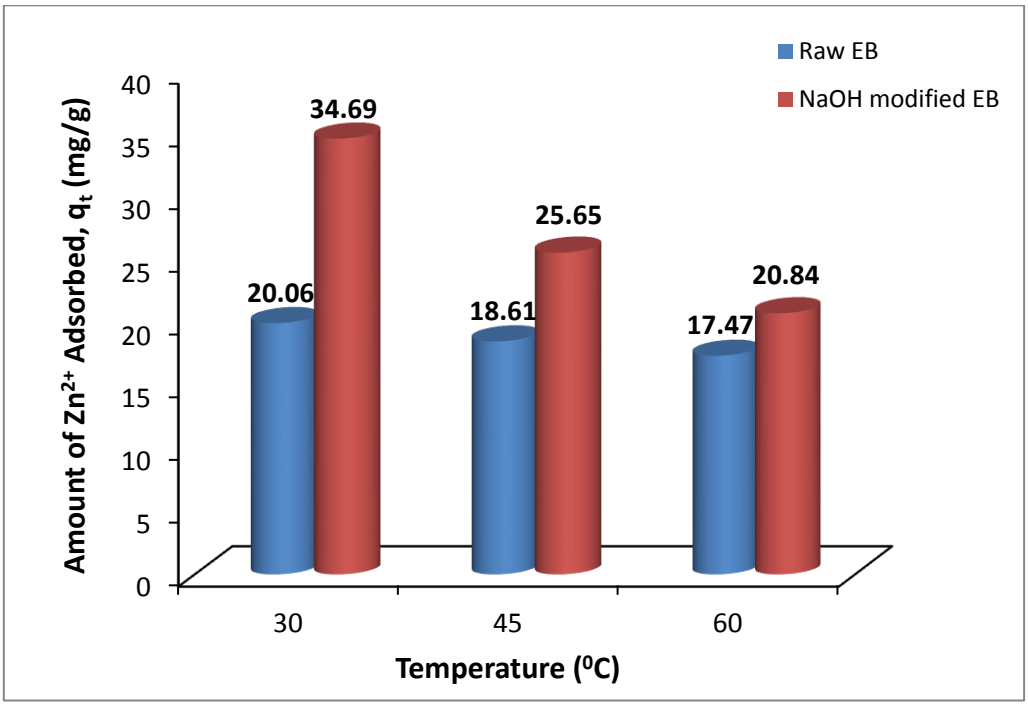

Figure 6.5 Effect of temperature on Zn^{2+} adsorption onto raw and NaOH modified EB powder

(Conditions: Mass of Adsorbent = 20 mg, Volume of Zn^{2+} Solution = 50 mL, Solution pH = 5.1, Initial Zn^{2+} Concentration = 20 ppm and Shaker Speed = 120 rpm)

The adsorption of Zn^{2+} metal ions was not in favor of temperature indicates that the attractive forces and mobility of the adsorbate Zn^{2+} metal ions towards eucalyptus bark adsorbent decreased with increase in temperature which resulted in decreased sorption. This reduction in adsorption capacity with increasing temperature suggests that the process of Zn^{2+} removal by both raw and modified eucalyptus bark biomass is exothermic in nature. It is also indicating that the adsorption process is sustainable and energy efficient as it is favorable at room temperature. Similar types of results

were also obtained by earlier investigators for different adsorbent systems (Gupta and Bhattacharyya 2006, Sen and Gomez 2011).

Thermodynamic parameters allow to estimate if the process is favourable or not from thermodynamic point of view. Hence, to understand the changes in the reaction during the process, the thermodynamic parameters: change in Gibbs free energy (ΔG^o), change in enthalpy ΔH^o) and change in entropy (ΔS^o) have been calculated using Eq. (2.11) and Eq. (2.12) illustrated in Section 2.8 from the linear form of the Van't Hoff plot [log (q_e/C_e) vs. 1/T] in Fig. 6.6. Further, the corresponding values of thermodynamic parameters for raw and NaOH modified eucalyptus bark are presented in Table 6.1.

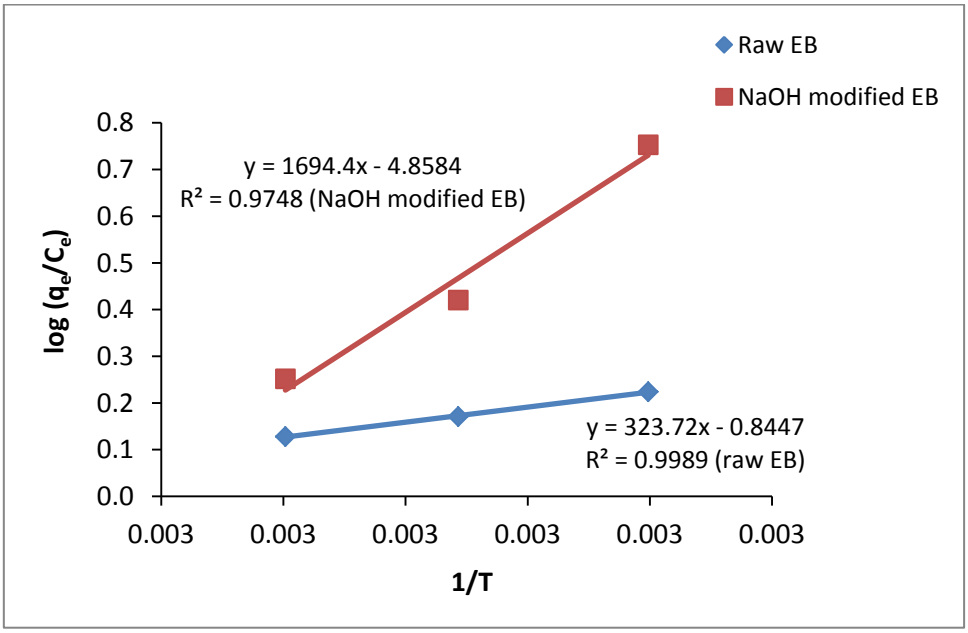

Figure 6.6 Van't Hoff plot for adsorption of Zn^{2+} onto raw and NaOH modified EB

From Table 6.1, the change in Gibbs free energy (ΔG^o) and enthalpy (ΔH^o) were found to be negative at all temperatures suggesting exothermic and spontaneous nature of the process. The negative value of entropy (ΔS^o) indicates decreased randomness during adsorption. Similar results for thermodynamic parameters were also reported by earlier researchers for the adsorption of Zn^{2+} from aqueous solution on various adsorbents (Bhattacharya, Mandal et al. 2006, Arias and Sen 2009, Sen and Gomez 2011). The change in enthalpy (ΔH^o) obtained for modified adsorbent is higher compared to the raw biomass and the value of ΔG^o was found to increase with

NaOH treatment indicating that the adsorption of Zn^{2+} is more favourable and spontaneous with NaOH treatment.

Table 6.1: Thermodynamic parameters for adsorption of Zn^{2+} at different temperatures onto raw and NaOH modified eucalyptus bark

Adsorbent	*Temp. (K)*	*ΔG˚(KJ/mole)*	*ΔH˚(KJ/mole)*	*ΔS˚(KJ/mole.K)*
Raw eucalyptus bark	303.15	-4.05	-32.43	-0.093
	318.15	-2.85		
	333.15	-1.45		
NaOH modified eucalyptus bark	303.15	-1.29	-6.53	-0.016
	318.15	-1.05		
	333.15	-0.81		

6.3.5 Effect of Presence of Salts on Zn^{2+} Adsorption Kinetics

Industrial wastes and natural water often contain dissolved salts in a wide range of concentrations depending on the source and the quality of water. Presence of electrolytes in solution strongly influences interfacial potential, compete with heavy metal ions for binding sites on the sorbent which affect the sorption of metal ions and thus influences adsorption process also. Hence, there is a need to ascertain the influence of this factor on eucalyptus bark material. The effect of salt concentration (ionic strength) on the amount of Zn^{2+} sorbed by eucalyptus bark (raw and modified) was analysed over a series of experiments by adding NaCl, $CaCl_2$ and $FeCl_3$ salts of initial concentrations ranging from 100 – 300 mg/L (ppm) to the Zn^{2+} solution. The obtained results for raw and NaOH modified bark biomass are reported in Figs. 6.7 and 6.8 respectively. The results presented in Fig. 6.7 and Fig. 6.8 indicate that due to the presence of mono (Na^{+}), di (Ca^{2+}) and trivalent (Fe^{3+}) salt ions in metal Zn^{2+} solution, the removal efficiency of Zn^{2+} by eucalyptus bark biomass was reduced for both the systems and by increasing the salt concentrations the adsorption capacity of eucalyptus bark further decreased more significantly.

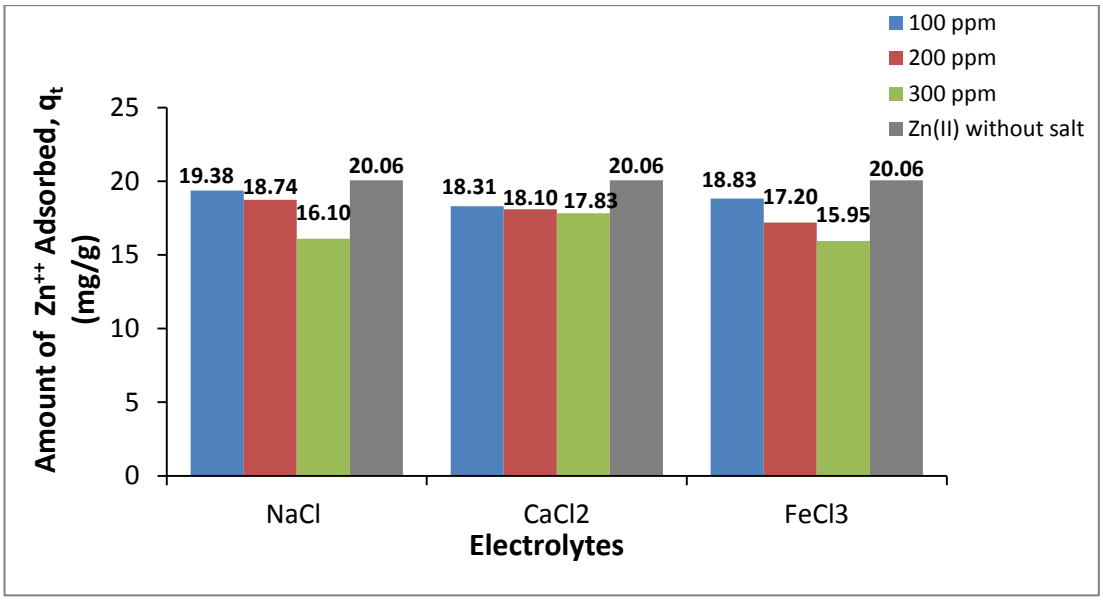

Figure 6.7 Effect of presence of salts on the amount of Zn^{2+} adsorption onto raw EB powder

(Conditions: Mass of Adsorbent = 20 mg, Total Reaction Volume = 50 mL (48 mL of Zn^{2+} Solution + 2 mL salt solution), Initial Zn^{2+} Concentration = 20 ppm, Solution pH = 5.1, Temp = 30°C, Shaker Speed = 120 rpm and Time of Adsorption = 100 min)

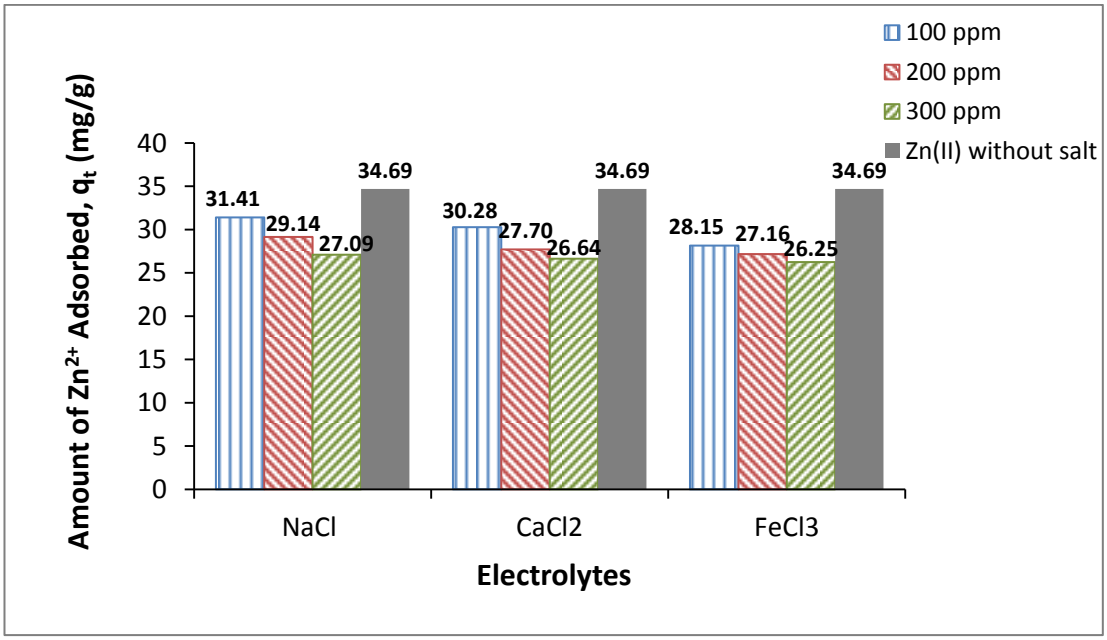

Figure 6.8 Effect of presence of salts on the amount of Zn^{2+} adsorption onto NaOH modified EB powder

(Conditions: Mass of Adsorbent = 20 mg, Total Reaction Volume = 50 mL (48 mL of Zn^{2+} Solution + 2 mL salt solution), Initial Zn^{2+} Concentration = 20 ppm, Solution pH = 5.1, Temp = 30°C, Shaker Speed = 120 rpm and Time of Adsorption = 100 min)

The trends of Figs. 6.7 and 6.8 indicate that adsorbed amount of Zn^{2+} by raw and modified eucalyptus bark decreased due to the presence of ionic strength which could be attributed to the competitive effect between Zn^{2+} ions and cations from the salt ($Na^{+}/Ca^{2+}/Fe^{3+}$) for available adsorption sites and it was more significantly decreased with increasing salt concentration. However, in every test series we experienced that the higher the Na^{+} ionic concentration, the smaller the percentage amount that adsorbed onto the adsorbent. This may be due to the increase in salt concentration (Na^{+}) that changes the equilibrium constant between the interface and the bulk of the liquid with increasing sorption. Similar trend was also observed for divalent ($CaCl_{2)}$ and trivalent ($FeCl_3$) salts but comparatively to a lesser extent.

The molecular weight, size, atomic radii and charge density may also play a major role of the adsorption efficiency (Arivoli, Hema et al. 2010). From Figs. 6.7 and 6.8, it was also observed that removal efficiency of Zn^{2+} adsorption significantly decreased with divalent/trivalent salt cations compared to monovalent cations. Hence, divalent calcium may apparently reduce more effectively than monovalent ions binding sites of eucalyptus bark for co-adsorbing ions (Karppi, Åkerman et al. 2010). Again, transition metals (Fe) have a much greater affinity for the surface as compared to alkaline earth metals (Ca) (Trivedi, Axe et al. 2001). Therefore, due to relatively small atomic radius of transition metal element (Fe) and having more electrons that can participate in the chemical bonding (Sahin and Peeters 2013), stronger binding of Fe^{3+} to the eucalyptus bark is expected which further reduces adsorption efficiency of Zn^{2+}. From Figs. 6.7 and 6.8, the adsorbed amounts suggest that adsorption affinity of studied cations onto raw and modified EB biomass followed the order $Na^{+} < Ca^{2+} < Fe^{3+}$. The decrease in adsorption amount of Zn^{2+} by studied adsorbents with increasing ionic strength is primarily attributed to the reduction in difference in the ionic osmotic pressure between the sorbent and the external solution (Adeyinka, Liang et al. 2007, Ansari and Pornahad 2010). The difference in osmotic pressure between the sorbent and the external solution decreases as the ionic strength of external solution increases. Therefore, the sorption of metal ion decreases when the ionic strength of external solution increases. Similar results were also reported by Osemeahon et al. 2013 on the removal of Zinc ions by *Immobilized Bombax costatum calyx* (Osemeahon, Barminas et al. 2013) and by Ghodbane et al. 2008 on the adsorption of Cadmium ions by eucalyptus bark

(Ghodbane, Nouri et al. 2008). However, despite decrease of adsorption efficiency with the presence of salts, sorbent potential is still relatively high and it may still effectively remove Zn^{2+} metal ions from heavy metal bearing solutions.

6.4 Desorption Studies

Desorption behaviour helps to explain the mechanism and recovery of the adsorbate and adsorbent. The study of desorption is also important for the determination of the amount of metal ions that may possibly be washed out when it is exposed to the natural erosion agent such as water. The desorption percentages of Zn^{2+} loaded on raw and modified eucalyptus bark at different concentrations are presented in Table 6.2. Desorption studies on Zn^{2+} loaded raw and base modified eucalyptus bark adsorbents indicated that Zn^{2+} was poorly desorbed from the biomass. Percentage desorption was less than 15% for the concentration range studied for raw eucalyptus bark system and lesser amounts of Zn^{2+} were desorbed from adsorbent biomass with higher Zn^{2+} concentration. About 14% and 7% of the bound Zn^{2+} was recovered from raw and NaOH treated bark biomass respectively. This suggests that strong binding affinity exists between the biomass and Zn^{2+} implying possible presence of strong complexes and ligands between adsorbent and Zn^{2+}. Further eucalyptus bark is an abundant solid agricultural waste with no value and hence regeneration of adsorbent is insignificant. Therefore the exhausted eucalyptus bark could be dried and used as a fuel in boilers/incinerators.

Table 6.2: Percentage desorption of Zn^{2+} from raw and NaOH modified eucalyptus bark

Initial Zn^{2+} Concentration (mg/L)	***Desorption (%)***	
	Raw eucalyptus bark	***NaOH modified eucalyptus bark***
20	13.89	6.91
30	6.98	3.22
40	4.90	1.15
50	3.54	0.56
60	2.85	0.23
70	1.43	0.14

6.5 Application of Adsorption Kinetic Models

The prediction of batch adsorption kinetics is compulsory for the design of industrial adsorption columns. The nature of the adsorption process will depend on the system conditions and also on chemical and physical characteristics of the adsorbent. In this present study, the applicability of pseudo-first-order, pseudo-second-order and intraparticle diffusion models were tested for the adsorption of inorganic Zn^{2+} metal ions onto raw and NaOH modified eucalyptus bark. The theories of all these models are presented in Section 2.6. These models have been evaluated and analysed by fitting experimental data at different physicochemical process conditions.

There are several error analysis methods used to predict the best fit of models. In this work, the best fitted model was selected not only based on linear regression correlation coefficient R^2 values but also by error estimation technique. R^2 value closest to unity is assumed to provide the best fit meanwhile for the error function, the minor value of the error indicates the better fitted model. The error estimation employed is Chi-square analysis which is given below:

$$\chi^2 = \sum \frac{(q_e - q_{calc})^2}{q_{calc}} \tag{6.3}$$

where q_{calc} presents the calculated adsorption capacity (mg/g) and q_e is the equilibrium capacity (mg/g) from the experimental data.

6.5.1 Pseudo First Order Kinetic Model

Linear plots of log ($q_e - q_t$) vs. t for experimental data at various physico-chemical conditions are fitted to test the applicability for pseudo first order model using Eq. (2.1). Figs. 6.9 and 6.10 represent the plots for raw and modified eucalyptus bark respectively where q_e refers to the amount of Zn^{2+} adsorbed (mg/g) at equilibrium and q_t refers to the amount of Zn^{2+} adsorbed (mg/g) at time, t (min). From those plots, the calculated low values of pseudo-first-order rate constant (K_1) and linear regression co-efficient (R^2) are presented in Table 6.3 for both the systems. Also, for both raw and modified adsorbents; pseudo-first-order kinetic model predicted a significantly lower value of the calculated equilibrium adsorption capacity (q_e) than

the experimental value as shown in Table 6.3. The error function, Chi-square analysis (χ^2) was performed as per Eq. (6.3) which provided very high value as displayed in Table 6.3 also suggesting the inapplicability of pseudo first order model.

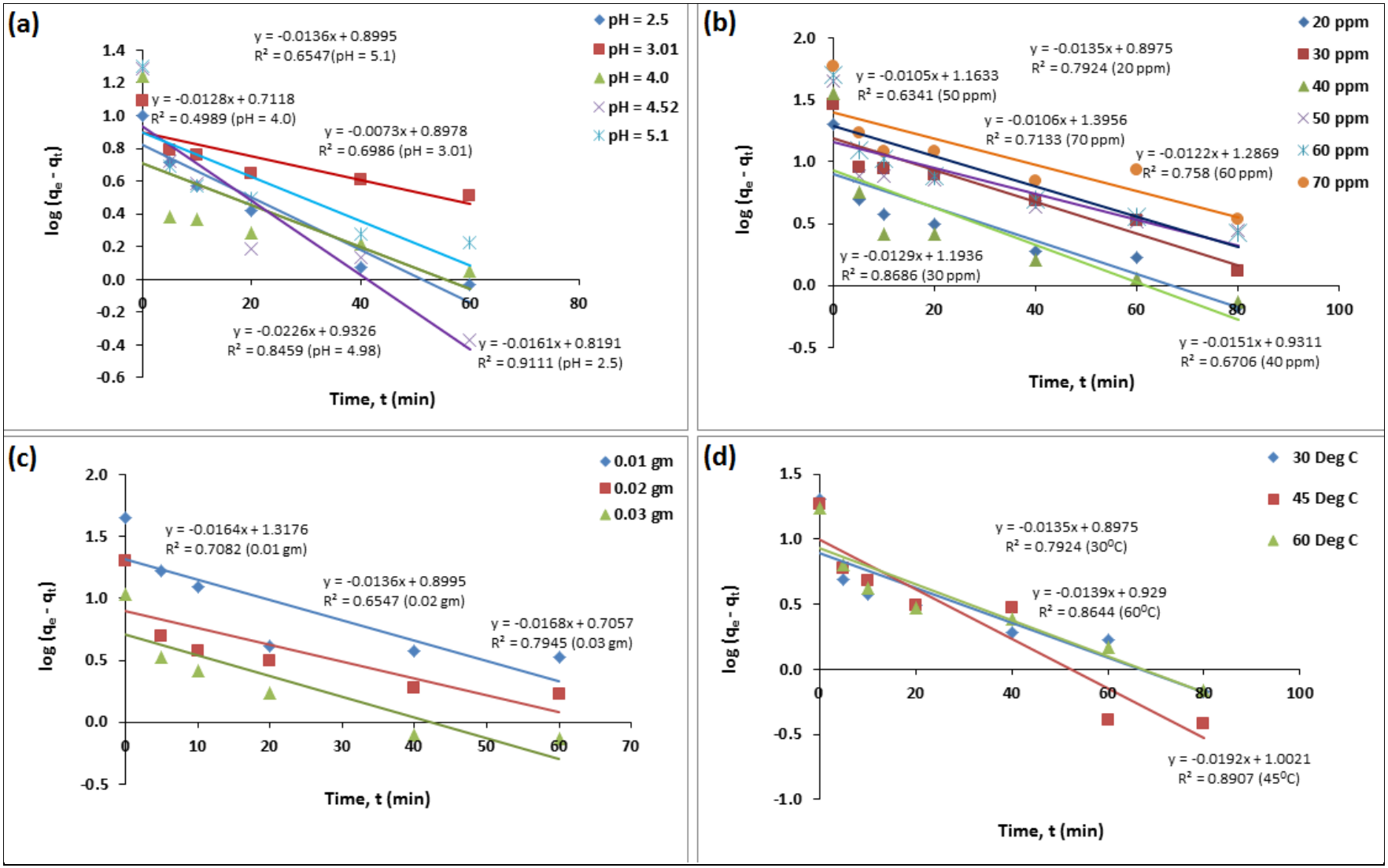

Figure 6.9 Pseudo-first-order kinetic model for the adsorption of Zn^{2+} onto raw eucalyptus bark at different (a) initial pH (b) initial concentrations (c) adsorbent dosages and (d) solution temperatures

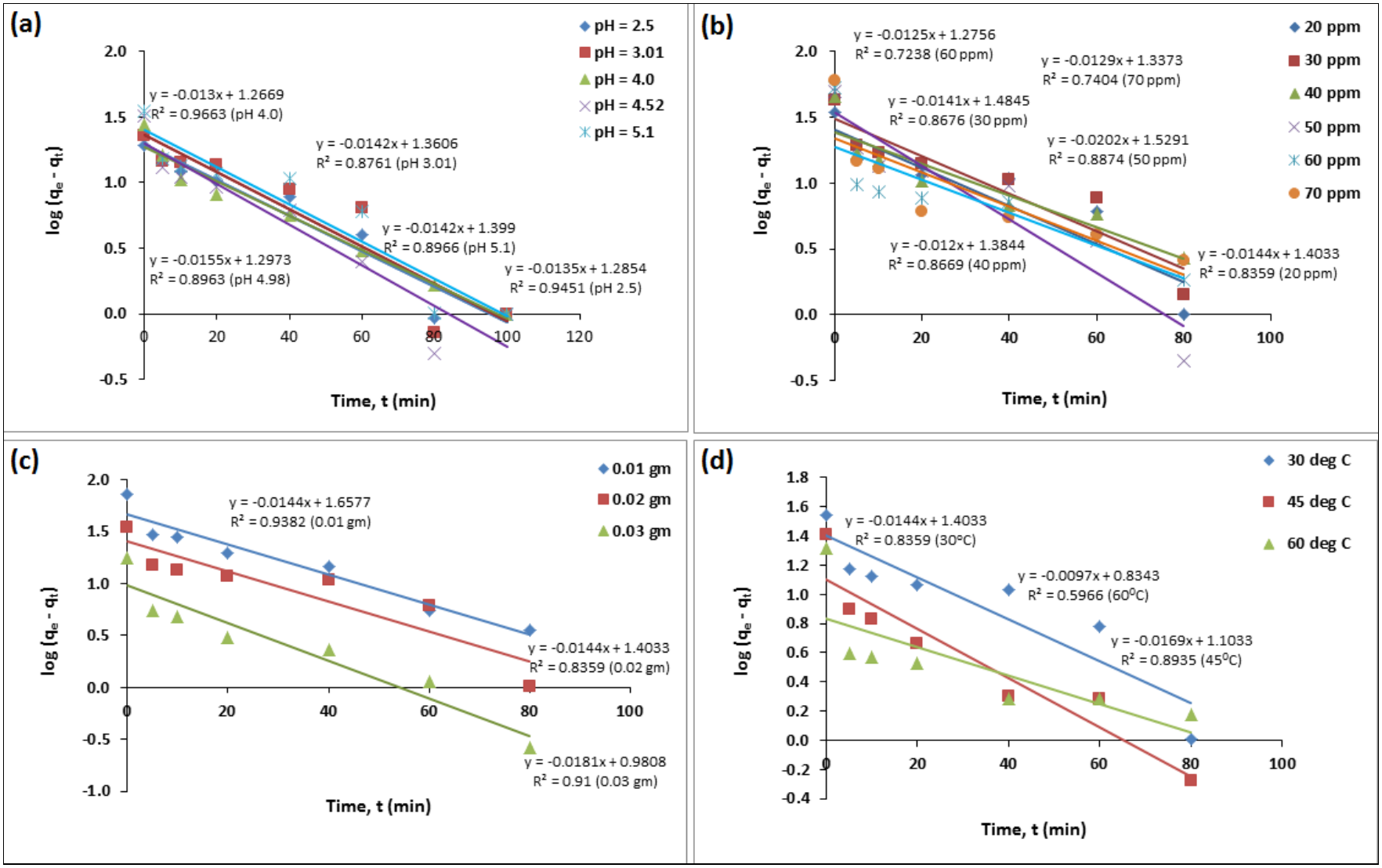

Figure 6.10 Pseudo-first-order kinetic model for the adsorption of Zn^{2+} onto NaOH modified eucalyptus bark at different (a) initial pH (b) initial concentrations (c) adsorbent dosages and (d) solution temperatures

Table 6.3: Pseudo-first-order kinetic model parameters for adsorption of Zn^{2+} on raw and NaOH modified eucalyptus bark

Pseudo-first-order kinetic model parameters					
System Parameters	***q_e (mg/g), Experimental***	***K_1 (min^{-1})***	***q_e (mg/g), Calculated***	***R^2***	***χ2***
Adsorbent Dosage (mg) for raw EB					
10	44.94	0.0378	3.73	0.7082	454.66
20	20.06	0.0313	2.46	0.6547	126.03
30	10.74	0.0387	2.03	0.7945	37.50
Adsorbent Dosage (mg) for modified EB					
10	72.52	0.0332	5.25	0.9382	862.48
20	34.69	0.0332	4.07	0.8359	230.46
30	17.57	0.0417	2.67	0.9100	83.29
Initial Zn^{2+} Concentration (ppm) for raw EB					
20	20.06	0.0311	2.45	0.7924	126.35
30	29.43	0.0297	3.30	0.8686	206.99
40	36.18	0.0348	2.54	0.6706	446.08
50	44.74	0.0242	3.20	0.6341	539.15
60	50.69	0.0281	3.62	0.7580	611.74
70	59.06	0.0244	4.04	0.7133	749.86
Initial Zn^{2+} Concentration (ppm) for modified EB					
20	34.69	0.0332	4.07	0.8359	230.46
30	43.04	0.0325	4.41	0.8676	338.12
40	45.26	0.0276	3.99	0.8669	426.56
50	49.26	0.0465	4.61	0.8874	432.00
60	53.01	0.0288	3.58	0.7238	682.31
70	59.82	0.0297	3.81	0.7404	823.70
pH for raw EB					
2.5	9.93	0.0371	2.27	0.9111	25.88
3.01	12.37	0.0168	2.45	0.6986	40.06
4.0	17.54	0.0295	2.04	0.4989	117.94
4.52	19.25	0.0520	2.54	0.8459	109.87
5.1	20.06	0.0313	2.46	0.6547	126.03
pH for modified EB					
2.5	19.40	0.0311	3.62	0.9451	68.89
3.01	22.58	0.0327	3.90	0.8761	89.52
4.0	27.89	0.0299	3.55	0.9663	166.89
4.52	31.84	0.0357	3.66	0.8963	217.02
5.1	34.69	0.0327	4.05	0.9451	231.72
Temperature (^oC) for raw EB					
30	20.06	0.0311	2.45	0.7924	126.35
45	18.61	0.0442	2.72	0.8907	92.65
60	17.47	0.0320	2.53	0.8644	88.13

Temperature (^oC) for modified EB					
30	34.69	0.0332	4.07	0.8359	230.46
45	25.65	0.0389	3.01	0.8935	170.00
60	20.84	0.0223	2.30	0.5966	149.19

6.5.2 Pseudo Second Order Kinetic Model

The adsorption experimental data were further analysed using the pseudo-second-order kinetic model. Eq. (2.2) is used to construct plots of t/q versus t to fit experimental data at various physico-chemical process conditions which plots are presented in Figs. 6.11 and 6.12 for raw and modified eucalyptus bark respectively. For both raw and modified eucalyptus bark system, all the pseudo-second-order kinetic model parameters including the values of q_e, K_2, h and R^2 are determined from the slope and intercept of plot t/q_t vs. t which are tabulated in Table 6.4. The R^2 values were found to be close to 1. The higher R^2 values confirm that the sorption process follows pseudo-second-order mechanism. It was further supported by low Chi-square error function which is presented in Table 6.4. Again, under different physico-chemical process conditions, the values of calculated equilibrium adsorption capacity ($q_{e,calc}$) were much closer to the experimental adsorption uptake at equilibrium ($q_{e,expt}$) values (Table 6.4) which indicated the applicability of pseudo-second-order kinetic model.

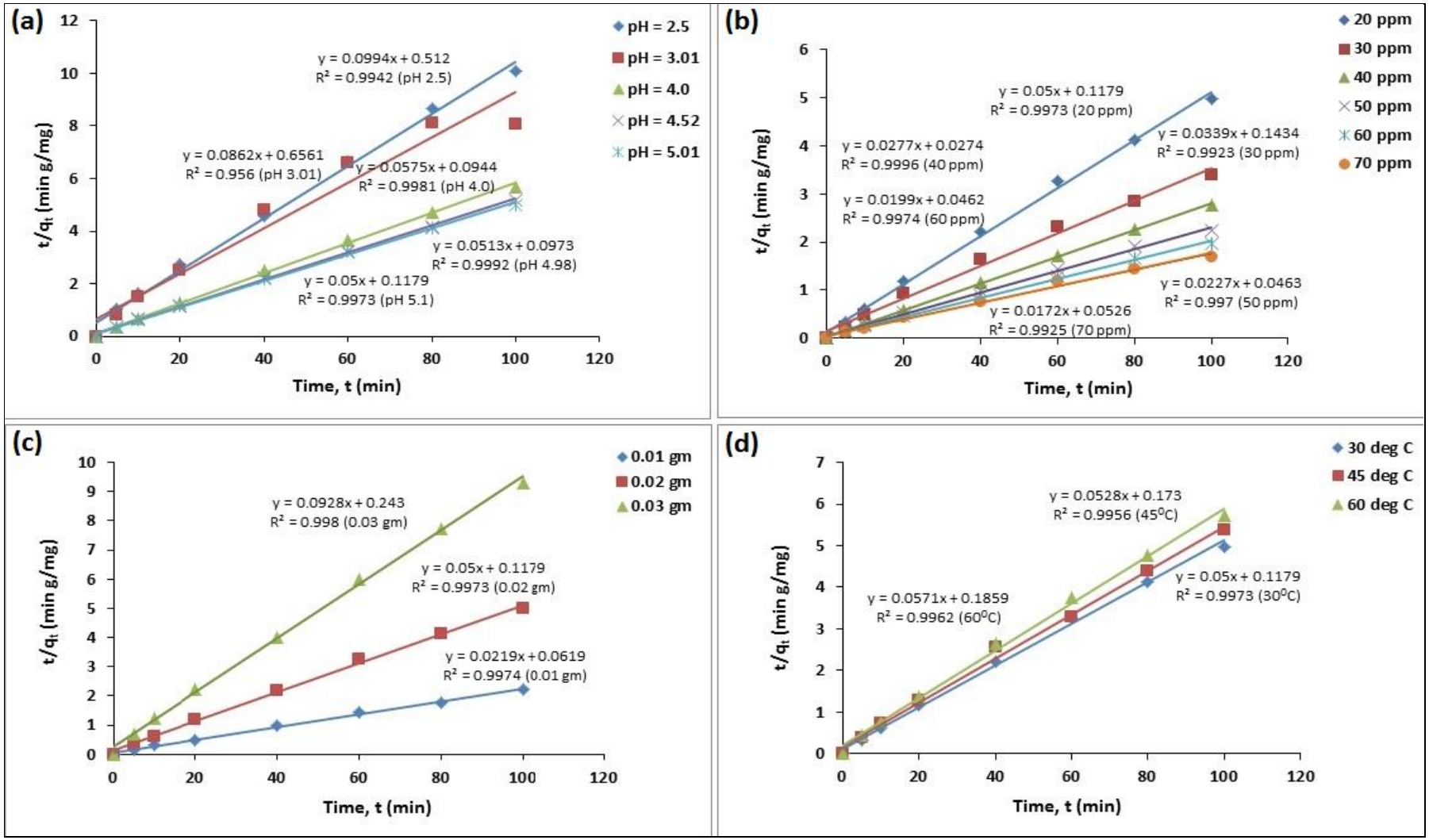

Figure 6.11 Pseudo-second-order kinetic model for the adsorption of Zn^{2+} onto raw eucalyptus bark at different (a) initial pH (b) initial concentrations (c) adsorbent dosages and (d) solution temperatures

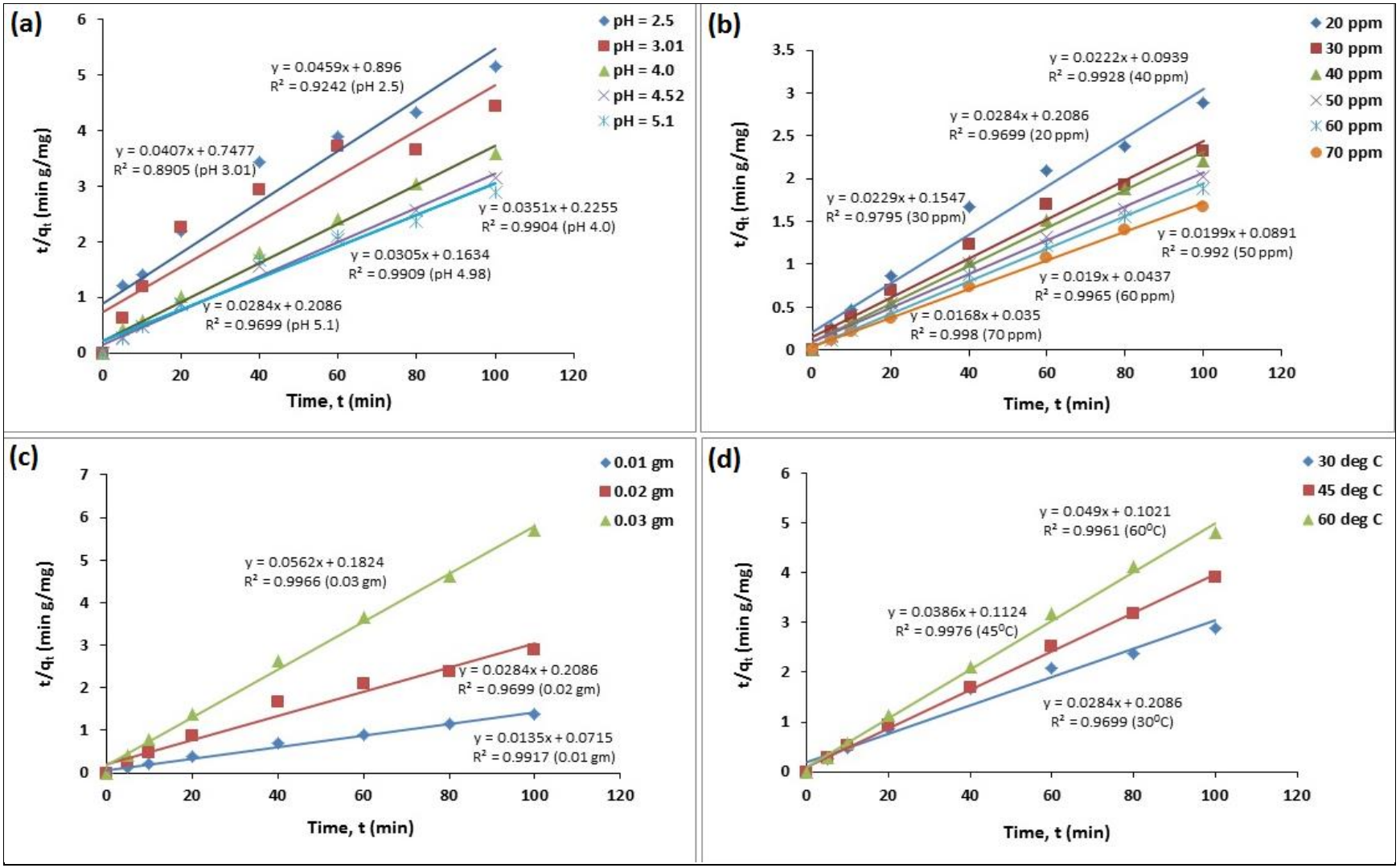

Figure 6.12 Pseudo-second-order kinetic model for the adsorption of Zn^{2+} onto NaOH modified eucalyptus bark at different (a) initial pH (b) initial concentrations (c) adsorbent dosages and (d) solution temperatures

Table 6.4: Pseudo second order model parameters for adsorption of Zn^{2+} on raw and NaOH modified eucalyptus bark (EB)

Pseudo-second-order kinetic model parameters						
System Parameters	***q_e (mg/g), Experimental***	***K_2 (mg/g-min)***	***q_e (mg/g), Calculated***	***h (mg/g-min)***	***R^2***	**χ2**
Adsorbent Dosage (mg) for raw EB						
10	44.94	0.0077	45.66	16.16	0.9974	0.0114
20	20.06	0.0212	20.00	8.48	0.9973	0.0002
30	10.74	0.0354	10.78	4.12	0.9980	0.0001
Adsorbent Dosage (mg) for modified EB						
10	72.52	0.0025	74.07	13.99	0.9917	0.0326
20	34.69	0.0039	35.21	4.79	0.9699	0.0077
30	17.57	0.0173	17.79	5.48	0.9966	0.0028
Initial Zn^{2+} Concentration (ppm) for raw EB						
20	20.06	0.0212	20.00	8.48	0.9973	0.0002
30	29.43	0.0080	29.50	6.97	0.9923	0.0002
40	36.18	0.0280	36.10	36.50	0.9996	0.0002
50	44.74	0.0111	44.05	21.60	0.9970	0.0107
60	50.69	0.0086	50.25	21.65	0.9974	0.0038
70	59.06	0.0056	58.14	19.01	0.9925	0.0146
Initial Zn^{2+} Concentration (ppm) for modified EB						
20	34.69	0.0039	35.21	4.79	0.9699	0.0077
30	43.04	0.0034	43.67	6.46	0.9795	0.0090
40	45.26	0.0052	45.05	10.65	0.9928	0.0010
50	49.26	0.0044	50.25	11.22	0.9920	0.0196
60	53.01	0.0083	52.63	22.88	0.9965	0.0027
70	59.82	0.0081	59.52	28.57	0.9980	0.0015
pH for raw EB						
2.5	9.93	0.0193	10.06	7.95	0.9942	0.0017
3.01	12.37	0.0113	11.60	9.66	0.9560	0.0510
4.0	17.54	0.0350	17.39	12.52	0.9981	0.0013
4.52	19.25	0.0270	19.49	11.39	0.9992	0.0030
5.1	20.06	0.0212	20.00	4.77	0.9973	0.0002
pH for modified EB						
2.5	19.40	0.0024	21.79	1.12	0.9242	0.2614
3.01	22.58	0.0022	24.57	1.34	0.8905	0.1612
4.0	27.89	0.0055	28.49	4.43	0.9904	0.0126
4.52	31.84	0.0057	32.79	6.12	0.9909	0.0273
5.1	34.69	0.0039	35.21	4.79	0.9699	0.0077
Temperature (^oC) for raw EB						
30	20.06	0.0212	20.00	8.48	0.9973	0.0002
45	18.61	0.0161	18.94	5.78	0.9956	0.0057
60	17.47	0.0175	17.51	5.38	0.9962	0.0001

Temperature (^oC) for modified EB						
30	34.69	0.0039	35.21	4.79	0.9699	0.0077
45	25.65	0.0133	25.91	8.90	0.9976	0.0025
60	20.84	0.0235	20.41	9.79	0.9961	0.0091

6.5.3 Intraparticle Diffusion Model and Mechanism of Adsorption

Understanding the adsorption mechanism that is originated from the dynamic behaviour of the system is significant for process design. The most commonly used technique for identifying the mechanism involved in the sorption process is by fitting the adsorption experimental data with intra-particle diffusion plot using Eq. (2.4). The intraparticle diffusion plot is the plot of amount sorbed per unit weight of sorbent, q_t (mg/g) versus square root of time, $\sqrt{t}$. Therefore, the experimental data were fitted into the intraparticle diffusion plot of q_t (the amount of Zn^{2+} sorbed per unit mass of sorbent, mg/g) against $t^{0.5}$ (the square root of contact time, $min^{0.5}$) for both raw and modified systems. The obtained plots of q_t vs. $t^{0.5}$ for Zn^{2+} adsorption on raw and modified eucalyptus bark at various physico-chemical process parameters are shown in Figs. 6.13 and 6.14 respectively. Both the Figs. 6.13 and 6.14 represent that the sorption process is not linear over the whole period of time and tends to be split into two to three regions which confirms the multi-stage nature of adsorption. These plots indicated that metal ions were transported to the external surface of the adsorbent particles through film diffusion and its rate was very fast. After that, Zn^{2+} ions were entered into biomass particles by intraparticle diffusion through pores. The initial linear portion of each plot is due to the boundary layer effect, while the second portion is controlled by intraparticle diffusion and the third one may be due to the chemical reaction (Ofomaja 2008).

Generally, when adsorption steps are not dependent of one another, the plot of q_t against $\sqrt{t}$ should give two or more intercepting lines depending on the actual mechanism (Sen and Gomez 2011). Moreover from Figs. 6.13 and 6.14, conclusions can be made that none of plots give linear straight line segment passing through the origin, $I \neq 0$ which is not shown here. This specifies that the intraparticle diffusion is involved in the adsorption process but not the only rate-controlling step. As the lines did not pass through the origin which indicating film diffusion and intraparticle diffusion occurred simultaneously.

The half-adsorption time of adsorbate, $t_{1/2}$, i.e. the time required for adsorbent to uptake half of the amount adsorbed at equilibrium, is often considered as a measure of the rate of adsorption. The values of the half-adsorption time of Zn^{2+} ions, $t_{1/2}$, for Zn^{2+} - raw eucalyptus bark and for Zn^{2+} - modified eucalyptus bark were individually estimated from Eq. (4.2). For raw bark biomass, the calculated values of $t_{1/2}$ for Zn^{2+} metal adsorption were found to be 2.35 min, 4.24 min, 0.99 min, 2.01 min, 2.30 min and 3.01 min for an initial concentration range of 20, 30, 40, 50, 60 and 70 ppm respectively. Also, $t_{1/2}$ were calculated as 7.46 min, 6.85 min, 4.21 min, 4.57 min, 2.28 min and 2.07 min for an initial concentration range of 20, 30, 40, 50, 60 and 70 ppm respectively for NaOH modified system.

The diffusion coefficient, D_p, largely depends on the surface properties of adsorbents. The diffusion coefficient for the intra-particle transport of different Zn^{2+} initial concentrations was also calculated using Eq. (4.3). For raw adsorbent, the calculated D_p values were found to be 3.39×10^{-10} cm^2/sec, 1.88×10^{-10} cm^2/sec, 8.08×10^{-10} cm^2/sec, 3.97×10^{-10} cm^2/sec, 3.47×10^{-10} cm^2/sec and 2.65×10^{-10} cm^2/sec for an initial Zn^{2+} concentration of 20, 30, 40, 50, 60 and 70 ppm respectively. Further, for modified biomass material, D_p values were calculated as 1.07×10^{-10} cm^2/sec, 1.16×10^{-10} cm^2/sec, 1.89×10^{-10} cm^2/sec, 1.75×10^{-10} cm^2/sec, 3.49×10^{-10} cm^2/sec and 3.85×10^{-10} cm^2/sec for an initial Zn^{2+} concentration of 20, 30, 40, 50, 60 and 70 ppm respectively.

For raw and NaOH modified eucalyptus bark system, the calculated amount of Zn^{2+} adsorbed, q_e, (mg/g), the intraparticle diffusion parameter, K_{id} (mg/(g $min^{0.5}$)) are obtained under various process conditions using Eq. (2.4) for which the results are tabulated in Table 6.5. The observed linear regression coefficient R^2 values in Table 6.5 are lower with respect to pseudo-second-order kinetic model which makes intraparticle diffusion model incompatible for this system.

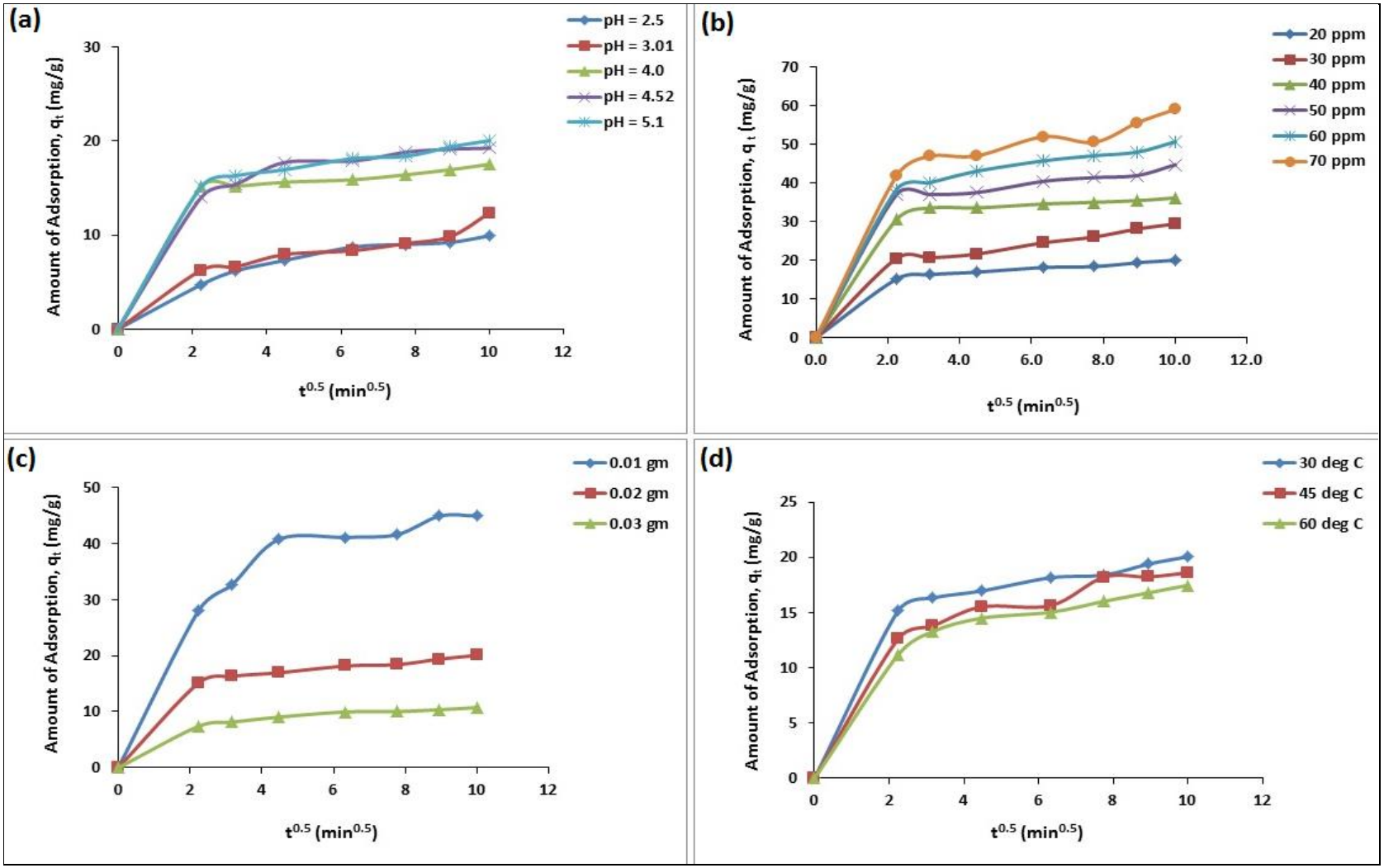

Figure 6.13 Intraparticle diffusion model for the adsorption of Zn^{2+} onto raw eucalyptus bark at different (a) initial pH (b) initial concentrations (c) adsorbent dosages and (d) solution temperatures

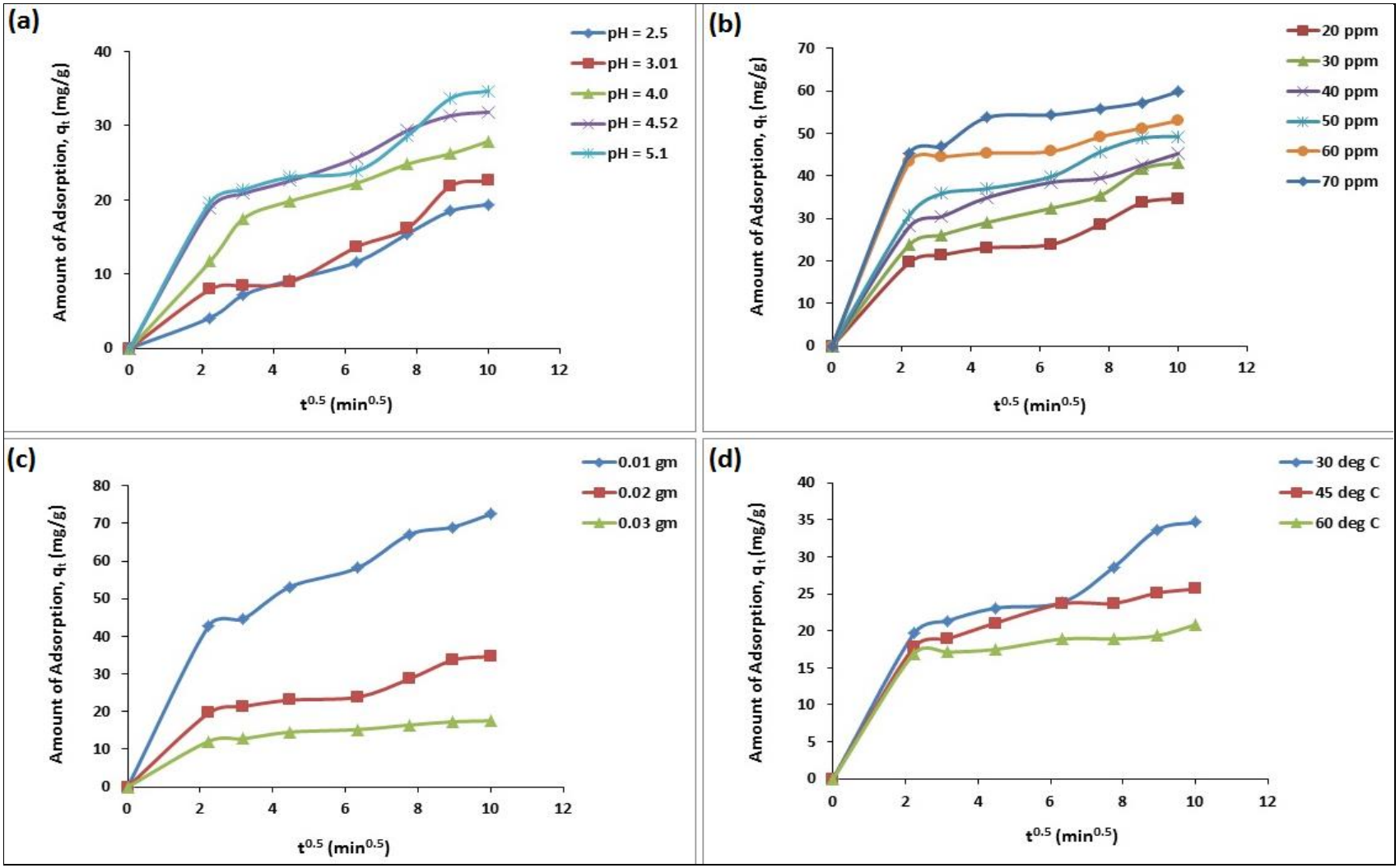

Figure 6.14 Intraparticle diffusion model for the adsorption of Zn^{2+} onto NaOH modified eucalyptus bark at different (a) initial pH (b) initial concentrations (c) adsorbent dosages and (d) solution temperatures

Table 6.5: Intraparticle diffusion model parameters for adsorption of Zn^{2+} on raw and NaOH modified eucalyptus bark (EB)

Intraparticle diffusion model parameters				
System Parameters	***q_e (mg/g), Experimental***	***q_e (mg/g), Calculated***	***K_{id} (mg/g.min$^{0.5}$)***	***R^2***
Adsorbent Dosage (mg) for raw EB				
10	44.94	51.30	3.6748	0.7245
20	20.06	22.40	1.4762	0.6299
30	10.74	12.10	0.8397	0.6971
Adsorbent Dosage (mg) for modified EB				
10	72.52	79.29	6.1183	0.8362
20	34.69	36.42	2.8672	0.8473
30	17.57	19.72	1.3912	0.7223
Initial Zn^{2+} Concentration (ppm) for raw EB				
20	20.06	22.40	1.4762	0.6299
30	29.43	31.97	2.2843	0.7393
40	36.18	41.46	2.5005	0.5118
50	44.74	49.48	3.1176	0.5690
60	50.69	56.43	3.7323	0.6348
70	59.06	64.20	4.3272	0.6567
Initial Zn^{2+} Concentration (ppm) for modified EB				
20	34.69	36.42	2.8672	0.8473
30	43.04	45.64	3.6047	0.8611
40	45.26	49.17	3.6185	0.7779
50	49.26	54.59	4.0307	0.7801
60	53.01	58.83	3.7292	0.5768
70	59.82	67.11	4.4157	0.6249
pH for raw EB				
2.5	9.93	10.93	0.8716	0.8576
3.01	12.37	11.99	0.9546	0.8503
4.0	17.54	19.66	1.1995	0.5277
4.52	19.25	22.19	1.4890	0.6481
5.1	20.06	22.40	1.4762	0.6299
pH for modified EB				
2.5	19.40	19.80	1.9673	0.9923
3.01	22.58	22.45	2.1577	0.9648
4.0	27.89	30.30	2.4845	0.8866
4.52	31.84	35.09	2.7011	0.8343
5.1	34.69	36.42	2.8672	0.8473
Temperature (^oC) for raw EB				
30	20.06	22.40	1.4762	0.6299
45	18.61	20.97	1.4879	0.7258
60	17.47	19.40	1.3742	0.7234

Temperature (^oC) for modified EB				
30	34.69	36.42	2.8672	0.8473
45	25.65	28.90	2.0260	0.7123
60	20.84	22.91	1.4484	0.5730

6.6 Adsorption Equilibrium Isotherm Models and Error Analysis

Adsorption isotherms describe how adsorbates interact with adsorbents and are important in optimizing the use of adsorbents. Therefore, the analysis of equilibrium adsorption data by fitting them to isotherm models is an important step to find out the suitable model to be used for design purposes (Dawood and Sen 2012). For this, the experimental data were fitted to the most popular and commonly used isotherm models of Langmuir and Freundlich which are described in Section 2.6 and isotherm parameters were calculated. Linear regression analysis was then used to determine the best fitted isotherm.

The Langmuir isotherm fittings for raw and NaOH modified eucalyptus bark are shown in Figs. 6.15(a) and 6.15(b) respectively. The maximum adsorption capacity, q_m (mg/g) and K_a values for Langmuir constants are obtained from the slope and intercept of Figs. 6.15(a) and 6.15(b) using Eq. (2.6) for Langmuir isotherm I and Eq. (2.7) for Langmuir isotherm II. The Langmuir isotherms fit the experimental data very well and Langmuir I showed higher adsorption capacity (mg/g) compared to Langmuir II model for both raw and modified bark adsorbents. The calculated values for Langmuir I show that the monolayer capacities for raw eucalyptus bark are 131.58 mg/g and 222.22 mg/g for modified eucalyptus bark (Table 6.6). These results indicate that monolayer capacity increases with NaOH pre-treatment. Moreover, the Langmuir II isotherm shows that the trends in the parameters, q_m and K_a are similar to those of the Langmuir I isotherm. The obtained results for Langmuir isotherms are found to be fitted well by both raw and modified eucalyptus barks for Zn^{2+} adsorption which make this study suitable to optimize the operating conditions for effective adsorption.

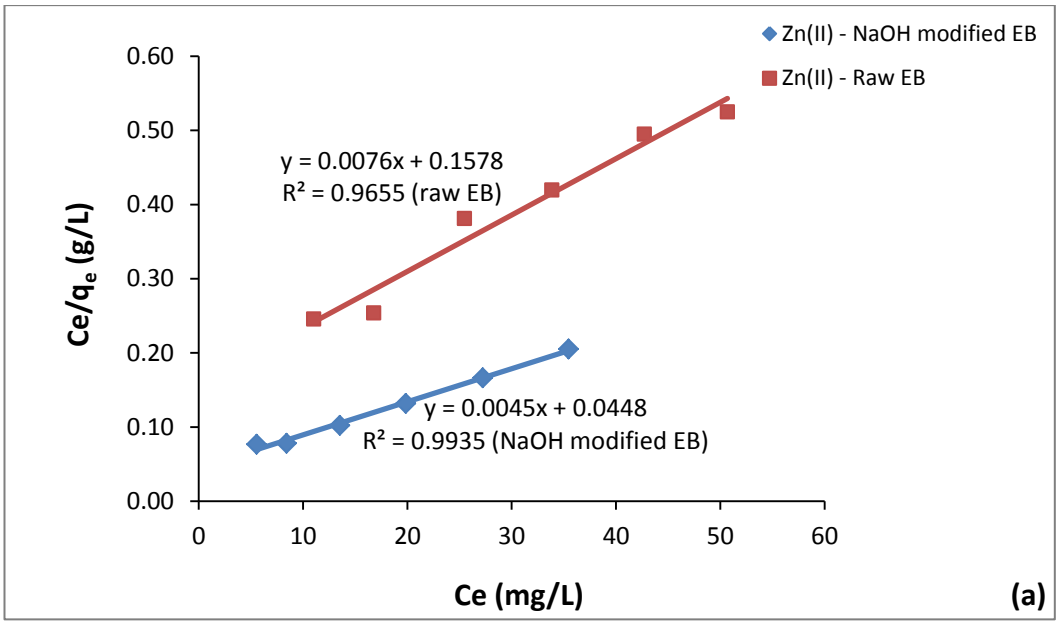

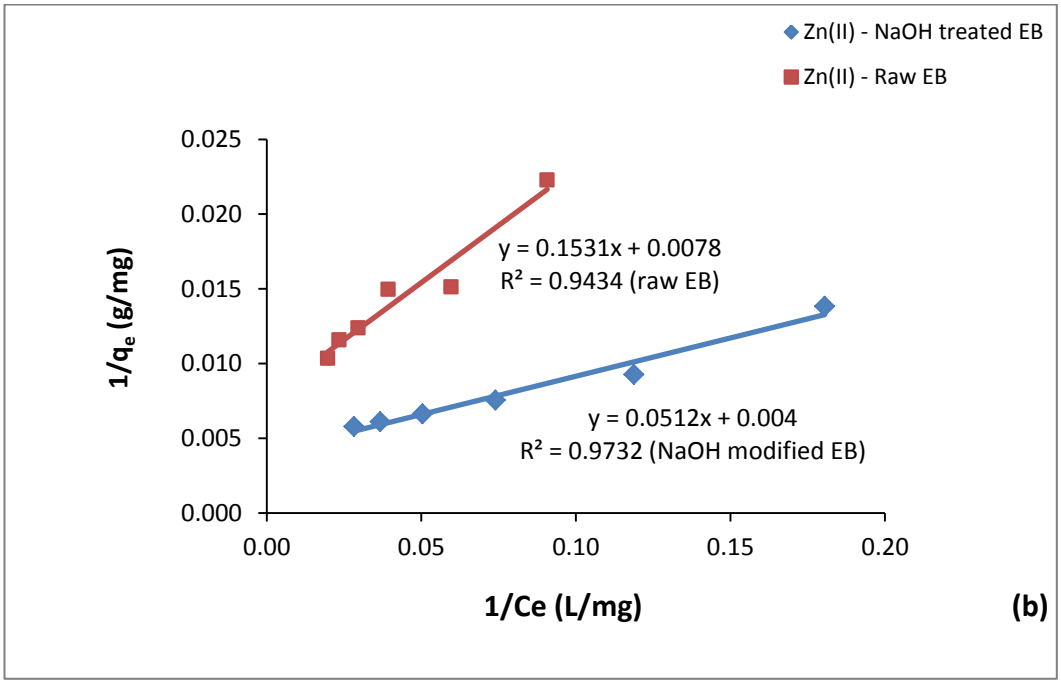

Figure 6.15 Equilibrium Adsorption Isotherm fitted to (a) Langmuir-I and (b) Langmuir-II Model

(Conditions: Amount of Adsorbent added = 10 mg; initial Zn^{+2} Concentration = 20, 30, 40, 50, 60, 70 ppm; Soluiton pH ≈ 5.1; Temperature = 30°C; Shaker Speed = 120 rpm and Time of Adsorption = 2 hr)

Fig. 6.16 shows Freundlich isotherm fittings of adsorption equilibrium experimental data for raw and NaOH modified eucalyptus bark system. Freundlich constants, i.e. adsorption capacity (K_f) and rate of adsorption (n) are calculated from the slope and

intercept of the plot lnq_e vs. lnC_e (Fig. 6.16) using Eq. (2.10). In Fig 6.16, the high value of linear correlation coefficient (R^2) of the Freundlich isotherm is 0.9331 for raw eucalyptus bark and 0.9273 for NaOH modified eucalyptus bark indicating the applicability of this model. The achieved values of K_f, n and R^2 are tabulated on Table 6.6. As shown in Table 6.6, the Freundlich isotherm constant, K_f was found to increase with NaOH pre-treatment. The low K_f value for raw EB compared to modified EB indicates that base pre-treatment improved adsorption capacity. Further, the obtained numerical values of n for the studied adsorbents are always greater than unity, indicating that Zn^{2+} are favourably adsorbed by raw and base modified eucalyptus barks (Demiral, Demiral et al. 2008).

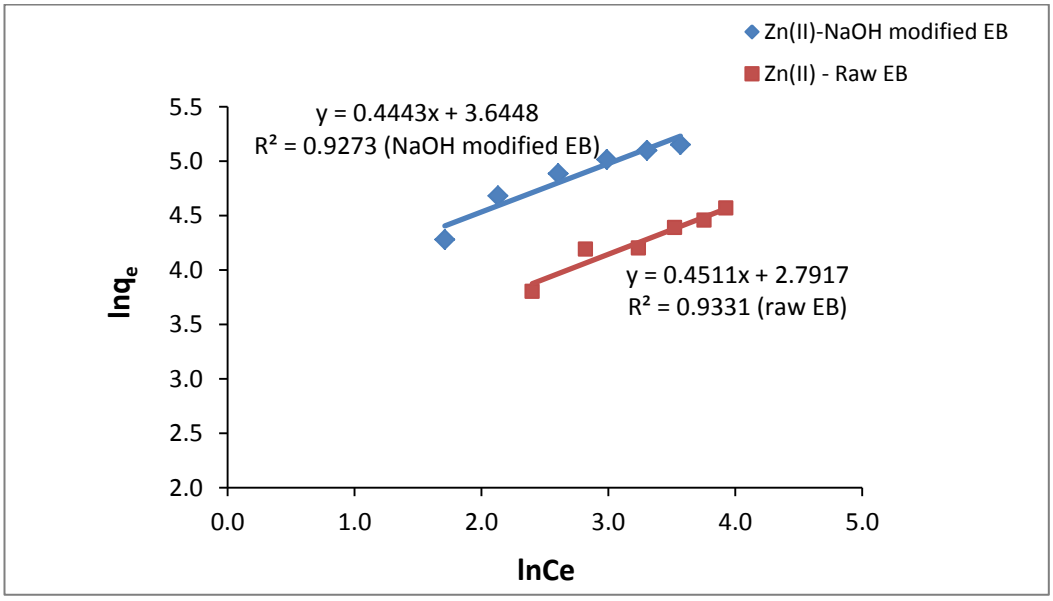

Figure 6.16 Freundlich plot for raw and NaOH treated EB: Amount of adsorbent 10 mg; Initial Zn^{2+} Concentration = 20, 30, 40, 50, 60 and 70 ppm, Soluiton pH ≈ 5.1, Temperature = 30°C; Shaker Speed = 120 rpm and Time of Adsorption = 2 hr

The correlation coefficient, R^2, for the equilibrium isotherm models applied in this study showed that the Langmuir I isotherm had the highest R^2 values followed by the Langmuir II and Freundlich isotherms. The Langmuir I isotherm is therefore the best fitting of the three models; indicating monolayer coverage of the adsorbate on the adsorbent and homogeneity of the actives sites on the adsorbent surface. The values of Freundlich & Langmuir model parameters for the adsorption of Zn^{2+} ions onto raw and modified eucalyptus bark adsorbents are summarised and presented in Table 6.6.

Error Analysis:

The use of R^2 is limited to solve linear forms of isotherm equation, which measures the difference between experimental and theoretical data in linearized plots only, but not the errors in non-linear form of isotherm curves. For that reason, the Marquardt's percent standard deviation (MPSD) error function was used to test the adequacy of the isotherm equations to represent the experimental data. The error function of Marquardt's Percent Standard Deviation (MPSD) (Marquardt 1963) is given as:

$$MPSD = 100\sqrt{\frac{1}{x-p}\sum_{i=1}^{x}\left(\frac{q_{e,meas}-q_{e,calc}}{q_{e,meas}}\right)_i^2} \quad (6.4)$$

The MPSD account for the number of degrees of freedom of the system where x is the number of data point and p is the number of parameters of the isotherm and is similar in some respects to a geometric mean error distribution.

For each parameter set, the values of MPSD error function for adsorption of Zn^{2+} on raw and NaOH modified eucalyptus bark are calculated and presented in Table 6.6. By comparing the results of the values for the MPSD error function, it can be concluded that the Freundlich isotherms result in the lowest values for the error function and therefore fits the data better than Langmuir isotherm models.

Table 6.6: A summary of Langmuir and Freundlich calculated values

Model	***Parameters***	***Raw eucalyptus bark***	***NaOH modified eucalyptus bark***
LANGMUIR (TYPE I)	q_m (mg/g)	131.58	222.22
	K_a (L/g)	0.0482	0.1004
	R^2	0.9655	0.9935
	MPSD	69.01	74.44
LANGMUIR (TYPE II)	q_m (mg/g)	128.21	250.00
	K_a (L/g)	0.0509	0.0781
	R^2	0.9434	0.9732
	MPSD	37.02	53.35
FREUNDLICH	K_f $(L/g)^{1/n}$	16.31	38.28
	$1/n$	0.4511	0.4443
	R^2	0.9331	0.9273
	MPSD	1.91	2.13

The separation factor (R_L) which is a dimensionless constant, further used to investigate the feasibility of adsorption process at different initial Zn^{2+} concentrations. The obtained R_L values, calculated from Langmuir plots using Eq. (4.4) were observed to decrease with the increase in initial Zn^{2+} solution concentration for both raw and treated eucalyptus bark and the values are in between $0<R_L<1$. This confirms the favourable uptake of Zn^{2+} metal ions onto raw and NaOH modified eucalyptus bark biomass.

The adsorption capacities, q_m (mg/g) of the adsorbents obtained in the present study for the removal of Zn^{2+} from its aqueous solution have been compared with those of other adsorbents reported in literature and the values of adsorption capacities are presented in Table 6.7. The experimental data of the present investigations are comparable with the reported values for many other agricultural solid wastes and activated carbon adsorbents.

Table 6.7: Comparison of the adsorption capacity (q_m in mg/g) of different sorbents for the removal of Zn^{2+}

Adsorbent	***Maximum Adsorption Capacity, q_m (mg/g)***	***Reference***
Activated carbon (sulphurised)	23.7	(Krishnan, Sreejalekshmi et al. 2016)
Okra biomass (modified)	57.11	(Singha and Guleria 2015)
Activated neem bark	11.90	(Maheshwari, Mathesan et al. 2015)
Rapeseed waste	13.86	(Paduraru, Tofan et al. 2015)
Sugarcane bagasse	40.00	(Putra, Kamari et al. 2014)
Coconut tree sawdust	23.81	(Putra, Kamari et al. 2014)
Orange Peel (Modified by sodium hydroxide and calcium chloride)	56.18	(Feng and Guo 2012)
Orange Peel (raw)	21.25	(Feng and Guo 2012)
Water melon rind	6.85	(Liu, Ngo et al. 2012)
Citrus reticulata waste biomass	138.42	(Boota, Bhatti et al. 2009)
Moringa oleifera biomass (NaOH treated)	45.76	(Bhatti, Mumtaz et al. 2007)
Neem bark	13.29	(Bhattacharya, Mandal et al. 2006)
Papaya wood	13.45	(Saeed, Akhter et al. 2005)
Raw eucalyptus bark	128.21	In this present study
Modified eucalyptus bark (NaOH treated)	250.00	In this present study

6.7 Design of Single Stage Batch Adsorber from Isotherm Data

Langmuir II adsorption isotherm data have been used to design a single-stage batch adsorber system as per method mentioned in Section 4.7. a series of plots derived from Eq. (4.6) between different solution volumes and the predicted amount of raw and modified eucalyptus bark particles required to remove Zn^{2+} solutions of initial concentrations of 100 ppm for 90%, 80%, 70%, 60% removal is shown in Fig. 6.17(a) and Fig 6.17(b) respectively.

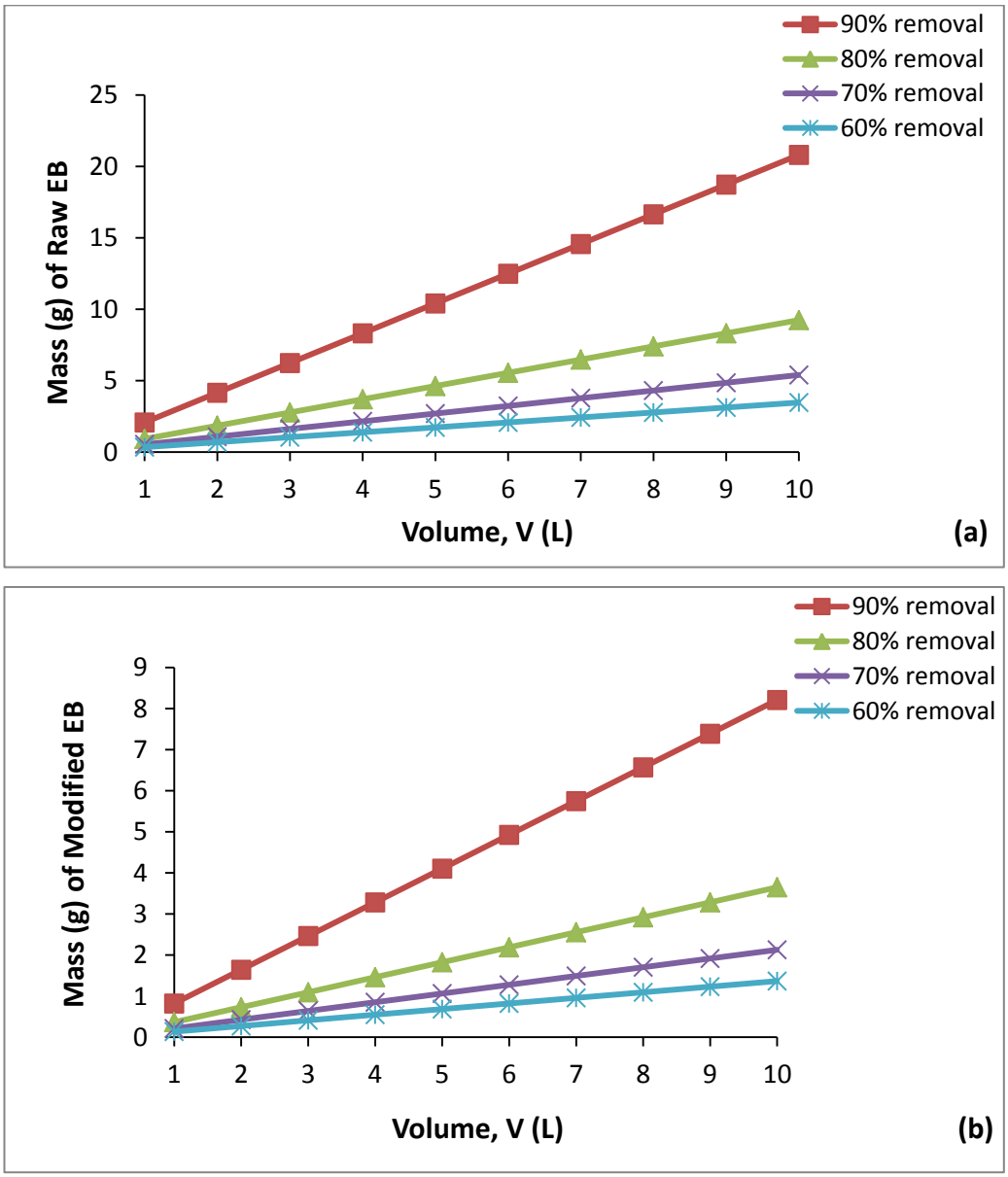

Figure 6.17 Adsorbent mass (g) against volume (litres) of solution treated for (a) raw eucalyptus bark system (b) NaOH modified eucalyptus bark

It is observed that the mass of adsorbent needed from modified bark was less [Fig. 6.17(b)] than the mass needed from raw bark biomass [Fig. 6.17(a)]; this means treated biomass adsorbent is more favourable compared to raw material.

6.8 Summary

The effectiveness of raw and modified eucalyptus bark for the removal of Zn^{2+} from its aqueous solution was tested under different experimental conditions in a batch process. Hence, the following conclusion can be made from this chapter:

- Batch kinetic experiments revealed that the adsorption of Zn^{2+} was rapid at initial stage followed by a slower intraparticle phase and equilibrium was attained within 100 min.
- The sorption kinetics was found to be dependent upon contact time, initial metal ion concentration, sorbent dose, solution initial pH, ionic strength and temperature and their optimum values are determined. The adsorptive effectiveness of raw eucalyptus bark was increased by chemical treatment with NaOH.
- The amount of Zn^{2+} removal on raw and modified eucalyptus bark was found to increase with an increase in initial solution pH, initial Zn^{2+} concentration and contact time but decreased with the increase in adsorbent dosage, solution temperature and salt concentration.
- Desorption experiments clearly indicated that adsorption of Zn^{2+} metal followed ion-exchange and strong physical-chemical adsorption.
- Modelling of sorption kinetics showed good agreement of experimental data with the pseudo-second-order kinetic equation for various process operating conditions and the adsorption was controlled by chemisorption process.
- Both the Freundlich and Langmuir isotherm models were fitted well with the isotherm experimental data. At optimum pH 5.1, the highest monolayer adsorption capacity obtained was 250.00 mg/g for NaOH modified eucalyptus bark whereas 128.21 mg/g for raw eucalyptus bark which are comparative to commercial activated carbon and other biomass based adsorbents.
- Thermodynamic studies indicate that the adsorption process is spontaneous and exothermic in nature for both raw and modified adsorbents.

6.9 References

Adeyinka, A., Liang, H. and Tina, G. (2007). "Removal of metal ion form waste water with natural waste." School of Engineering and Technology **33**: 1-8.

Afroze, S., Sen, T. K., Ang, M. and Nishioka, H. (2015). "Adsorption of methylene blue dye from aqueous solution by novel biomass Eucalyptus sheathiana bark: equilibrium, kinetics, thermodynamics and mechanism." Desalination and Water Treatment **57**(13): 5858-5878.

Ansari, R. and Pornahad, A. (2010). "Removal of cerium (IV) ion from aqueous solutions using sawdust as a very low coast bioadsorbent." Journal of Applied Science and Environmental Sanitation: 239-247.

Arias, F. and Sen, T. K. (2009). "Removal of zinc metal ion (Zn 2+) from its aqueous solution by kaolin clay mineral: a kinetic and equilibrium study." Colloids and Surfaces A: Physicochemical and Engineering Aspects **348**(1): 100-108.

Arivoli, S., Hema, M., Parthasarathy, S. and Manju, N. (2010). "Adsorption dynamics of methylene blue by acid activated carbon." Journal of Chemical and Pharmaceutical Research **2**(5): 626-641.

Bhattacharya, A., Mandal, S. and Das, S. (2006). "Adsorption of Zn (II) from aqueous solution by using different adsorbents." Chemical Engineering Journal **123**(1): 43-51.

Bhatti, H. N., Mumtaz, B., Hanif, M. A. and Nadeem, R. (2007). "Removal of Zn (II) ions from aqueous solution using Moringa oleifera Lam.(horseradish tree) biomass." Process Biochemistry **42**(4): 547-553.

Boota, R., Bhatti, H. N. and Hanif, M. A. (2009). "Removal of Cu (II) and Zn (II) using lignocellulosic fiber derived from Citrus reticulata (Kinnow) waste biomass." Separation Science and Technology **44**(16): 4000-4022.

Davis, J. A. and Leckie, J. O. (1978). "Surface ionization and complexation at the oxide/water interface II. Surface properties of amorphous iron oxyhydroxide and adsorption of metal ions." Journal of Colloid and Interface Science **67**(1): 90-107.

Dawood, S. and Sen, T. K. (2012). "Removal of anionic dye Congo red from aqueous solution by raw pine and acid-treated pine cone powder as adsorbent: Equilibrium, thermodynamic, kinetics, mechanism and process design." Water Research **46**(6): 1933-1946.

Demiral, H., Demiral, I., Tümsek, F. and Karabacakoğlu, B. (2008). "Adsorption of chromium (VI) from aqueous solution by activated carbon derived from olive bagasse and applicability of different adsorption models." Chemical Engineering Journal **144**(2): 188-196.

Feng, N.-c. and Guo, X.-y. (2012). "Characterization of adsorptive capacity and mechanisms on adsorption of copper, lead and zinc by modified orange peel." Transactions of Nonferrous Metals Society of China **22**(5): 1224-1231.

Ghodbane, I., Nouri, L., Hamdaoui, O. and Chiha, M. (2008). "Kinetic and equilibrium study for the sorption of cadmium (II) ions from aqueous phase by eucalyptus bark." Journal of Hazardous Materials **152**(1): 148-158.

Gupta, S. S. and Bhattacharyya, K. G. (2006). "Adsorption of Ni (II) on clays." Journal of Colloid and Interface Science **295**(1): 21-32.

Karppi, J., Åkerman, S., Åkerman, K., Sundell, A. and Penttilä, I. (2010). "Adsorption of metal cations from aqueous solutions onto the pH responsive poly (vinylidene fluoride grafted poly (acrylic acid)(PVDF-PAA) membrane." Journal of Polymer Research **17**(1): 71-76.

Krishnan, K. A., Sreejalekshmi, K., Vimexen, V. and Dev, V. V. (2016). "Evaluation of adsorption properties of sulphurised activated carbon for the effective and economically viable removal of Zn (II) from aqueous solutions." Ecotoxicology and Environmental Safety **124**: 418-425.

Liu, C., Ngo, H. H. and Guo, W. (2012). "Watermelon rind: agro-waste or superior biosorbent?" Applied Biochemistry and Biotechnology **167**(6): 1699-1715.

Maheshwari, U., Mathesan, B. and Gupta, S. (2015). "Efficient adsorbent for simultaneous removal of Cu (II), Zn (II) and Cr (VI): Kinetic, thermodynamics and mass transfer mechanism." Process Safety and Environmental Protection **98**: 198-210.

Marquardt, D. W. (1963). "An algorithm for least-squares estimation of nonlinear parameters." Journal of the Society for Industrial & Applied Mathematics **11**(2): 431-441.

Nandi, B., Goswami, A. and Purkait, M. (2009). "Removal of cationic dyes from aqueous solutions by kaolin: Kinetic and equilibrium studies." Applied Clay Science **42**(3-4): 583-590.

Nasernejad, B., Zadeh, T. E., Pour, B. B., Bygi, M. E. and Zamani, A. (2005). "Camparison for biosorption modeling of heavy metals (Cr (III), Cu (II), Zn (II)) adsorption from wastewater by carrot residues." Process Biochemistry **40**(3): 1319-1322.

Ofomaja, A. and Naidoo, E. (2010). "Biosorption of lead (II) onto pine cone powder: studies on biosorption performance and process design to minimize biosorbent mass." Carbohydrate Polymers **82**(4): 1031-1042.

Ofomaja, A. and Naidoo, E. (2011). "Biosorption of copper from aqueous solution by chemically activated pine cone: a kinetic study." Chemical Engineering Journal **175**: 260-270.

Ofomaja, A., Naidoo, E. and Modise, S. (2009). "Removal of copper (II) from aqueous solution by pine and base modified pine cone powder as biosorbent." Journal of Hazardous Materials **168**(2): 909-917.

Ofomaja, A. E. (2008). "Sorptive removal of Methylene blue from aqueous solution using palm kernel fibre: Effect of fibre dose." Biochemical Engineering Journal **40**(1): 8-18.

Osemeahon, S., Barminas, J. and HammaAdama, M. (2013). "Studies on the removal of metal ions from aqueous solution using Immobilized Bombax costatum calyx." IOSR Journal Of Environmental Science, Toxicology And Food Technology (IOSR-JESTFT) **3**(6): 6-13.

Paduraru, C., Tofan, L., Teodosiu, C., Bunia, I., Tudorachi, N. and Toma, O. (2015). "Biosorption of zinc (II) on rapeseed waste: Equilibrium studies and thermogravimetric investigations." Process Safety and Environmental Protection **94**: 18-28.

Putra, W. P., Kamari, A., Yusoff, S. N. M., Ishak, C. F., Mohamed, A., Hashim, N. and Isa, I. M. (2014). "Biosorption of Cu (II), Pb (II) and Zn (II) ions from aqueous solutions using selected waste materials: Adsorption and characterisation studies." Journal of Encapsulation and Adsorption Sciences **4**(1).

Saeed, A., Akhter, M. W. and Iqbal, M. (2005). "Removal and recovery of heavy metals from aqueous solution using papaya wood as a new biosorbent." Separation and Purification Technology **45**(1): 25-31.

Sahin, H. and Peeters, F. M. (2013). "Adsorption of alkali, alkaline-earth, and 3d transition metal atoms on silicene." Physical Review B **87**(8): 085423.

Sen, T. K., Afroze, S. and Ang, H. (2011). "Equilibrium, kinetics and mechanism of removal of methylene blue from aqueous solution by adsorption onto pine cone biomass of Pinus radiata." Water, Air, & Soil Pollution **218**(1-4): 499-515.

Sen, T. K. and Gomez, D. (2011). "Adsorption of zinc (Zn 2+) from aqueous solution on natural bentonite." Desalination **267**(2): 286-294.

Singha, A. S. and Guleria, A. (2015). "Utility of chemically modified agricultural waste okra biomass for removal of toxic heavy metal ions from aqueous solution." Engineering in Agriculture, Environment and Food **8**(1): 52-60.

Trivedi, P., Axe, L. and Dyer, J. (2001). "Adsorption of metal ions onto goethite: single-adsorbate and competitive systems." Colloids and Surfaces A: Physicochemical and Engineering Aspects **191**(1): 107-121.

Wang, L., Chen, Z., Yang, J. and Ma, F. (2015). "Pb (II) biosorption by compound bioflocculant: performance and mechanism." Desalination and Water Treatment **53**(2): 421-429.

Every reasonable effort has been made to acknowledge the owners of copyright material. I would be pleased to hear from any copyright owner who has been omitted or incorrectly acknowledged.

CHAPTER 7

CONCLUSIONS AND RECOMMENDATIONS

7.1 Introduction

The increase in the volume of organic-inorganic contaminated industrial wastewater generated and discharged into the environment appears unavoidable and therefore, the presence of these pollutants is of great concern and their removal is essential. In last few decades, for the treatment of wastewater effluents; adsorption is considered to be a very effective separation technique and superior over other methods in the removal of dyes and heavy metals from aqueous solution. On the other hand, day by day large amount of industrial and agricultural solid waste is generated and need proper solid waste management. Recent trend of research interest is to develop cost-effective and non-conventional potential adsorbents such as clays, minerals, raw and modified agricultural solid waste and biomass based activated carbon. In view of this quest, this research work has reported a cost effective, environmentally friendly and readily available alternative agricultural by-product based sustainable novel adsorbent from agricultural solid waste. Eucalyptus bark is an agricultural solid waste. In this study, eucalyptus *sheathiana* bark has been used as a highly cost-effective new alternative adsorbent for the removal of MB dye and Zn^{2+} metal ions from aqueous solution by adsorption. This chapter summarizes the overall achieved research results and indicates the suitability of the selected adsorbent as an inexpensive potentially alternative adsorbent in comparison to existing commercial activated carbon. Batch adsorption kinetic studies show the effectiveness of organic MB dye removal using the prepared raw eucalyptus bark and the removal of inorganic Zn^{2+} metal ions was done by using the prepared raw and base modified eucalyptus bark adsorbent. Further, the different operational parameters observed during the process of investigations reveal that pH, temperature, contact time, adsorbent dose and concentrations of the adsorbate govern the overall process of adsorption. Besides, adsorption performance of adsorbents in continuous system is important in accessing the feasibility of adsorbents in real industrial applications and to find key parameters required for the design of fixed-bed adsorber. For this purpose, the breakthrough curve shape and the breakthrough time appearance characteristics via various column operating parameters such as adsorbate flow rate, concentration of solute in the feed and the bed height of adsorbent were evaluated here. Hence, column studies show that eucalyptus bark powder can be used in wastewater treatment containing organic pollutants. In order to complete the existing

data, recommendations for future work include the possibilities of conducting further similar experiments by using new materials.

7.2 Conclusion

This thesis investigates the feasibility of using an agricultural by-product, eucalyptus bark, as an effective adsorbent to remove organic MB dye and inorganic Zn^{2+} contaminants from their aqueous solutions. In this study, raw eucalyptus bark was modified with base (NaOH) treatment and characterisation of raw and modified adsorbent was performed. Next, raw eucalyptus bark was tested for MB dye removal and separately, raw and modified bark biomass was studied for Zn^{2+} removal from its aqueous solution. This conclusion is generally in agreement with the outcomes reported in research literature thereby confirming that the findings from this study can be used as a reliable guide to predicting the sorption affinities of sorbent materials. Specifically this study considers the following aspects:

i. Collection and characterisation of prepared adsorbents
ii. Batch adsorption study of raw eucalyptus bark biomass for MB dye removal
iii. Column adsorption study of raw eucalyptus bark biomass for MB dye removal
iv. Batch adsorption study of raw and modified eucalyptus bark materials for Zn^{2+} removal

My chapter wise conclusions with prime findings are as follows:

7.2.1 Chapter 3: Characterisation of Prepared Adsorbents

Several techniques were employed to characterise eucalyptus bark to understand the properties of raw and modified bark materials as well as to study the effects of modification on the textural and surface properties of the raw eucalyptus bark. The outcomes based on the results of the characterisation of prepared raw and modified eucalyptus bark using various analytical instruments including SEM, EDS, XRD, FT-IR, BET method along with bulk density, point of zero charge, etc. are as follows:

- The scanning electron microscopy (SEM) of all the prepared adsorbents showed the highly irregular shapes and sizes. The chemically modified

surface appeared to be rough, indicating that the surface had been covered with organic molecules. EDS study exposed that calcium is the major element where oxygen, hydrogen, nitrogen, sodium, magnesium and chloride are homogeneously distributed all over the adsorbent surface.

- The chemical analysis using XRD technique identifies no major changes in the XRD patterns of raw and NaOH treated eucalyptus bark and the peaks obtained gave good indication of highly organized crystalline cellulose on the adsorbent biomass.
- FTIR spectra of raw and treated eucalyptus bark materials did not show any radical changes indicating that the treatment with mild base solutions did not significantly alter the chemical properties of the raw eucalyptus bark biomass. The FTIR of modified bark revealed a new peak at 2922.5 cm^{-1} which allocates the aliphatic group C–H stretching vibrations. This shows that the treatment of biomass with alkali resulted in the exposure of buried aliphatic groups of the adsorbent surface which leads to higher adsorption capacity of modified biomass.
- For the chemically treated eucalyptus bark, higher BET surface area was observed. Lower bulk density of treated biomass was due to the chemically modified eucalyptus bark surfaces. The bulk density for eucalyptus bark was 0.39 gm/cm^3, whereas 0.27 gm/cm^3 bulk density was found for NaOH modified eucalyptus bark. The point of zero charge for modified eucalyptus bark was 4.5 whereas for raw bark, it was observed at 5.0.

7.2.2 Chapter 4: Batch Adsorption Study of Raw Eucalyptus Bark for MB Dye Removal

In this study, the effectiveness of raw eucalyptus bark was tested for the removal of organic Methylene Blue (MB) dye from its aqueous solution under various physico-chemical process operating conditions and the outcomes are as follows:

- Around 90% of MB dye was removed by raw eucalyptus bark adsorbent at optimum MB dye solution pH of 10.0 with 20 ppm initial MB dye concentration.
- The adsorption equilibrium was reached within 140 min. Kinetic experiments clearly indicated that adsorption of MB dye on raw eucalyptus bark biomass

is a multi-step process: a rapid adsorption of dye onto the external surface of adsorbent followed by intra-particle diffusion into the interior of adsorbent which was also confirmed by intra-particle diffusion model. Overall, the kinetic studies showed that the process of MB dye adsorption followed pseudo-second order kinetic model. The thermodynamic analysis showed that the adsorption process is endothermic, irreversible and spontaneous in nature.

- From the mixed contaminant study, it was found that eucalyptus bark has a good adsorption capacity to adsorb both cationic dye methylene blue (MB) and anionic dye congo red (CR) simultaneously. At a particular solution pH of 7.4, the removal percentage of MB dye was 86.33% with CR dye removal of 57.95%.
- The experimental data correlated reasonably well by both Langmuir I and Langmuir II adsorption isotherms with an adsorption capacity of 204.08 mg/g. The dimensionless separation factor (R_L) gives an indication of favourable adsorption.
- The results of the batch desorption studies showed that ion-exchange and chemisorption played a prominent role in the sorption process and as the regeneration of eucalyptus bark is not economically viable, the exhausted eucalyptus bark could be used as a fuel in incinerators. This will further help waste management by reducing the cost of waste disposal.

7.2.3 Chapter 5: Column Adsorption Study of Raw Eucalyptus Bark for MB Dye Removal

The outcomes from adsorption dynamics study of fixed bed column for the removal of methylene blue (MB) dye on raw eucalyptus bark are as follows:

- High bed height, low flow rate and high initial dye concentration were studied to be better operating conditions for maximum MB dye adsorption in a fixed bed column. A maximum dye uptake of 45.24, 48.29 and 49.55 mg g^{-1} was observed at 10 mL min^{-1} MB flow rate, 100 mg L^{-1} initial dye concentration and 10 cm bed height of raw eucalyptus bark respectively.
- To investigate the breakthrough curve performance, to describe the adsorption kinetics for the calculation of column kinetic parameters and to determine the adsorption capacity of the fixed bed column; Thomas, Yoon–

Nelson and BDST models were applied in this study. From the results, it can be stated that the regression coefficient (R^2) values are very close for all the three models and hence all these three models can be applied satisfactorily to describe the experimental data well.

- The results such as sorption capacity and prediction of the time necessary for the effective column operation indicates that the external mass transfer resistance plays a dominating role together with the axial dispersion for the mechanism of the process.

7.2.4 Chapter 6: Batch Adsorption Study of Raw and Modified Eucalyptus Bark for Zn^{2+} Removal

The effectiveness of raw and modified eucalyptus bark for the removal of Zn^{2+} from its aqueous solution was conducted under different experimental conditions in batch process. The outcomes drawn from this study can be concluded as follows:

- The sorption kinetics was found to be dependent upon contact time, initial metal ion concentration, sorbent dose, solution initial pH, ionic strength and temperature. The adsorption effectiveness of raw eucalyptus bark was increased by treatment with NaOH.
- With 20 ppm of initial metal Zn^{2+} concentration, 30^0C solution temperature, 20 mg of adsorbent dosage and at 5.1 solution pH; the maximum removal percent of Zn^{2+} was found to be 40.12% and 69.38% for raw and modified adsorbent respectively.
- In batch studies, the kinetic experiments revealed that the adsorption of Zn^{2+} was rapid at initial stage followed by a slower phase where equilibrium was attained within 100 min. Modelling of sorption kinetics showed good agreement of experimental data with the pseudo-second-order kinetic equation for various process operating conditions and the adsorption was controlled by chemisorption process.
- Desorption experiments clearly indicated that adsorption of Zn^{2+} metal followed ion-exchange and strong physical-chemical adsorption.
- Both the Freundlich and Langmuir isotherm models were fitted well in the selected range of concentrations. The monolayer adsorption capacity obtained

was 250.00 mg/g for NaOH modified eucalyptus bark and 128.21 mg/g for raw eucalyptus bark at optimum pH 5.1.

- Overall, for both raw and modified adsorbents; the thermodynamic parameters indicated that Zn^{2+} sorption process is spontaneous and exothermic in nature.

Finally, it can be concluded that eucalyptus bark (*Eucalyptus sheathiana*) biomass is a good and cheap precursor for the production of raw and modified adsorbents. Further, the adsorption capacity of raw and modified eucalyptus bark is much comparative with other adsorbents including activated carbon in the removal of organic-inorganic materials from aqueous solution. The accumulated research data would significantly assist in moving towards the potential commercial use of eucalyptus bark biomass to be scaled up and used in field applications to treat and clean industrial water pollution.

7.3 Recommendations for Future Research

The applicability of eucalyptus bark biomass from eucalyptus *sheathiana* tree for the removal of Methylene Blue (MB) dye and Zn^{2+} was thoroughly studied. The results showed the effectiveness of raw and modified eucalyptus bark as a better adsorbent material for the removal of MB dye and Zn^{2+} contaminated wastewater respectively. However, some issues need to be addressed in an effort to compliment and improve the current study before considering the real applications. Some of the findings to date and need for future researches are as follows:

- Similar research should be done on locally available agricultural waste materials such as grass, eucalyptus tree leaves, straw, wheat straw, etc. and the potential of using these adsorbent biomass materials need to be evaluated. Other chemical and physical treatments could also be used. It is interesting to further find out the potential of utilizing different types of treatments as well as other types of biomasses.
- In this study, eucalyptus bark was tested discretely for the removal of MB dye and Zn^{2+} ions from their individual aqueous solution. The majority of industrial effluents contain more than one toxic pollutant. Hence, there is a

potential for mixtures to be used to see the affinity for the sorption of organic-inorganic simultaneously and to further advance the use of sorbent to enhance the sorption affinity of dyes-metals in a multi effluent system.

- Much work is necessary to predict the performance of adsorption process for inorganic removal from real industrial effluents under a wide range of operating conditions. The scale up of batch adsorption system to pilot system provides vital information in order to evaluate the applicability of a technique for the design of a treatment system for commercial use. In this research study, batch kinetic adsorption experiments were carried out in the removal of Zn^{2+} from aqueous solution by eucalyptus bark derived adsorbents. However more research is required for column study and pilot plant case study.
- In literature review, few efforts were made to relate the thermodynamic parameters. Therefore, more extensive studies should be performed in this direction.
- Leaching of agricultural solid wastes in water is very important in order to perceive the dissolution of various substances present in the industrial wastes. This interference will lead to erroneous results in the adsorption experiments. Therefore, more research work should be performed in this direction.

APPENDIX A

Raw data for the adsorption of methylene blue (MB) dye onto raw eucalyptus bark

Appendix A-1 Effect of initial solution pH on adsorption of methylene blue (MB) dye onto raw eucalyptus bark at initial solution pH of 2.5

Time, t (min)	C_t (mg/L)	q_t (mg/g)	% Adsorption
0	0.000	0.000	0.00
10	10.010	24.975	49.95
20	9.921	25.198	50.40
40	9.921	25.198	50.40
60	9.564	26.090	52.18
80	9.493	26.268	52.54
100	8.940	27.650	55.30
120	8.851	27.873	55.75
140	9.011	27.472	54.94
160	8.654	28.364	56.73
180	8.440	28.899	57.80

Experimental Conditions:

Amount of adsorbent = 20 mg
Initial MB dye concentration = 20 ppm
Volume of dye solution = 50 mL
Shaking speed = 120 rpm
Temperature = 30^0C

Appendix A-2 Effect of initial solution pH on adsorption of methylene blue (MB) dye onto raw eucalyptus bark at initial solution pH of 3.5

Time, t (min)	C_t (mg/L)	q_t (mg/g)	% Adsorption
0	0.000	0.000	0.00
10	8.583	28.542	57.08
20	7.870	30.325	60.65
40	6.158	34.605	69.21
60	6.122	34.695	69.39
80	6.015	34.962	69.92
100	5.676	35.809	71.62
120	5.587	36.032	72.06
140	5.569	36.077	72.15
160	5.498	36.255	72.51
180	4.660	38.350	76.70

Experimental Conditions:

Amount of adsorbent = 20 mg
Initial MB dye concentration = 20 ppm
Volume of dye solution = 50 mL
Shaking speed = 120 rpm
Temperature = 30^0C

Appendix A-3 Effect of initial solution pH on adsorption of methylene blue (MB) dye onto raw eucalyptus bark at initial solution pH of 5.25

Time, t (min)	C_t (mg/L)	q_t (mg/g)	% Adsorption
0	0.000	0.000	0.00
10	6.550	33.625	67.25
20	6.086	34.784	69.57
40	4.374	39.064	78.13
60	4.339	39.153	78.31
80	4.232	39.420	78.84
100	3.893	40.267	80.53
120	3.804	40.490	80.98
140	3.786	40.535	81.07
160	3.715	40.713	81.43
180	2.877	42.809	85.62

Experimental Conditions:

Amount of adsorbent = 20 mg
Initial MB dye concentration = 20 ppm
Volume of dye solution = 50 mL
Shaking speed = 120 rpm
Temperature = 30^0C

Appendix A-4 Effect of initial solution pH on adsorption of methylene blue (MB) dye onto raw eucalyptus bark at initial solution pH of 7.4

Time, t (min)	C_t (mg/L)	q_t (mg/g)	% Adsorption
0	0.000	0.000	0.00
10	6.978	32.555	65.11
20	4.909	37.726	75.45
40	4.749	38.128	76.26
60	4.678	38.306	76.61
80	3.733	40.669	81.34
100	3.643	40.892	81.78
120	3.626	40.936	81.87
140	3.429	41.427	82.85
160	3.108	42.229	84.46
180	2.805	42.987	85.97

Experimental Conditions:

Amount of adsorbent = 20 mg
Initial MB dye concentration = 20 ppm
Volume of dye solution = 50 mL
Shaking speed = 120 rpm
Temperature = 30^0C

Appendix A-5 Effect of initial solution pH on adsorption of methylene blue (MB) dye onto raw eucalyptus bark at initial solution pH of 8.3

Time, t (min)	C_t (mg/L)	q_t (mg/g)	% Adsorption
0	0.000	0.000	0
10	7.246	31.886	63.77
20	6.782	33.045	66.09
40	6.746	33.134	66.27
60	6.193	34.516	69.03
80	6.122	34.695	69.39
100	4.357	39.108	78.22
120	3.715	40.713	81.43
140	3.590	41.025	82.05
160	2.627	43.433	86.87
180	2.627	43.433	86.87

Experimental Conditions:

Amount of adsorbent = 20 mg
Initial MB dye concentration = 20 ppm
Volume of dye solution = 50 mL
Shaking speed = 120 rpm
Temperature = 30^0C

Appendix A-6 Effect of initial solution pH on adsorption of methylene blue (MB) dye onto raw eucalyptus bark at initial solution pH of 10.0

Time, t (min)	C_t (mg/L)	q_t (mg/g)	% Adsorption
0	0.000	0.000	0.00
10	5.658	35.854	71.71
20	5.427	36.433	72.87
40	4.374	39.064	78.13
60	4.214	39.465	78.93
80	3.608	40.981	81.96
100	3.572	41.070	82.14
120	3.376	41.560	83.12
140	3.162	42.095	84.19
160	2.770	43.076	86.15
180	2.110	44.726	89.45

Experimental Conditions:

Amount of adsorbent = 20 mg
Initial MB dye concentration = 20 ppm
Volume of dye solution = 50 mL
Shaking speed = 120 rpm
Temperature = 30^0C

Appendix A-7 Effect of initial dye concentration on adsorption of methylene blue (MB) dye onto raw eucalyptus bark at MB dye initial concentration of 20 ppm (mg/L)

Time, t (min)	C_t (mg/L)	q_t (mg/g)	% Adsorption
0	0.000	0.000	0.00
10	6.978	32.555	65.11
20	4.909	37.726	75.45
40	4.749	38.128	76.26
60	4.678	38.306	76.61
80	3.733	40.669	81.34
100	3.643	40.892	81.78
120	3.626	40.936	81.87
140	3.429	41.427	82.85
160	3.108	42.229	84.46
180	2.805	42.987	85.97

Experimental Conditions:

Amount of adsorbent = 20 mg
Initial solution pH = 7.4
Volume of dye solution = 50 mL
Shaking speed = 120 rpm
Temperature = 30^0C

Appendix A-8 Effect of initial dye concentration on adsorption of methylene blue (MB) dye onto raw eucalyptus bark at MB dye initial concentration of 30 ppm (mg/L)

Time, t (min)	C_t (mg/L)	q_t (mg/g)	% Adsorption
0	0.000	0.000	0.00
10	12.259	44.351	59.14
20	11.992	45.020	60.03
40	11.323	46.692	62.26
60	8.648	53.379	71.17
80	7.525	56.188	74.92
100	7.204	56.991	75.99
120	6.776	58.061	77.41
140	5.706	60.736	80.98
160	5.545	61.137	81.52
180	5.545	61.137	81.52

Experimental Conditions:

Amount of adsorbent = 20 mg
Initial solution pH = 7.4
Volume of dye solution = 50 mL
Shaking speed = 120 rpm
Temperature = 30^0C

Appendix A-9 Effect of initial dye concentration on adsorption of methylene blue (MB) dye onto raw eucalyptus bark at MB dye initial concentration of 40 ppm (mg/L)

Time, t (min)	C_t (mg/L)	q_t (mg/g)	% Adsorption
0	0.000	0.000	0.00
10	28.972	27.570	27.57
20	24.835	37.914	37.91
40	22.124	44.690	44.69
60	22.017	44.958	44.96
80	20.769	48.078	48.08
100	17.880	55.301	55.30
120	17.416	56.460	56.46
140	15.989	60.027	60.03
160	15.668	60.829	60.83
180	15.561	61.097	61.10

Experimental Conditions:

Amount of adsorbent = 20 mg
Initial solution pH = 7.4
Volume of dye solution = 50 mL
Shaking speed = 120 rpm
Temperature = 30^0C

Appendix A-10 Effect of initial dye concentration on adsorption of methylene blue (MB) dye onto raw eucalyptus bark at MB dye initial concentration of 50 ppm (mg/L)

Time, t (min)	C_t (mg/L)	q_t (mg/g)	% Adsorption
0	0.000	0.000	0.00
10	36.037	34.909	27.93
20	31.846	45.386	36.31
40	31.311	46.723	37.38
60	29.884	50.290	40.23
80	29.305	51.739	41.39
100	28.101	54.748	43.80
120	27.833	55.417	44.33
140	27.031	57.423	45.94
160	25.604	60.990	48.79
180	25.470	61.324	49.06

Experimental Conditions:

Amount of adsorbent = 20 mg
Initial solution pH = 7.4
Volume of dye solution = 50 mL
Shaking speed = 120 rpm
Temperature = 30^0C

Appendix A-11 Effect of initial dye concentration on adsorption of methylene blue (MB) dye onto raw eucalyptus bark at MB dye initial concentration of 60 ppm (mg/L)

Time, t (min)	C_t (mg/L)	q_t (mg/g)	% Adsorption
0	0.000	0.000	0.00
10	46.828	32.929	21.95
20	42.495	43.763	29.18
40	41.692	45.769	30.51
60	41.318	46.705	31.14
80	41.264	46.839	31.23
100	38.536	53.660	35.77
120	37.198	57.004	38.00
140	35.700	60.749	40.50
160	35.433	61.418	40.95
180	35.112	62.220	41.48

Experimental Conditions:

Amount of adsorbent = 20 mg
Initial solution pH = 7.4
Volume of dye solution = 50 mL
Shaking speed = 120 rpm
Temperature = 30^0C

Appendix A-12 Effect of initial dye concentration on adsorption of methylene blue (MB) dye onto raw eucalyptus bark at MB dye initial concentration of 70 ppm (mg/L)

Time, t (min)	C_t (mg/L)	q_t (mg/g)	% Adsorption
0	0.000	0.000	0.00
10	60.937	22.657	12.95
20	51.887	45.283	25.88
40	51.575	46.063	26.32
60	50.077	49.808	28.46
80	47.330	56.674	32.39
100	46.457	58.859	33.63
120	45.708	60.731	34.70
140	43.773	65.568	37.47
160	43.024	67.441	38.54
180	42.836	67.909	38.81

Experimental Conditions:

Amount of adsorbent = 20 mg
Initial solution pH = 7.4
Volume of dye solution = 50 mL
Shaking speed = 120 rpm
Temperature = 30^0C

Appendix A-13 Effect of adsorbent doses on adsorption of methylene blue (MB) dye onto raw eucalyptus bark at 10 mg

Time, t (min)	C_t (mg/L)	q_t (mg/g)	% Adsorption
0	0.000	0.000	0.00
10	10.349	48.257	48.26
20	9.956	50.218	50.22
40	9.154	54.231	54.23
60	9.082	54.588	54.59
80	8.868	55.658	55.66
100	6.853	65.733	65.73
120	6.407	67.963	67.96
140	6.318	68.408	68.41
160	6.140	69.300	69.30
180	5.409	72.956	72.96

Experimental Conditions:

Initial MB dye concentration = 20 ppm
Initial solution pH = 7.4
Volume of dye solution = 50 mL
Shaking speed = 120 rpm
Temperature = 30^0C

Appendix A-14 Effect of adsorbent doses on adsorption of methylene blue (MB) dye onto raw eucalyptus bark at 20 mg

Time, t (min)	C_t (mg/L)	q_t (mg/g)	% Adsorption
0	0.000	0.000	0.00
10	6.978	32.555	65.11
20	4.909	37.726	75.45
40	4.749	38.128	76.26
60	4.678	38.306	76.61
80	3.733	40.669	81.34
100	3.643	40.892	81.78
120	3.626	40.936	81.87
140	3.429	41.427	82.85
160	3.108	42.229	84.46
180	2.805	42.987	85.97

Experimental Conditions:

Initial MB dye concentration = 20 ppm
Initial solution pH = 7.4
Volume of dye solution = 50 mL
Shaking speed = 120 rpm
Temperature = 30^0C

Appendix A-15 Effect of adsorbent doses on adsorption of methylene blue (MB) dye onto raw eucalyptus bark at 30 mg

Time, t (min)	C_t (mg/L)	q_t (mg/g)	% Adsorption
0	0.000	0.000	0.00
10	4.357	26.072	78.22
20	3.376	27.707	83.12
40	3.340	27.766	83.30
60	3.251	27.915	83.74
80	3.180	28.034	84.10
100	3.055	28.242	84.73
120	2.235	29.609	88.83
140	2.128	29.787	89.36
160	1.753	30.412	91.23
180	1.218	31.303	93.91

Experimental Conditions:

Initial MB dye concentration = 20 ppm
Initial solution pH = 7.4
Volume of dye solution = 50 mL
Shaking speed = 120 rpm
Temperature = 30^0C

Appendix A-16 Effect of temperature on adsorption of methylene blue (MB) dye onto raw eucalyptus bark at 30°C

Time, t (min)	C_t (mg/L)	q_t (mg/g)	% Adsorption
0	0.000	0.000	0.00
10	6.978	32.555	65.11
20	4.909	37.726	75.45
40	4.749	38.128	76.26
60	4.678	38.306	76.61
80	3.733	40.669	81.34
100	3.643	40.892	81.78
120	3.626	40.936	81.87
140	3.429	41.427	82.85
160	3.108	42.229	84.46
180	2.805	42.987	85.97

Experimental Conditions:

Amount of adsorbent = 20 mg
Initial MB dye concentration = 20 ppm
Initial solution pH = 7.4
Volume of dye solution = 50 mL
Shaking speed = 120 rpm

Appendix A-17 Effect of temperature on adsorption of methylene blue (MB) dye onto raw eucalyptus bark at 45°C

Time, t (min)	C_t (mg/L)	q_t (mg/g)	% Adsorption
0	0.000	0.000	0.00
10	5.944	35.140	70.28
20	5.070	37.325	74.65
40	4.660	38.350	76.70
60	4.535	38.663	77.33
80	3.929	40.178	80.36
100	3.233	41.917	83.83
120	2.698	43.255	86.51
140	2.591	43.522	87.04
160	2.466	43.834	87.67
180	2.217	44.458	88.92

Experimental Conditions:

Amount of adsorbent = 20 mg
Initial MB dye concentration = 20 ppm
Initial solution pH = 7.4
Volume of dye solution = 50 mL
Shaking speed = 120 rpm

Appendix A-18 Effect of temperature on adsorption of methylene blue (MB) dye onto raw eucalyptus bark at 60°C

Time, t (min)	C_t (mg/L)	q_t (mg/g)	% Adsorption
0	0.000	0.000	0.00
10	5.819	35.453	70.91
20	5.070	37.325	74.65
40	4.374	39.064	78.13
60	3.857	40.357	80.71
80	3.697	40.758	81.52
100	3.233	41.917	83.83
120	2.698	43.255	86.51
140	2.591	43.522	87.04
160	2.217	44.458	88.92
180	1.842	45.395	90.79

Experimental Conditions:

Amount of adsorbent = 20 mg
Initial MB dye concentration = 20 ppm
Initial solution pH = 7.4
Volume of dye solution = 50 mL
Shaking speed = 120 rpm

Appendix A-19 Effect of surfactant (Triton X-100) on adsorption of methylene blue (MB) dye onto raw eucalyptus bark

Time, t (min)	C_t (mg/L)	q_t (mg/g)	% Adsorption
0	0.000	0.000	0.00
10	7.210	32.615	63.95
20	7.067	32.978	64.66
40	5.872	36.025	70.64
60	5.855	36.071	70.73
80	5.462	37.071	72.69
100	5.106	37.981	74.47
120	5.016	38.208	74.92
140	4.981	38.299	75.10
160	4.945	38.390	75.27
180	4.785	38.799	76.08

Experimental Conditions:

Amount of Adsorbent = 20 mg
Initial MB dye Concentration = 20 ppm
Initial Solution pH = 7.4
Volume of Triton X-100 = 1.0 mL
Volume of MB dye solution = 50 mL
Total Reaction Volume, V = 51.0 mL
Temperature = 30^0C
Shaking speed = 120 rpm

Appendix A-20 Effect of mixed dye on adsorption of methylene blue (MB) dye onto raw eucalyptus bark

Time, t (min)	Methylene Blue (MB)			Congo Red (CR)		
	C_t (mg/L)	q_t (mg/g)	% Adsorption of MB	C_t (mg/L)	q_t (mg/g)	% Adsorption of CR
0	0.000	0.000	0.00	0.000	0.000	0
10	3.180	21.025	84.10	9.466	13.167	52.67
20	3.144	21.070	84.28	9.349	13.314	53.26
40	3.019	21.226	84.90	9.114	13.607	54.43
60	2.966	21.293	85.17	8.880	13.900	55.60
80	2.877	21.404	85.62	8.880	13.900	55.60
100	2.877	21.404	85.62	8.704	14.120	56.48
120	2.841	21.449	85.80	8.645	14.194	56.77
140	2.823	21.471	85.88	8.587	14.267	57.07
160	2.752	21.560	86.24	8.469	14.413	57.65
180	2.734	21.583	86.33	8.411	14.487	57.95

Experimental Conditions:

Amount of Adsorbent = 20 mg
Initial MB Concentration = 20 ppm
Initial CR Concentration = 20 ppm
Initial Solution pH = 7.4
Volume of Congo Red solution = 25 mL
Volume of MB Solution = 25 mL
Total Reaction Volume, V = 50 mL
Temperature = 30^0C
Shaking speed = 120 rpm

Appendix A-21 Effect of monovalent ions concentration on adsorption of methylene blue (MB) dye onto raw eucalyptus bark at initial NaCl concentration of different concentrations

Time, t (min)	NaCl Concentration 100 mg L^{-1}		NaCl Concentration 200 mg L^{-1}		NaCl Concentration 300 mg L^{-1}	
	C_t (mg/L)	q_t (mg/g)	C_t (mg/L)	q_t (mg/g)	C_t (mg/L)	q_t (mg/g)
0	0.0	0.0	0.0	0.0	0.0	0.0
10	16.501	8.747	18.320	4.200	17.250	6.875
20	15.556	11.110	16.804	7.989	15.877	10.308
40	15.021	12.448	15.556	11.110	15.074	12.314
60	14.290	14.276	15.413	11.467	13.523	16.193
80	12.399	19.001	14.468	13.830	13.416	16.460
100	11.312	21.721	12.025	19.938	13.041	17.396
120	11.205	21.988	10.580	23.549	12.667	18.333
140	10.010	24.975	7.888	30.281	10.295	24.262
160	8.440	28.899	7.424	31.440	9.867	25.332
180	8.244	29.389	7.156	32.109	6.015	34.962

Experimental Conditions:

Amount of adsorbent = 20 mg
Initial MB dye concentration = 20 ppm
Initial solution pH = 7.4
Total volume of reaction solution = 50 mL (48 mL of MB solution + 2 mL of NaCl salt solution)
Shaking speed = 120 rpm
Temperature = 30^0C

Appendix A-22 Effect of divalent ions concentration on adsorption of methylene blue (MB) dye onto raw eucalyptus bark at initial $CaCl_2$ concentration of different concentrations

Time, t (min)	$CaCl_2$ Concentration 100 mg L^{-1}		$CaCl_2$ Concentration 200 mg L^{-1}		$CaCl_2$ Concentration 300 mg L^{-1}	
	C_t (mg/L)	q_t (mg/g)	C_t (mg/L)	q_t (mg/g)	C_t (mg/L)	q_t (mg/g)
0	0.0	0.0	0.0	0.0	0.0	0.0
10	14.094	14.766	13.024	17.441	4.125	39.688
20	12.810	17.976	12.631	18.422	2.894	42.764
40	11.436	21.409	11.579	21.052	2.395	44.012
60	10.117	24.708	10.955	22.613	2.306	44.235
80	10.063	24.842	9.653	25.867	2.163	44.592
100	9.956	25.109	9.510	26.224	1.967	45.082
120	8.815	27.963	6.693	33.268	1.949	45.127
140	8.654	28.364	5.605	35.988	1.896	45.261
160	7.995	30.013	5.462	36.344	1.789	45.528
180	7.781	30.548	5.641	35.898	1.771	45.573

Experimental Conditions:

Amount of adsorbent = 20 mg
Initial MB dye concentration = 20 ppm
Initial solution pH = 7.4
Total volume of reaction solution = 50 mL (48 mL of MB solution + 2 mL of $CaCl_2$ salt solution)
Shaking speed = 120 rpm
Temperature = 30^0C

Appendix A-23 Effect of trivalent ions concentration on adsorption of methylene blue (MB) dye onto raw eucalyptus bark at initial $FeCl_3$ concentration of different concentrations

Time, t (min)	$FeCl_3$ Concentration 100 mg L^{-1}		$FeCl_3$ Concentration 200 mg L^{-1}		$FeCl_3$ Concentration 300 mg L^{-1}	
	C_t (mg/L)	q_t (mg/g)	C_t (mg/L)	q_t (mg/g)	C_t (mg/L)	q_t (mg/g)
0	0.0	0.0	0.0	0.0	0.0	0.0
10	12.774	18.065	11.347	21.632	9.564	26.090
20	10.456	23.861	9.600	26.001	8.387	29.033
40	9.564	26.090	8.672	28.319	6.425	33.937
60	8.672	28.319	6.889	32.778	5.106	37.236
80	6.889	32.778	5.997	35.007	3.322	41.694
100	5.997	35.007	4.571	38.573	2.217	44.458
120	4.571	38.573	3.322	41.694	1.040	47.401
140	3.679	40.802	1.700	45.751	0.968	47.579
160	2.787	43.032	1.503	46.242	0.861	47.847
180	2.431	43.923	1.307	46.732	0.808	47.980

Experimental Conditions:

Amount of adsorbent = 20 mg
Initial MB dye concentration = 20 ppm
Initial solution pH = 7.4
Total volume of mixed solution = 50 mL (48 mL of MB solution + 2 mL of $FeCl_3$ salt solution)
Shaking speed = 120 rpm
Temperature = 30^0C

APPENDIX B

Raw data for the adsorption of methylene blue (MB) dye onto raw eucalyptus bark through fixed bed column study

Appendix B-1 Effect of flow rate on adsorption of methylene blue (MB) dye onto raw eucalyptus bark at 10 mL/min using packed bed column

Time, t (min)	C_t (mg/L)	C_t/C_o (mg/L)	Time, t (min)	C_t (mg/L)	C_t/C_o (mg/L)
5	0	0	225	20.3900	0.2719
10	0	0	240	23.6515	0.3154
15	0	0	255	29.4916	0.3932
20	0	0	270	39.5604	0.5275
25	0	0	285	44.9015	0.5987
30	0	0	300	51.7480	0.6900
40	0.2269	0.0030	320	56.5491	0.7540
50	0.3206	0.0043	340	60.7498	0.8100
60	0.4297	0.0057	360	64.8095	0.8641
75	0.5545	0.0074	380	67.0338	0.8938
90	0.6572	0.0088	400	68.9870	0.9198
105	0.8590	0.0115	420	70.5774	0.9410
120	1.2250	0.0163	440	71.8282	0.9577
135	1.5605	0.0208	460	72.6923	0.9692
150	2.5752	0.0343	480	73.4372	0.9792
165	5.4301	0.0724	500	73.8128	0.9842
180	8.6566	0.1154	520	74.2234	0.9896
195	12.0045	0.1601	540	74.5545	0.9941
210	14.6168	0.1949	565	75	1.0

Experimental Conditions:

Column bed height = 12 cm
Initial MB dye concentration = 75 ppm
Initial solution pH = 7.4
Temperature = 25±1°C

Appendix B-2 Effect of flow rate on adsorption of methylene blue (MB) dye onto raw eucalyptus bark at 12 mL/min using packed bed column

Time, t (min)	C_t (mg/L)	C_t/C_o (mg/L)	Time, t (min)	C_t (mg/L)	C_t/C_o (mg/L)
5	0	0	210	27.2404	0.3632
10	0	0	225	32.6250	0.4350
15	0	0	240	38.7103	0.5161
20	0	0	255	45.6850	0.6091
25	0	0	270	49.5230	0.6603
30	0.2380	0.0032	285	53.1701	0.7089
40	0.3110	0.0041	300	56.1453	0.7486
50	0.4000	0.0053	320	60.7625	0.8102
60	0.5941	0.0079	340	65.0277	0.8670
75	0.8960	0.0119	360	68.8332	0.9178
90	1.3681	0.0182	380	70.6054	0.9414
105	1.9323	0.0258	400	72.2804	0.9637
120	3.0302	0.0404	420	73.4289	0.9791
135	4.5628	0.0608	440	73.9089	0.9855
150	6.5013	0.0867	460	74.2830	0.9904
165	10.2490	0.1367	480	74.6630	0.9955
180	16.1987	0.2160	500	74.7830	0.9971
195	20.7476	0.2766	520	75	1.0

Experimental Conditions:

Column bed height = 12 cm
Initial MB dye concentration = 75 ppm
Initial solution pH = 7.4
Temperature = 25±1°C

Appendix B-3 Effect of flow rate on adsorption of methylene blue (MB) dye onto raw eucalyptus bark at 15 mL/min using packed bed column

Time, t (min)	C_t (mg/L)	C_t/C_o (mg/L)	Time, t (min)	C_t (mg/L)	C_t/C_o (mg/L)
5	0	0	195	33.2007	0.4427
10	0	0	210	38.3844	0.5118
15	0	0	225	42.1641	0.5622
20	0	0	240	49.5540	0.6607
25	0	0	255	53.5850	0.7145
30	0.4777	0.0064	270	58.1939	0.7759
40	0.6875	0.0092	285	63.2374	0.8432
50	0.8473	0.0113	300	67.1943	0.8959
60	1.2955	0.0173	320	69.5942	0.9279
75	2.1646	0.0289	340	71.5237	0.9536
90	3.8021	0.0507	360	72.5320	0.9671
105	5.2491	0.0700	380	73.2653	0.9769
120	7.5457	0.1006	400	73.9619	0.9862
135	9.5963	0.1280	420	74.3240	0.9910
150	14.1765	0.1890	440	74.6131	0.9948
165	20.8704	0.2783	460	74.7650	0.9969
180	26.7386	0.3565	480	75	1.0

Experimental Conditions:

Column bed height = 12 cm
Initial MB dye concentration = 75 ppm
Initial solution pH = 7.4
Temperature = 25±1°C

Appendix B-4 Effect of initial MB dye concentration on adsorption of methylene blue (MB) dye onto raw eucalyptus bark at 50 ppm (mg/L) using packed bed column

Time, t (min)	C_t (mg/L)	C_t/C_o (mg/L)	Time, t (min)	C_t (mg/L)	C_t/C_o (mg/L)
5	0	0	240	18.251	0.3650
10	0	0	255	21.290	0.4258
15	0	0	270	25.330	0.5066
20	0	0	285	29.942	0.5988
25	0	0	300	32.055	0.6411
30	0	0	320	34.278	0.6856
40	0	0	340	35.625	0.7125
50	0.188	0.0038	360	37.275	0.7455
60	0.243	0.0049	380	41.205	0.8241
75	0.522	0.0104	400	43.045	0.8609
90	0.723	0.0145	420	46.105	0.9221
105	1.325	0.0265	440	47.005	0.9401
120	1.505	0.0301	460	48.125	0.9625
135	1.869	0.0374	480	48.275	0.9655
150	2.505	0.0501	500	48.98	0.9796
165	4.105	0.0821	520	49.275	0.9855
180	6.523	0.1305	540	49.445	0.9889
195	8.495	0.1699	560	49.785	0.9957
210	11.225	0.2245	580	50	1
225	15.382	0.3076			

Experimental Conditions:

Column bed height = 12 cm
Influent MB dye flow rate = 12 mL/min
Initial solution pH = 7.4
Temperature = 25±1°C

Appendix B-5 Effect of initial MB dye concentration on adsorption of methylene blue (MB) dye onto raw eucalyptus bark at 75 ppm (mg/L) using packed bed column

Time, t (min)	C_t (mg/L)	C_t/C_o (mg/L)	Time, t (min)	C_t (mg/L)	C_t/C_o (mg/L)
5	0	0	210	27.240	0.3632
10	0	0	225	32.625	0.4350
15	0	0	240	38.710	0.5161
20	0	0	255	45.685	0.6091
25	0	0	270	49.523	0.6603
30	0.238	0.0032	285	53.170	0.7089
40	0.311	0.0041	300	56.145	0.7486
50	0.400	0.0053	320	60.763	0.8102
60	0.594	0.0079	340	65.028	0.8670
75	0.896	0.0119	360	68.833	0.9178
90	1.368	0.0182	380	70.605	0.9414
105	1.932	0.0258	400	72.280	0.9637
120	3.030	0.0404	420	73.429	0.9791
135	4.563	0.0608	440	73.909	0.9855
150	6.501	0.0867	460	74.283	0.9904
165	10.249	0.1367	480	74.663	0.9955
180	16.199	0.2160	500	74.783	0.9971
195	20.748	0.2766	520	75	1

Experimental Conditions:

Column bed height = 12 cm
Influent MB dye flow rate = 12 mL/min
Initial solution pH = 7.4
Temperature = 25±1°C

Appendix B-6 Effect of initial MB dye concentration on adsorption of methylene blue (MB) dye onto raw eucalyptus bark at 100 ppm (mg/L) using packed bed column

Time, t (min)	C_t (mg/L)	C_t/C_o (mg/L)	Time, t (min)	C_t (mg/L)	C_t/C_o (mg/L)
5	0	0	180	37.501	0.3750
10	0	0	195	45.050	0.4505
15	0	0	210	57.932	0.5793
20	0	0	225	63.212	0.6321
25	0	0	240	73.142	0.7314
30	0	0	255	77.256	0.7726
40	0.963	0.0096	270	81.925	0.8193
50	1.198	0.0120	285	85.849	0.8585
60	1.653	0.0165	300	89.109	0.8911
75	2.583	0.0258	320	93.814	0.9381
90	4.091	0.0409	340	96.033	0.9603
105	6.582	0.0658	360	97.899	0.9790
120	10.136	0.1014	380	98.510	0.9851
135	14.507	0.1451	400	99.265	0.9927
150	21.880	0.2188	420	99.652	0.9965
165	28.943	0.2894	440	100	1.0

Experimental Conditions:

Column bed height = 12 cm
Influent MB dye flow rate = 12 mL/min
Initial solution pH = 7.4
Temperature = 25±1°C

Appendix B-7 Effect of column adsorbent bed height on adsorption of methylene blue (MB) dye onto raw eucalyptus bark at 10 cm using packed bed column

Time, t (min)	C_t (mg/L)	C_t/C_o (mg/L)	Time, t (min)	C_t (mg/L)	C_t/C_o (mg/L)
5	0	0	180	26.2850	0.3505
10	0	0	195	31.7460	0.4233
15	0	0	210	36.6068	0.4881
20	0	0	225	41.9998	0.5600
25	0	0	240	50.2256	0.6697
30	0.2980	0.0040	255	51.2318	0.6831
40	0.4374	0.0058	270	54.1082	0.7214
50	0.6700	0.0089	285	58.1865	0.7758
60	1.1160	0.0149	300	63.1425	0.8419
75	1.8904	0.0252	320	68.4714	0.9130
90	3.0284	0.0404	340	71.6105	0.9548
105	4.5565	0.0608	360	72.8847	0.9718
120	7.1167	0.0949	380	73.9850	0.9865
135	11.1701	0.1489	400	74.3933	0.9919
150	14.9087	0.1988	420	74.6250	0.9950
165	20.3478	0.2713	440	75	1.0

Experimental Conditions:

Influent MB dye flow rate = 12 mL/min
Initial MB dye concentration = 75 ppm
Initial solution pH = 7.4
Temperature = 25±1°C

Appendix B-8 Effect of column adsorbent bed height on adsorption of methylene blue (MB) dye onto raw eucalyptus bark at 12 cm using packed bed column

Time, t (min)	C_t (mg/L)	C_t/C_o (mg/L)	Time, t (min)	C_t (mg/L)	C_t/C_o (mg/L)
5	0	0	210	27.2404	0.3632
10	0	0	225	32.6250	0.4350
15	0	0	240	38.7103	0.5161
20	0	0	255	45.6850	0.6091
25	0	0	270	49.5230	0.6603
30	0.2380	0.0032	285	53.1701	0.7089
40	0.3110	0.0041	300	56.1453	0.7486
50	0.4000	0.0053	320	60.7625	0.8102
60	0.5941	0.0079	340	65.0277	0.8670
75	0.8960	0.0119	360	68.8332	0.9178
90	1.3681	0.0182	380	70.6054	0.9414
105	1.9323	0.0258	400	72.2804	0.9637
120	3.0302	0.0404	420	73.4289	0.9791
135	4.5628	0.0608	440	73.9089	0.9855
150	6.5013	0.0867	460	74.2830	0.9904
165	10.2490	0.1367	480	74.6630	0.9955
180	16.1987	0.2160	500	74.7830	0.9971
195	20.7476	0.2766	520	75	1

Experimental Conditions:

Influent MB dye flow rate = 12 mL/min
Initial MB dye concentration = 75 ppm
Initial solution pH = 7.4
Temperature = 25±1°C

Appendix B-9 Effect of column adsorbent bed height on adsorption of methylene blue (MB) dye onto raw eucalyptus bark at 15 cm using packed bed column

Time, t (min)	C_t (mg/L)	C_t/C_o (mg/L)	Time, t (min)	C_t (mg/L)	C_t/C_o (mg/L)
5	0	0	285	20.2504	0.2700
10	0	0	300	24.5848	0.3278
15	0	0	320	27.9203	0.3723
20	0	0	340	33.1781	0.4424
25	0	0	360	35.4668	0.4729
30	0	0	380	43.2036	0.5760
40	0	0	400	45.3284	0.6044
50	0	0	420	49.8106	0.6641
60	0	0	440	53.2886	0.7105
75	0.3095	0.0041	460	57.1635	0.7622
90	0.4352	0.0058	480	60.4288	0.8057
105	0.6294	0.0084	500	63.8247	0.8510
120	0.9783	0.0130	520	66.8320	0.8911
135	1.5534	0.0207	540	69.4518	0.9260
150	2.2723	0.0303	560	70.9133	0.9455
165	3.1336	0.0418	580	71.9478	0.9593
180	4.0987	0.0546	600	72.9818	0.9731
195	5.4508	0.0727	620	73.4979	0.9800
210	6.9373	0.0925	645	73.9125	0.9855
225	8.5331	0.1138	670	74.2563	0.9901
240	11.6274	0.1550	695	74.5815	0.9944
255	14.1525	0.1887	720	75	1
270	16.5485	0.2206			

Experimental Conditions:

Influent MB dye flow rate = 12 mL/min
Initial MB dye concentration = 75 ppm
Initial solution pH = 7.4
Temperature = 25±1°C

APPENDIX C

Raw data for the adsorption of Zinc(II) metal ions onto raw and modified eucalyptus bark

Appendix C-1 Effect of initial solution pH on adsorption of Zn^{2+} ions onto raw and modified eucalyptus bark at initial solution pH of 2.5

Time, t (min)	Raw Eucalyptus Bark		Modified Eucalyptus Bark	
	C_t (mg/L)	q_t (mg/g)	C_t (mg/L)	q_t (mg/g)
0	0.000	0.000	0.000	0.000
5	18.113	4.718	18.354	4.115
10	17.526	6.185	17.136	7.160
20	17.080	7.300	16.332	9.170
40	16.507	8.733	15.354	11.615
60	16.399	9.003	13.831	15.423
80	16.309	9.228	12.611	18.473
100	16.030	9.925	12.241	19.398

Experimental Conditions:

Amount of adsorbent = 20 mg
Initial Zn^{2+} concentration = 20 ppm
Volume of Zn^{2+} solution = 50 mL
Shaking speed = 120 rpm
Temperature = 30^0C

Appendix C-2 Effect of initial solution pH on adsorption of Zn^{2+} ions onto raw and modified eucalyptus bark at initial solution pH of 3.01

Time, t (min)	Raw Eucalyptus Bark		Modified Eucalyptus Bark	
	C_t (mg/L)	q_t (mg/g)	C_t (mg/L)	q_t (mg/g)
0	0.000	0.000	0.000	0.000
5	17.494	6.265	16.831	7.923
10	17.348	6.630	16.630	8.425
20	16.827	7.933	16.441	8.898
40	16.661	8.348	14.541	13.648
60	16.356	9.110	13.527	16.183
80	16.062	9.845	11.257	21.858
100	15.052	12.370	10.970	22.575

Experimental Conditions:

Amount of adsorbent = 20 mg
Initial Zn^{2+} concentration = 20 ppm
Volume of Zn^{2+} solution = 50 mL
Shaking speed = 120 rpm
Temperature = 30^0C

Appendix C-3 Effect of initial solution pH on adsorption of Zn^{2+} ions onto raw and modified eucalyptus bark at initial solution pH of 4.0

Time, t (min)	Raw Eucalyptus Bark		Modified Eucalyptus Bark	
	C_t (mg/L)	q_t (mg/g)	C_t (mg/L)	q_t (mg/g)
0	0.000	0.000	0.000	0.000
5	13.949	15.128	15.322	11.695
10	13.917	15.208	13.018	17.455
20	13.751	15.623	12.066	19.835
40	13.643	15.893	11.104	22.240
60	13.431	16.423	10.068	24.830
80	13.215	16.963	9.514	26.215
100	12.983	17.543	8.845	27.888

Experimental Conditions:

Amount of adsorbent = 20 mg
Initial Zn^{2+} concentration = 20 ppm
Volume of Zn^{2+} solution = 50 mL
Shaking speed = 120 rpm
Temperature = 30^0C

Appendix C-4 Effect of initial solution pH on adsorption of Zn^{2+} ions onto raw and modified eucalyptus bark at initial solution pH of 4.52

Time, t (min)	Raw Eucalyptus Bark		Modified Eucalyptus Bark	
	C_t (mg/L)	q_t (mg/g)	C_t (mg/L)	q_t (mg/g)
0	0.000	0.000	0.000	0.000
5	14.394	14.015	12.449	18.878
10	13.850	15.375	11.663	20.843
20	12.910	17.725	10.969	22.578
40	12.846	17.885	9.734	25.665
60	12.470	18.825	8.260	29.350
80	12.343	19.143	7.466	31.335
100	12.299	19.253	7.265	31.838

Experimental Conditions:

Amount of adsorbent = 20 mg
Initial Zn^{2+} concentration = 20 ppm
Volume of Zn^{2+} solution = 50 mL
Shaking speed = 120 rpm
Temperature = 30^0C

Appendix C-5 Effect of initial solution pH on adsorption of Zn^{2+} ions onto raw and modified eucalyptus bark at initial solution pH of 5.01

Time, t (min)	Raw Eucalyptus Bark		Modified Eucalyptus Bark	
	C_t (mg/L)	q_t (mg/g)	C_t (mg/L)	q_t (mg/g)
0	0.0000	0.000	0.0000	0.000
5	13.9410	15.148	12.1380	19.655
10	13.4730	16.318	11.4550	21.363
20	13.2190	16.953	10.7710	23.073
40	12.7390	18.153	10.4570	23.858
60	12.6450	18.388	8.5440	28.640
80	12.2450	19.388	6.5320	33.670
100	11.976	20.060	6.1250	34.688

Experimental Conditions:

Amount of adsorbent = 20 mg
Initial Zn^{2+} concentration = 20 ppm
Volume of Zn^{2+} solution = 50 mL
Shaking speed = 120 rpm
Temperature = 30^0C

Appendix C-6 Effect of initial metal (Zn^{2+}) concentration on adsorption of Zn^{2+} ions onto raw and modified eucalyptus bark at Zn^{2+} initial concentration of 20 ppm (mg/L)

Time, t (min)	Raw Eucalyptus Bark		Modified Eucalyptus Bark	
	C_t (mg/L)	q_t (mg/g)	C_t (mg/L)	q_t (mg/g)
0	0.000	0.000	0.0000	0.000
5	13.941	15.148	12.1380	19.655
10	13.473	16.318	11.4550	21.363
20	13.219	16.953	10.7710	23.073
40	12.739	18.153	10.4570	23.858
60	12.645	18.388	8.5440	28.640
80	12.245	19.388	6.5320	33.670
100	11.976	20.060	6.1250	34.688

Experimental Conditions:

Amount of adsorbent = 20 mg
Initial solution pH = 5.1
Volume of Zn^{2+} solution = 50 mL
Shaking speed = 120 rpm
Temperature = 30^0C

Appendix C-7 Effect of initial metal (Zn^{2+}) concentration on adsorption of Zn^{2+} ions onto raw and modified eucalyptus bark at Zn^{2+} initial concentration of 30 ppm (mg/L)

Time, t (min)	Raw Eucalyptus Bark		Modified Eucalyptus Bark	
	C_t (mg/L)	q_t (mg/g)	C_t (mg/L)	q_t (mg/g)
0	0.000	0.000	0.000	0.000
5	21.801	20.498	20.466	23.835
10	21.729	20.678	19.568	26.081
20	21.344	21.641	18.396	29.010
40	20.178	24.555	17.046	32.385
60	19.580	26.051	15.846	35.385
80	18.747	28.133	13.358	41.606
100	18.230	29.426	12.786	43.035

Experimental Conditions:

Amount of adsorbent = 20 mg
Initial solution pH = 5.1
Volume of Zn^{2+} solution = 50 mL
Shaking speed = 120 rpm
Temperature = 30^0C

Appendix C-8 Effect of initial metal (Zn^{2+}) concentration on adsorption of Zn^{2+} ions onto raw and modified eucalyptus bark at Zn^{2+} initial concentration of 40 ppm (mg/L)

Time, t (min)	Raw Eucalyptus Bark		Modified Eucalyptus Bark	
	C_t (mg/L)	q_t (mg/g)	C_t (mg/L)	q_t (mg/g)
0	0.000	0.000	0.000	0.000
5	27.794	30.515	28.760	28.100
10	26.580	33.550	27.846	30.385
20	26.560	33.600	26.058	34.855
40	26.170	34.575	24.618	38.455
60	25.986	35.035	24.230	39.425
80	25.822	35.445	22.984	42.540
100	25.528	36.180	21.896	45.260

Experimental Conditions:

Amount of adsorbent = 20 mg
Initial solution pH = 5.1
Volume of Zn^{2+} solution = 50 mL
Shaking speed = 120 rpm
Temperature = 30^0C

Appendix C-9 Effect of initial metal (Zn^{2+}) concentration on adsorption of Zn^{2+} ions onto raw and modified eucalyptus bark at Zn^{2+} initial concentration of 50 ppm (mg/L)

Time, t (min)	Raw Eucalyptus Bark		Modified Eucalyptus Bark	
	C_t (mg/L)	q_t (mg/g)	C_t (mg/L)	q_t (mg/g)
0	0.000	0.000	0.000	0.000
5	35.200	37.000	37.695	30.763
10	35.188	37.031	35.675	35.813
20	34.983	37.544	35.198	37.006
40	33.823	40.444	34.078	39.806
60	33.430	41.425	31.738	45.656
80	33.218	41.956	30.473	48.819
100	32.105	44.738	30.295	49.263

Experimental Conditions:

Amount of adsorbent = 20 mg
Initial solution pH = 5.1
Volume of Zn^{2+} solution = 50 mL
Shaking speed = 120 rpm
Temperature = 30^0C

Appendix C-10 Effect of initial metal (Zn^{2+}) concentration on adsorption of Zn^{2+} ions onto raw and modified eucalyptus bark at Zn^{2+} initial concentration of 60 ppm (mg/L)

Time, t (min)	Raw Eucalyptus Bark		Modified Eucalyptus Bark	
	C_t (mg/L)	q_t (mg/g)	C_t (mg/L)	q_t (mg/g)
0	0.000	0.000	0.000	0.000
5	44.697	38.258	42.657	43.358
10	43.959	40.103	42.237	44.408
20	42.774	43.065	41.868	45.330
40	41.709	45.728	41.706	45.735
60	41.166	47.085	40.329	49.178
80	40.797	48.008	39.525	51.188
100	39.723	50.693	38.796	53.010

Experimental Conditions:

Amount of adsorbent = 20 mg
Initial solution pH = 5.1
Volume of Zn^{2+} solution = 50 mL
Shaking speed = 120 rpm
Temperature = 30^0C

Appendix C-11 Effect of initial metal (Zn^{2+}) concentration on adsorption of Zn^{2+} ions onto raw and modified eucalyptus bark at Zn^{2+} initial concentration of 70 ppm (mg/L)

Time, t (min)	Raw Eucalyptus Bark		Modified Eucalyptus Bark	
	C_t (mg/L)	q_t (mg/g)	C_t (mg/L)	q_t (mg/g)
0	0.000	0.000	0.000	0.000
5	53.267	41.834	51.881	45.299
10	51.223	46.944	51.268	46.830
20	51.191	47.023	48.517	53.708
40	49.207	51.984	48.272	54.320
60	49.781	50.549	47.688	55.781
80	47.758	55.606	47.107	57.234
100	46.375	59.063	46.074	59.815

Experimental Conditions:

Amount of adsorbent = 20 mg
Initial solution pH = 5.1
Volume of Zn^{2+} solution = 50 mL
Shaking speed = 120 rpm
Temperature = 30^0C

Appendix C-12 Effect of adsorbent doses on adsorption of Zn^{2+} ions onto raw and modified eucalyptus bark at 10 mg

Time, t (min)	Raw Eucalyptus Bark		Modified Eucalyptus Bark	
	C_t (mg/L)	q_t (mg/g)	C_t (mg/L)	q_t (mg/g)
0	0.000	0.000	0.0000	0.000
5	14.392	28.040	11.4310	42.845
10	13.473	32.635	11.0960	44.520
20	11.844	40.780	9.3660	53.170
40	11.773	41.135	8.3660	58.170
60	11.682	41.590	6.5950	67.025
80	11.015	44.925	6.1980	69.010
100	11.012	44.940	5.4960	72.520

Experimental Conditions:

Initial Zn^{2+} concentration = 20 ppm
Initial solution pH = 5.1
Volume of Zn^{2+} solution = 50 mL
Shaking speed = 120 rpm
Temperature = 30^0C

Appendix C-13 Effect of adsorbent doses on adsorption of Zn^{2+} ions onto raw and modified eucalyptus bark at 20 mg

Time, t (min)	Raw Eucalyptus Bark		Modified Eucalyptus Bark	
	C_t (mg/L)	q_t (mg/g)	C_t (mg/L)	q_t (mg/g)
0	0.000	0.000	0.0000	0.000
5	13.941	15.148	12.1380	19.655
10	13.473	16.318	11.4550	21.363
20	13.219	16.953	10.7710	23.073
40	12.739	18.153	10.4570	23.858
60	12.645	18.388	8.5440	28.640
80	12.245	19.388	6.5320	33.670
100	11.976	20.060	6.1250	34.688

Experimental Conditions:

Initial Zn^{2+} concentration = 20 ppm
Initial solution pH = 5.1
Volume of Zn^{2+} solution = 50 mL
Shaking speed = 120 rpm
Temperature = 30^0C

Appendix C-14 Effect of adsorbent doses on adsorption of Zn^{2+} ions onto raw and modified eucalyptus bark at 30 mg

Time, t (min)	Raw Eucalyptus Bark		Modified Eucalyptus Bark	
	C_t (mg/L)	q_t (mg/g)	C_t (mg/L)	q_t (mg/g)
0	0.000	0.000	0.000	0.000
5	15.564	7.393	12.712	12.147
10	15.128	8.120	12.312	12.813
20	14.583	9.028	11.257	14.572
40	14.025	9.958	10.853	15.245
60	13.995	10.008	10.134	16.443
80	13.785	10.358	9.614	17.310
100	13.554	10.743	9.457	17.572

Experimental Conditions:

Initial Zn^{2+} concentration = 20 ppm
Initial solution pH = 5.1
Volume of Zn^{2+} solution = 50 mL
Shaking speed = 120 rpm
Temperature = 30^0C

Appendix C-15 Effect of temperature on adsorption of Zn^{2+} ions onto raw and modified eucalyptus bark at 30°C

Time, t (min)	Raw Eucalyptus Bark		Modified Eucalyptus Bark	
	C_t (mg/L)	q_t (mg/g)	C_t (mg/L)	q_t (mg/g)
0	0.000	0.000	0.0000	0.000
5	13.941	15.148	12.1380	19.655
10	13.473	16.318	11.4550	21.363
20	13.219	16.953	10.7710	23.073
40	12.739	18.153	10.4570	23.858
60	12.645	18.388	8.5440	28.640
80	12.245	19.388	6.5320	33.670
100	11.976	20.060	6.1250	34.688

Experimental Conditions:

Amount of adsorbent = 20 mg
Initial Zn^{2+} concentration = 20 ppm
Initial solution pH = 5.1
Volume of dye solution = 50 mL
Shaking speed = 120 rpm

Appendix C-16 Effect of temperature on adsorption of Zn^{2+} ions onto raw and modified eucalyptus bark at 45°C

Time, t (min)	Raw Eucalyptus Bark		Modified Eucalyptus Bark	
	C_t (mg/L)	q_t (mg/g)	C_t (mg/L)	q_t (mg/g)
0	0.000	0.000	0.000	0.000
5	14.954	12.615	12.872	17.820
10	14.489	13.778	12.426	18.935
20	13.794	15.515	11.578	21.055
40	13.750	15.625	10.536	23.660
60	12.720	18.200	10.511	23.723
80	12.710	18.225	9.950	25.125
100	12.556	18.610	9.739	25.653

Experimental Conditions:

Amount of adsorbent = 20 mg
Initial Zn^{2+} concentration = 20 ppm
Initial solution pH = 5.1
Volume of dye solution = 50 mL
Shaking speed = 120 rpm

Appendix C-17 Effect of temperature on adsorption of Zn^{2+} ions onto raw and modified eucalyptus bark at 60°C

Time, t (min)	Raw Eucalyptus Bark		Modified Eucalyptus Bark	
	C_t (mg/L)	q_t (mg/g)	C_t (mg/L)	q_t (mg/g)
0	0.000	0.000	0.000	0.000
5	15.534	11.165	13.225	16.938
10	14.692	13.270	13.155	17.113
20	14.203	14.493	13.004	17.490
40	13.988	15.030	12.441	18.898
60	13.596	16.010	12.434	18.915
80	13.285	16.788	12.260	19.350
100	13.012	17.470	11.665	20.838

Experimental Conditions:

Amount of adsorbent = 20 mg
Initial Zn^{2+} concentration = 20 ppm
Initial solution pH = 5.1
Volume of dye solution = 50 mL
Shaking speed = 120 rpm

Appendix C-18 Effect of monovalent ions concentration on adsorption of Zn^{2+} onto raw and modified eucalyptus bark at initial NaCl concentration of 100 mg L^{-1}

Time, t (min)	Raw Eucalyptus Bark		Modified Eucalyptus Bark	
	C_t (mg/L)	q_t (mg/g)	C_t (mg/L)	q_t (mg/g)
0	0.000	0.000	0.000	0.000
5	13.449	16.378	13.621	15.948
10	13.419	16.453	11.187	22.033
20	13.294	16.765	10.087	24.783
40	12.888	17.780	9.096	27.260
60	12.750	18.125	8.506	28.735
80	12.550	18.625	7.547	31.133
100	12.250	19.375	7.434	31.415

Experimental Conditions:

Amount of adsorbent = 20 mg
Initial Zn^{2+} concentration = 20 ppm
Initial solution pH = 5.1
Total volume of reaction solution = 50 mL (48 mL of Zn^{2+} solution + 2 mL of 100 ppm NaCl salt solution)
Shaking speed = 120 rpm
Temperature = 30^0C

Appendix C-19 Effect of monovalent ions concentration on adsorption of Zn^{2+} onto raw and modified eucalyptus bark at initial NaCl concentration of 200 mg L^{-1}

Time, t (min)	Raw Eucalyptus Bark		Modified Eucalyptus Bark	
	C_t (mg/L)	q_t (mg/g)	C_t (mg/L)	q_t (mg/g)
0	0.000	0.000	0.000	0.000
5	14.348	14.130	14.121	14.698
10	14.310	14.225	12.852	17.870
20	13.771	15.573	11.213	21.968
40	13.507	16.233	9.887	25.283
60	13.259	16.853	9.097	27.258
80	12.514	18.715	8.543	28.643
100	12.504	18.740	8.345	29.138

Experimental Conditions:

Amount of adsorbent = 20 mg
Initial Zn^{2+} concentration = 20 ppm
Initial solution pH = 5.1
Total volume of reaction solution = 50 mL (48 mL of Zn^{2+} solution + 2 mL of 200 ppm NaCl salt solution)
Shaking speed = 120 rpm
Temperature = 30^0C

Appendix C-20 Effect of monovalent ions concentration on adsorption of Zn^{2+} onto raw and modified eucalyptus bark at initial NaCl concentration of 300 mg L^{-1}

Time, t (min)	Raw Eucalyptus Bark		Modified Eucalyptus Bark	
	C_t (mg/L)	q_t (mg/g)	C_t (mg/L)	q_t (mg/g)
0	0.000	0.000	0.000	0.000
5	14.965	12.588	15.108	12.230
10	14.147	14.633	13.365	16.588
20	13.847	15.383	12.468	18.830
40	13.705	15.738	11.473	21.318
60	13.572	16.070	10.779	23.053
80	13.572	16.070	9.468	26.330
100	13.562	16.095	9.163	27.093

Experimental Conditions:

Amount of adsorbent = 20 mg
Initial Zn^{2+} concentration = 20 ppm
Initial solution pH = 5.1
Total volume of reaction solution = 50 mL (48 mL of Zn^{2+} solution + 2 mL of 300 ppm NaCl salt solution)
Shaking speed = 120 rpm
Temperature = 30^0C

Appendix C-21 Effect of divalent ions concentration on adsorption of Zn^{2+} onto raw and modified eucalyptus bark at initial $CaCl_2$ concentration of 100 mg L^{-1}

Time, t (min)	Raw Eucalyptus Bark		Modified Eucalyptus Bark	
	C_t (mg/L)	q_t (mg/g)	C_t (mg/L)	q_t (mg/g)
0	0.000	0.000	0.000	0.000
5	13.965	15.088	12.504	18.740
10	13.916	15.210	10.179	24.553
20	13.351	16.623	9.706	25.735
40	13.108	17.230	9.568	26.080
60	12.965	17.588	8.428	28.930
80	12.686	18.285	7.898	30.255
100	12.676	18.310	7.888	30.280

Experimental Conditions:

Amount of adsorbent = 20 mg
Initial Zn^{2+} concentration = 20 ppm
Initial solution pH = 5.1
Total volume of reaction solution = 50 mL (48 mL of Zn^{2+} solution + 2 mL of 100 ppm $CaCl_2$ salt solution)
Shaking speed = 120 rpm
Temperature = 30^0C

Appendix C-22 Effect of divalent ions concentration on adsorption of Zn^{2+} onto raw and modified eucalyptus bark at initial $CaCl_2$ concentration of 200 mg L^{-1}

Time, t (min)	Raw Eucalyptus Bark		Modified Eucalyptus Bark	
	C_t (mg/L)	q_t (mg/g)	C_t (mg/L)	q_t (mg/g)
0	0.000	0.000	0.000	0.000
5	14.335	14.163	12.828	17.930
10	13.663	15.843	10.828	22.930
20	13.663	15.843	10.668	23.330
40	13.126	17.185	9.875	25.313
60	12.856	17.860	9.799	25.503
80	12.772	18.070	9.436	26.410
100	12.761	18.098	8.921	27.698

Experimental Conditions:

Amount of adsorbent = 20 mg
Initial Zn^{2+} concentration = 20 ppm
Initial solution pH = 5.1
Total volume of reaction solution = 50 mL (48 mL of Zn^{2+} solution + 2 mL of 200 ppm $CaCl_2$ salt solution)
Shaking speed = 120 rpm
Temperature = 30^0C

Appendix C-23 Effect of divalent ions concentration on adsorption of Zn^{2+} onto raw and modified eucalyptus bark at initial $CaCl_2$ concentration of 300 mg L^{-1}

Time, t (min)	Raw Eucalyptus Bark		Modified Eucalyptus Bark	
	C_t (mg/L)	q_t (mg/g)	C_t (mg/L)	q_t (mg/g)
0	0.000	0.000	0.000	0.000
5	14.904	12.740	13.596	16.010
10	14.318	14.205	12.408	18.980
20	14.171	14.573	11.937	20.158
40	13.708	15.730	11.398	21.505
60	13.610	15.975	9.889	25.278
80	13.185	17.038	9.452	26.370
100	12.867	17.833	9.346	26.635

Experimental Conditions:

Amount of adsorbent = 20 mg
Initial Zn^{2+} concentration = 20 ppm
Initial solution pH = 5.1
Total volume of reaction solution = 50 mL (48 mL of Zn^{2+} solution + 2 mL of 300 ppm $CaCl_2$ salt solution)
Shaking speed = 120 rpm
Temperature = 30^0C

Appendix C-24 Effect of trivalent ions concentration on adsorption of Zn^{2+} onto raw and modified eucalyptus bark at initial $FeCl_3$ concentration of 100 mg L^{-1}

Time, t (min)	Raw Eucalyptus Bark		Modified Eucalyptus Bark	
	C_t (mg/L)	q_t (mg/g)	C_t (mg/L)	q_t (mg/g)
0	0.000	0.000	0.000	0.000
5	15.904	10.240	12.867	17.833
10	15.643	10.893	10.184	24.540
20	15.049	12.378	9.757	25.608
40	14.862	12.845	9.487	26.283
60	13.838	15.405	9.445	26.388
80	13.112	17.220	8.950	27.625
100	12.468	18.830	8.739	28.153

Experimental Conditions:

Amount of adsorbent = 20 mg
Initial Zn^{2+} concentration = 20 ppm
Initial solution pH = 5.1
Total volume of mixed solution = 50 mL (48 mL of Zn^{2+} solution + 2 mL of 100 ppm $FeCl_3$ salt solution)
Shaking speed = 120 rpm
Temperature = 30^0C

Appendix C-24 Effect of trivalent ions concentration on adsorption of Zn^{2+} onto raw and modified eucalyptus bark at initial $FeCl_3$ concentration of 200 mg L^{-1}

Time, t (min)	Raw Eucalyptus Bark		Modified Eucalyptus Bark	
	C_t (mg/L)	q_t (mg/g)	C_t (mg/L)	q_t (mg/g)
0	0.000	0.000	0.000	0.000
5	14.924	12.690	13.384	16.540
10	14.867	12.833	11.083	22.293
20	14.861	12.848	9.906	25.235
40	14.523	13.693	9.855	25.363
60	14.226	14.435	9.566	26.085
80	13.898	15.255	9.189	27.028
100	13.121	17.198	9.135	27.163

Experimental Conditions:

Amount of adsorbent = 20 mg
Initial Zn^{2+} concentration = 20 ppm
Initial solution pH = 5.1
Total volume of mixed solution = 50 mL (48 mL of Zn^{2+} solution + 2 mL of 200 ppm $FeCl_3$ salt solution)
Shaking speed = 120 rpm
Temperature = 30^0C

Appendix C-24 Effect of trivalent ions concentration on adsorption of Zn^{2+} onto raw and modified eucalyptus bark at initial $FeCl_3$ concentration of 300 mg L^{-1}

Time, t (min)	Raw Eucalyptus Bark		Modified Eucalyptus Bark	
	C_t (mg/L)	q_t (mg/g)	C_t (mg/L)	q_t (mg/g)
0	0.000	0.000	0.000	0.000
5	14.708	13.230	13.922	15.195
10	14.624	13.440	12.831	17.923
20	14.385	14.038	11.578	21.055
40	14.137	14.658	10.973	22.568
60	14.020	14.950	9.863	25.343
80	13.642	15.895	9.511	26.223
100	13.621	15.948	9.501	26.248

Experimental Conditions:

Amount of adsorbent = 20 mg
Initial Zn^{2+} concentration = 20 ppm
Initial solution pH = 5.1
Total volume of mixed solution = 50 mL (48 mL of Zn^{2+} solution + 2 mL of 300 ppm $FeCl_3$ salt solution)
Shaking speed = 120 rpm
Temperature = 30^0C